University of Cyprus

DEPARTMENT OF CHEMISTRY

DEGRADABLE POLYMERS CONTAINING LABILE PYRIDINYLALKYL ESTER GROUPS IN THE MONOMER UNIT, CROSS-LINKER, INITIATOR OR INIMER

DOCTOR OF PHILOSOPHY DISSERTATION

MARIOS ELLADIOU

2017

University of Cyprus

DEPARTMENT OF CHEMISTRY

DEGRADABLE POLYMERS CONTAINING LABILE PYRIDINYLALKYL ESTER GROUPS IN THE MONOMER UNIT, CROSS-LINKER, INITIATOR OR INIMER

A Dissertation Submitted to the University of Cyprus in Partial Fulfillment of the Requirements for the Degree of Doctor of Philosophy

MARIOS ELLADIOU

April 2017

VALIDATION PAGE

Doctoral Candidate: Marios Elladiou

Doctoral Thesis Tittle: Degradable Polymers Containing Labile Pyridinylalkyl Ester Groups in the Monomer Unit, Cross-linker, Initiator or Inimer

The present doctoral dissertation was submitted in partial fulfillment of the requirements for the Degree of Doctor of Philosophy at the Department of Chemistry and was approved on the 22nd March 2017 by the members of the ***Examination Committee***

Examination Committee:

Research Supervisor: …….
(Name, position and signature)

Committee Member: …….
(Name, position and signature)

Committee Member: …….
(Name, position and signature)

Committee Member: …….
(Name, position and signature)

Committee Member: …….
(Name, position and signature)

DECLARATION OF DOCTORAL CANDIDATE

The present doctoral dissertation was submitted in partial fulfillment of the requirements for the degree of Doctor of Philosophy of the University of Cyprus. It is a product of original work of my own, unless otherwise mentioned through references, notes, or any other statements.

……..[Full Name of Doctoral Candidate]

……..[Signature]

Περίληψη

Η παρούσα Διδακτορική Διατριβή πραγματεύεται το σχεδιασμό, τη σύνθεση, τον πολυμερισμό και τη μελέτη της σταθερότητας μίας οικογένειας εννέα ομόλογων μονομερών μεθακρυλικών πυριδινυλαλκυλεστέρων και μερικών συναφών μονομερών, καθώς και τριών ενώσεων βασισμένων στο διεστέρα της 2,6-δισ(υδροξυαιθυλο)πυριδίνης: ένα διασπώμενο διασταυρωτή, ένα διασπώμενο διδραστικό εκκινητή, και ένα διασπώμενο ίνιμερ. Οι ομόλογοι μεθακρυλικοί πυριδινυλαλκυλεστέρες διέφεραν ως προς τη θέση του ατόμου του αζώτου στο δακτύλιο της πυριδίνης (2-, 3- ή 4-πυριδίνη) ή/και το μήκος της συνδετικής ομάδας (από μέθυλο- μέχρι και πρόπυλο-) μεταξύ του εστέρα και της πυριδίνης. Τα πολυμερή των ομόλογων μεθακρυλικών πυριδινυλαλκυλεστέρων μελετήθηκαν ως προς τη θερμική σταθερότητά τους, αλλά και την υδρολυτική τους σταθερότητα κάτω από αλκαλικές και όξινες συνθήκες. Όλα τα ομόλογα πολυμερή ήταν σταθερά σε συνθήκες όξινης υδρόλυσης, αλλά ήταν μερικώς ή πλήρως ασταθή σε συνθήκες αλκαλικής υδρόλυσης ή θερμόλυσης, με διάσπαση της πλευρικής πυριδινυλαλκυλομάδας. Τα τρία ισομερή ομόλογα πολυμερή που φέρουν αιθυλομάδα μεταξύ του εστέρα και της πυριδίνης διασπάστηκαν πλήρως κάτω από αλκαλικές συνθήκες σχηματίζοντας πολυ(μεθακρυλικό οξύ) (poly(methacrylic acid), pMAA) και την αντίστοιχη βινυλοπυριδίνη, ενώ τα υπόλοιπα έξι ομόλογα πολυμερή των μεθακρυλικών πυριδινυλαλκυλεστέρων διασπάστηκαν μερικώς προς pMAA και την αντίστοιχη υδροξυαλκυλοπυριδίνη. Επιπλέον, τα δύο ομόλογα ισομερή που φέρουν αιθυλομάδα με το άτομο του αζώτου στη θέση 2 ή 4 στο δακτύλιο της πυριδίνης διασπώνται πλήρως σε θερμοκρασία γύρω στους 200 ºC σχηματίζοντας pMAA και την αντίστοιχη βινυλοπυριδίνη, ενώ το άλλο ισομερές πολυμερές με το άζωτο στη θέση 3 στο δακτύλιο της πυριδίνης ήταν θερμικά πιο σταθερό, παρουσιάζοντας μόνο μερική διάσπαση προς pMAA και 3-βινυλοπυριδίνη. Τα υπόλοιπα έξι ομόλογα πολυμερή ήταν θερμικά πιο σταθερά από τα τρία προαναφερθέντα ισομερή ομόλογα πολυμερή με τις πυριδινυλαιθυλομάδες. Επιπλέον, συντέθηκαν και κάποια συναφή πολυμερή, των οποίων η χημική δομή είναι παρόμοια με αυτή του πολυ(μεθακρυλικού 2-(πυριδιν-2-υλ)αιθυλεστέρα) (poly(2-(pyridin-2-yl)ethyl methacrylate), p2PyEMA), όπου όμως είχε αντικατασταθεί το άτομο του αιθερικού οξυγόνου του εστέρα με άζωτο ή θείο δίνοντας αμίδιο ή θειεστέρα, ή ο δακτύλιος της πυριδίνης με αυτόν του βενζολίου, ή είχε αυξηθεί η υποκατάσταση στην ομάδα που συνδέει τον εστέρα και την πυριδίνη, με την προσθήκη μίας ή δύο μεθυλομάδων στον άνθρακα της θέσης 2 του αιθυλεστέρα. Αυτά τα πολυμερή

ήταν σταθερότερα, τόσο θερμικά όσο και υδρολυτικά, από το p2PyEMA, με το πολυαμίδιο να είναι εξαιρετικά σταθερό. Ακολούθως, συντέθηκαν και μελετήθηκαν συμπολυμερή του 2PyEMA με το μεθακρυλικό 2-τετραϋδροπυρανυλεστέρα (tetrahydro-2*H*-pyran-2-yl methacrylate, THPMA), μονομερές γνωστό για την αστάθειά του σε όξινες συνθήκες. Με αυτή τη μελέτη αποδείχτηκε η αμοιβαία εκλεκτική («ορθογωνική») αποπροστασία των μονάδων του 2PyEMA και του THPMA. Επιπλέον, τα πολυμερή που έφεραν το διασταυρωτή, το ίνιμερ, ή το διδραστικό εκκινητή, ενώσεις βασισμένες στη 2,6-δισ(υδροξυαιθυλο)πυριδίνη, διασπώνται θερμικά ή υδρολυτικά σε αλκαλικές συνθήκες στις ευαίσθητες μονάδες του διεστέρα της διόλης, μετατρέποντας υπερδιακλαδισμένα πολυμερή, γραμμικά πολυμερή, και διασυνδεδεμένα στα άκρα πολυμερικά πλέγματα σε γραμμικά πολυμερή, γραμμικά πολυμερή με το μισό μοριακό βάρος από το αρχικό, και αστεροειδή πολυμερή, αντίστοιχα. Όλα τα παραπάνω, αποτελούν μία καινούρια πλατφόρμα μορίων τα οποία αναμένεται να είναι χρήσιμα στη μακρομοριακή μηχανική, παρέχοντας νέες προστατευτικές ομάδες για την ομάδα του καρβοξυλικού οξέος, ή, αντίθετα, πιο σταθερές επαναλαμβανόμενες μονομερικές μονάδες, ή, τελικά, καινοτόμα διασπώμενα σημεία διακλάδωσης.

Abstract

This PhD Thesis is concerned with the design, synthesis, polymerization, and stability of a series of nine pyridinylalkyl methacrylate monomers and related monomers, as well as three compounds based on 2,6-pyridinediethanol diesters: a degradable cross-linker, a degradable bifunctional initiator and a degradable inimer. The pyridinylalkyl methacrylates were homologues differing in the position of the nitrogen atom in the pyridine ring (2-, 3- or 4-pyridine) or/and in the length of the spacer (from methyl to propyl) between the ester moiety and the pyridine ring. The thermal and hydrolytic stability under alkaline and acidic hydrolysis conditions of the pyridinylalkyl methacrylate homologous polymers was investigated. All polymer homologues were stable under acidic hydrolysis conditions, but presented partial or complete lability to alkaline hydrolysis conditions or thermally, as manifested by the cleavage of the pyridinylalkyl side-group. The three isomeric polymer homologues bearing an ethyl spacer were fully cleaved under alkaline hydrolysis conditions yielding poly(methacrylic acid) (pMAA) and the corresponding vinylpyridine, while the other six poly(pyridinylalkyl methacrylate) homologues were partially cleaved to pMAA and the corresponding hydroxyalkylpyridine. Furthermore, the two isomeric polymer homologues bearing an ethyl spacer with the nitrogen placed at position 2 or 4 in the pyridine ring were also cleaved at around 200 ºC yielding pMAA and the corresponding vinylpyridine, while the other isomeric polymer ethyl homologue with the nitrogen placed at position 3 was thermally more stable, presenting only partial cleavage to pMAA units and 3-vinylpyridine. The other six polymer homologues were thermally more stable than the three above-mentioned isomeric polymer ethyl homologues. Additionally, some related polymers were also synthesized, whose chemical structure was similar to that of poly(2-(pyridin-2-yl)ethyl methacrylate) (p2PyEMA), but having a non-ester side-group by replacing the ester linkage for amide or thioester, or a non-pyridine aromatic group by replacing the pyridine ring for a benzene ring, or a substituted ethyl ester spacer, by introducing one or two methyl groups on the carbon at 2-position in the ethyl spacer. These related polymers were more stable than p2PyEMA both toward thermolysis and alkaline hydrolysis conditions, with the polyamide homologue being extremely stable. Subsequently, by preparing and studying the copolymers of 2PyEMA with tetrahydro-2*H*-pyran-2-yl methacrylate (THPMA), a well-known acid labile monomer, it was proven that the 2PyEMA and THPMA units are orthogonally deprotectable. Finally, polymers bearing the cross-linker, inimer, or bifunctional initiator based on 2,6-pyridinediethanol were

shown to cleave under thermolysis or alkaline hydrolysis conditions at the sensitive diester moieties of the diol, converting hyperbranched polymers, linear polymers and end-linked polymer networks to linear polymers, linear polymers with half the initial molecular weight, and star polymers, respectively. All the above, newly-developed monomers, cross-linker, inimer, and bifunctional initiator form a new platform of molecules which are expected to be useful for macromolecular engineering, so as to provide novel carboxylic acid group protection, or, conversely, more stable monomer repeating units, or, finally, novel cleavable branching points.

Acknowledgments

The author would like to express his sincere thanks and gratitude to his Supervisor Dr. Costas S. Patrickios, Professor of Department of Chemistry in University of Cyprus for his valuable guidance and assistance given throughout the PhD period.

His thanks are extended to the European Regional Development Fund (ERDF) and the Republic of Cyprus (RoC) for funding a part of this work through the Cyprus Research Promotion Foundation (CRPF) within the project NEA YPODOMH/NEKYP/0311/27. Additionally, the author wish to thanks the European Commission which through the project SELFMEM (grant agreement no. NMP3-SL-2009-228652) also funded a part of this work.

To my mother for her appreciate assistance

throughout the performance of this work

PUBLICATIONS

1. Elladiou, M.; Patrickios, C. S. "2-(Pyridin-2-yl)ethanol as a Protecting Group for Carboxylic Acids: Chemical and Thermal Cleavage, and Conversion of Poly[2-(pyridin-2-yl)ethyl Methacrylate] to Poly(methacrylic Acid)." *Polym. Chem.* **2012**, *3*, 3228−3231.

2. Pafiti, K. S.; Elladiou, M.; Patrickios, C. S. "Inverse Polyampholyte" Hydrogels from Double-cationic Hydrogels: Synthesis by RAFT Polymerization and Characterization." *Macromolecules* **2014**, *47*, 1819−1827.

3. Rikkou-Kalourkoti, M.; Elladiou, M.; Patrickios, C. S. "Synthesis and Characterization of Hyperbranched Amphiphilic Block Copolymers Prepared via Self-condensing RAFT Polymerization." *J. Polym. Sci., Part A: Polym. Chem.* **2015**, *53*, 1310−1319.

4. Elladiou, M.; Patrickios, C. S. "ABC Triblock Terpolymers with Orthogonally Deprotectable Blocks: Synthesis, Characterization, and Deprotection." *Macromolecules* **2015**, *48*, 7503−7512.

5. Constantinou, A. P.; Elladiou, M.; Patrickios, C. S. "Regular and Inverse Polyampholyte Hydrogels: A Detailed Comparison." *Macromolecules* **2016**, *49*, 3869−3880.

6. Elladiou, M.; Patrickios, C. S. "A Dimethacrylate Cross-linker Cleavable Under Thermolysis or Alkaline Hydrolysis Conditions: Synthesis, Polymerization, and Degradation." *Chem. Commun.* **2016**, *52*, 3135−3138.

7. Elladiou, M.; Kalogirou A. S.; Patrickios, C. S. "Symmetrical Polymer Systems Prepared Using a Degradable Bifunctional ATRP Initiator: Synthesis, Polymerization, and Degradation." Under revision in *The Journal of Polymer Science Part A: Polymer Chemistry*. February 2017.

8. Elladiou, M.; Patrickios, C. S. "A Degradable ATRP Inimer Cleavable Under Thermolysis or Alkaline Hydrolysis Conditions: Synthesis, Polymerization and Cleavage." In preparation for submission in *Macromolecular Rapid Communications*.

9. Elladiou, M.; Patrickios, C. S. "Poly(Pyridinylalkyl Methacrylates): A Class of Addition Polymers With Rich Chemical Properties." In preparation for submission in *Chemical Science.*

Table of Contents

List of Figures

Figure 4.1 Chemical structures of molecules proposed to be investigated in future work.

List of Schemes

Scheme 3.16 Chemical reaction for the alkaline hydrolysis of the 2PyEMA monomer, along with its ^{1}H NMR spectra before (a, black) and after alkaline hydrolysis (b, red), both in d_6-DMSO.

Scheme 3.17 Chemical reaction for the alkaline hydrolysis of the 4PyEMA monomer, along with its ^{1}H NMR spectra before (a, black) and after alkaline hydrolysis (b, red), both in d_6-DMSO.

Scheme 3.18 (Co)polymerization of 2PyEMA, and Polymer Chemical and Thermal Deprotection.

Scheme 3.19 Synthesis of THPMA monomer, along with its ^{1}H and ^{13}C NMR spectra.

Scheme 3.20 Addition Sequences Followed for the Preparation of the Two ABC Triblock Terpolymers.

Scheme 3.21 Cleavage Sequences Followed for the Step-wise and Selective Deprotection of the $BzMA_{20}$-*b*-$THPMA_{20}$-*b*-($THPMA_{20}$-*co*-$PyEMA_{20}$) Triblock Terpolymer All the Way to MAA_{80}.

Scheme 3.22 Chemical Reaction of hydroxymethylation od 2,6-lutidine leading to synthesis of 2,6-pyridinediethanol, along with its (a) ^{1}H and (b) ^{13}C NMR Spectra.

Scheme 3.23 Chemical Reaction for the Synthesis of the PyDMA Cross-linker, Along with its (a) ^{1}H and (b) ^{13}C NMR Spectra.

Scheme 3.24 RAFT (Co)Polymerization of the PyDMA Cross-Linker, and the Thermal and the Alkaline Hydrolysis Treatments of the Resulting Polymers.

Scheme 3.25 Chemical reactions performed for the synthesis of 2,6-pyridinediethanol and the PyDEDBrMeP degradable bifunctional ATRP initiator, together with their ^{1}H NMR spectra.

Scheme 3.26 Esterification reaction of 2,6-pyridinedimethanol for the synthesis of the PyDMDBrMeP more stable bifunctional ATRP initiator, and their ^{1}H NMR spectra.

Scheme 3.27 Chemical reaction for the alkaline hydrolysis of the PyDEDBrMeP degradable bifunctional ATRP initiator, its ^{1}H NMR spectrum (a, black) in $CDCl_3$ and the ^{1}H NMR spectrum after alkaline hydrolysis (b, red) in d_6-DMSO.

Scheme 3.28 Synthesis of the Hyperbranched MMA Homopolymers and the Hyperbranched Amphiphilic MMA-DMA Diblock Copolymers and the Products Obtained after Thermolysis or Alkaline Hydrolysis of the PyDEBrMA Residues.

Scheme 3.29 Synthesis of 2,6-pyridinediethanol, the intermediate monofunctional ATRP initiator, and the 2PyDEBrMA ATRP inimer, along with their ^{1}H and ^{13}C NMR spectra.

Scheme 3.30 Chemical Reaction of the Alkaline Hydrolysis of the PyDEBrMA *Inimer* in d_6-DMSO using NaOD, along with the ^{1}H NMR spectra before (black) and after (red) alkaline hydrolysis of the PyDEBrMA ATRP Inimer.

List of Tables

Table 3.14 Micellar Characteristics of the hyperbranched amphiphilic [MMA-Inimer]-*b*-DMAEMA diblock copolymers and their products obtained after alkaline hydrolysis of the PyDEBrMA residue.

Abbreviation

2PyMMA	pyridin-2-ylmethyl methacrylate
2PyEMA	2-(pyridin-2-yl)ethyl methacrylate
2PyPMA	3-(pyridin-2-yl)propyl methacrylate
3PyMMA	pyridin-3-ylmethyl methacrylate
3PyEMA	2-(pyridin-3-yl)ethyl methacrylate
3PyPMA	3-(pyridin-3-yl)propyl methacrylate
4PyMMA	pyridin-4-ylmethyl methacrylate
4PyEMA	2-(pyridin-4-yl)ethyl methacrylate
4PyPMA	3-(pyridin-4-yl)propyl methacrylate
2PheMA	2-phenethyl methacrylate
2PyEMAAm	*N*-(2-(pyridin-2-yl)ethyl) methacrylamide
2PyESMA	*S*-(2-(pyridin-2-yl)ethyl) methacrylthioate
FMMA	(*9H*-fluoren-9-yl)methyl methacrylate
THPMA	tetrahydro-2*H*-pyran-2-yl methacrylate
2PyEmeMA	2-((pyridine-2-yl)2-methyl)ethyl methacrylate
2PyEdimeMA	2-((pyridine-2-yl)2,2-dimethyl)ethyl methacrylate
PyDEDBrMeP	2,6-pyridinediethanol di-(2-bromo-2-methyl propanoate)
PyDMDBrMeP	2,6-pyridinedimethanol di-(2-bromo-2-methyl propanoate)
PyDMA	2,6-pyridine dimethacrylate
DMOEM	di-(methacryloyloxy-1-ethoxy)methane
PyDEBrMA	2-(6-(2-((2-bromo-2-methylpropanoyl)oxy)ethyl)pyridin-2-yl)ethyl methacrylate
BzMA	benzyl methacrylate
DMAEMA	2-(dimethylamino)ethyl methacrylate
MMA	methyl methacrylate
Sty	styrene

MAA	methacrylic acid
EGDMA	ethylene glycol dimethacrylate
DPPH	2,2-diphenyl-1-picrylhydrazyl hydrate
VPy	vinyl pyridine
THF	tetrahydrohuran
ET_3N	triethylamine
DMSO	dimethylsulfoxide
d_6-DMSO	deuterated dimethylsulfoxide
$CDCl_3$	deuterated chloroform
D_2O	deuterated oxide
NaOH	sodium hydroxide
NaOD	sodium deuteroxide
HCl	hydrochloric acid
DCl	deuterium chloride
HMTETA	1,1,4,7,10,10-hexamethyltriethylenetetramine
EBbrBu	ethyl *a*-bromoisobutyrate
MTS	1-methoxy-1-trimethylsiloxy-2-methyl propene
TBABB	tetrabutylammonium dibenzoate
AIBN	*N*,*N*′-azobisisobutylnitrile
MTS	1-methoxy-1-trimethylsiloxy-2-methyl propene
CPDB	2-cyanoprop-2-yl dithiobenzoate
ATRP	Atom transfer radical polymerization
RAFT	reversible addition-fragmentation chain transfer polymerization
GTP	group transfer polymerization
GPC	gel permeation chromatography
NMR	nuclear magnetic resonance spectroscopy
DSC	differential scanning calorimetry

TGA	thermal gravimetric analysis
DLS	dynamic light scattering
SLS	static light scattering
AFM	atomic force microscopy
$\boldsymbol{M_p}$	peak molecular weight
$\boldsymbol{M_n}$	number-average molecular weight
$\boldsymbol{M_w}$	weight-average molecular weight
$\boldsymbol{Đ}$	molecular weight dispersities
DP	degree of polymerization
DI	degree of ionization
DS	degree of swelling

Chapter 1 – Introduction

1.1 Aim and Novelty of this PhD Thesis

The initial target of this research was the synthesis of linear amphiphilic diblock copolymers of 2- or 4-vinylpyridine with styrene of various compositions, using reversible addition-fragmentation chain transfer (RAFT) polymerization. The combination of the very polar vinylpyridine units in the one block with the less polar styrene units in the other block strongly drives microphase separation, leading to the formation of various morphologies,[1,2,3] which can be exploited for the fabrication of membranes for use in water purification and separation of gases and proteins.[4] The RAFT polymerization of vinylpyridine did not result in highly homogeneous polymers because of undesired side – reactions triggered by the highly reactive 2- and, particularly, 4-vinylpyridines. We attempted to solve this problem by preparing methacrylate analogues of vinylpyridine, suitable for group transfer polymerization (GTP). The first monomer we prepared was 2-(pyridin-2-yl)ethyl methacrylate (2PyEMA). GTP allowed the polymerization of 2PyEMA, leading to the preparation of rather homogeneous polymers. However, it was soon realized that these polymers were labile, as the 2PyEMA units could readily lose their pyridine side – groups under certain conditions, whereas they were stable under other conditions. A literature survey indicated that this was highly unexplored within polymer chemistry, and warranted further investigation. Based on the initial discovery of the lability of the 2PyEMA units in their polymers, the following objectives were formulated for this Thesis:

1) Investigate conditions of stability / lability of the 2PyEMA units in their homopolymers, and study their degradation kinetics.
2) Investigate the selectivity of degradation of 2PyEMA in its copolymers with other stable comonomers.
3) Investigate the orthogonality of the degradation of 2PyEMA in its copolymers with other unstable monomer repeating units exhibiting lability under different conditions than 2PyEMA.
4) Expand the study to investigate the stability of the homopolymers of the two isomers of 2PyEMA, 2-(pyridin-3-yl)ethyl methacrylate (3PyEMA), and 2-(pyridin-4-yl)ethyl methacrylate (4PyEMA), differing in the position of the nitrogen atom in the pyridine ring, and also the homopolymers of the six remaining homologues having different spacer length (methyl and propyl rather than ethyl,

i.e., pyridin-2-ylmethyl methacrylate (2PyMMA), and 3-(pyridin-2-yl)propyl methacrylate (2PyPMA) and covering the three possible nitrogen atom positions in the ring (pyridin-3-ylmethyl methacrylate (3PyMMA), 3-(pyridin-3-yl)propyl methacrylate (3PyPMA), pyridin-4-ylmethyl methacrylate (4PyMMA), and 3-(pyridin-4-yl)propyl methacrylate (4PyPMA)).

5) Further expand the stability study in order to compare with the homopolymers of related monomers, such as the methacrylamide and methacrylthioate analogues of 2PyEMA, and also the homopolymers of 2PyEMA analogues with its ethyl group in the pendant being singly- and doubly- substituted.
6) Expand the established lability of the 2-(pyridin-2-yl)ethyl ester by preparing the symmetrical, also degradable 2,6-pyridinediethanol diesters, based on which to design and synthesize three new degradable compounds, together with the relevant polymeric products: a cross-linker, a bifunctional initiator, and an inimer.

This Thesis lies in the import in the labile 2-(pyridin-2-yl)ethyl ester group in polymer chemistry, and the design and preparation several novel compounds, both small molecules and polymeric bearing it. First, as a side – group, the 2-(pyridin-2-yl)ethyl ester constitutes a novel protective group for MAA, which, unlike the most common protecting groups which can be cleaved under acidic conditions, this can be readily removed under thermolysis or alkaline hydrolysis conditions. Furthermore, the thermal and alkaline hydrolytic lability of the 2-(pyridin-2-yl)ethyl ester group was also exploited to prepare degradable symmetrical linear (co-)polymers, hyperbranched polymers, and polymer networks, through its incorporation with in a novel bifunctional initiator, inimer and cross-linker.

1.2 Pyridine

Pyridine possesses a central role in this PhD Thesis. All polymers prepared in this study contained the pyridine ring in the monomer repeating units or in the cross-linker, initiator or inimer residue. The presence of the pyridine ring in polymers can confer upon them certain properties.

Pyridine is a fundamentally important basic heterocyclic compound with the empirical formula C_5H_5N. It is a liquid with a distinctively putrid, fishy odor. It has a six-membered ring structure, related to the structure of benzene, with one methine replaced by a nitrogen atom. The pyridine ring can be found in many important compounds and has numerous

applications. Pyridine is used as solvent and as starting material in the manufacture of insecticides, herbicides, pharmaceuticals, food flavorings, dyes, adhesives, paints, explosives and disinfectants. In addition, it is used in polymers and in coordination chemistry as a ligand. Worldwide, between 100 and 1000 tons of pyridine or pyridine-containing products are produced annually.[5]

1.2.1 Pyridine: History. In 1849, the Scottish scientist Thomas Anderson obtained 2-methylpyridine and subsequently pyridine as well as some dimethylpyridines, when examining the contents of the oil from animal bones.[6,7] Anderson described it as a colorless liquid, highly soluble in water, readily soluble in concentrated acids and salts upon heating, and only slightly soluble in oils. Due to its flammability, Anderson named it pyridine, from the Greek *πυρ* (*pyr*) meaning fire. The suffix *idine* was added in compliance with the chemical nomenclature, to indicate a carbon ring containing a nitrogen atom. The chemical structure of pyridine was elucidated by Wilhelm Körner and James Dewar, decades after its original isolation by Anderson. Körner and Dewar independently suggested that the structure of pyridine is related to benzene, by substituting one methine (C-H) with a nitrogen atom. In 1876, Sir William Ramsey was the first to report a synthesis of pyridine that involved passing a mixture of acetylene and hydrogen cyanide through a hot tube.[8] Increased demand for pyridine and pyridine derivatives led to the development of new synthetic methods. In 1881, Arthur Rudolf Hantzsch reported the synthesis of pyridine from an aldehyde, a *β*-ketoester and ammonia,[9] while, in 1906, Russian chemist Aleksei Chichibabin reported a vapour phase synthesis of pyridine, which was based on inexpensive reagents, formaldehyde, acetaldehyde and ammonia.[10] It is noteworthy that these last two methods are still used for the industrial production of pyridine.

In its general form, Chichibabin pyridine synthesis can be described as a condensation reaction of aldehydes, ketones, *α*,*β*-unsaturated carbonyl compounds, or any combination of the above, with ammonia or ammonia derivatives.[11] In particular, unsubstituted pyridine is produced from formaldehyde, acetaldehyde and ammonia, which are inexpensive and widely available. Chichibabin pyridine synthesis involves an aldol condensation between acetaldehyde and formaldehyde, forming the simplest unsaturated aldehyde, acrolein, and its subsequent condensation with acetaldehyde and ammonia, where finally an oxidation reaction takes place forming the pyridine ring. Figure 1.1 displays the general procedure of Chichibabin pyridine synthesis. This process is carried out in gas phase at 400–450 °C. Practical application of the traditional Chichibabin pyridine synthesis is limited by its

consistently low yield, typically about 20%. This low yield, together with the high prevalence of byproducts, render unmodified forms of Chichibabin's method unpopular.

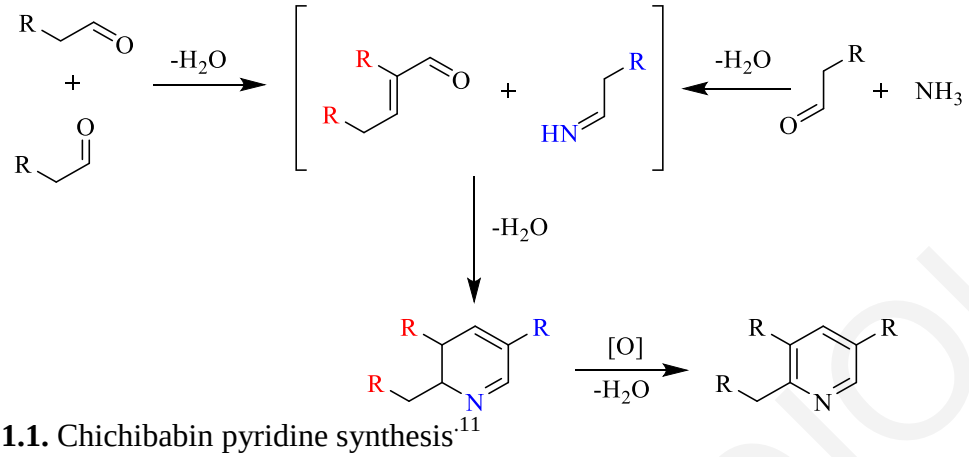

Figure 1.1. Chichibabin pyridine synthesis[11]

The Hantzsch pyridine synthesis is a multi-component organic reaction between an aldehyde, such as formaldehyde, 2 equivalents of a *β*-ketoester such as ethyl acetoacetate, and a nitrogen donor such as ammonium acetate or mmonia.[12] The initial reaction product is a dihydropyridine which can be oxidized in a subsequent step to a pyridine. The driving force for this second reaction step is aromatization. Figure 1.2 displays Hantzsch pyridine synthesis, whose yield exceeds 90%.

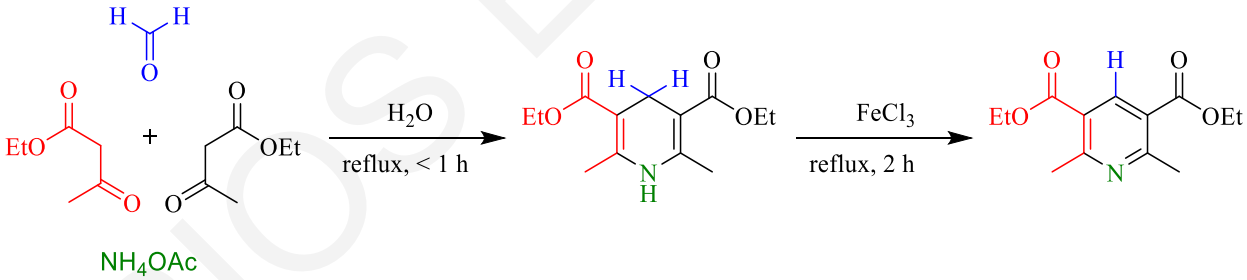

Figure 1.2. Hantzsch pyridine synthesis.[9]

1.2.2 Pyridine: Physical and Chemical Properties.[13] The physical properties of pyridine are the consequence of a stable, cyclic, 6-π-electron, π-deficient, aromatic structure containing a ring nitrogen atom. The ring nitrogen is more electronegative than the ring carbons, making the two-, four-, and six-ring carbons more electropositive. The aromatic π-electron system does not require the participation of the lone pair of the electrons on the nitrogen atom. Because this lone pair is not delocalized into the aromatic system of π-electrons, pyridine can act like base, with chemical properties similar to those of organic tertiary amines. Pyridine is protonated by reaction with acids, forming a positively charged aromatic polyatomic ion called a pyridinium cation. This cation is the conjugate acid of

pyridine and its pK_a has a value of 5.30. The bond lengths and bond angles in pyridine and the pyridinium ion are almost identical. This is because protonation of pyridine does not affect the aromatic π-system. Liquid pyridine and alkylpyridines are considered to be polar aprotic solvents, similar to dimethylformamide or dimethylsulfoxide. Pyridine is fully miscible with a broad range of other solvents, including hexane and water.

Many physical properties of pyridine are unlike those of benzene, its homocyclic counterpart. For instance, pyridine has a boiling point by 35.10 °C higher than benzene (115.20 *vs.* 80.10 °C) and a melting point by 47.13 °C lower than benzene (−41.60 *vs.* 5.53 °C), and, unlike benzene, it is miscible with water in all proportions at ambient temperatures. Its density, 0.9819 g cm^{-3}, is close to that of water, and its refractive index at a wavelength of 589 nm and a temperature of 20 °C is 1.5093. The much higher dipole moment of pyridine relative to benzene is responsible, in a significant part, for the higher boiling point and water solubility. Benzene and pyridine are aromatic compounds having resonance energies of similar magnitude, and both are miscible with most other organic solvents. Pyridine is a weak organic base, less than aliphatic, tertiary amines, being both an electron-pair donor and a proton acceptor, whereas benzene has little tendency to donate electron pairs or accept protons.

Most chemical properties of pyridine are typical of those of a heteroaromatic compound. Pyridine behaves both as a tertiary amine undergoing protonation reactions, alkylation, acylation and *N*-oxidation,[14-17] and as an aromatic compound, allowing easy nucleophilic substitution reactions[18] and difficult electrophilic substitution reactions,[19] due to the presence of the electronegative nitrogen in the pyridine ring (the molecule is relatively electron deficient). The reactivity of pyridine can be distinguished for three chemical groups. With electrophiles, electrophilic substitution takes place where pyridine expresses aromatic properties. With nucleophiles, pyridine reacts via its 2nd and 4th carbon atoms and thus behaves similar to imines and carbonyls. The reaction with many Lewis acids results in the addition to the nitrogen atom of pyridine, which is similar to the reactivity of tertiary amines. The nitrogen atom of pyridine features a basic lone pair of electrons. Pyridine can act as a Lewis base, donating its pair of electrons to a Lewis acid as in the sulfur trioxide pyridine complex. Additionally, pyridine itself is a relatively weak ligand in forming complexes with transition metal ions.

The increased chemical reactivity of pyridine leads to the formation of several side reactions during the polymerization of monomers which contain it, especially in the case

where anionic polymerization is used, due to the presence of strong nucleophiles. Schmitz et al. reported a detailed description of the most prevalent side reaction that takes place, both to monomers and polymers containing pyridine.[20] Gas chromatography (GC) and mass spectrometry (MS) indicated that strong nucleophiles attack the *a*-position of nitrogen in the pyridine ring converting the nitrogen atom to negative, and, thereby able for several subsequent side reactions as shown in Figure 1.3. Lee et al. also reported the presence of side reactions in the pyridine ring of monomers during their polymerization, and the formation of high molecular weight polymers due to the formation of several side-branches.[21,22] Furthermore, this chemical reactivity of pyridine was also reported by Cui and Lattermann,[23] where the increased reactivity of the pyridine ring led to the spontaneous *in situ* polymerization of 3-(pyridin-4-yl)propyl acrylate. Fetters et al. synthesized cross-linked polymers using small amounts of 2- or 4-vinylpyridine, which can act as bifunctional monomers.

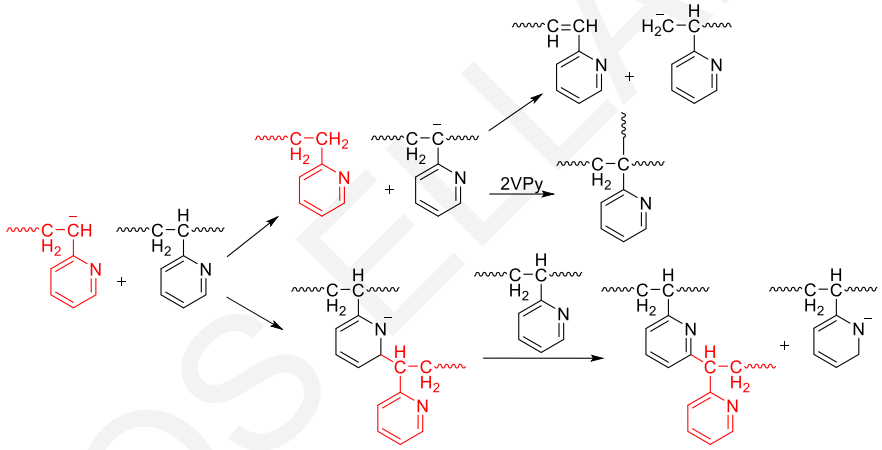

Figure 1.3. Most prevalent side reaction that takes place during polymerization of 2VPy, described by Schmitz et al.[20]

1.2.3 Pyridine: Uses. The pyridine ring is one of the most important heterocycles in drug discovery.[24,25] It is present in more than 100 currently marketed drugs, including the blockbuster drugs esomeprazole (Nexium, dyspepsia) and loratadine (Claritin, antiallergic), in addition to the recently approved cancer therapeutic crizotinib (Xalkori). Other drugs that contain the pyridine ring, or some related compounds, include the life-changing medicines montelukast sodium (Singulair, for asthma/allergies), pioglitazone (Actos, for diabetes), eszopiclozone (Lunesta, for insomnia), imatinib mesylate (Gleevec, for various cancers), lansoprazole (Prevacid, for acid reflux/ulcers) and mirtazapine (for depression). As a result of the immense value of pyridines, for decades methods to access functionalized derivatives of this privileged heterocycle have been highly sought. Additionally, the pyridine ring is present in the chemical structure of many agrochemical

products such as insecticides and herbicides, such as Chlorantraniliprole, Nicosulfuron, Rynaxypyr, Imidacloprid, and Nitrapyrin.

Pyridine can also be used in the field of metal complexes as ligand,[26] acting through the nitrogen atom, forming strong bonds with oxidized metals.[27-30] Pyridine and several pyridine derivative metal complexes, and especially those of silver, cobalt, platinum and gold metal, can be used for their anticancer activity. The chemical and biological activity of these complexes is not possessed only by the metal or organic ligand but also this activity can be due to the changes in the electronic and steric properties of the complexes or by variation of the oxidation state of the metal. These complexes can bind to DNA in noncovalent modes such as electrostatic and intercalation which involves stacking of the planar ligand between adjacent base pairs of the DNA duplex,[31,32] inhibiting its synthesis, and, therefore, show anticancer activity. There is a variety of anticancer pyridine based metal complexes showing anticancer activity, such as $[PtCl_2(pyridine)_2]$,[33] $[Co(ethylenediamine)_2(pyridine)_2]^{3+}$, $[Co(ethylenediamine)_2(methyl\ pyridine)_2]^{3+}$,[34] and some derivatives 2,6-bis(substituted)pyridine Ag(I) nitrate complexes.[35]

Pyridine is also used in the field of Polymer Science, and plays an important role in this area, finding numerous applications. The physical and chemical properties of pyridine are expected to also be displayed by the polymers bearing it. Polymers containing pyridine have such properties as high polarity, increased chemical reactivity and sensitivity to pH, and these polymers can find a host of applications in various fields.[36-38] The presence of pyridine groups in one block of block copolymers whose other block is less polar, e.g., polystyrene, leads to block copolymer self-assembly in solution or in the bulk,[1,2] thus enabling the formation of polymeric membranes for use in water purification and separation of gases and proteins.[4,39-45] The passive diffusion of proteins through membranes is a versatile method for protein separation or long term release, and water purification for desalination applying reverse osmosis effect.[42] Size-based separation of proteins can be carried out by ultrafiltration membrane systems when the proteins have significantly different molecular sizes.[46-49] Isoporous poly(styrene)-*b*-poly(4-vinylpyridine) (PS-*b*-P4VP) membranes with pore size of 34 nm were used for the effective separation of bovine serum albumin (BSA) and immunoglobulin-γ (lgG) as described by Peinemann et al.[45] Another remarkable property of this membrane is that it is pH-responsive, allowing the selective separation of similarly sized proteins based on charge effects, as stated for the separation of BSA and bovine hemoglobin. Furthermore, after quaternization of the

membrane, it was possible to separate these proteins effectively by varying the pH due to their different isoelectric points.

The presence of the pH-responsive pyridine in the polymers offers the possibility of selective drug delivery.[50-53] Yang et al.[53] used a pH-responsive PS-*b*-P4VP block copolymer and formed well-defined spherical and/or worm-like micelles with PS cores and P4VP coronas in selective solvents. The self-assembled worm-like morphology exhibited a pH-responsive behavior due to the protonation of the P4VP block at low pH and its deprotonation at high pH, thus constituting a switchable "off/on" system. Doxorubicin (Dox), a drug used in cancer chemotherapy, was loaded as cargo to test the formed PS-*b*-P4VP micelles. Luminescence experiments indicated that this polymer system was able to store Dox molecules within its micellar structure at neutral pH and then release them as soon as the pH was raised to 8.0.

Yoshikawa et al.[39,54] investigated carbon dioxide separation using polymer membranes having pyridine moieties or the pyridine-Cu(II) complex group, and noticed the selective separation-permeation of CO_2 from a mixture with O_2 and N_2, through a P4VP-*co*-polyacrylonitrile (PACN) membrane. The pyridine moiety was adopted to make use of acid-base interaction for the separation of CO_2, where CO_2 act like acid and pyridine as base. Additionally, Yoshikawa et al.[55] reported halogen ion transport through P4VP-*co*-PACN and P4VP-*co*-PS membranes. Membranes of pyridine-based polybenzimidazole copolymers were thermally stable and maintained mechanical integrity even at high phopsphoric acid doping levels, demonstrating their ability for application in fuel cells at temperatures exceeding 120 ºC without any external humidification.[56]

Furthermore, the presence of pyridine in polymers confers upon them the ability of complexing with various salts or metals. The resulting polymer complexes can find application as solid electrolytes, and may also be used for other electrochemical, electrical and optical applications.[57-59]

1.3 Polymer Architecture

Since this PhD Thesis is concerned with the preparation and characterization of several polymer architectures, we review here information about the structure and properties of these architectures. A polymer may exist in different architectures, the most common of which are linear chains, branched chains, and cross-linked networks (Figure 1.4).[60]

Polymers belonging to all three of these architectures were prepared and characterized for the purposes of this PhD Thesis.

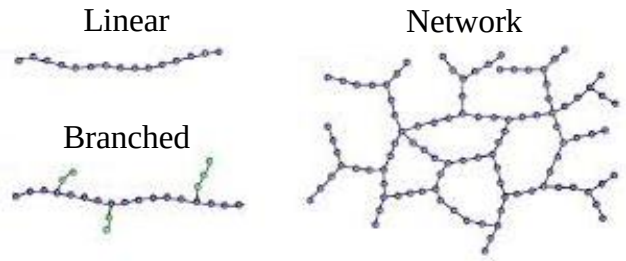

Figure 1.4 Most common polymer architectures.[60]

Linear polymers comprise monomer repeating units interconnected in a linear fashion. Hyperbranched polymers are highly branched soluble polymers, consisting of a basic chain from which several side branches emanate. These branches may have further branches, and so on. Hyperbranched polymers have properties intermediate between linear polymers and networks. Compared to linear polymers, hyperbranched polymers have lower viscosity, easier processability, more compact structure, multiple chain-end functional groups, and unique interfacial and association behavior. Hyperbranched polymers [61] find numerous applications in biological and biomedical systems,[62-64] in coatings,[65,66] and in nonlinear optics,[67,68] or in nanoimprint lithography.[69] Hyperbranched polymers were first reported by DuPont, in order to replace dendrimers, whose synthesis is complicated and time consuming, and therefore difficult for industrial application.

Hyperbranched polymers can be easily synthesized following one of several approaches. One of the easiest routes is the copolymerization of monovinyl with a small amount of di- or multivinyl monomers.[70] Another possibility is the copolymerization of di- or multivinyl monomers with a very large amount of initiator.[71] These two methods can be used either in controlled or non-controlled polymerization methods. A third method for hyperbranched polymer synthesis is the self-condensing vinyl polymerization (SCVP) [72] of an AB* initiator-functionalized monomer, known as *inimer*. An *inimer* can act both as *ini*-tiator and mono-*mer*, containing both a polymerizable group (A) (monomeric) and an initiating group (B*). An advantage of using *inimers* in a controlled polymerization method is the synthesis of hyperbranched polymers which can be easily prepared and purified containing multifunctional groups, without the risk of network formation. SCVP has been applied in ATRP,[73-88] RAFT polymerization,[89-93] photopolymerization,[94] nitroxide-mediated radical polymerization (NMRP),[95,96] living ionic,[97] and GTP.[98-100] In this PhD Thesis, hyperbranched (co)polymers were synthesized following the first approach, polymerization

of monomer in the presence of small amount of cross-linker, and the third route, SCVP-ATRP, using an inimer.

Polymer networks are polymers whose constituting linear chains are cross-linked forming an insoluble matrix,[101] which can absorb large amounts of a particular solvent. Regarding their structure, polymer networks can be distinguished into two categories, randomly cross-linked polymer networks,[102] and model polymer networks.[103,104] Randomly cross-linked polymer networks possess a less perfect structure, because the chains between the cross-links do not have a fixed length. The preparation of randomly cross-linked polymer networks is easy, as it can be performed in one stage, from the simultaneously copolymerization of the monomer with the cross-linker. In contrast, model polymer networks are more difficult to prepare as they must possess chains between cross-links of fixed length. Valles et al.[105] reported the synthesis of model polymer networks by the interconnection of linear chains using a trifunctional cross-linker. Additionally, Katime et al.[106] prepared model networks interconnecting linear chains with a tetrafunctional cross-linker. Weissmüller and Burchard [107] reported the synthesis of model networks by the preparation of star polymers with functional end-groups, which were subsequently interconnected in a final reaction step.

1.4 Protective Groups for MAA Units

Since one of the first findings in this PhD Thesis is a new protective group for MAA, we review here information about the polymers of MAA and chemical groups currently employed to protect its carboxylic acid group.

PMAA and poly(acrylic acid) (PAA) are weak polyelectrolytes, in which the degree of ionization is mainly governed by the pH of the aqueous solution. For example, PMAA and PAA are virtually undissociated at low pH (pH 2), but fully charged at pH 8. PMAA and PAA are known to form interpolymer complexes with various non-ionic proton accepting polymers, e.g., polyethylene oxide, and with cationic polyelectrolytes in aqueous and organic media.[108–114] It has been shown that the nature and molecular weight (MW) of the interacting polymers as well as various environmental parameters (the nature of the solvent, the pH, the ionic strength of the solution, the temperature, and the polymer concentration) have significant influence on the complex formation. Numerous studies have also been devoted to the interaction of PMAA and PAA with metal ions,[114-118] since the knowledge of the association phenomena of metal ions with charged macromolecules is of importance for the understanding of their physicochemical behavior in environmental

and biological systems. PAA could be successfully used as a component of characteristic 'intelligent' organic–inorganic hybrid materials.[119]

Block copolymers containing MAA segments belong to the class of ionic (or polyelectrolytic) block copolymers, which combine structural features of polyelectrolytes, block copolymers, and surfactants. If the ionic block is rather short compared to the non-ionic one, they are also named 'block ionomers'. Ionic block copolymers possess quite unique and attractive properties, potentially connecting materials science, pharmacy, biochemistry and polymer science, which make them a challenging subject for researchers. In particular, there has been much interest for the self-assembly of block copolymers, because of their capability to generate nanostructured materials and their numerous potential applications in separation technology, and controlled drug delivery and release.[120–126] Recent advances in controlled/living polymerization techniques made it possible to produce well-defined polymer structures, such as graft copolymers, star polymers, and polymer brushes. The interest in the synthesis and characterization of such complex polymer systems containing MAA segments has increased enormously. Their chemical structure and three-dimensional (3D) architectures may be tuned for a wide range of applications covering such different aspects as stabilization of colloids, crystal growth modification, induced micelle formation, components of intelligent materials, and polyelectrolyte complexing towards novel drug carrier systems.

For the synthesis of well-defined polymers, living polymerization techniques have traditionally been employed, proceeding without irreversible chain transfer or chain termination reactions. These characteristics are encountered in a nearly ideal way in living anionic polymerization, and less ideally in living cationic polymerization. However, the application of these techniques for the synthesis of functional polymers is sometimes not straightforward, as these systems are not tolerant to many functional groups. Thus, typically, protected functional monomers have been employed for the polymerization, followed by a polymer-analogous deprotection reaction, e.g., hydrolysis of the protecting ester group. A variety of protected monomers have been developed in the past few decades, and polymerized using controlled / living technique, to obtain various types of tailor-made polymers with interesting architectures and functional groups.[127,128]

A wide range of protecting groups, with various degrees of stability, have been developed for MAA during the past 20-30 years. Figure 1.5 shows these protective groups. Most of the (meth)acrylic acid protective groups in synthetic polymers are acid labile, and are

stable under alkaline hydrolysis conditions. Trimethylsilyl,[129,130] 2-tetrahydropyranyl,[130-133] 1-ethoxyethyl,[134,135] and *tertiary*-butyl groups [129,136,137] can be removed under acidic hydrolysis conditions. Benzyl esters [129,138,139] and *p*-nitrophenyl group [140,141] can be readily removed by catalytic hydrogenolysis and photolysis, respectively. In the literature, there are only three examples of carboxylic acid protective groups cleavable under mildly basic conditions, the pentafluorophenyl, the succinimidyl and the fluorenyl esters.[142-146]

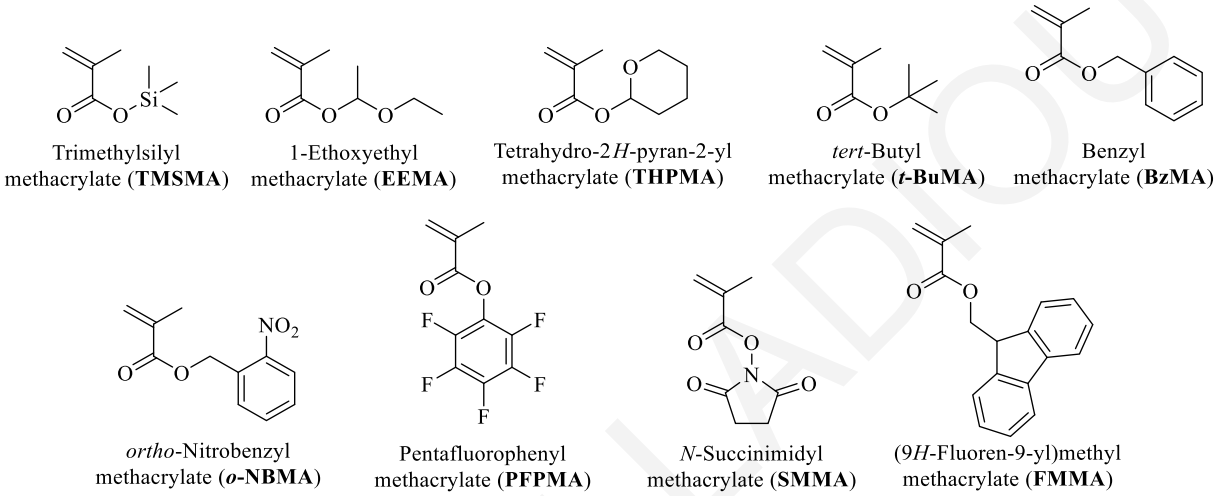

Figure 1.5 Chemical structures and names of protected forms of the MAA monomer.

The units of the polymerized commercially available TMSMA can be converted to MAA units by methanolysis or hydrolysis with or without mild acid catalysis.[129,130] THPMA units can be smoothly converted to MAA units by heating at 130 ºC under vacuum for several hours, or under acidic hydrolysis conditions using HCl at room temperature for a few hours.[130-133] EEMA units can be easily deprotected by thermolysis, without the need for a time-consuming purification step.[134] EEMA units can be alternatively deprotected at lower temperatures under acid-catalyzed conditions.[135] The *t*-butyl protective group can be easily removed via acid-catalyzed processes, in the presence [147] or absence of water.[148] The *t*-butyl group can also be removed thermally.[149] BzMA units can be converted to MAA units after catalytic hydrogenolysis using a palladium catalyst on charcoal at room temperature. The *o*-NBMA group can be cleaved to MAA units and *o*-nitrobenzaldehyde when exposed to 300 – 365 nm light. The monomer repeating units of PFPMA, FMMA and *N*-hydroxysuccinimide esters can be converted to MAA units after treatment with excess primary amine, alcohol or base, respectively.

1.5 Degradable Polymers

The central theme in this PhD Thesis is the preparation and study of degradable polymers, with the degradation observedin the main chain or in the side-group of the monomer repeating unit, or in the residues of the cross-linker, the bifunctional initiator or the inimer. Thus, this section briefly reviews literature on degradable polymers.

Degradable polymers have acquired a prominent position within polymer science in the last decades because of their ability to undergo a reduction in their molecular weight which can be exploited in a number of important applications.[150] These applications include use in microelectronics as the polymeric material for microlithography,[151-155] in waste management as packaging material,[156-159] and in medicine as matrices for controlled drug release [160-166] or absorbable surgical implants, artificial skin and bone grafts.[167-173] It should be noted that the controlled release technology can also be used in the agricultural and cosmetic industries.[174,175]

Degradable polymers comprise at least one degradable component, the monomer, the cross-linker, the initiator or the inimer. Although degradable monomers are the most common components of degradable polymers, degradable cross-linkers have also been incorporated in polymers leading to the formation of degradable branches, whose cleavage results in less branched, even linear, polymers. Degradable (mostly bifunctional) initiators have also been used for the preparation of degradable polymers. Upon their degradation, these polymers are cut into two equal parts (when the degradable initiator used is bifunctional), and the two terminal points of scission are endowed with functional groups. Finally, degradable polymers can also be synthesized using degradable *inimers*, which act both as *ini*-tiators and mono-*mers*.

1.5.1 Degradable Monomers. The most common degradable polymers are based on degradable monomer repeating units, such as polymers of aliphatic esters poly(ε-caprolactone), poly(α-hydroxyacids), poly(anhydrides), and poly(orthoesters).[176-181]

1.5.2 Degradable Cross-linkers. There is a variety of degradable polymers prepared using degradable cross-linkers. Most of these cross-linkers are acid-degradable, based on acetal di(meth)acrylates and diacrylamides,[182-195] hemiacetal ester dimethacrylates,[196,197] ketal di(meth)acrylates, diacrylamides, or di(*N*-vinylformamides),[198-205] silyl ether di(meth)acrylates,[206,207] and tertiary ester di(meth)acrylates.[208-212] One rare example of cross-linker spontaneously degradable under alkaline hydrolysis conditions is

tetrafluorophenylene diacrylate,[213] which is, however, very costly to prepare because the perfluorinated aromatic ring component is very expensive. Other cross-linkers, also sensitive to alkaline hydrolysis conditions, but degrading at much slower rates, include a trithiocarbonate di(meth)acrylate (aminolyzable too),[214,215] a carbonate dimethacrylate (cleavable at a slightly alkaline pH),[216,217] a dilactone dimethacrylate,[218] 1,1-ethylene diol (acylal) dimethacrylate,[125,219] (small molecule labile to alkaline conditions, but not after polymerization! however, readily thermolyzable), methacrylic anhydride,[220] and aliphatic ester dimethacrylates.[221-223] Figure 1.6 shows the main degradable groups incorporated in labile cross-linkers.

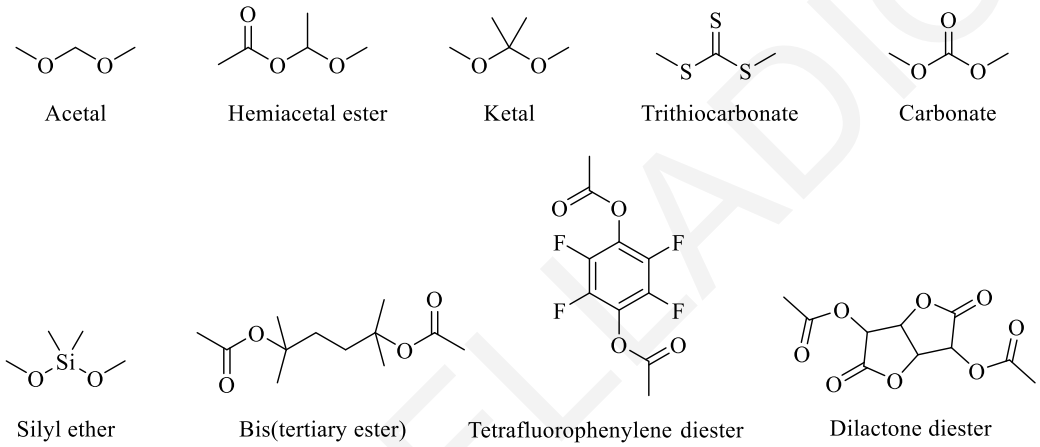

Figure 1.6 Chemical structures of labile groups in main degradable cross-linkers.

1.5.3 Degradable Initiators. Although the majority of degradable polymers are primarily based on degradable monomers, and, secondarily, on degradable cross-linkers, a small number of degradable polymers are based on degradable bifunctional initiators.[224] These polymers have the important property of degradability at a precise location in the polymer chain, and, namely in the middle of the chain. Thus, degradation of the initiator fragment in the polymer leads to the reduction of the initial polymer molecular weight exactly by a factor of two. Furthermore, functional polymer end-groups are formed at the location of the cleavage. These degradable initiators concern controlled/living polymerization methods, most recently controlled radical polymerization methods, i.e., ATRP,[225-228] NMP,[229] and RAFT polymerization,[230-233] although earlier examples of degradable bifunctional initiators were suitable for GTP,[234-239] and ring opening polymerization (ROP).[240,241]

Figure 1.7 illustrates the labile groups employed in degradable bifunctional initiators. These initiators contain the reducible disulfide group,[242-247] the hydrolyzable hemiacetal

ester group,[248-252] the ozonolyzable olefinic group,[253] the thermoreversible Diels-Alder group,[254] the photocleavable *o*-nitrobenzyl ester group,[140,255-256] and the aminolyzable trithiocarbonate group.[257]

The most common degradable bifunctional initiator contains the disulfide group which can be cleaved reversibly using a thiol as a reducing agent, or irreversibly using performic acid where the disulfide bond is converted to the corresponding sulfonic acid.[246] Tsarevsky and Matyjaszewski [245] reported the synthesis of well-defined degradable linear polymethacrylates with an internal degradable disulfide bond. The hemiacetal ester group can be cleaved under acidic hydrolysis conditions. Patrickios and co-workers [249,250] reported the synthesis of cleavable well-defined MMA homopolymer end-linked networks and amphiphilic end-linked co-networks using GTP initiated by a hydrolyzable hemiacetal ester-containing bifunctional initiator, which were degraded in dilute mineral acid, yielding carboxylic acid end-fuctinalized star polymers. Olefinic groups can be oxidized with a large number of oxidizing agents, e.g., ozone, yielding a carbonyl compound.[253] Koberstein and co-workers reported the use of a bifunctional initiator bearing in the middle an olefinic group, for the ATRP synthesis of linear polymers of *tert*-butyl acrylate (*t*-BuA), which were then end-linked using a cross-linker, yielding model polymer networks with well-defined functionalities at the cross-linking nodes. The olefinic group in the middle of each linear polymer chain in these networks was ozonolyzed, converting the swollen networks to star polymer solutions.[253]

The Diels–Alder adduct, known for its thermal reversibility, can also be used in bifunctional initiators. Hadletton and co-workers [254] reported the synthesis of a bifunctional ATRP initiator bearing Diels-Alder adduct, which was used for the synthesis of linear MMA homopolymers. The presence of the Diels-Alder adduct in the middle of the polymer chains allowed for their temperature-modulated reversible cleavage, by heating at high temperature, while it is regenerated by heating at lower temperature. Trithiocarbonates and dithioesters can be readily cleaved to thiols using primary amines, and can, therefore, also be incorporated as the labile groups in degradable initiators. Liu and co-workers [257] reported the use of a symmetrical bifunctional macroCTA (chain transfer agent for RAFT polymerization) bearing a symmetrical trithiocarbonate group in the middle of the CTA for the controlled RAFT polymerization of *N*-isopropylacrylamide (NIPAAm), to obtain dendritic-linear-dendritic triblock copolymers, which after aminolysis, gave dendritic-linear diblock copolymers with half the molecular weight of the parent ABA triblock copolymer. The *ortho*-nitrobenzyl ester group undergoes

photocleavage upon irradiation with UV-light with high efficiency to produce *ortho*-nitrosobenzaldehyde and a carboxylic acid. Koberstein [256] introduced a photocleavable *ortho*-nitrobenzyl ester group to an ATRP bifunctional initiator, and used for the preparation of linear *t*-BuA homopolymer. The parent linear *t*-BuA homopolymer was used for the preparation of model networks, which was degraded upon exposure to UV light of 350 nm to yield four-armed star polymers.

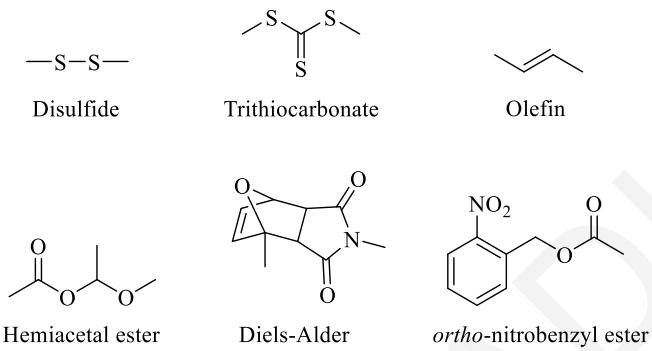

Figure 1.7 Chemical structures of labile groups used in degradable bifunctional initiators.

1.5.4 Degradable Inimers. Several degradable polymers based on degradable inimers have recently been reported. As already mentioned, an *inimer* can act both as *ini*-tiator and as mono-*mer*, containing both a functional initiating group and a polymerizable group, respectively. An advantage of using *inimers* in a controlled polymerization is the facile, one-step synthesis of hyperbranched polymers, in contrast to dendrimers, whose synthesis is difficult because it requires multiple reaction and purification steps. As already noted, SCVP has been applied in ATRP,[73-88] RAFT polymerization,[89-93] photopolymerization,[94] nitroxide-mediated radical polymerization (NMRP),[64, 258] living anionic polymerization,[97] and GTP.[98-100]

Despite the availability of numerous non-degradable *inimers* for SCVP-ATRP, there is only a limited number of reported degradable counterparts.[83-88] First, Matyjaszewski et al.[83] reported the synthesis of two degradable ATRP inimers, the one containing a degradable ester group, (2-(2′-bromopropionyloxy)ethyl acrylate), and the other bearing a degradable disulfide group, (2-(2′-bromoisobutyryloxy)ethyl 2′′-methacryloyloxyethyl disulfide). These inimers were copolymerized with styrene and methyl methacrylate (MMA), respectively. The hyperbranched polymers derived from the ester-type inimer were hydrolytically degradable under basic conditions, whereas those derived from the disulfide-containing inimer could be efficiently degraded in the presence of reducing agents. Since, numerous degradable hyperbranched polymers were synthesized using the

latter labile ATRP inimer.[84,85] Subsequently, Rikkou et al.[86] reported the synthesis of a novel degradable inimer for SCVP-ATRP bearing a thermolyzable acylal group and its copolymerization with MMA. Afterward, Gao et al.[87] also reported the synthesis of a degradable inimer bearing an acid-labile acetal group, and, finally, Sumerlin et al.[88] reported the synthesis of hyperbranched MMA homopolymers using the thermally reversible Diels-Alder adduct ATRP-inimer. Figure 1.8 shows the chemical structures of the degradable inimers described above, as well as the chemical structure of a degradable inimer for NMRP and one for RAFT polymerization, bearing the reversibly thermolyzable nitroxide group[64] and the aminolyzable dithiobenzoate group,[91] respectively.

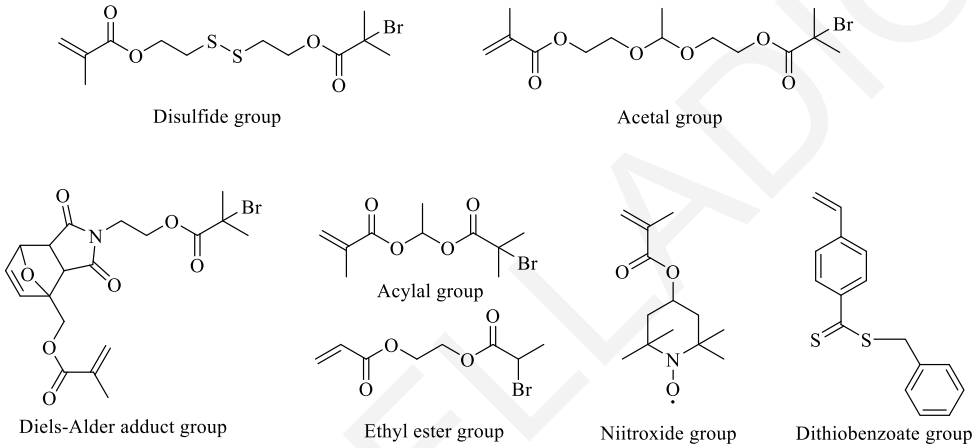

Figure 1.8 Chemical structures of various degradable inimers.

1.6 Polymer Synthesis and Characterization

1.6.1 Polymerization Methods. During the last 3-4 decades, a large research effort in Polymer Science was directed toward the development of new controlled or "living" polymerization methods, allowing the preparation of polymers with controlled molecular weight and narrow molecular weight distribution. "Living" polymerization methods are those in which the active polymerization centers in the polymer chains remain active even after the completion of the polymerization, allowing for the polymerization of a second, newly-added monomer. Since polymers prepared by such methods contain one initiator residue per polymer chain, the degree of polymerization (DP) can be calculated as the ratio of the monomer molar concentration divided by the initiator molar concentration.

In this PhD Thesis, three controlled polymerization methods were employed: group transfer polymerization (GTP),[234,237] reversible addition-fragmentation chain transfer (RAFT) polymerization.,[230,233] and atom transfer radical polymerization (ATRP).[225,227]

1.6.1.1 Group Transfer Polymerization (GTP). Group transfer polymerization (GTP) was announced in 1979 by Webster and co-workers at the DuPont Central Research and Development Laboratories in Wilmington, Delaware, USA, as a method for the controlled synthesis of acrylic block copolymers, and was published later, in 1983.[234] GTP can operate in a broad temperature range, from −100 °C to +100 °C, which, importantly, includes room temperature. GTP uses a trimethylsilyl ketene acetal initiator whose activation is catalyzed by nucleophilic anions. Recent studies indicated that *N*-heterocyclic carbenes can also be employed as catalysts for initiator activation, allowing now the controlled polymerization of acrylamides too.[259] Initial GTP mechanism studies in the 1980's pointed out that the trimethylsilyl group was covalently transferring to the monomer as it was adding to the polymer chain ends and the technique was, therefore, named group transfer polymerization. This mechanism now appears to be incorrect, but the name remained. Even today, the GTP mechanism has not been completely elucidated. However, two are the prevailing mechanistic routes for the GTP process, the dissociative pathway and the associative pathway. The former route involves the cleavage of the initiator unit, while the latter does not require this cleavage. Figure 1.9 shows the dissociative mechanism which is believed to be the most probable.

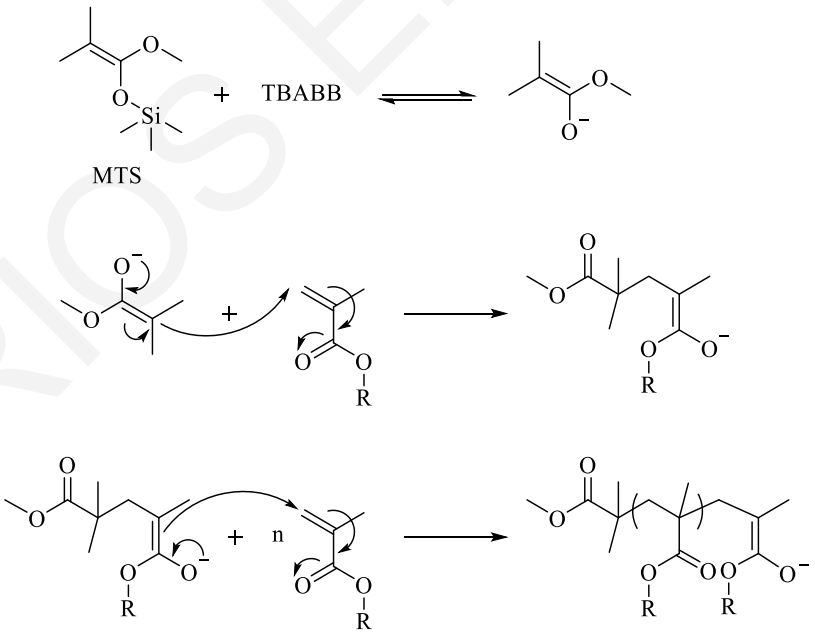

Figure 1.9 Steps involved in the dissociative mechanism of group transfer polymerization (GTP).[234]

GTP presents several important advantages:

1. Simple and fast polymerization method, requiring only 5 – 15 min for each polymerization step.

2. Quantitative monomer conversion to polymer.
3. Wide temperature range (−100 to 100 °C).
4. Narrow molecular weight distribution and controlled DP of the produced polymers.
5. Capability for preparation of block copolymers.
6. Capability for preparation of polymers with various architectures.

From the above-mentioned advantages, number 1 and number 3 stand out. Regarding number 1, other controlled / living polymerization methods require from a few hours to 1-2 days. Regarding number 3, GTP can readily take place at room temperature whereas other controlled / living polymerization methods require either very low temperatures (living anionic polymerization, −78 °C) or temperatures, above room temperature (controlled radical polymerization, ~70 °C)

GTP also presents some disadvantages:

1. Polymers with relatively low molecular weight and, therefore, low DP.
2. Applicable for the polymerization of only specific types of monomers, acrylates and methacrylates, and, more recently, acrylamides and methacrylamides (when *N*-heterocyclic carbenes are used as polymerization catalysts), whose chemical structures are shown in Figure 1.10. The important class of styrenic monomers cannot be polymerized by GTP.

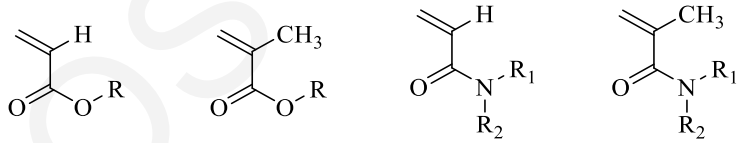

Figure 1.10 Chemical structures of (meth)acrylate and (meth)acrylamide monomers, appropriate for GTP.

Similar to classical anionic polymerization, GTP is terminated in the presence of compounds bearing acidic protons which irreversibly neutralize the enolate active polymerization sites of GTP. Thus, polymerization must take place in aprotic organic solvents, which should be completely dry to avoid termination reactions.[108] Similarly, the *R* group in the monomers must also be aprotic, such as hydrocarbon-based (aliphatic or aromatic) or tertiary amine, with groups bearing free carboxylic acids, alcohols or phenols not being allowed. Monomers carrying such acidic groups may be polymerized by GTP only after appropriate protection.

1.6.1.2 Reversible Addition-Fragmentation chain Transfer (RAFT) Polymerization. RAFT polymerization was reported in 1995 by Moad et al.[230] RAFT polymerization can be employed for the polymerization of almost all types of vinylic monomers, and it tolerates many functional groups in the side chain, without the necessity for protection.[74,232] RAFT polymerization can also be applied in a variety of reaction configurations (in solution, emulsion or bulk), and a range of temperatures, from 20 up to 150 ºC.[232,261] RAFT polymerization can produce polymers with different structures, with controlled molecular weight (linear relationship between the molecular weight of the polymer and the conversion of monomer to polymer) and relatively narrow molecular weight distribution.

RAFT polymerization is a "living" radical polymerization method. The "living" character of this method is secured *via* the use of dithioester or trithiocarbonate compounds, which act as chain transfer agents (CTA) *via* a reversible addition-fragmentation reaction. Figure 1.11 shows the general chemical structure of the CTA used in RAFT polymerization, whose ability for chain transfer depends on the nature of its Z and R groups, to activate the C=S bond of the CTA in order to initiate and propagate the polymerization. RAFT polymerization involves a reversible-fragmentation sequence in which the transfer of the S=C(Z)S- moiety between active and dormant chains serves to maintain the living character of the polymerization.

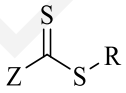

Figure 1.11 General chemical structure of the dithioester chain transfer agent (CTA) necessary in RAFT polymerization.

Figure 1.12 presents the mechanism of RAFT polymerization. The first stage in RAFT polymerization is initiation *via* the cleavage of the initiator to two similar radical fragments (**I•**) each added to a single monomer molecule to yield a propagating polymeric radical of length 1, P_1•. P_1• can be repeatedly added to monomer, M, forming a longer propagating radical, P_n•. P_n• reacts with the CTA to form a RAFT adduct radical, which may undergo a fragmentation reaction in either direction to yield either the starting species or a radical (R•) plus a polymeric R RAFT agent S=C(Z)S-P_n. This is a reversible step in which the intermediate RAFT adduct radical is capable of losing either the R group (R•) or the polymeric species (P_n•). The leaving group radical (R•) then reacts with another monomer species, starting another active polymer chain. Equilibration is the most important part in the RAFT process, in which, by a process of rapid interchange, an equilibrium is achieved between P_n• and P_m•, allowing the two polymer chains equal opportunities for growth.

Finally, termination can occur through a biradical termination reaction between two active polymer chains, P_n• and P_m•, forming P_{n+m}, or through a recombination and the formation of P_n with an extra hydrogen atom and P_m with one double bond at the end of the polymer chain.

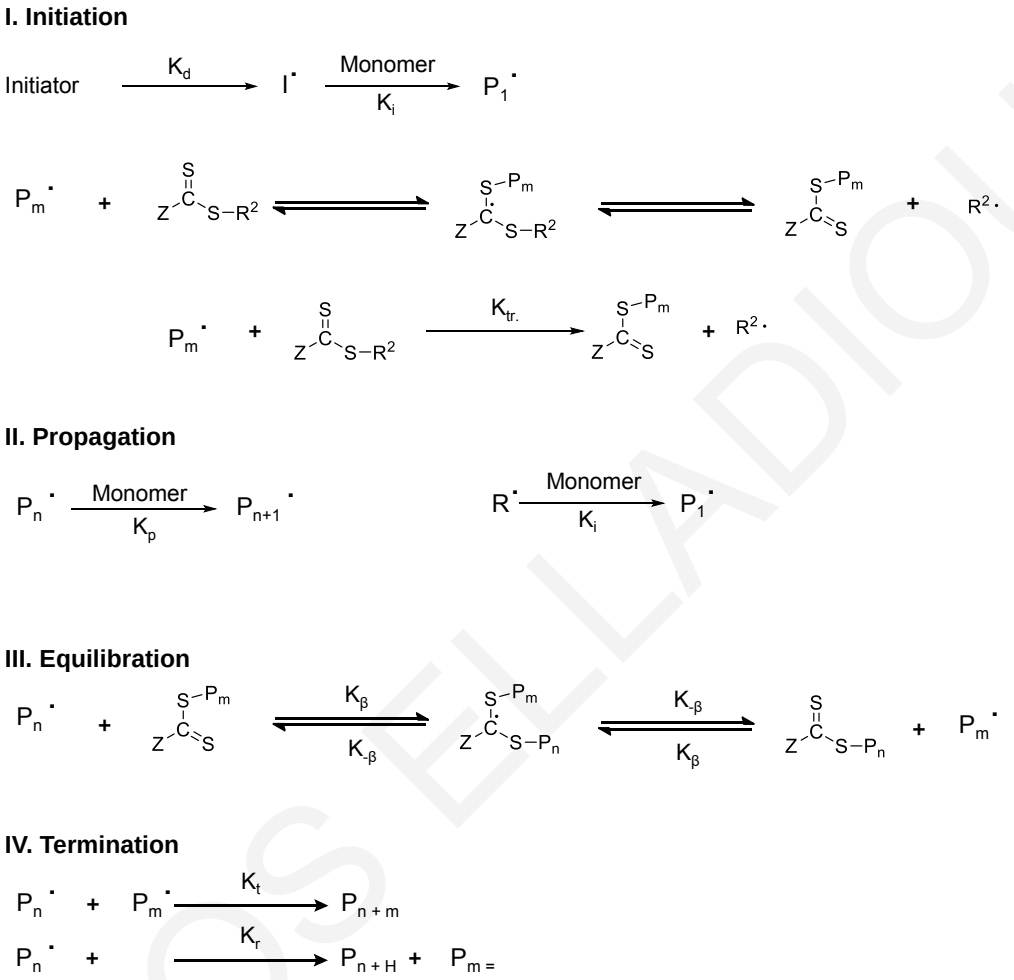

Figure 1.12 Steps and mechanism of reversible addition-fragmentation chain transfer (RAFT) polymerization.[230]

1.6.1.3 Atom Transfer Radical Polymerization (ATRP). Similar to atom transfer radical addition (ATRA), ATRP [225,227] is a polymerization method that involves the carbon-carbon couplings using a transition metal catalyst through reversible-deactivation radical polymerization. ATRP usually employs a transition metal (Mt^n) of a low oxidative state as the catalyst and an alkyl halide (R-X) as the initiator, forming a transition metal complex at a higher oxidative state (Mt^{n+1}) and a radical fragment (R•) which is added to the double bond of a monomer, forming RM•. The RM• species then takes back the halogen from the metal complex, regenerating the metal catalyst at its lower oxidative state (Mt^n). ATRP also employs a ligand which may cause a reversible equilibrium between the active

radicals of the polymer chains and the inactive polymer chains, and also has a key role in the metal dissolution.

Figure 1.13 presents the mechanism of ATRP. The first stage is the initiation of the polymerization, involving the oxidation reaction of the catalyst and the reduction of the initiator forming a radical (R•) which can react with a monomer to yield a propagating polymeric radical (RM•). RM• can then react reversibly with the metal complex to form RMCl and regenerate the catalyst at its lower oxidation state. In the propagation step, there is a reversible equilibrium reaction between the metal complex plus the polymer chain on the one hand, with the free radical polymer chain (which can react with monomer molecules for propagation of the polymerization) plus the metal complex at the higher oxidation state, on the other hand. Like RAFT polymerization termination, ATRP termination can occur through a biradical termination reaction. Controlled polymerization in ATRP is achieved by establishing a dynamic equilibrium between the propagating and dormant species with copper complexes acting as a reversible halogen atom transfer agent. As a result, the concentration of the propagating species is greatly lowered, and, therefore, slowing down of the termination reaction.[228,262]

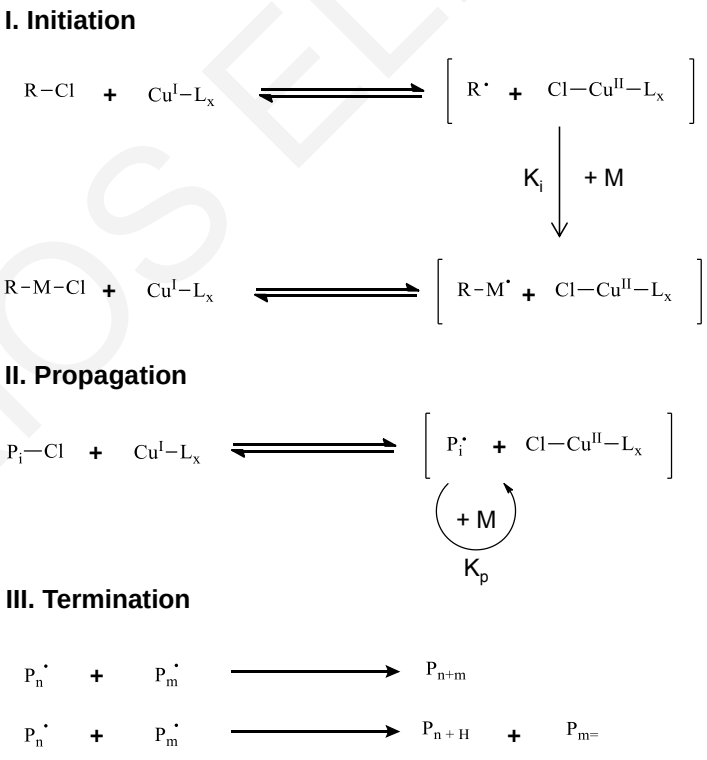

Figure 1.13 Steps and mechanism of atom transfer radical polymerization (ATRP).[227]

1.6.2 Polymer Characterization Methods.

1.6.2.1 Gel Permeation Chromatography (GPC). Gel permeation chromatography (GPC) or size exclusion chromatography (SEC) [263] is a type of high pressure liquid chromatography (HPLC), most appropriate for characterizing the molecular weight and the molecular weight distribution of a polymer, which are its most fundamental size characteristics. GPC is based on the principle of size exclusion, hence the name size exclusion chromatography. Historically, the porous medium in the GPC column was made of a gel and, therefore, the name gel permeation chromatography was also coined.

A GPC/SEC instrument consists of a pump to force the solvent through the column, an injection port to introduce the sample into the column, a column to hold the stationary phase, a detector to detect the components as they are eluted from the column, and software to control the different parts of the instrument and calculate and display the results. The polymer sample is first dissolved in a solvent.

GPC employs a stagnant liquid present in the pores of the porous beads constitute the stationary phase (silica or polymer network), and a flowing liquid as the mobile phase. The mobile phase can, therefore, flow between the beads and also in and out of the pores in the beads. The separation mechanism is illustrated schematically in Figure 1.14, and is based on the size of the polymer molecules in solution (hydrodynamic volume). The smaller analytes can enter the pores more easily, and, therefore, spend more time in these pores, increasing their retention time. Conversely, larger analytes spend shorter, if any, time in the pores and are eluted quickly. All columns have a range of polymer molecular weights that can be separated.

If an analyte is either too large or too small, it will be either not retained or completely retained, respectively. Analytes that are not retained are eluted with the free volume outside of the particles (V_0), while analytes that are completely retained are eluted with the volume of solvent held in the pores (V_i). The total volume, V_t, can be calculated using the following equation, where V_g is the volume of the polymer gel:

$$V_t = V_g + V_i + V_0$$

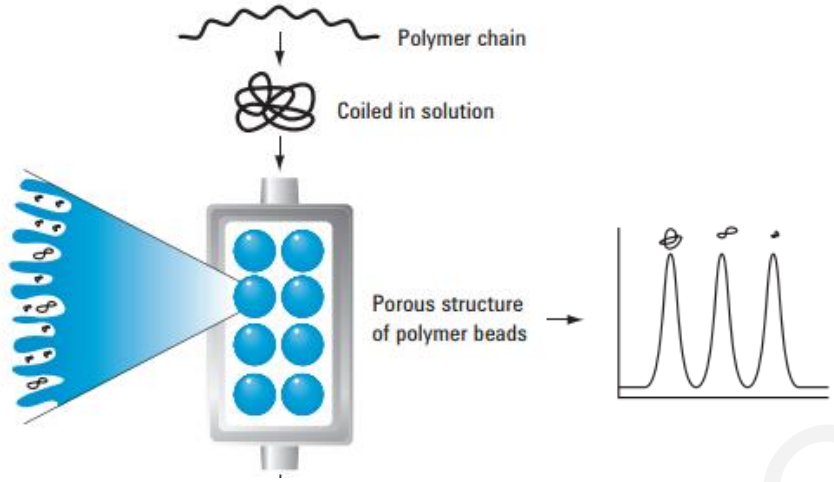

Figure 1.14 Principle of the GPC method. Larger molecules are eluted first, while smaller molecules enter the pores and are eluted last.[263]

GPC can be used to calculate the number-average molecular weight, M_n, the peak molecular weight, M_p, the weight-average molecular weight, M_w, and the molecular weight dispersity ($Đ$). The $Đ$ value is identified as the ratio of M_w/M_n. A $Đ$ value close to 1 implies a narrow molecular weight distribution, with all polymer chains possessing approximately the same size, while a high $Đ$ value means a broad molecular weight distribution. The M_n value calculated from GPC must be compared with the theoretical molecular weight calculated from the monomer to initiator ratio, taking into account monomer to polymer conversion determined using ^{1}H NMR spectroscopy.

1.6.2.2 Nuclear Magnetic Resonance (NMR) Spectroscopy. Nuclear magnetic resonance (NMR) spectroscopy [264] is a powerful and theoretically complex tool, exploiting the magnetic properties of certain atomic nuclei, from which one can determine the chemical and physical properties of the molecules in which they are contained. NMR spectroscopy can help obtain information about the structure, dynamics, reaction state, and chemical environment of molecules. The NMR spectroscopy measurements take place in a strong magnetic field. Figure 1.15 shows the main component parts of an NMR spectrometer. The intramolecular magnetic field around an atom in a molecule changes the resonance frequency, thus giving access to details of the electronic structure of the molecule.

The nucleic spins of a magnetic nucleus are randomly oriented in the absence of a magnetic field, while, when this magnetic nucleus is placed in a strong magnetic field, its nucleic spins acquire specific orientations. A rotatable nucleus (^{13}C, ^{1}H) can acquire these orientations, and its own magnetic field can be oriented either parallel or antiparallel to the external magnetic field. If the nucleus is irradiated with the appropriate frequency of

electromagnetic radiation, the lower energy parallel orientation transforms to a higher energy antiparallel orientation, and, therefore, the nucleus has been resonated, hence the term nuclear magnetic resonance.

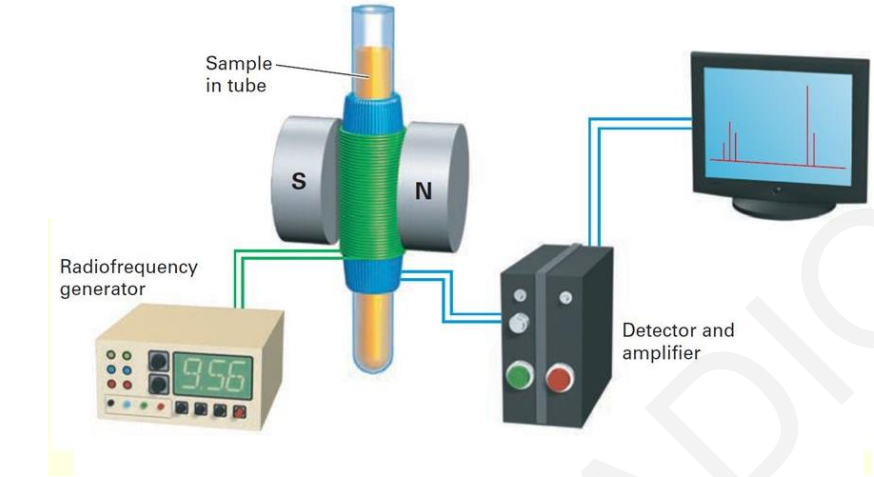

Figure 1.15 Main component parts of an NMR spectrometer.[264]

1.6.2.3 Differential Scanning Calorimetry (DSC). Differential scanning calorimetry is a thermoanalytical technique in which the difference in the amount of heat required to increase the temperature of a sample and the reference is measured as a function of temperature.[265,266] Both the sample and the reference are maintained at nearly the same temperature throughout the experiment as shown in Figure 1.16. Generally, the temperature program for a DSC analysis is designed such that the sample holder temperature increases linearly as a function of time. The reference sample should have a well-defined heat capacity over the range of temperatures to be scanned.

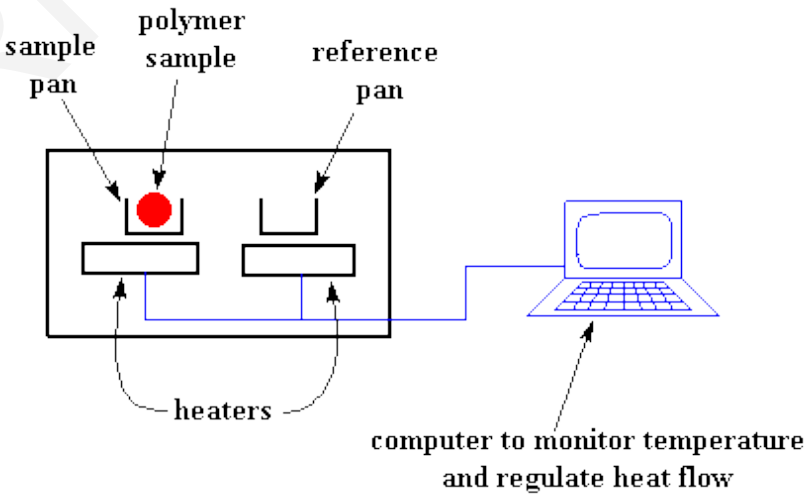

Figure 1.16 Simplified layout of a differential scanning calorimeter with focus on the sample compartment and the heaters.[266]

The basic principle underlying this technique is that, when the sample undergoes a transformation, such as a phase transition or a chemical reaction, more or less heat will need to flow to it than the reference to maintain both at the same temperature. Whether less or more heat must flow to the sample depends on whether the process is exothermic or endothermic, respectively. By observing the difference in heat flow between the sample and the reference, differential scanning calorimeters are able to measure the amount of heat absorbed or released during such transitions. In a DSC measurement, the heat flow q/t of the sample is calculated and compared to the reference. A typical DSC thermogram plots the difference in heat output of the two heaters (y-axis) against temperature (x-axis).

Figure 1.17 displays a typical DSC plot for a semicrystalline polymer. In the Figure, T_g is the glass transition temperature of the polymer, T_c its crystallization temperature, and T_m its melting temperature. The figure shows that the polymer has a higher heat capacity above the T_g than below. The figure also indicates that at T_c, the polymer gives out heat, as crystallization is an exothermic transition. Finally, at higher temperature, the T_m is reached, where the polymer crystals absorb heat and begin to melt. As already mentioned, DSC can also be used to determine not only the physical transformations of a polymer, but also any temperature-induced chemical reactions that may take place.

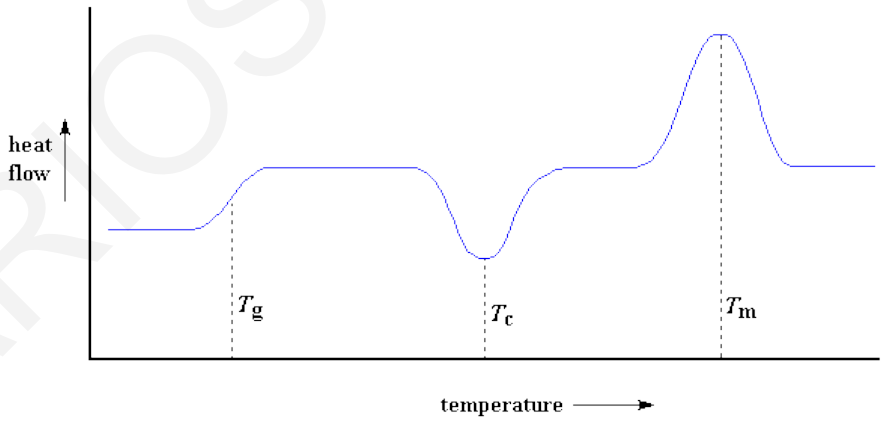

Figure 1.17 Typical DSC plot for a semicrystalline polymer.[266]

1.6.2.4 Thermal Gravimetric Analysis (TGA). Thermal gravimetric analysis (TGA) is a technique which measures the change in the mass of a sample over a range of temperatures.[267] A TGA instrument consists of a sample pan which hangs off a hook and is connected by a microgram balance arm to a tare pan. The basic principle of TGA is that, as a sample is heated, its mass changes. This change can be used to determine the

composition of a material or its thermal stability, up to 1000 ^{o}C. Usually, a sample loses weight as it is heated up due to decomposition or evaporation. A TGA instrument tracks the change in weight of the sample *via* the microgram balance and the temperature is monitored *via* a thermocouple, as displayed in Figure 1.18, usually under an inert atmosphere, to avoid the oxidation from the atmospheric oxygen and moisture. The TGA results are usually plotted with the *y*-axis representing remaining weight percentage and the *x*-axis representing temperature (or time), from which one can determine several characteristics of materials that exhibit either mass loss or gain due to decomposition, chemical reaction, oxidation or loss of volatiles.

Common applications of TGA are (1) materials characterization through analysis of decomposition patterns, (2) studies of degradation mechanisms and reaction kinetics, (3) determination of organic content in a sample, and (4) determination of inorganic (e.g., ash) content in a sample, which may be useful for corroborating predicted material structures or simply used as a chemical analysis. It is an especially useful technique for the study of polymeric materials, including thermoplastics, thermosets, elastomers, composites, plastic films, fibers, coatings and paints.

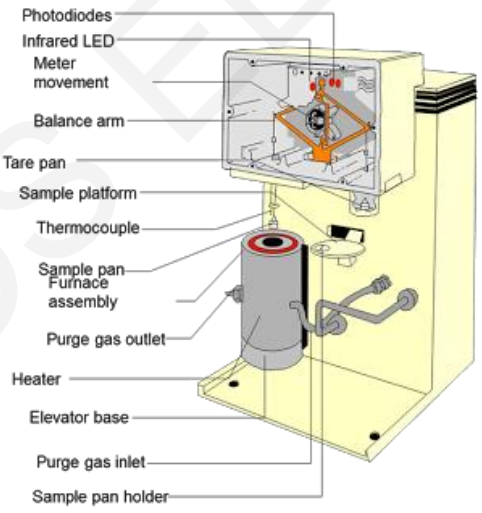

Figure 1.18 Component parts of a thermal gravimetric analyzer.[268]

1.6.2.5 Dynamic Light Scattering (DLS). Dynamic light scattering (DLS) is one of the most popular methods used to determine the average size and size distribution of small particles in suspension or polymers in solution.[269-271] When a monochromatic light beam, such as a laser, hits into a solution with spherical particles in Brownian motion, it causes a Doppler shift, changing the wavelength of the incoming light. This change is related to the size of the particle. Usually, DLS measurements detect the scattered light at 90°. It is

possible to compute the sphere size distribution and give a description of the particle's motion in the medium, by measuring the diffusion coefficient of the particle, using the following two autocorrelation functions:

$$G_1(\tau)= \frac{\langle E_{sc}(t)E^*_{sc}(t+\tau)\rangle}{\langle I_{sc}\rangle} \qquad G_2(\tau)= \frac{\langle I_{sc}(t)\, I_{sc}(t+\tau)\rangle}{\langle I_{sc}\rangle^2} \tag{1.1}$$

where E_{sc} or I_{sc} is the intensity of the scattered light at time t, and the brackets indicate averaging over all t. The autocorrelation function depends on the delay time, τ, that is the time that a duplicate intensity trace is shifted from the original before the averaging is performed. A typical autocorrelation function for a monodisperse sample is shown in Figure 1.19.

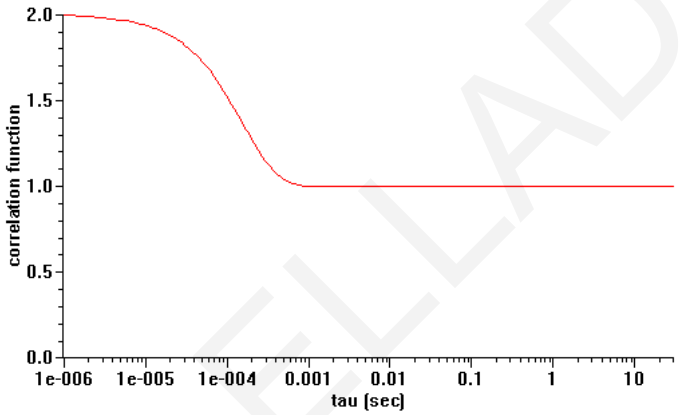

Figure 1.19 Autocorrelation function for a monodisperse sample.[270]

The autocorrelation function for a monodisperse sample can also be analyzed using the equation:

$$G_1(\tau)= B + \beta e^{-2\Gamma\tau} \tag{1.2}$$

where B is the baseline of the correlation function at infinite delay, β is the correlation function amplitude at zero delay, and Γ is the decay rate. Γ can be converted to the diffusion coefficient D *via* the relation:

$$D = \frac{\Gamma}{q^2} \tag{1.3}$$

where q is the magnitude of the scattering vector, and is given by:

$$q = \frac{4\pi n_0}{\lambda_0} \sin\left(\frac{\theta}{2}\right) \tag{1.4}$$

where n_0 is the solvent index of refraction, λ_0 is the vacuum wavelength of the incident light, and θ is the scattering angle.

Finally, the diffusion coefficient can be used to calculate the hydrodynamic radius, R_h, of a diffusing sphere *via* the Stokes-Einstein equation:

$$R_h = \frac{kT}{6\pi\eta D} \tag{1.5}$$

where k is Boltzmann's constant, T is the absolute temperature (in K), and η is the solvent viscosity.

DLS has several advantages. It is a non-destructive method, fast, and needs only small quantities of sample. The most important disadvantage of DLS is its sensitivity to dust and that it works better in dilute solutions.

1.6.2.6 Static Light Scattering (SLS). In contrast to DLS, static light scattering (SLS) measures the average intensity of the scattered light at different scattering angles and different polymer concentrations.[269-271] Using SLS, one can calculate the weight-average molecular weight of a polymer, M_w, the radius of gyration, R_g, and the second virial coefficient, A_2. These relationships are described by Debye theory which states that the molecular weight of a molecule is proportional to the Rayleigh ratio of the scattered light, i.e., the ratio of the intensity of the scattered light divided by the intensity of the incident light.

The most common equation to determine M_w is the Zimm equation:

$$\frac{KC}{R_\theta} \cong \left(\frac{1}{M_w} + 2A_2C\right)\left(1 + \frac{16\pi^2 R_g^2}{3\lambda^2}\sin^2\frac{\theta}{2} - \ldots\right) \tag{1.6}$$

where C is the sample concentration (in g/L), θ is the measurement angle, R_θ is the Rayleigh ratio at the measurement angle θ, while K defined as:

$$K = \frac{4\pi^2}{\lambda_0^4 N_A}\left(n_0\frac{dn}{dc}\right)^2 \tag{1.7}$$

where λ_0 is the wavelength of the incident radiation (laser) in vacuum, N_A is the Avogadro number, n_0 is the refractive index of the solvent, and dn/dc is the refractive index increment of the sample in the given solvent.

The analysis of the static light scattering data involves plotting KC/R_θ as a function of $\sin^2(\theta/2) + C$, from which two extrapolations can be obtained (Zimm plot), as shown Figure 1.20. One is an extrapolation to zero angle to remove the large particle size effect. The other is an extrapolation to zero concentration to remove the effect of non-ideal solutions (interparticle interactions). The slope of the first extrapolation gives the radius of gyration, R_g, whereas the slope of the second extrapolation gives the second virial coefficient, A_2. The intercept of the two extrapolations gives the weight-average molecular weight, M_w.

$$slope_1 = 2A_2 \tag{1.8}$$

$$slope_2 = \frac{16\pi^2 R_g^2}{3\lambda^2} \tag{1.9}$$

$$intercept = \frac{1}{M_w} \tag{1.10}$$

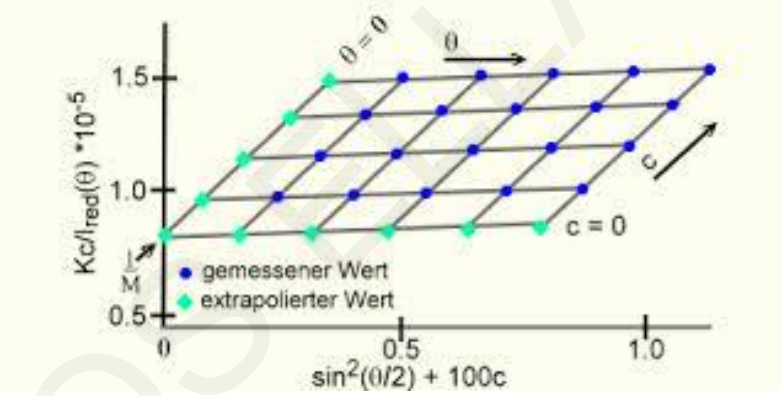

Figure 1.20 Typical Zimm plot. The experimental data points are in blue at the grid intersection points. The points in green along the θ = 0 and the C = 0 lines are extrapolations of the experimental points.[270]

1.6.2.7 Atomic Force Microscopy (AFM). Atomic force microscopy is a powerful characterization tool for polymer science, capable of revealing surface structures with superior spatial resolution.[272,273] The universal character of repulsive forces between the tip and the sample, which are employed for surface analysis in AFM enables examination of even single polymer molecules without disturbance of their integrity. Being initially developed as the analogue of scanning tunneling microscopy (STM) for the high-resolution profiling of non-conducting surfaces, AFM has developed into a multifunctional technique suitable for characterization of topography, adhesion, mechanical, and other properties on scales from tens of microns down to nanometers.[274]

AFM operates by measuring the force between a probe and the sample. Normally, the probe is a sharp tip, which is a 3-6 μm tall pyramid with 15-40 nm end radius. Though the lateral resolution of AFM is low (~20 nm) due to convolution, the vertical resolution can be down to 0.1 nm. To acquire the image resolution, AFM microscopes can generally measure the vertical and lateral deflections of the cantilever using the optical lever. The optical lever operates by reflecting a laser beam off the cantilever. The reflected laser beam strikes a position-sensitive photo-detector consisting of a four-segment photo-detector. The differences between the segments of the photo-detector signals indicate the position of the laser spot on the detector and, therefore, the angular deflections of the cantilever, as shown in Figure 1.21.

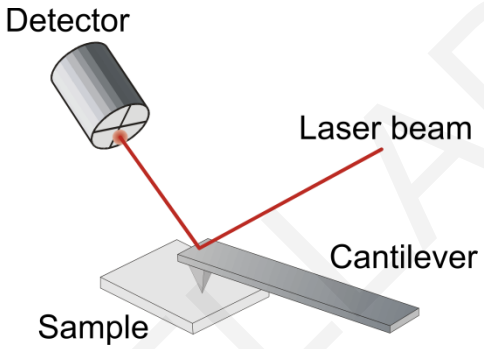

Figure 1.21 Main component parts of the detection system of an atomic force microscope.[273]

Piezo-ceramics position the tip with high resolution. Piezoelectric ceramics are a class of materials that expand or contract when located in a voltage gradient. Piezo-ceramics make it possible to create three-dimensional positioning devices of arbitrarily high precision. In contact mode, AFM microscopes use feedback to regulate the force on the sample. Thus, these microscopes not only measure the force on the sample but also regulate it, allowing acquisition of images at very low forces. The feedback loop usually consists of the tube scanner that controls the height of the tip, the cantilever and optical lever, which measures the local height of the sample, and a feedback circuit that attempts to keep the cantilever deflection constant by adjusting the voltage applied to the scanner.

1.7 Preview of Results

This work deals with the synthesis of polymers bearing pyridine, introduced through an alcohol (becoming the side group of a monomer) or a diol (becoming the middle part of a cross-linker, a bifunctional initiator or inimer) and the study of their thermal and hydrolytic lability under alkaline and acidic hydrolysis conditions. The monomers were homologues

with the pyridine nitrogen located in different positions in the pyridine ring, and / or different lengths of the spacer between the ester moiety and the pyridine ring. The polymerizations were pursued *via* one of three different controlled polymerization methods, GTP, RAFT polymerization and ATRP. The placement of the pyridine moieties as side groups of polymers confers upon them various properties, both physical and chemical.

In total, nine pyridinylalkyl methacrylate homologues were synthesized, differing in the length of the spacer (from methyl to propyl) between the ester moiety and the pyridine ring or/and in the position of the nitrogen atom in the pyridine ring (2-, 3- or 4-pyridine). These nine monomers were polymerized to obtain the corresponding homopolymers. All homopolymers were stable under acidic hydrolysis conditions, but presented partial or complete lability under alkaline hydrolysis conditions or thermally, as manifested by the cleavage of the pyridinylalkyl side-group. Alkaline hydrolysis fully converted the three isomeric poly(pyridinylethyl methacrylate) (polyPyEMA) homologues to polyMAA and the corresponding vinylpyridines, while it caused only partial cleavage in the other six homologues even after 2 weeks of reaction. However, thermal treatment converted to polyMAA and the corresponding vinylpyridines only the poly(2-(pyridin-2-yl)ethyl methacrylate) (poly2PyEMA) and poly(2-(pyridin-4-yl)ethyl methacrylate) (poly4PyEMA) isomeric homologues at around 200 ºC, but did not affect the poly(2-(pyridin-3-yl)ethyl methacrylate) (poly3PyEMA) isomeric homologue which was thermally stable. Additionally, some related polymers, poly(2-phenylethyl methacrylate) (p2PheMA), poly[9*H*-fluoren-9-yl)methyl methacrylate] (pFMMA), poly[*N*-(2-(pyridin-2-yl)ethyl) methacrylamide] (p2PyEMAAm), poly[*S*-(2-(pyridin-2-yl)ethyl) methacrylthioate] (p2PyESMA), poly[2-((pyridin-2-yl)2-methyl)ethyl methacrylate] (p2PyEmeMA) and poly[2-((pyridin-2-yl)2,2-dimethyl)ethyl methacrylate] (p2PyEdimeMA) were also synthesized. These polymers were also subjected to thermolysis or acidic or alkaline hydrolysis conditions, presenting stability after acidic hydrolysis treatment, but none, partial or complete lability under alkaline hydrolysis conditions or thermally. The thioester p2PyESMA presented similar lability under alkaline hydrolysis conditions or thermally to that of p2PyEMA, while the amide p2PyEMAAm was stable. P2PheMA and pFMMA were thermally stable up to ~300 ºC and presented partial and complete cleavage under alkaline hydrolysis conditions, respectively. Finally, p2PyEmeMA was partially cleaved under alkaline hydrolysis conditions and was slightly thermally more stable than p2PyEMA, while p2PyEdimeMA was stable under these conditions.

An interesting result from the above observations was the lability of the 2PyEMA units under alkaline hydrolysis conditions or thermally, at or above 110 ºC in bulk or in solution, while it was stable under acidic hydrolysis conditions and resisted catalytic hydrogenolysis.[275] Therefore, 2-(pyridin-2-yl)ethanol can be employed as a good protective group for MAA units. Most of the (meth)acrylic acid protective groups in synthetic polymers are acid labile, and are stable under alkaline hydrolysis conditions.[276] Thus, the developed 2-(pyridin-2-yl)ethyl moiety emerges as a rare protective group that can be removed under alkaline hydrolysis conditions.

2PyEMA was then terpolymerized with the acid-labile tetrahydro-2*H*-pyran-2-yl methacrylate (THPMA) and the hydrogenolyzable benzyl methacrylate (BzMA) to yield two ABC triblock terpolymers. One of the terpolymers was prepared by RAFT polymerization and the other by GTP.[277] Subsequently, the two ABC triblock terpolymers were sequentially subjected to conditions of alkaline hydrolysis, acidic hydrolysis and catalytic hydrogenolysis, leading to the selective cleavage of the 2PyEMA, the THPMA and the BzMA units, respectively. Similarly selective was the acidic hydrolysis followed by alkaline hydrolysis.

Furthermore, 2PyEMA was also randomly terpolymerized with one of the lower homologous, (pyridin-2-yl)methyl methacrylate (2PyMMA) which was thermally stable up to 300 °C and presented partial alkaline hydrolysis at room temperature, and a dimethacrylate cross-linker, ethylene glycol dimethacrylate (EGDMA).[278] Using RAFT polymerization, three randomly cross-linked networks, with different molar ratios of the weakly basic 2PyEMA and 2PyMMA units, were prepared. Upon thermal treatment, the 2PyEMA units were converted to MAA units. Thus, the double-cationic polyelectrolyte networks were converted to polyampholyte hydrogels. While the parent double-cationic polyelectrolyte hydrogels exhibited a swelling response only to low-pH conditions, the daughter polyampholyte hydrogels presented swelling responses to both high and low pH conditions. Owing to the relative values of the effective pK_a's of the weakly acidic and weakly basic units, with the latter being lower than the former ("inverse polyampholyte" behavior), the swelling profiles of the daughter hydrogels were insensitive to polyampholyte composition.

As already mentioned, the ester of 2-pyridineethanol is a good protective group for MAA units. As a subsequent step, we extended the idea of mono-substituted ester to a di-substituted ester, going from a protected monomer to a degradable cross-linker, 2,6-

pyridinediethanol dimethacrylate, PyDMA, bearing two labile 2-(pyridin-2-yl)ethyl ester groups.[279] PyDMA was synthesized by the esterification of 2,6-pyridinediethanol with a slight excess of methacryloyl chloride. Given the lability of the 2PyEMA monomer units, the resulting PyDMA cross-linker units would also be cleavable thermally or under alkaline hydrolysis conditions. This latter property is rare among labile cross-linkers, as most cleavable dimethacrylates break under acidic hydrolysis conditions. Hyperbranched (co)polymers and (co)polymer networks obtained *via* the RAFT polymerization of the PyDMA cross-linker were shown to be cleavable both thermally (either in the bulk or in solution) and under alkaline hydrolysis conditions at room temperature, resulting in the expected linear degradation polymeric products.

We also designed, synthesized and used a new bifunctional ATRP initiator, 2,6-pyridinediethanol di(2-bromo-2-methyl propanoate), PyDEDBrMeP.[280] PyDEDBrMeP was synthesized by the esterification of 2,6-pyridinediethanol with excess *α*-bromoisobutyrylbromide. The bifunctional PyDEDBrMeP ATRP initiator also bears two labile 2-(pyridin-2-yl)ethyl ester groups and, it was, therefore, cleaved either under alkaline hydrolysis conditions or thermally. This is the first example of a bifunctional ATRP initiator readily degradable under alkaline hydrolysis conditions. Additionally, the more stable ATRP initiator, 2,6-pyridinedimethanol di(2-bromo-2-methyl propanoate) (PyDMDBrMeP), was also synthesized, bearing two more stable (pyridin-2-yl)methyl ester groups. PyDEDBrMeP and PyDMDBrMeP were separately used for the preparation of linear homopolymers of methyl methacrylate (MMA), linear amphiphilic ABA and BAB triblock copolymers of 2-(dimethylamino)ethyl methacrylate (DMAEMA) and MMA, and end-linked homopolymer networks of MMA. After the characterization of their molecular weights, these polymers were subjected to alkaline hydrolysis and thermolysis conditions and the products obtained were characterized also in terms of their molecular weights to determine the degree of cleavage of the parent polymers. In the case of the polymers prepared using PyDEDBrMeP, thermal or hydrolytic treatment led to a reduction of the molecular weights of the linear polymers by a factor of two, and to the conversion of the polymer networks to soluble branched (star) structures, consistent with the expected cleavage of the initiator residue located in the middle of the polymer chain. In the case of the polymers prepared using PyDMDBrMeP, thermal treatment did not affect the initiator residue due to the thermal stability of the (pyridin-2-yl)methyl ester group, while treatment under alkaline hydrolysis conditions resulted in a reduction of the molecular weights of the linear polymers by a factor of two and to the conversion of the polymer networks to

soluble star polymers, indicating the hydrolytic lability of (pyridin-2-yl)methyl esters as well.

Amphiphilic ABA and BAB triblock copolymers prepared using these two bifunctional initiators, composed of the hydrophilic DMAEMA and the MMA, formed spherical micelles in water. After treatment by alkaline hydrolysis, ABA and BAB triblock copolymers prepared using both bifunctional initiators, again formed spherical micelles in water of the same size as their untreated counterparts.

The labile under alkaline hydrolysis and thermolysis conditions bifunctional ATRP initiator, PyDEDBrMeP, and cross-linker, PyDMA, were conceptually combined to obtain a degradable ATRP *inimer*, 2-(6-(2-((2-bromo-2-methylpropanoyl)oxy)ethyl)pyridin-2-yl)ethyl methacrylate (PyDEBrMA),[281] which can act both as *ini*tiator and mono*mer*. The synthesis of the cleavable *inimer* PyDEBrMA was achieved by the two-step esterification of 2,6-pyridinediethanol, first with α-bromoisobutyryl bromide in order to introduce the initiator moiety, and then with methacryloyl chloride in order to introduce the monomer moiety. PyDEBrMA was used for the preparation of three hyperbranched MMA homopolymers with different MMA to inimer molar ratios, 50, 100 and 200, using self-condensing vinyl polymerization (SCVP) ATRP. Furthermore, three hyperbranched amphiphilic diblock copolymers were also synthesized using as macroinitiator the smallest hyperbranched MMA homopolymer (hydrophobic core) and hydrophilic DMAEMA at three loadings, yielding copolymers with DMAEMA contents of 25, 50 and 75 mol%. Alkaline hydrolysis, using sodium deuteroxide in d_6-DMSO, or thermolysis, at or above 130 °C, of these polymeric materials, led to a reduction in their molecular weight and conversion of their architecture from hyperbranched to linear. The hyperbranched amphiphilic diblock copolymers and their cleavage products formed spherical micelles in toluene, after quaternization of DMAEMA units using methyl iodide, and acidified water, respectively, with latter copolymers forming micelles of smaller sizes due to the cleavage of the PyDEBrMA residue branches.

Chapter 2 – Experimental Part

Chapter 2 describes the experimental procedures undertaken in this Thesis, that concern both synthesis and characterization. The former includes the preparation and homopolymerization of a series of nine pyridinylalkyl methacrylate monomers differing in the position of the nitrogen atom in the pyridine ring (2-, 3- or 4-pyridine) or/and in the length of the spacer (from methyl to propyl) between the ester moiety and the pyridine ring. This was followed by the evaporation of the thermal and hydrolytic stabilities of the above-produced homopolymers. The chapter also describes the formation and homopolymerization of some related monomers, in order to compare the thermal and hydrolytic stabilities of their polymers with those of the homopolymers of the pyridinylalkyl methacrylate homologues. These monomers were 2-phenylethyl methacrylate (2PheMA), 9*H*-fluoren-9-ylmethyl methacrylate (FMMA), *N*-(2-(pyridin-2-yl)ethyl) methacrylamide (2PyEMAAm), *S*-(2-(pyridin-2-yl)ethyl) methacrylthioate (2PyESMA), 2-((pyridin-2-yl)2-methyl)ethyl methacrylate (2PyEmeMA) and 2-((pyridin-2-yl)2,2-dimethyl)ethyl methacrylate (2PyEdimeMA).

Furthermore, the most labile of the above monomers, 2PyEMA, was combined in linear statistical copolymers and randomly cross-linked polymer networks with the more stable 2PyMMA. Moreover, 2PyEMA was incorporated in linear ABC triblock terpolymers with THPMA and BzMA, representing two other forms of protected MAA. Finally, the labile structure of the 2PyEMA monomer monoester was expanded to a labile diol diester, from which non-monomer labile structures were designed, synthesized and used in controlled polymerizations. In particular, 2,6-pyridinediethanol was in-house synthesized, from which three different diesters were prepared which represent a new degradable cross-linker, 2,6-pyridinediethanol dimethacrylate (PyDMA), a new degradable bifunctional atom transfer radical polymerization (ATRP) initiator, 2,6-bis(2-bromo-2-methylpropanoylethyl)pyridine (PyDEDBrMeP), and a new degradable ATRP *inimer*, 2-(6-(2-((2-bromo-2-methylpropanoyl)oxy) ethyl)pyridin-2-yl)ethyl methacrylate (PyDEBrMA).

2.1 Materials and Methods.

2.1.1 Materials. Almost all reagents used in this PhD Thesis for synthesis, purification and characterization were purchased from Aldrich, Germany. In particular, 2-pyridinemethanol (98%), 2-pyridineethanol (98%), 2-pyridinepropanol (96%), 3-pyridinemethanol (98%), 3-pyridinepropanol (98%), 4-pyridinemethanol (99%), 4-pyridinepropanol (96%), 2-

phenylethanol (≥98%), ethyl 3-pyridylacetate (99%), methacryloyl chloride (97%), methyl methacrylate (MMA, 99%), 2-(dimethylamino)ethyl methacrylate (DMAEMA, 99%), methacrylic acid (MAA, 99%), styrene (Sty, > 99%), ethylene glycol dimethacrylate (EGDMA, 98%), 3,4-dihydro-2*H*-pyran (DHP, 97%), sodium hydrogen carbonate ($NaHCO_3$, ≥99.9%), toluene (99.8%), 1-methoxy-1-trimethylsiloxy-2-methyl propene (MTS, 95%), 2-cyanoprop-2-yl dithiobenzoate (CPDB, 97%), 1,1,4,7,10,10-hexamethyltriethylenetetramine (HMTETA, 97%), copper(I) chloride (CuCl, ≥99.9%), tetrabutylammonium hydroxide (40% w/w in water), benzoic acid (99.5%), 1,4-dioxane (99.8%), 2,2-diphenyl-1-picrylhydrazyl hydrate (DPPH, 95%), calcium hydride (CaH_2, 90-95%), potassium metal (99%), deuterium chloride (35 wt.% solution in D_2O, 99 atom % D), benzyl methacrylate (BzMA, 96%), basic alumina (60 Å, 150 mesh, pH 9.5 ± 0.5), neutral alumina (60 Å, 150 mesh, pH 7.0 ± 0.5), 2,6-lutidine (96%), *n*-hexane (≥97%), diethyl ether (≥98%), ethyl acetate (≥99.5%), methanol (≥99.8%), *p*-toluenesulfonic acid monohydrate (≥98.5%), paraformaldehyde (reagent grade, crystalline), basic alumina (Al_2O_3·KOH, ≥98%), sodium deuteroxide (40 wt.% in D_2O, 99.5 atom % D), deuterated methanol (CD_3OD, 99.8%), sodium carbonate (≥99.5%), sodium hydrogen carbonate (≥99.7%), potassium carbonate (≥99%), 2,6-pyridinedimethanol (98%), 4-methylpyridine (98%), *α*-bromoisobutyryl bromide (98%), 1,1,4,7,10,10-hexamethyltriethylenetetramine (HMTETA, 97%), thiourea (≥99%), ammonium hydroxide solution (28% NH_3 in H_2O) and anisole (99%) were purchased from Aldrich, Germany. Synthesis grade triethylamine (≥99%) and tetrahydrofuran (THF, 99.8%) were obtained from Scharlau, Spain. THF was also used as the mobile phase in chromatography (HPLC grade). 2,2′-Azobis(isobutyronitrile) (AIBN, 95%), silica gel (60 Å, 230-400 mesh), sodium hydroxide (NaOH, 99%), dimethyl sulfoxide (DMSO, 99%), deuterated dimethyl sulfoxide (d_6-DMSO, 99.9%), deuterated chloroform ($CDCl_3$, 99.8%), deuterium oxide (D_2O, 99.9%), hydrochloric acid (HCl, 99%), sulfuric acid (H_2SO_4, 98%) and sodium hydroxide (NaOH, 99%) were purchased from Merck, Germany. Finally, sodium metal (98%) was from Fluka, Germany, and acetone (99.5%) was from Labscan, Ireland.

2.1.2 Purification of Solvents, Monomers and Catalysts. The solvent for GTP, THF, was purified by being refluxed in a specially-constructed glass still over a potassium-sodium-benzophenone complex (a deep purple color indicated an oxygen- and moisture-free solvent). 1,4-Dioxane and anisole, solvents for RAFT polymerization and ATRP, respectively, were distilled from CaH_2. Tetrabutylammonium bibenzoate (TBABB, GTP catalyst) was synthesized by the reaction of tetrabutylammonium hydroxide and benzoic

acid in water, following the procedure of Dicker et al.,[282] and was kept under vacuum until use. MMA, DMAEMA, BzMA and EGDMA were passed through basic alumina columns to remove the polymerization inhibitors and any other acidic impurities, and they were subsequently stirred over CaH_2 (to remove the last traces of moisture and protonic impurities) in the presence of added DPPH free-radical inhibitor, and stored in the refrigerator at about 5 ºC. Finally, they were freshly distilled under vacuum just before their use and kept under a dry argon atmosphere. The GTP initiator, MTS, was distilled once prior to the polymerization, without any contact with calcium hydride or basic alumina to avoid the risk of hydrolysis. AIBN, the radical source for RAFT polymerization, was recrystallized twice from ethanol. In the case of GTP, all glassware was dried overnight at 150 ºC and assembled hot under dynamic vacuum prior to use. The ATRP catalyst, CuBr, was purified by being stirred in glacial acetic acid and being rinsed with methanol and diethyl ether and being dried in a vacuum oven, while the ATRP ligand, HMTETA, was distilled under vacuum.[283]

2.2 Synthesis of Monomers

2.2.1. Synthesis of Pyridinylalkyl Methacrylate Monomers. Nine homologous pyridinylalkyl methacrylate monomers were synthesized. The chemical structures of these monomers are displayed in Table 2.1. These homologues differed in the size of the alkyl spacer between the ester moiety and pyridine or/and in the position of the nitrogen atom in the pyridine ring. All monomers were synthesized from the esterification of the corresponding hydroxyalkylpyridine (seven of which were commercially available) with about 25% molar excess of methacryloyl chloride in absolute tetrahydrofuran (THF) in the presence of a large excess (~8-fold) triethylamine base at 0 °C. The two commercially unavailable alcohols were 3-pyridineethanol and 4-pyridineethanol which were synthesized in our laboratory.

Table 2.1 Chemical Structures of All Pyridinylalkyl Methacrylate Homologues.[a]

	methyl	ethyl	propyl
2-Pyridine	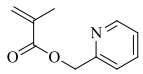 **2PyMMA**	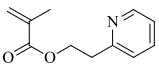 **2PyEMA**	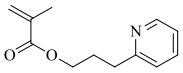 **2PyPMA**
3-Pyridine	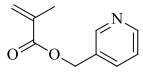 **3PyMMA**	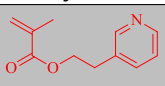 **3PyEMA**	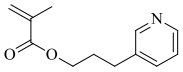 **3PyPMA**
4-Pyridine	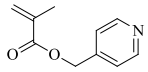 **4PyMMA**	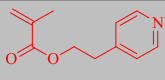 **4PyEMA**	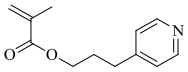 **4PyPMA**

[a.] For the two chemical structures in red, the corresponding alcohols were not commercially available. Thus, those two alcohols were produced from other, commercially available reagents.

Figure 2.1 shows the chemical reaction for the synthesis of the pyridinylalkyl methacrylate monomers by the esterification of hydroxyalkylpyridines with methacryloyl chloride using triethylamine base in dry THF.[275,278]

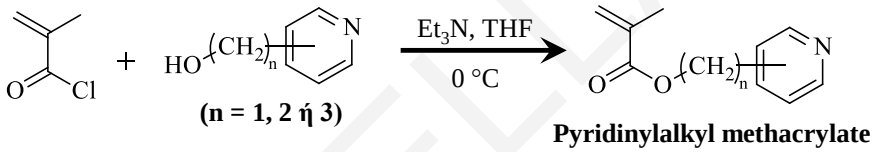

Figure 2.1 Chemical reaction for the synthesis of the pyridinylalkyl methacrylate monomers by the esterification of hydroxyalkylpyridines with methacryloyl chloride.

2.2.1.1 Synthesis of 2-(pyridin-2-yl)ethyl methacrylate (2PyEMA). 2-Pyridineethanol (10 mL, 10.93 g, 0.0888 mol), Et_3N (99 mL, 72 g, 0.71 mol) and absolute THF (62.5 mL) were transferred to a 500-mL round-bottomed flask containing a magnetic stirring bar. The solution was stirred and cooled down to 0 °C. After stabilization of the temperature, methacryloyl chloride (10.74 mL, 11.60 g, 0.111 mol) was added dropwise using a glass syringe and the reaction mixture was stirred for 2 h at 0 °C. Subsequently, the mixture was filtered to remove triethylamine hydrochloride and passed twice through a basic alumina column to remove methacrylic acid (hydrolysis product of excess methacryloyl chloride) and any other acidic impurities. Then, the solvent was evaporated off to give pure monomer in 90% yield (15.3 g). 2PyEMA was stirred over CaH_2 in the presence of DPPH to remove all moisture and the last traces of protic impurities. Finally, 2PyEMA was distilled under reduced pressure and was characterized using ^1H and ^{13}C NMR spectroscopy. **^1H NMR ($CDCl_3$, δ):** 1.80 ppm (s, CH_2=CCH_3, 3 H), 3.09 ppm (t, -OCH_2CH_2-, J = 6.70, 2 H), 4.45 ppm (t, -OCH_2CH_2-, J = 6.71, 2 H), 5.44 ppm (s, olefinic

H *trans* to CO_2, 1 H), 5.95 ppm (s, olefinic H *cis* to CO_2, 1 H), 7.09 ppm (t, *J* = 4.90, 1 H), 7.24 ppm (d, *J* = 7.71, 1 H), 7.51 ppm (t, *J* = 7.62, 1 H), and 8.48 ppm (d, *J* = 4.70, 1 H). **^{13}C NMR ($CDCl_3$, δ):** 18.24 ppm (s, CH_2=C*C*H_3, 1 C), 37.43 ppm (s, -OCH_2*C*H_2-, 1 C), 63.84 ppm (s, -O*C*H_2CH_2-, 1 C), 121.60 ppm (s, aromatic, 1 C), 123.43 ppm (s, aromatic, 1 C), 125.46 ppm (s, *C*H_2=CCH_3, 1 C), 136.24 ppm (s, CH_2=*C*CH_3, 1 C), 136.32 ppm (s, aromatic, 1 C), 149.46 ppm (s, aromatic, 1 C), 158.12 ppm (s, aromatic, 1 C) and 167.25 ppm (s, *C*O_2, 1 C).

With the exception of two homologous monomers, 3PyEMA and 4PyEMA (isomers of 2PyEMA), the synthesis of the other six homologues, 2PyMMA, 2PyPMA, 3PyMMA, 3PyPMA, 4PyMMA and 4PyPMA, were performed in the same way as that of 2PyEMA, directly from the esterification of the commercially available alcohol with 25% excess methacryloyl chloride in absolute THF containing a large excess of triethylamine base as catalyst at 0 °C.

2.2.1.2 Synthesis of 2-(pyridin-3-yl)ethyl methacrylate (3PyEMA). Due to the commercial unavailability of 3-pyridineethanol, necessary for the synthesis of the 3PyEMA monomer, 3-pyridineethanol was prepared according to the procedure of Almond et al.[284] which followed a modification of the method of Barnden.[285]

Synthesis of 3-pyridineethanol: 3-Pyridineethanol was synthesized by the reduction of ethyl 3-pyridylacetate using lithium aluminum hydride in tetrahydrofuran (THF). In this modified procedure, 22 mL of a 1.0 M solution of lithium aluminum hydride in THF (0.0218 mol) was added dropwise to a stirred solution of ethyl 3-pyridylacetate (3.6 g, 0.0218 mol) in anhydrous THF (58 mL) maintained at 0 °C using an ice bath, under a nitrogen atmosphere. After the addition of the lithium aluminum hydride solution, the ice bath was removed and the reaction was stirred for 2 extra hours. A saturated aqueous solution of potassium sodium tartrate (20 mL) was slowly added to the reaction, followed by diethyl ether, and the layers were vigorously mixed and then allowed to separate. The aqueous layer was filtered over celite to remove the solids, and it was subsequently extracted twice with ethyl acetate (2 × 25 mL). The organic phases were combined and dried using anhydrous magnesium sulfate. The solvent was removed using a rotary evaporator and the residue was fractionated by column chromatography using a chloroform/methanol solvent mixture of varying composition, starting from 100% chloroform and ending up in 95% chloroform. Pure 3-pyridineethanol eluted at a 95/5 v/v chloroform/methanol solvent composition (2.02 g recovered, 75.4% yield). 3-

Pyridineethanol was characterized using ^{1}H and ^{13}C NMR spectroscopy. **^{1}H NMR ($CDCl_3$, δ):** 2.80 ppm (t, -C*H*$_2$-CH_2OH, *J* = 6.6, 2 H), 3.81 ppm (t, -CH_2C*H*$_2$OH, *J* = 6.42, 2 H), 7.17 ppm (m, aromatic, *J* = 2.84, 1 H), 7.54 ppm (d, aromatic, *J* = 7.70, 1 H), 8.33 ppm (d, aromatic, *J* = 4.25, 1 H), 8.37 ppm (s, aromatic, 1 H). **^{13}C NMR ($CDCl_3$, δ):** 36.26 ppm (s, -*C*H_2-CH_2OH, 1 C), 62.51 ppm (s, -CH_2*C*H_2-OH, 1 C), 123.39 ppm (s, aromatic, 1 C), 134.89 ppm (s, aromatic, 1 C),), 136.93 ppm (s, aromatic, 1 C), 146.98 ppm (s, aromatic, 1 C), 149.71 ppm (s, aromatic, 1 C).

Synthesis of 3PyEMA: 3PyEMA was synthesized by the esterification of 3-pyridineethanol with 25% molar excess of methacryloyl chloride. To this end, 3-pyridineethanol (2.0 g, 0.0162 mol), Et_3N (18.12 mL, 13.14 g, 0.1299 mol) and absolute THF (12.5 mL) were transferred to a 100-mL round-bottomed flask containing a magnetic stirring bar, thermostated at 0 °C under an inert atmosphere. Then, methacryloyl chloride (1.98 mL, 2.12 g, 0.0203 mol) was added dropwise using a glass syringe and the reaction mixture was stirred for 2 h at 0 °C. Subsequently, the mixture was filtered and passed twice through a basic alumina column to remove methacrylic acid (hydrolysis product of excess methacryloyl chloride) and any other acidic impurities. The solvent was evaporated off to give pure 3PyEMA monomer in 58% yield. 3PyEMA was stirred over CaH_2 in the presence of DPPH to remove all moisture and the last traces of protonic impurities. Finally, 3PyEMA was distilled under vacuum at 80 °C, and was characterized using ^{1}H and ^{13}C NMR spectroscopy.**^{1}H NMR ($CDCl_3$, δ):** 1.89 ppm (s, CH_2=CC*H*$_3$, 3 H), 2.97 ppm (t, -C*H*$_2$$CH_2O$, *J* = 6.7, 2 H), 4.34 ppm (t, -CH_2C*H*$_2$O, *J* = 6.6, 2 H), 5.33 ppm (s, C*H*$_2$=CCH_3 H *trans* to CO_2, 1 H), 6.04 ppm (s, C*H*$_2$=CCH_3 H *cis* to CO_2, 1 H), 7.22 ppm (m, aromatic, *J* = 2.84 and 4.88, 1 H), 7.53 ppm (d, aromatic, *J* = 7.88, 1 H), 8.46 ppm (d, aromatic, *J* = 4.88, 1 H), 8.48 ppm (s, aromatic, 1 H). **^{13}C NMR ($CDCl_3$, δ):** 18.27 ppm (s, CH_2=C*C*H_3, 1 C), 32.28 ppm (s, -*C*$H_2$$CH_2O$, 1 C), 64.39 ppm (s, -$CH_2$*C*$H_2$O, 1 C), 123.30 ppm (s, aromatic, 1 C), 125.69 ppm (s, *C*H_2=CCH_3, 1 C), 133.43 ppm (s, aromatic, 1 C), 136.01 ppm (s, CH_2=*C*CH_3, 1 C), 136.23 ppm (s, aromatic, 1 C), 148.06 ppm (s, aromatic, 1 C), 150.27 ppm (s, aromatic, 1 C), 167.09 ppm (s, *C*O_2, 1 C).

2.2.1.3 Synthesis of 2-(pyridin-4-yl)ethyl methacrylate (4PyEMA). Due to the commercial unavailability of 4-pyridineethanol, necessary for the synthesis of 4PyEMA, 4-pyridineethanol was prepared according to the procedure of Vaganova et al.[286] from the reaction of 4-methylpyridine (4-picoline) with formaldehyde under reflux.

Synthesis of 4-pyridineethanol: 83.6 mL of 4-picoline (80.00 g, 0.859 mol) was dispersed in 160 mL of water, giving an emulsion, and 44 g of a 37 wt.% aqueous solution of formaldehyde (0.543 mol) was added. The reaction mixture was refluxed under stirring for 20 h. Subsequently, the reaction mixture was cooled down to room temperature, and a few drops of a saturated aqueous sodium carbonate solution were then added to it. Water, formaldehyde and unreacted 4-methylpyridine were removed by steam distillation, and the liquid residue was evaporated on a steam bath until distillation stopped at 100 °C. The residue was distilled off on the vacuum line at 80 °C, and the distilled product consisted of 95% of 4-pyridineethanol. Pure 4-pyridineethanol was obtained after column chromatography in a solvent mixture of *n*-hexane/acetone of varying composition, starting from a 90/10 v/v *n*-hexane/acetone mixture. 4-Pyridineethanol eluted at a 55/45 v/v *n*-hexane/acetone solvent composition. Pure 4-pyridineethanol (5.01 g, 4.73%) was characterized using ^{1}H and ^{13}C NMR spectroscopy. **^{1}H NMR ($CDCl_3$, δ):** 2.82 ppm (t, -C*H*$_2$-CH$_2$OH, *J* = 6.46, 2 H), 3.86 ppm (t, -CH$_2$C*H*$_2$OH, *J* = 6.46, 2 H), 7.13 ppm (d, aromatic, *J* = 5.83, 2H), 8.37 ppm (d, aromatic, *J* = 5.83, 2 H). **^{13}C NMR ($CDCl_3$, δ):** 38.51 ppm (s, -*C*H$_2$-CH$_2$OH, 1 C), 62.12 ppm (s, -CH$_2$*C*H$_2$-OH, 1 C), 124.51 ppm (s, aromatic, 2 C), 148.58 ppm (s, aromatic, 1 C), 149.30 ppm (s, aromatic, 2 C).

Synthesis of 2-(pyridin-4-yl)ethyl methacrylate (4PyEMA): Although for the synthesis by esterification of all other pyridinylalkyl methacrylates, (excess) triethylamine proved to be an efficient esterification catalyst, this was not the case for 4PyEMA, for whose alcohol, the esterification using triethylamine base was not efficient. Thus, pyridine was used instead, which appeared to solve the problems. In particular, 4-pyridineethanol (4.88 g, 0.0396 mol), freshly distilled pyridine (19.15 mL, 18.80 g, 0.2377 mol) and absolute $CHCl_3$ (30 mL) were transferred to a 250-mL round-bottomed flask containing a magnetic stirring bar, and maintained under an argon atmosphere. The solution was stirred and cooled down to 0 °C. After stabilization of the temperature, methacryloyl chloride (5.03 mL, 5.38 g, 0.0515 mol) was added dropwise using a glass syringe and the reaction mixture was stirred for 2 h at 0 °C. Subsequently, the mixture was filtered and passed thrice through a basic alumina column to remove methacrylic acid (hydrolysis product of excess methacryloyl chloride) and any other acidic impurities. Then, the pyridine was distilled off on the vacuum line, and the residue was pure 4PyEMA monomer (1.8 g) in 24% yield. The purified 4PyEMA was characterized using ^{1}H and ^{13}C NMR spectroscopy. **^{1}H NMR ($CDCl_3$, δ):** 1.89 ppm (s, CH$_2$=CC*H*$_3$, 3 H), 2.97 ppm (t, -C*H*$_2$CH$_2$O, *J* = 6.69, 2 H), 4.37 ppm (t, -CH$_2$C*H*$_2$O, *J* = 6.71, 2 H), 5.54 ppm (s, C*H*$_2$=CCH$_3$ H *trans* to CO$_2$, 1 H),

6.04 ppm (s, CH_2=CCH_3 H *cis* to CO_2, 1 H), 7.15 ppm (d, aromatic, J = 5.83, 2 H), 8.52 ppm (d, aromatic, J = 3.94, 2 H). **^{13}C NMR ($CDCl_3$, δ):** 18.27 ppm (s, CH_2=CCH_3, 1 C), 32.28 ppm (s, -CH_2CH_2O, 1 C), 64.39 ppm (s, -CH_2CH_2O, 1 C), 123.30 ppm (s, aromatic, 1 C), 125.69 ppm (s, CH_2=CCH_3, 1 C), 133.43 ppm (s, aromatic, 1 C), 136.01 ppm (s, CH_2=CCH_3, 1 C), 136.23 ppm (s, aromatic, 1 C), 148.06 ppm (s, aromatic, 1 C), 150.27 ppm (s, aromatic, 1 C), 167.09 ppm (s, CO_2, 1 C).

***2.2.2. Synthesis of Related Monomers*.** Figure 2.2 shows the chemical structures of some related monomers which were also synthesized, and subsequently homopolymerized.

These monomers were 2-phenylethyl methacrylate (2PheMA), (9*H*-fluoren-9-yl)methyl methacrylate (FMMA), *N*-(2-(pyridin-2-yl)ethyl) methacrylamide (2PyEMAAm), *S*-(2-(pyridin-2-yl)ethyl) methacrylthioate (2PyESMA), 2-((pyridin-2-yl)2-methyl)ethyl methacrylate (2PyEmeMA) and 2-((pyridin-2-yl)2,2-dimethyl)ethyl methacrylate (2PyEdimeMA) prepared from the esterification reaction of methacryloyl chloride with 2-phenylethanol, 9-fluorenemethanol, 2-(pyridin-2-yl)ethan-1-amine, 2-pyridineethanethiol, 2-(pyridin-1-methyl)ethan-2-ol and 2-(pyridin-1,1-dimethyl)ethan-2-ol, respectively. Due to the commercial unavailability of the last three alcohols, these were synthesized in our laboratory. 2-(Pyridin-2-yl)ethane-1-thiol was prepared from the reaction of 2-vinylpyridine with thiourea in ammonia according to Tsutsuminai et al.[287] 2-(Pyridin-2-yl)propan-1-ol was synthesized according to Gade et al.[288] by the reaction of 2-ethylpyridine with formaldehyde in water under high pressure and temperature, and 2-(pyridin-1,1-dimethyl)ethan-2-ol was synthesized according to Fraenkel et al.[289] by the reaction of 2-isopropylpyridine with paraformaldehyde in water under high pressure and temperature, where 2-isopropylpyridine was prepared by the alkylation of deprotonated (using *n*-BuLi) 2-ethylpyridine using iodomethane.[290] These related monomers were synthesized in order to compare the stabilities under alkaline hydrolysis or thermolysis conditions of their polymers with that of the polymers of the pyridinylalkyl methacrylate homologues.

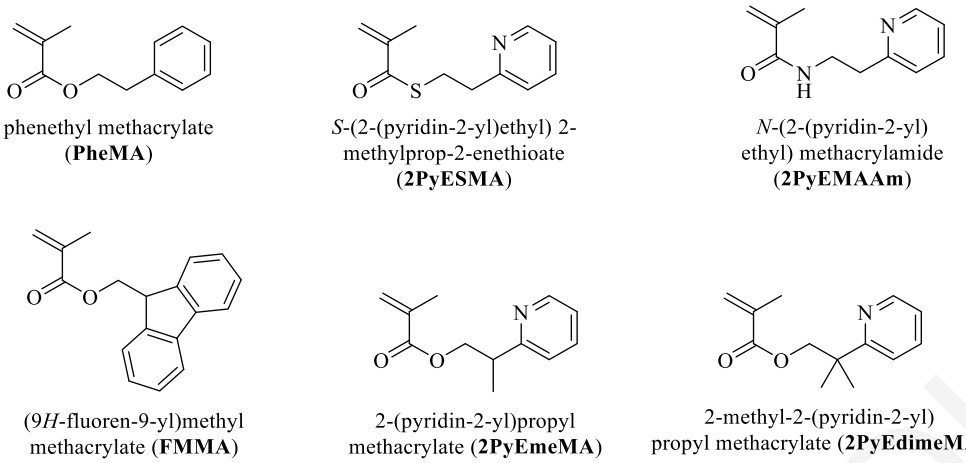

Figure 2.2 Chemical structures of monomers related to pyridinylalkyl methacrylates.

2.2.2.1 Synthesis of 2-phenylethyl methacrylate (PheMA). The synthesis of PheMA was achieved by the esterification of phenylethanol with 25% molar excess of methacryloyl chloride. In particular, in a 250-mL round-bottomed flask containing a magnetic stirring bar, and kept under an inert atmosphere, were transferred of 5 mL phenylmethanol (5.10 g, 0.0417 mol), 46.6 mL Et_3N (33.80 g, 0.3339 mol) and 31.3 mL of dry THF, which were subsequently thermostated at 0 °C. Then, 5.10 mL of methacryloyl chloride (5.45 g, 0.0522 mol) was added dropwise using a glass syringe and the reaction mixture was stirred for 2 h at 0 °C. Subsequently, the mixture was filtered and passed twice through a basic alumina column to remove methacrylic acid (hydrolysis product of excess methacryloyl chloride) and any other acidic impurities. The solvent was evaporated off to give 6.90 g pure PheMA monomer (87% yield). PheMA was stirred over CaH_2, in the presence of DPPH, to remove all moisture and the last traces of protonic impurities, and was distilled under vacuum. Finally, PheMA was characterized using ^{1}H and ^{13}C NMR spectroscopy. **^{1}H NMR ($CDCl_3$, δ):** 1.83 ppm (s, CH_2=CC*H*$_3$, 3 H), 2.89 ppm (t, -OCH$_2$C*H*$_2$-, *J* = 7.01, 2 H), 4.26 ppm (t, -OC*H*$_2$CH$_2$-, *J* = 6.93, 2 H), 5.44 ppm (s, olefinic H *trans* to CO_2, 1 H), 5.99 ppm (s, olefinic H *cis* to CO_2, 1 H), 7.14 ppm (d, aromatic, *J* = 7.25, 3 H), 7.21 ppm (d, aromatic, *J* = 7.09, 2 H). **^{13}C NMR ($CDCl_3$, δ):** 18.21 ppm (s, CH_2=C*C*H$_3$, 1 C), 37.05 ppm (s, -OCH$_2$*C*H$_2$-, 1 C), 65.12 ppm (s, -O*C*H$_2$CH$_2$-, 1 C), 125.39 ppm (s, *C*H$_2$=CCH$_3$, 1 C), 126.45 ppm (s, aromatic, 1 C), 128.39 ppm (s, aromatic, 2 C), 128.87 ppm (s, aromatic, 2 C), 136.24 ppm (s, *C*H$_2$=CCH$_3$, 1 C), 137.86 ppm (s, aromatic, 1 C) and 167.24 ppm (s, *C*O$_2$, 1 C).

2.2.2.2 Synthesis of (9H-fluoren-9-yl)methyl methacrylate (FMMA). The synthesis of FMMA was achieved by the esterification of (9*H*-fluoren-9-yl)methanol with 25% molar

excess of methacryloyl chloride. To this end, in a 250-mL round-bottomed flask containing a magnetic stirring bar, and preserved under an inert atmosphere, were transferred 5.0 g of (9*H*-fluoren-9-yl)methanol (0.0255 mol), 28.4 mL Et_3N (20.62 g, 0.2038 mol) and 31.3 mL of dry THF, which were subsequently thermostated at 0 °C. Then, 3.11 mL of methacryloyl chloride (3.33 g, 0.0318 mol) was added dropwise using a glass syringe and the reaction mixture was stirred for 2 h at 0 °C. Subsequently, the mixture was filtered and passed twice through a basic alumina column to remove methacrylic acid (hydrolysis product of excess methacryloyl chloride) and any other acidic impurities. The solvent was evaporated off to give 6.06 g of pure FMMA monomer (90% yield). **^{1}H NMR ($CDCl_3$, δ):** 2.02 ppm (s, CH_2=CC*H*$_3$, 3 H), 4.29 ppm (t, -OCH_2C*H*-, *J* = 7.25, 1 H), 4.46 ppm (t, -OC*H*$_2$CH-, *J* = 7.41, 2 H), 5.65 ppm (s, olefinic H *trans* to CO_2, 1 H), 6.20 ppm (s, olefinic H *cis* to CO_2, 1 H), 7.33 ppm (t, aromatic, *J* = 7.49, 2 H), 7.42 ppm (t, aromatic, *J* = 7.41, 2 H), 7.62 ppm (d, aromatic, *J* = 7.57, 2 H), 7.79 ppm (d, aromatic, *J* = 7.57, 2 H). **^{13}C NMR ($CDCl_3$, δ):** 18.38 ppm (s, CH_2=C*C*H$_3$, 1 C), 46.83 ppm (s, -OCH_2*C*H-, 1 C), 66.74 ppm (s, -O*C*H$_2$CH-, 1 C), 120.00 ppm (s, aromatic, 2 C), 125.00 ppm (s, aromatic, 2 C), 125.87 ppm (s, *C*H$_2$=CCH$_3$, 1 C), 126.70 ppm (s, aromatic, 2 C), 127.07 ppm (s, aromatic, 2 C), 136.18 ppm (s, *C*H$_2$=CCH$_3$, 1 C), 141.27 ppm (s, aromatic, 2 C), 143.81 ppm (s, aromatic, 2 C) and 167.24 ppm (s, *C*O$_2$, 1 C).

2.2.2.3 Synthesis of S-(2-(pyridin-2-yl)ethyl) methacrylthioate (2PyESMA). The synthesis of 2PyESMA was performed in two stages. The first stage included the synthesis of 2-(pyridin-2-yl)ethane-1-thiol, followed by the esterification of the thiol with methacryloyl chloride in the second stage. 2-(Pyridin-2-yl)ethane-1-thiol was prepared from the reaction of 2-vinylpyridine with thiourea in ammonia according to Tsutsuminai et al.[287]

Synthesis of 2-(pyridin-2-yl)ethane-1-thiol: In a two-necked round-bottomed flask equipped with a pressure-equalizing dropping funnel, containing a magnetic stirring bar, and maintained under an inert argon atmosphere, were transferred 12.58 mL of a 29 wt.% aqueous sulfuric acid solution (0.1258 mol) and 4.61 g of thiourea (0.0605 mol), which were, subsequently, thermostated at 70 °C. Then, 5.13 mL of 2-vinylpyridine (5.00 g, 0.0488 mol) dissolved in 9.0 mL of toluene were added dropwise using a pressure-equalizing dropping funnel and the reaction mixture was stirred for 5 h at 70 °C. After 5 h, the reaction mixture was cooled down to 20 °C, and 20 mL of a 28 wt.% ammonia solution (0.30 mol) was added dropwise, ensuring that the liquid temperature did not rise above 22 °C. After all ammonia solution was added, the mixture was heated to 40 °C for 3 h. After

this time, the reaction mixture was cooled down to room temperature, and solid sodium hydrogen carbonate ($NaHCO_3$) was added carefully (~5.5 g, 0.0655 mol), until gas evolution stopped, in order to neutralize the sulfuric acid. Subsequently, the mixture was extracted with toluene (3 × 50 mL). The organic phases were combined and dried using anhydrous magnesium sulfate, and toluene was evaporated off to give 4.84 g of pure 2-(pyridin-2-yl)ethane-1-thiol at 73.1% yield. 2(-Pyridin-2-yl)ethane-1-thiol was characterized using ^{1}H and ^{13}C NMR spectroscopy. **^{1}H NMR (D_2O, δ):** 3.51 ppm (t, -CH_2CH_2SH, J = 6.83, 2 H), 3.63 ppm (t, -CH_2CH_2SH, J = 6.94, 2 H), 3.76 ppm (t, -CH_2CH_2SH, 1 H), 7.89 ppm (t, aromatic, J = 6.44, 1 H), 7.94 ppm (d, aromatic, J = 8.04, 1 H), 8.45 ppm (t, aromatic, J = 7.95, 1 H), 8.71 ppm (d, aromatic, J = 5.67, 1 H). **^{13}C NMR (D_2O, δ):** 29.54 ppm (s, -CH_2-CH_2-SH, 1 C), 32.91 ppm (s, -CH_2CH_2SH, 1 C), 125.21 ppm (s, aromatic, 1 C), 127.30 ppm (s, aromatic, 1 C), 142.50 ppm (s, aromatic, 1 C), 145.57 ppm (s, aromatic, 1 C), 153.44 ppm (s, aromatic, 1 C).

Synthesis of 2PyESMA: 2PyESMA was synthesized by the esterification of 2-(pyridin-2-yl)ethane-1-thiol with 25% molar excess of methacryloyl chloride. To this end, in a 250-mL round-bottomed flask containing a magnetic stirring bar, kept under an inert atmosphere, were transferred 3.0 g of 2-(pyridin-2-yl)ethane-1-thiol (0.0215 mol), 24.1 mL Et_3N (17.44 g, 0.1724 mol) and 18.8 mL of dry THF, which were subsequently thermostated at 0 °C. Then, 2.63 mL of methacryloyl chloride (2.82 g, 0.0269 mol) was added dropwise using a glass syringe and the reaction mixture was stirred for 2 h at 0 °C. Subsequently, the mixture was filtered and passed twice through a basic alumina column to remove methacrylic acid (hydrolysis product of excess methacryloyl chloride) and any other acidic impurities. The solvent was evaporated off to give 3.79 g of pure 2PyESMA monomer (85% yield). **^{1}H NMR ($CDCl_3$, δ):** 1.97 ppm (s, CH_2=CCH_3, 3 H), 3.09 ppm (t, -OC$H_2$$CH_2$-, J = 7.39, 2 H), 3.34 ppm (t, -OCH_2CH_2-, J = 7.41, 2 H), 5.56 ppm (s, olefinic H *trans* to CO_2, 1 H), 6.05 ppm (s, olefinic H *cis* to CO_2, 1 H), 7.14 ppm (t, aromatic, J = 6.68, 1 H), 7.20 ppm (d, aromatic, J = 7.72, 1 H), 7.61 ppm (t, aromatic, J = 7.64, 1 H), 8.55 ppm (d, aromatic, J = 4.57, 1 H). **^{13}C NMR ($CDCl_3$, δ):** 17.57 ppm (s, CH_2=CCH_3, 1 C), 27.42 ppm (s, -SCH_2CH-, 1 C), 36.72 ppm (s, -SCH_2CH-, 1 C), 121.69 ppm (s, aromatic, 1 C), 123.07 ppm (s, aromatic, 1 C), 123.63 ppm (s, CH_2=CCH_3, 1 C), 136.51 ppm (s, CH_2=CCH_3, 1 C), 143.01 ppm (s, aromatic, 1 C), 148.98 ppm (s, aromatic, 1 C), 158.94 ppm (s, aromatic, 1 C), 192.48 ppm (s, COS, 1 C).

2.2.2.4 Synthesis of N-(2-(pyridin-2-yl)ethyl) methacrylamide (2PyEMAAm). 2PyEMAAm was synthesized by the esterification of 2-(pyridin-2-yl)ethan-1-amine with 25% molar excess of methacryloyl chloride. To this end, 4.89 mL of 2-(pyridin-2-yl)ethan-1-amine (5.00 g, 0.0409 mol), 45.66 mL of Et_3N (33.13 g, 0.3274 mol) and 31.3 mL absolute THF were transferred to a 250-mL round-bottomed flask, containing a magnetic stirring bar, and preserved under an inert argon atmosphere. The solution was stirred and cooled down to 0 °C. After stabilization of the temperature, 5.0 mL of methacryloyl chloride (5.35 g, 0.0512 mol) was added dropwise using a glass syringe and the reaction mixture was stirred for 2 h at 0 °C. Subsequently, the mixture was filtered to remove triethylamine hydrochloride and was passed twice through a basic alumina column to remove methacrylic acid (hydrolysis product of excess methacryloyl chloride) and any other acidic impurities. Then, the solvent was evaporated off to give 6.38 g of pure 2PyEMAAm in 82% yield. 2PyEMAAm was characterized using ^{1}H and ^{13}C NMR spectroscopy. **^{1}H NMR ($CDCl_3$, δ):** 1.94 ppm (s, CH_2=CC*H*$_3$, 3 H), 3.02 ppm (t, -NHCH$_2$C*H*$_2$-, *J* = 6.29, 2 H), 3.70 ppm (t, -NHC*H*$_2$CH$_2$-, *J* = 6.02, 2 H), 5.28 ppm (s, olefinic H *trans* to CONH, 1 H), 5.68 ppm (s, olefinic H *cis* to CO_2, 1 H), 7.08 ppm (s, -CON*H*-, 1 H), 7.16 – 7.20 ppm (m, aromatic, *J* = 7.57, 2 H), 7.62 ppm (t, aromatic, *J* = 7.64, 1 H), 8.52 ppm (d, aromatic, *J* = 4.57, 1 H). **^{13}C NMR ($CDCl_3$, δ):** 18.32 ppm (s, CH_2=C*C*H$_3$, 1 C), 36.34 ppm (s, -NHCH$_2$*C*H$_2$-, 1 C), 38.63 ppm (s, -NH*C*H$_2$CH$_2$-, 1 C), 119.15 ppm (**c**, s, *C*H$_2$=CCH$_3$, 1 C), 121.35 ppm (s, aromatic, 1 C), 123.22 ppm (s, aromatic, 1 C), 136.43 ppm (s, aromatic, 1 C), 139.72 ppm (s, CH$_2$=*C*CH$_3$, 1 C), 148.83 ppm (s, aromatic, 1 C), 159.51 ppm (s, aromatic, 1 C), 167.94 ppm (s, *C*ONH, 1 C).

2.2.2.5 Synthesis of 2-(pyridin-2-yl)propyl methacrylate (2PyEmeMA). 2PyEmeMA was synthesized by the esterification of 2-(pyridin-2-yl)propan-1-ol with 30% molar excess of methacryloyl chloride. 2-(Pyridin-2-yl)propan-1-ol was synthesized according to Gade et al.[288] by the reaction of 2-ethylpyridine with formaldehyde in water under high pressure and temperature.

Synthesis of 2-(pyridin-2-yl)propan-1-ol. 2-Ethylpyridine (15 mL, 14.06 g, 0.1312 mol) and an aqueous solution of formaldehyde (45.20 mL, 0.6561 mol) were transferred to a 500-mL round-bottomed pressure flask with an Ace-Thread 15 PTFE front-seal plug containing a magnetic stirring bar. The mixture was stirred and heated at 140 °C. After 2 days, the reaction mixture was cooled down to room temperature, and a few drops of a 20% w/w sodium carbonate aqueous solution were added. The unreacted 2-ethylpyridine

and formaldehyde were removed by steam distillation, and the liquid residue was evaporated on a steam bath until the distillation stopped at 100 °C. Afterwards, potassium carbonate (0.5 g, 0.0036 mol) was added and the resulting mixture was extracted twice with 80 mL of chloroform. The organic phases were then concentrated and the mixture was separated by silica gel column chromatography using a solvent mixture of *n*-hexane/acetone of varying composition, starting with a composition of 90/10 v/v *n*-hexane/acetone. Pure 2-(pyridin-2-yl)propan-1-ol eluted at a 75/25 v/v *n*-hexane/acetone solvent composition (2.79 g, 15.5% yield). 2-(Pyridin-2-yl)propan-1-ol was characterized using ^{1}H and ^{13}C NMR spectroscopy. **^{1}H NMR ($CDCl_3$, δ):** 1.32 ppm (d, -C*H*$_3$CH-, *J* = 7.09, 3 H), 3. 07 ppm (m, -C*H*CH$_2$OH, *J* = 3.01 and 3.94 , 1 H), 3.82 – 3.93 (m, -CHC*H*$_2$OH, *J* = 3.94 and 6.77, 2 H), 7.14 ppm (m, aromatic, *J* = 1.58 and 5.67, 1H), 7.18 ppm (d, aromatic, *J* = 7.72, 1 H), 7.63 ppm (m, aromatic, *J* = 1.57 and 7.72, 1 H), 8.49 ppm (d, aromatic, *J* = 4.41, 1 H). **^{13}C NMR ($CDCl_3$, δ):** 17.12 ppm (s, -*C*H$_3$CH-, 1 C), 41.90 ppm (s, -*C*HCH$_2$OH, 1 C), 67.05 ppm (s, -CH*C*H$_2$OH, 1 C), 121.48 ppm (s, aromatic, 1 C), 122.16 ppm (s, aromatic, 1 C), 136.79 ppm (s, aromatic, 1 C), 148.57 ppm (s, aromatic, 1 C), 164.90 ppm (s, aromatic, 1 C).

Synthesis of 2PyEmeMA. The synthesis of 2PyEmeMA was achieved by the esterification of 2-(pyridin-2-yl)propan-1-ol with 30% molar excess of methacryloyl chloride. In particular, in a 100-mL round-bottomed flask containing a magnetic stirring bar, and maintained under an inert argon atmosphere, were transferred 2.7 g of 2-(pyridin-2-yl)propan-1-ol (0.0197 mol), 21.96 mL Et_3N (15.93 g, 0.1574 mol) and absolute THF (16.8 mL) which were subsequently thermostated at 0 °C. Then, methacryloyl chloride (2.67 mL, 2.50 g, 0.0256 mol) was added dropwise using a glass syringe and the reaction mixture was stirred for 2 h at 0 °C. Subsequently, the mixture was filtered and passed twice through a basic alumina column to remove methacrylic acid (hydrolysis product of excess methacryloyl chloride) and any other acidic impurities. The solvent was evaporated off to give 3.23 g of pure 2PyEmeMA monomer (80.0% yield). 2PyEmeMA was stirred over CaH_2 in the presence of DPPH to remove all moisture and the last traces of any other protonic impurities, and was distilled under vacuum at 80 °C. 2PyEmeMA was characterized using ^{1}H and ^{13}C NMR spectroscopy. **^{1}H NMR (d_6-DMSO, δ):** 1.26 ppm (d, -C*H*$_3$CH-, *J* = 6.94, 3 H), 1.78 ppm (s, CH$_2$=CC*H*$_3$, 3 H), 3.26 ppm (m, -C*H*CH$_2$O-, *J* = 6.94 and 7.09, 1 H), 4.26 – 4.34 (m, -CHCH$_2$O-, *J* = 7.72, 6.62 and 4.10, 2 H), 5.59 ppm (s, C*H*$_2$=CCH$_3$ H *trans* to CO_2, 1 H), 5.88 ppm (s, C*H*$_2$=CCH$_3$ H *cis* to CO_2, 1 H), 7.23 ppm (m, aromatic, *J* = 1.73 and 5.67, 1H), 7.31 ppm (d, aromatic, *J* = 7.88, 1 H), 7.72 ppm (m,

aromatic, J = 1.73 and 7.57, 1 H), 8.51 ppm (d, aromatic, J = 4.73, 1 H). **^{13}C NMR (d_6-DMSO, δ):** 16.83 ppm (s, -*C*H_3CH-, 1 C), 17.73 ppm (s, CH_2=C*C*H_3, 1 C), 30.30 ppm ppm (s, -*C*HCH_2O-, 1 C), 68.02 ppm (s, -CH*C*H_2O-, 1 C), 121.73 ppm (s, aromatic, 1 C), 122.25 ppm (s, *C*H_2=CCH_3, 1 C), 125.45 ppm (s, aromatic, 1 C), 135.71 ppm (s, aromatic, 1 C), 136.43 ppm (s, CH_2=*C*CH_3, 1 C), 148.94 ppm (s, aromatic, 1 C), 161.98 ppm (s, aromatic, 1 C), 166.23 ppm (s, *C*O_2, 1 C).

2.2.2.6 Synthesis of 2-methyl-2-(pyridin-2-yl)propyl methacrylate (2PyEdimeMA). The synthesis of 2PyEdimeMA was accomplished by the esterification of 2-(pyridin-1,1-dimethyl)ethan-2-ol with 30% molar excess of methacryloyl chloride. 2-(Pyridin-1,1-dimethyl)ethan-2-ol was synthesized according to Fraenkel et al.[289] by the reaction of 2-isopropylpyridine with paraformaldehyde in water under high pressure and temperature. 2-Isopropylpyridine was prepared by the alkylation, using iodomethane, of deprotonated (using *n*-BuLi) 2-ethylpyridine.[290]

Synthesis of 2-isopropylpyridine. 2-Isopropylpyridine was synthesized by the alkylation of 2-ethylpyridine using *n*-BuLi and iodomethane. In particular, to a dried, argon-flushed 500 mL 2-necked round-bottomed flask fitted with a pressure-equalizing dropping funnel and containing a magnetic stirring bar, were transferred 15 mL of 2-ethylpyridine (14.06 g, 0.1312 mol) and absolute THF (78.6 mL), which were subsequently cooled down to −30 °C. Afterward, 56.91 mL of a 2.4 M solution of *n*-BuLi (0.1377 mol) in *n*-hexane was slowly added over 30 min, using the pressure-equalizing dropping funnel, ensuring that the temperature did not rise above −20 °C. After an additional hour of stirring at −20 °C, the deep red solution was cooled down to −50 °C. Subsequently, iodomethane (8.98 mL, 20.48 g, 0.1443 mol) in absolute THF (32.8 mL) was added dropwise making sure that the temperature did not exceed −40 °C. After 30 minutes of stirring at −40 °C, the reaction mixture was made acidic by the addition of a 66 mL H_2O / 16.4 mL HCl (37% w/w in H_2O) mixture, and was then extracted with 150 mL diethyl ether (once). The aqueous layer was treated with potassium carbonate (K_2CO_3), extracted with dichloromethane (DCM) (3 × 150 mL) and dried using anhydrous $MgSO_4$. The solvent was evaporated off to give 14.51 g of pure 2-isopropylpyridine (91.3% yield). 2-Isopropylpyridine was characterized using ^{1}H and ^{13}C NMR spectroscopy. **^{1}H NMR ($CDCl_3$, δ):** 1.32 ppm (d, (CH_3)$_2$CH-, J = 6.94, 6 H), 2.99 ppm (m, -CH(CH_3)$_2$, J = 6.94, 1 H), 7.01 ppm (m, aromatic, J = 4.99, 1H), 7.10 ppm (m, aromatic, J = 7.88, 1 H), 7.51 ppm (m, aromatic, J = 1.89 and 5.83, 1 H), 8.47 ppm (d, aromatic, J = 2.99, 1 H). **^{13}C NMR ($CDCl_3$, δ):** 22.40 ppm (s, (CH_3)$_2$CH-, 2

C), 36.18 ppm (s, -*C*H(CH_3), 1 C), 120.46 ppm (s, aromatic, 1 C), 122.82 ppm (s, aromatic, 1 C), 136.18 ppm (s, aromatic, 1 C), 148.88 ppm (s, aromatic, 1 C), 167.13 ppm (s, aromatic, 1 C).

Synthesis of 2-(Pyridin-1,1-dimethyl)ethan-2-ol. 2-(Pyridin-1,1-dimethyl)ethan-2-ol was prepared by the reaction of 2-isopropylpyridine with paraformaldehyde in water under high pressure and temperature. In particular, to a 500 mL round-bottomed pressure flask with an Ace-Thread 15 PTFE front-seal plug and containing a magnetic stirring bar were transferred 15.91 mL of 2-isopropylpyridine (14.51 g, 0.1197 mol), paraformaldehyde (21.57 g, 0.7184 mol) and water (15 mL), and heated to 160 °C. After 2 days, the reaction mixture was cooled down to room temperature. The unreacted 2-isopropylpyridine was removed by steam distillation, and the liquid residue was evaporated on a steam bath until distillation stopped at 100 °C. The mixture was fractionated by silica gel column chromatography using a solvent mixture of *n*-hexane/acetone of varying composition, starting from 100% *n*-hexane. Pure 2-(pyridin-1,1-dimethyl)ethan-2-ol was obtained at a 80/20 v/v *n*-hexane/acetone solvent composition (3.2 g, 17.68% yield). 2-(Pyridin-1,1-dimethyl)ethan-2-ol was characterized using ^{1}H and ^{13}C NMR spectroscopy. **^{1}H NMR ($CDCl_3$, δ):** 1.30 ppm (s, (CH_3)$_2$C-, 6 H), 3.71 ppm (s, -C(CH_3)$_2$CH_2OH, 2 H), 4.85 ppm (m, -CCH_2O*H*, 1 H), 7.11 ppm (m, aromatic, *J* = 2.68 and 4.88, 1H), 7.28 ppm (d, aromatic, *J* = 8.20, 1 H), 7.64 ppm (m, aromatic, *J* = 1.89 and 7.72, 1 H), 8.43 ppm (d, aromatic, *J* = 3.94, 1 H). **^{13}C NMR ($CDCl_3$, δ):** 25.51 ppm (s, (CH_3)$_2$C-, 2 C), 41.02 ppm (s, -*C*(CH_3)$_2$, 1 C), 71.94 ppm (s, -C*C*H_2OH, 1 C), 120.30 ppm (s, aromatic, 1 C), 121.20 ppm (s, aromatic, 1 C), 136.90 ppm (s, aromatic, 1 C), 147.67 ppm (s, aromatic, 1 C), 168.20 ppm (s, aromatic, 1 C).

Synthesis of 2PyEdimeMA. The synthesis of 2PyEdimeMA was achieved by the esterification of 2-methyl-2-(pyridin-2-yl)propan-1-ol with 30% molar excess of methacryloyl chloride. To this end, to a 100-mL round-bottomed flask containing a magnetic stirring bar, and kept under an inert atmosphere, were transferred 3.2 g of 2-methyl-2-(pyridin-2-yl)propan-1-ol (0.0212 mol), 23.61 mL Et_3N (17.13 g, 0.1693 mol) and absolute THF (20.0 mL), which were thermostated at 0 °C. Then, methacryloyl chloride (2.69 mL, 2.88 g, 0.0275 mol) was added dropwise using a glass syringe and the reaction mixture was stirred for 2 h at 0 °C. Subsequently, the mixture was filtered and passed twice through a basic alumina column to remove methacrylic acid (hydrolysis product of excess methacryloyl chloride) and any other acidic impurities. The solvent was

evaporated off to give 2.76 g of pure 2PyEdimeMA monomer (59.48% yield). 2PyEdimeMA was characterized using ^{1}H and ^{13}C NMR spectroscopy. **^{1}H NMR (d_6-DMSO, δ):** 1.34 ppm (s, (CH_3)$_2$CH-, 6 H), 1.77 ppm (s, CH_2=CCH_3, 3 H), 4.29 ppm (s, -CCH_2O-, 2 H), 5.56 ppm (s, CH_2=CCH$_3$ H *trans* to CO_2, 1 H), 5.86 ppm (s, CH_2=CCH$_3$ H *cis* to CO_2, 1 H), 7.21 ppm (m, aromatic, J = 2.68 and 4.73, 1H), 7.43 ppm (d, aromatic, J = 7.88, 1 H), 7.73 ppm (m, aromatic, J = 1.89 and 7.56, 1 H), 8.52 ppm (d, aromatic, J = 3.78, 1 H). **^{13}C NMR (d_6-DMSO, δ):** 17.69 ppm (s, (CH_3)$_2$C-, 2 C), 24.56 ppm (s, CH_2=CCH_3, 1 C), 40.67 ppm (s, -C(CH$_3$)$_2$, 1 C), 71.93 ppm (s, -CCH_2O, 1 C), 119.94 ppm (s, aromatic, 1 C), 121.28 ppm (s, aromatic, 1 C), 125.33 ppm (s, CH_2=CCH$_3$, 1 C), 135.73 ppm (s, CH_2=CCH$_3$, 1 C), 136.36 ppm (s, aromatic, 1), 148.40 ppm (s, aromatic, 1 C), 164.56 ppm (s, aromatic, 1 C), 166.18 ppm (s, CO_2, 1 C).

2.2.2.7 Synthesis of tetrahydro-2H-pyran-2-yl methacrylate (THPMA). The THPMA monomer was prepared by the esterification reaction of MAA with a 100% excess of 3,4-dihydro-2*H*-pyran.[291] To this end, 3,4-dihydro-2*H*-pyran (21.51 mL, 19.84 g, 0.2358 mol), methacrylic acid (10 mL, 10.15 g, 0.1179 mol) and a small amount of DPPH were transferred to a 100-mL two-neck round-bottomed flask containing a magnetic stirring bar. The solution was stirred at 65 °C over a 48 h period. The mixture was passed twice through a basic alumina column to remove methacrylic acid and any other protonic impurities. Then, the solvent was evaporated off to give pure monomer in 60% yield. Finally, THPMA was stirred over CaH_2 in the presence of DPPH to remove all moisture and the last traces of acidic impurities. THPMA was characterized using ^{1}H and ^{13}C NMR spectroscopy. **^{1}H NMR (CDCl$_3$, δ):** 1.4 – 1.8 ppm (m, -CH_2CH_2CH_2-, 6 H), 1.95 ppm (s, CH_2=CCH_3, 3 H), 3.6 – 3.9 ppm (m, -OCH_2CH$_2$-, J = 11.66, 2 H), 5.6 ppm (s, olefinic H *trans* to CO_2, 1 H), 6.05 ppm (t, O-CH-O, 1 H), 6.15 ppm (s, olefinic H *cis* to CO_2, 1 H). **^{13}C NMR (CDCl$_3$, δ):** 18.1 ppm (s, CH_2=CCH_3, 1 C), 18.51 ppm (s, -CH_2CH_2-, 1 C), 24.9 ppm (s, -CH$_2$CH$_2$-, 1 C), 29.15 ppm (s, -CH$_2$CH_2-, 1 C), 63.1 ppm (s, -OCH$_2$CH$_2$-, 1 C), 92.7 ppm (s, O-CH-O, 1 C), 125.8 ppm (s, CH_2=CCH$_3$, 1 C), 136.4 ppm (s, CH_2=CCH$_3$, 1 C) and 165.8 ppm (s, CO_2, 1 C).

2.2.3 Synthesis of the 2,6-pyridinediethanol di(2-bromo-2-methyl propanoate) (PyDEDBrMeP) degradable bifunctional ATRP initiator

The synthesis of the bifunctional ATRP initiator PyDEDBrMeP was accomplished by the esterification of 2,6-pyridinediethanol with 40% molar excess of α-bromoisobutyryl bromide.[290] 2,6-Pyridinediethanol was prepared following the method of Kelly et al.[292]

which was based on the high-pressure, high-temperature, aqueous hydroxymethylation of 2,6-lutidine using paraformaldehyde following the old, low-yield procedure of Löffler and Thiel.[293] Briefly, 2,6-pyridinediethanol was prepared from the reaction of 2,6-lutidine with paraformaldehyde in water under conditions of elevated pressure and temperature.

Synthesis of 2,6-pyridinediethanol. 2,6-Pyridinediethanol was prepared from the reaction of 2,6-lutidine with paraformaldehyde in water under conditions of elevated pressure and temperature. To this end, 2,6-lutidine (50 mL, 46.26 g, 0.4317 mol), paraformaldehyde (25.92 g, 0.8634 mol of formaldehyde units) and H_2O (25 mL) were transferred to a 500-mL round-bottomed pressure flask with an Ace-Thread 15 PTFE front-seal plug, containing a magnetic stirring bar. The mixture was stirred and heated at 135 °C for 12 h. Subsequently, the reaction mixture was cooled down to room temperature, and a few drops of sodium carbonate solution were then added to it. The unreacted 2,6-lutidine was removed by steam distillation, and the residue was evaporated on a steam bath until the distillation stopped at 100 °C. Afterwards, potassium carbonate was added and the resulting (mixture of) organic bases was extracted with chloroform (3 × 200 mL). Then, the solvent was removed, and the by-product, 2-(6-methylpyridin-2-yl)ethanol, was distilled off on the vacuum line at 80 °C. The residue was a mixture of two isomeric diols, 2,6-pyridinediethanol and the side product 2-(6-methylpyridin-2-yl)propane-1,3-diol. The mixture was separated by column chromatography (*n*-hexane/acetone) in a solvent mixture of varying composition, starting with a 90/10 *n*-hexane/acetone mixture. Pure 2-(6-methylpyridin-2-yl)propane-1,3-diol eluted at a 65/35 *n*-hexane/acetone solvent composition (5 g, 6.5%), while pure 2,6-pyridinediethanol (1.2 g, 1.6%) eluted at a 35/65 *n*-hexane/acetone composition. The diols were characterized using ^{1}H and ^{13}C NMR spectroscopy, and differential scanning calorimetry. **^{1}H NMR 2,6-pyridinediethanol ($CDCl_3$, δ):** 2.90 ppm (t, -CH_2-CH_2OH, J = 6.31, 4 H), 3.90 ppm (t, -C$H_2$$CH_2$OH, J = 6.31, 4 H), 4.50 ppm (s, -CH_2-CH_2O*H*, 2 H), 6.95 ppm (d, aromatic, J = 7.72, 2H), 7.45 ppm (t, aromatic, J = 7.72, 1 H). **^{13}C NMR ($CDCl_3$, δ):** 39.56 ppm (s, -*C*H_2-CH_2OH, 2 C), 61.39 ppm (s, -CH_2*C*H_2-OH, 2 C), 121.06 ppm (s, aromatic, 2 C), 136.94 ppm (s, aromatic, 1 C), 158.86 ppm (s, aromatic, 2 C). **^{1}H NMR (2-(6-methylpyridin-2-yl)propane-1,3-diol) ($CDCl_3$, δ):** 2.43 ppm (s, -CH_3, 3 H), 2.95 ppm (m, -C*H*-$(CH_2OH)_2$, J = 5.04, 1 H), 3.95 – 4.00 ppm (m, -CH-CH_2OH, J = 11.03, 4 H), 4.70 ppm (s, -CH-CH_2O*H*, 2 H), 6.98 ppm (m, aromatic, J = 4.10, 2 H), 7.47 ppm (t, aromatic, J = 7.57, 1 H). **^{13}C NMR ($CDCl_3$, δ):** 23.83 ppm (s, -*C*H_3, 1 C), 48.70 ppm (s, -*C*H-CH_2-OH, 1 C), 62.88 ppm (s, -CH-

CH_2OH, 2 C), 119.96 ppm (s, aromatic, 1 C), 121.14 ppm (s, aromatic, 1 C), 136.70 ppm (s, aromatic, 1 C), 156.95 ppm (s, aromatic, 1 C), 160.61 ppm (s, aromatic, 1 C).

Synthesis of PyDEDBrMeP. The PyDEDBrMeP degradable bifunctional ATRP initiator was prepared by the esterification of 2,6-pyridinediethanol with 40% molar excess of *α*-bromoisobutyryl bromide. To this end, 2,6-pyridinediethanol (1.0 g, 0.0060 mol), Et_3N (13.34 mL, 9.68 g, 0.0957 mol) and absolute THF (6.25 mL) were transferred to a 100-mL round-bottomed flask containing a magnetic stirring bar. The solution was stirred and cooled down to 0 °C. After stabilization of the temperature, *α*-bromoisobutyryl bromide (2.07 mL, 3.85 g, 0.0167 mol) was added dropwise using a glass syringe and the reaction was stirred for 2 h at 0 °C. Subsequently, the mixture was filtered and passed twice through a basic alumina column to remove 2-bromo-2-methylpropionic acid (hydrolysis product of excess *α*-bromoisobutyryl bromide) and any other acidic impurities. Finally, PyDEDBrMeP was purified by silica gel column chromatography using an 80/20 v/v *n*-hexane/ethyl acetate solvent mixture, and it was obtained as a transparent yellowish oil (1.78 g, 64%). PyDEDBrMeP was characterized using ^{1}H and ^{13}C NMR spectroscopy. **^{1}H NMR ($CDCl_3$, *δ*, ppm):** 1.84 (s, -CC*H*$_3$, 12 H), 3.11 (t, -C*H*$_2$CH$_2$O, *J* = 6.62, 4 H), 4.53 (t, -CH$_2$C*H*$_2$O, *J* = 6.62, 4 H), 7.05 (d, aromatic, *J* = 7.57, 2 H), 7.52 (t, aromatic, *J* = 7.72, 1 H). **^{13}C NMR ($CDCl_3$, *δ*, ppm):** 30.65 (s, -C*C*H$_3$, 4 C), 36.93 (s, -CH$_2$*C*H$_2$O, 2 C), 55.71 (s, -*C*(CH$_3$)$_2$, 2 C), 65.08 (s, -*C*H$_2$CH$_2$O, 2 C), 121.44 (s, aromatic, 2 C), 136.59 (s, aromatic, 1 C), 157.32 (s, aromatic, 2 C), 171.44 (s, *C*O$_2$, 2 C).

2.2.4 Synthesis of the 2,6-pyridinedimethanol di(2-bromo-2-methyl propanoate) (PyDMDBrMeP) bifunctional ATRP initiator.

The synthesis of the more stable bifunctional ATRP initiator, PyDMDBrMeP, was accomplished in a similar way as that for its degradable by the esterification of 2,6-pyridinedimethanol with 40% molar excess of *α*-bromoisobutyryl bromide.[280]

Synthesis of 2,6-pyridinedimethanol di(2-bromo-2-methyl propanoate) (PyDMDBrMeP). 2,6-Pyridinedimethanol (2.0 g, 0.0143 mol), Et_3N (32.07 mL, 23.27 g, 0.2299 mol) and absolute THF (25 mL) were transferred to a 250-mL round-bottomed flask containing a magnetic stirring bar. The solution was stirred and cooled down to 0 °C. After stabilization of the temperature, *α*-bromoisobutyryl bromide (4.97 mL, 9.25 g, 0.0402 mol) was added dropwise using a glass syringe and the reaction was stirred for 2 h at 0 °C. Subsequently, the mixture was filtered and passed twice through a basic alumina column to remove 2-bromo-2-methylpropionic acid (hydrolysis product of excess *α*-bromoisobutyryl

bromide) and any other acidic impurities. Finally, PyDMDBrMeP was purified by silica gel column chromatography using an 80/20 v/v *n*-hexane/ethyl acetate solvent mixture, and it was obtained as a transparent yellowish oil in 60.5% yield (3.80 g). PyDMDBrMeP was characterized by ^{1}H and ^{13}C NMR spectroscopy. **^{1}H NMR ($CDCl_3$, δ, ppm):** 1.98 (s, -CC*H*$_3$, 12 H), 5.30 (s, -C*H*$_2$O, 4 H), 7.35 (d, aromatic, *J* = 7.72, 2 H), 7.65 (d, aromatic, *J* = 7.88, 1 H). **^{13}C NMR ($CDCl_3$, δ, ppm):** 30.76 (s, -C*C*H$_3$, 4 C), 55.43 (s, -*C*(CH$_3$)$_2$, 2 C), 67.55 (s, -*C*H$_2$O, 2 C), 120.19 (s, aromatic, 2 C), 137.60 (s, aromatic, 1 C), 155.14 (s, aromatic, 2 C), 171.16 (s, *C*O$_2$, 2 C).

2.2.5 Synthesis of the 2,6-pyridinediethanol dimethacrylate (PyDMA) degradable cross-linker.

PyDMA was prepared from the esterification of 2,6-pyridinediethanol with excess methacryloyl chloride in absolute tetrahydrofuran in the presence of excess triethylamine base.[279]

Synthesis of PyDMA. The PyDMA cross-linker was prepared by the esterification of 2,6-pyridinediethanol with 40% molar excess of methacryloyl chloride. In particular, 2,6-pyridinediethanol (2.4 g, 0.0144 mol; two purified batches), Et_3N (32 mL, 23.24 g, 0.2296 mol) and absolute THF (15 mL) were transferred to a 100-mL round-bottomed flask containing a magnetic stirring bar. The solution was stirred and cooled down to 0 °C. After stabilization of the temperature, methacryloyl chloride (3.93 mL, 4.2 g, 0.0402 mol) was added dropwise using a glass syringe and the reaction was stirred for 2 h at 0 °C. Subsequently, the mixture was filtered and passed twice through a basic alumina column to remove methacrylic acid (hydrolysis product of excess methacryloyl chloride) and any other acidic impurities. Then, the solvent was evaporated off to give pure cross-linker in 60% yield. Afterwards, PyDMA was stirred for at least 24 h over CaH_2 to remove all the moisture and the last traces of protonic impurities, and was, finally, filtered just prior to the polymerizations. The thus-purified PyDMA was characterized using ^{1}H and ^{13}C NMR spectroscopy. **^{1}H NMR (d_6-DMSO, δ):** 1.88 ppm (s, CH$_2$=CC*H*$_3$, 6 H), 3.12 ppm (t, -C*H*$_2$CH$_2$O, *J* = 6.62, 4 H), 4.50 ppm (t, -CH$_2$C*H*$_2$O, *J* = 6.62, 4 H), 5.51 ppm (s, C*H*$_2$=CCH$_3$ H *trans* to CO$_2$, 2 H), 6.03 ppm (s, C*H*$_2$=CCH$_3$ H *cis* to CO$_2$, 2 H), 7.04 ppm (d, aromatic, *J* = 7.72, 2 H), 7.53 ppm (t, aromatic, *J* = 7.57, 1 H). **^{13}C NMR (d_6-DMSO, δ):** 17.77 ppm (s, CH$_2$=C*C*H$_3$, 2 C), 36.41 ppm (s, -CH$_2$*C*H$_2$O, 2 C), 63.44 ppm (s, -*C*H$_2$CH$_2$O, 2 C), 121.10 ppm (s, aromatic, 2 C), 125.40 ppm (s, *C*H$_2$=CCH$_3$, 2 C), 135.78

ppm (s, CH_2=*C*CH_3, 2 C), 136.74 ppm (s, aromatic, 1 C), 157.32 ppm (s, aromatic, 2 C), 166.33 ppm (s, *C*O_2, 2 C).

2.2.6 Synthesis of the 2-(6-(2-((2-bromo-2-methylpropanoyl)oxy)ethyl)pyridin-2-yl)ethyl methacrylate (PyDEBrMA) degradable ATRP Inimer. The synthesis of the cleavable *inimer* PyDEBrMA was achieved by the two-step esterification of 2,6-pyridinediethanol, first with *α*-bromoisobutyryl bromide, and, subsequently, with methacryloyl chloride.[281] Column chromatography purification of the product of the first esterification was performed before proceeding to the second esterification. The PyDEBrMA final product was also purified by column chromatography.

Synthesis of 2-(6-(2-hydroxyethyl)pyridin-2-yl)ethyl 2-bromo-2-methylpropanoate. 2,6-Pyridinediethanol was partially esterified with a sub-stoichiometric amount of *α*-bromoisobutyryl bromide (32.4% relative to the hydroxyl groups of 2,6-pyridinediethanol), in order to synthesize the intermediate monoester that is a monofunctional ATRP initiator, 2-(6-(2-hydroxyethyl)pyridin-2-yl)ethyl 2-bromo-2-methylpropanoate. For this reaction, 3.56 g of 2,6-pyridinediethanol (0.0213 mol), 23.75 mL Et_3N (17.23 g, 0.1703 mol) and absolute THF (22.3 mL) were transferred into a 250-mL round-bottomed flask containing a magnetic stirring bar, and kept under an inert argon atmosphere. Afterwards, the flask and its contents were thermostated at 0 °C. Then, *α*-bromoisobutyryl bromide (1.71 mL, 3.18 g, 0.0138 mol) was added dropwise using a glass syringe and the reaction was stirred for 2 h at 0 °C. Subsequently, the mixture was filtered and passed twice through a basic alumina column to remove *α*-bromoisobutyric acid (the hydrolysis product of *α*-bromoisobutyryl bromide) and any other acidic impurities. Then, the solvent was evaporated off, and the mixture was separated by silica gel column chromatography (*n*-hexane/ethyl acetate) in a solvent mixture of varying composition, starting with a 100% *n*-hexane. Pure intermediate monofunctional ATRP initiator was obtained at a 50/50 v/v *n*-hexane/ethyl acetate solvent composition (1.2 g, 27.5% yield). 2-(6-(2-Hydroxyethyl)pyridin-2-yl)ethyl 2-bromo-2-methylpropanoate was characterized using ^{1}H and ^{13}C NMR spectroscopy. **^{1}H NMR ($CDCl_3$, *δ*):** 1.87 ppm (s, (CH_3)$_2$C-, 6 H), 3.02 ppm (t, -C$H_2$$CH_2$OH, *J* = 5.36, 2 H), 3.26 ppm (m, -C$H_2$$CH_2$O, *J* = 6.62, 2 H), 4.01 ppm (t, -CH_2CH_2OH, *J* = 5.52, 2 H), 4.56 ppm (t, CH_2CH_2O, *J* = 6.62, 2 H), 7.04 ppm (d, aromatic, *J* = 7.72, 1H), 7.11 ppm (d, aromatic, *J* = 7.57, 1 H), 7.59 ppm (t, aromatic, *J* = 7.72, 1 H). **^{13}C NMR ($CDCl_3$, *δ*):** 30.66 ppm (s, (CH_3)$_2$C-Br, 2 C), 36.71 ppm (s, *C*$H_2$$CH_2$O-, 1 C), 38.41 ppm (s, *C*$H_2$$CH_2$OH, 1 C), 55.72 ppm (s, (CH_3)$_2$*C*-Br, 1 C), 61.73 ppm (s, CH_2*C*H_2OH, 1 C), 64.82 ppm (s, CH_2*C*H_2O-, 1

C), 121.53 ppm (s, aromatic, 2 C), 137.41 ppm (s, aromatic, 1 C), 156.62 ppm (s, aromatic, 1 C), 160.42 ppm (s, aromatic, 1 C), 171.49 ppm (s, CO_2, 1 C).

Synthesis of PyDEBrMA. The synthesis of the PyDEBrMA inimer was achieved by the esterification reaction of the intermediate monofunctional ATRP initiator, 2-(6-(2-hydroxyethyl)pyridin-2-yl)ethyl 2-bromo-2-methylpropanoate, with a 25% molar excess of methacryloyl chloride. In particular, in a 100-mL round-bottomed flask containing a magnetic stirring bar, kept under an inert argon atmosphere, were transferred 1.2 g of the intermediate monofunctional ATRP initiator (0.0038 mol), 4.23 mL Et_3N (3.07 g, 0.0303 mol) and absolute THF (7.5 mL). Afterwards, the flask and its contents were thermostated at 0 °C. Then, methacryloyl chloride (0.46 mL, 0.50 g, 0.0047 mol) was added dropwise using a glass syringe and the reaction was stirred for 2 h at 0 °C. Subsequently, the mixture was filtered and passed twice through a basic alumina column to remove methacrylic acid (the hydrolysis product of excess methacryloyl chloride) and any other acidic impurities. Then, the solvent was evaporated off, and the mixture was separated by silica gel column chromatography (*n*-hexane/ethyl acetate) in a solvent mixture of varying composition, starting with a 100% *n*-hexane. Pure PyDEBrMA was obtained at a 80/20 v/v *n*-hexane/ethyl acetate solvent composition (0.91 g, 63% yield). PyDEBrMA was characterized using ^{1}H and ^{13}C NMR spectroscopy. **^{1}H NMR (d_6-DMSO, δ):** 1.79 ppm (s, $(CH_3)_2$C-, 6 H), 1.81 ppm (s, CH_2=CCH_3, 3 H), 3.05 ppm (m, CH_2CH_2O, J = 3.15, 4 H), 4.41 – 4.49 (m, CH_2CH_2O, J = 6.62, 4 H), 5.61 ppm (s, CH_2=CCH_3 H *trans* to CO_2, 1 H), 5.92 ppm (s, CH_2=CCH_3 H *cis* to CO_2, 1 H), 7.16 ppm (t, aromatic, J = 6.78, 2H), 7.65 ppm (t, aromatic, J = 7.72, 1 H). **^{13}C NMR (d_6-DMSO, δ):** 17.83 ppm (s, -CH_3CH, 1 C), 30.07 ppm (s, $(CH_3)_2$CBr, 2 C), 36.09 ppm (s, CH_2CH_2O-(Br), 1 C), 36.40 ppm (s, CH_2CH_2O-, 1 C), 57.00 ppm (s, $(CH_3)_2$CBr, 1 C), 63.48 ppm (s, CH_2CH_2O-(Br), 1 C), C), 64.64 ppm (s, CH_2CH_2O-, 1 C), 121.22 ppm (s, aromatic, 1 C), 121.26 ppm (s, aromatic, 1 C), 125.54 ppm (s, CH_2=CCH_3, 1 C), 135.76 ppm (s, CH_2=CCH_3, 1 C), 136.78 ppm (s, aromatic, 1 C), 156.96 ppm (s, aromatic, 1 C), 157.32 ppm (s, aromatic, 1 C), 166.35 ppm (s, CO_2, 1 C), 170.58 ppm (s, CO_2-(Br), 1 C).

2.3 Polymer Synthesis

Within this PhD Thesis, we synthesized polymers of various structures, including linear and hyperbranched (co)polymers, and randomly cross-linked as well as end-linked (co)polymer networks. The preparation of these polymers was accomplished using three polymerization methods: reversible addition-fragmentation chain transfer (RAFT)

polymerization,[230,233] group transfer polymerization (GTP),[234,237] and atom transfer radical polymerization (ATRP).[225,227] These polymerization methods are suitable for (meth)acrylate monomers, ensuring their controlled polymerization, with the resulting polymers having molecular weights close to the theoretical, and narrow molecular weight distributions. In fact, most of the monomers could be polymerized *via* any of the three methods. The monomers whose polymerization required special care were 2PyEMA and 4PyEMA whose thermal lability precluded their RAFT polymerization typically performed at 65 °C. Thus, GTP was used for p2PyEMA preparation at a polymerization temperature of 0 °C. In the case of 4PyEMA, its extreme thermal lability and reactivity led to the use of ATRP, which can tolerate presence of moisture the monomer (thus avoiding heating necessary for vacuum distillation), and it can also be performed at room temperature (26 °C). A key factor for the success process of GTP is the purification of the monomer, solvent and initiator from moisture, thus the monomers of the homopolymers of 2PyMMA, 2PyPMA, 3PyMMA and 3PyPMA were also synthesized following the same procedure (at 0 °C), which were prior distilled in a vacuum line, were polymerized using GTP following the same procedure. Finally all related polymers were synthesized using RAFT polymerization.

Polymers with various compositions and architectures were synthesized. In total, nine linear poly(pyridinylalkyl methacrylate)s and six related linear polymers were synthesized using the above-mentioned polymerization methods. Additionally, linear (co)polymers and end-linked polymer networks cleavable in the middle of the polymer chain, either thermally or under alkaline hydrolysis conditions, were prepared *via* ATRP using a degradable bifunctional initiator, PyDEDBrMeP. Furthermore, linear (co)polymers and end-linked polymer networks were also synthesized using the more stable bifunctional ATRP initiator, PyDMDBrMeP. PyDMA cross-linker was homopolymerized using RAFT polymerization, at relatively low and at higher concentrations to produce a hyperbranched soluble polymer and an insoluble polymer network, respectively, and also was randomly copolymerized with MMA to obtain again an insoluble polymer network. Furthermore, four hyperbranched MMA copolymers containing the degradable PyDMA cross-linker, with variable molar ratio of PyDMA to CTA (1, 2, 3 and 4), were synthesized. Finally, the inimer, PyDEBrMA, was (co)polymerized using self-condensing vinyl atom transfer radical polymerization (SCVP-ATRP) with MMA to prepare hyperbranched hydrophobic homopolymers, and also a series of hyperbranched amphiphilic copolymers bearing the hydrophilic DMAEMA in the core and the hydrophobic MMA in shell.

2.3.1 Synthesis of Linear Homopolymers.

The preparation of linear homopolymers from all synthesized monomers was accomplished using three different polymerization methods, RAFT polymerization, GTP, and ATRP, all three of which are suitable for methacrylate monomers. Below is described the synthesis of the $2PyEMA_5$, $3PyEMA_{50}$ and $4PyEMA_{50}$ homopolymers.

2.3.1.1 Synthesis of linear $2PyEMA_{55}$ Homopolymer by GTP. To a 50 mL round-bottomed flask, containing a magnetic stirring bar, loaded with a catalytic amount of TBABB (~20 mg, ~40 μmol, ~4% mol relative to the initiator), and kept under an inert argon atmosphere, were added 0.3 mL of the MTS initiator (0.258 g, 1.48 mmol) and 45.10 mL freshly distilled THF, and was thermostated at 0 °C. Afterwards, 15.56 mL of freshly distilled 2PyEMA (15.56 g, 81.37 mmol) was slowly added using a glass syringe producing an exotherm (26 – 38 °C). The polymer was precipitated in *n*-hexane and dried *in vacuo* for 48 h. A key factor for the success process of GTP is the purification of the monomer, solvent and initiator from moisture, thus the monomers of 2PyMMA, 2PyPMA, 3PyMMA and 3PyPMA, which were prior distilled in a vacuum line, were polymerized using GTP following the same procedure.

2.3.1.2 Synthesis of linear $3PyEMA_{50}$ Homopolymer by RAFT polymerization. AIBN (0.0150 g, 0.0913 mmol), CPDB (0.0323 g, 0.1461 mmol) and 3PyEMA (1.4 g, 7.3218 mmol) were dissolved in 1,4-dioxane (1.0 mL), and the resulting solution was transferred into a 50 mL round-bottomed flask, fitted with a glass valve, and containing a magnetic stirring bar. The system was degassed by three freeze-pump-thaw cycles and was subsequently placed in an oil bath thermostated at 65 °C for 22 h. The polymer was precipitated in *n*-hexane and dried *in vacuo* for 48 h. The homopolymers of 4PyMMA, 4PyPMA, PheMA, FMMA, 2PyEMAAm, 2PyESMA, 2PyEmeMA and 2PyEdimeMA were also synthesized following the same procedure.

2.3.1.3 Synthesis of linear $4PyEMA_{50}$ Homopolymer by ATRP. CuCl (0.0103 g, 0.1046 mmol), EBiB (0.0204 g, 15.35 μL, 0.1046 mmol), 4PyEMA (1.00 g, 5.2299 mmol) and HMTETA (0.0241 g, 28.45 μL, 0.1046 mmol) were dissolved in anisole (1.0 mL), and the resulting solution was transferred into a 50 mL round-bottomed flask, fitted with a glass valve, and containing a magnetic stirring bar. The system was degassed by three freeze-pump-thaw cycles. During every cycle, the flask was filled with argon. Finally, the flask was placed in an oil bath thermostated at 26 °C for 3 days. The polymer was passed

through a neutral alumina column to remove the CuCl catalyst, precipitated in *n*-hexane, and dried *in vacuo* for 48 h.

2.3.2 Synthesis of linear ABC triblock terpolymers.

Below is described the synthesis of two ABC triblock terpolymers, one by GTP with nominal DP equal to 15, and the other by RAFT polymerization with DP 80. The ABC triblock terpolymers were based on 2PyEMA, THPMA and BzMA, which can be converted to MAA units by alkaline hydrolysis, acidic hydrolysis and catalytic hydrogenolysis, respectively.

2.3.2.1 Synthesis of linear $BzMA_5$-b-$2PyEMA_5$-b-$THPMA_5$ triblock terpolymer by GTP. A catalytic amount of TBABB was transferred to a 50-mL round-bottomed flask containing a stirring bar. The flask was immediately sealed with a rubber septum, and it was purged with dry argon. Subsequently, 9.8 mL of freshly distilled THF was transferred into the flask *via* a glass syringe, followed by the addition of 0.3 mL of the MTS initiator (0.258 g, 1.48 mmol). Then, 1.25 mL of BzMA (1.30 g, 7.4 mmol) was slowly added using a glass syringe, producing an exotherm (–20 – –17 °C). The exotherm abated within 5 min, and samples (2 × 0.1 mL) were withdrawn for analyses by gel permeation chromatography (GPC) (GPC number-average molecular weight = M_n = 1570 g mol^{-1} compared to the theoretical value expected on the basis of the monomer-initiator feed ratio of 980 g mol^{-1}; molecular weight dispersity = $Đ = M_w/M_n$ = 1.37; M_w is the weight-average molecular weight) and ^{1}H NMR spectroscopy (complete monomer conversion; degree of polymerization, DP, determined to be 5 by end-group analysis, identical to the theoretically expected value). Afterwards, 1.42 mL of PyEMA (1.42 g, 7.4 mmol) was slowly added using a glass syringe, producing an exotherm (–20 – –17 °C). The exotherm abated within 5 min, and samples (2 × 0.1 mL) were extracted for analyses by GPC (GPC M_n = 2060 g mol^{-1} compared to the theoretically expected value of 1940 g mol^{-1}; $Đ$ = 1.40) and ^{1}H NMR spectroscopy (100% monomer conversion; PyEMA content in copolymer = 50% mol compared to 50% mol expected from the comonomer feed ratio and given complete comonomer conversion). Afterwards, 1.22 mL of THPMA (1.26 g, 7.4 mmol) was slowly added using a glass syringe, producing an exotherm (–20 – –18 °C). The exotherm abated within 10 min, 0.5 mL methanol was added to terminate the polymerization, and samples (2 × 0.1 mL) were again obtained for analyses by GPC (GPC M_n = 3160 g mol^{-1} compared to the theoretically expected value of 2790 g mol^{-1}; $Đ$ = 1.36) and ^{1}H NMR spectroscopy (complete monomer conversion; THPMA content in the triblock terpolymer = 33% mol

compared to 33% mol expected from the comonomer feed ratio and given complete comonomer conversion).

2.3.2.2 Synthesis of linear BzMA$_{20}$-b-THPMA$_{20}$-b-[THPMA$_{20}$-co-2PyEMA$_{20}$] triblock terpolymer by RAFT polymerization. The BzMA$_{20}$-*b*-THPMA$_{20}$-*b*-(THPMA$_{20}$-*co*-PyEMA$_{20}$) triblock terpolymer was synthesized by a three-step sequential polymerization. AIBN (0.0454 g, 0.2766 mmol) and 2-(cyanoprop-2-yl) dithiobenzoate (CPDB) RAFT CTA (0.0979 g, 0.4426 mmol) was dissolved in 1,4-dioxane (1.45 mL) and was transferred to a 50-mL round-bottomed flask, fitted with a glass valve, containing BzMA (1.5 mL, 1.56 g, 8.85 mmol) and a magnetic stirring bar. This resulted in a monomer solution at a concentration of 3 M. The system was degassed by three freeze-pump-thaw cycles and was subsequently placed in an oil bath at 65 °C for 24 h. Monomer conversion, measured by ^{1}H NMR spectroscopy, was 100%, whereas poly(BzMA) molecular weight characteristics, as measured by GPC, were: M_n = 6880 g mol^{-1} (theoretically expected molecular weight = 3500 g mol^{-1}) and $Đ$ = 1.3. Afterwards, 1.45 mL of THPMA (1.51 g, 8.85 mmol) and Et_3N (0.2 mL), in order to protect THPMA from spontaneous hydrolysis,[31] were added to the solution of poly(BzMA). Monomer conversion, measured by ^{1}H NMR spectroscopy, was 100%, whereas BzMA$_{20}$-*b*-THPMA$_{20}$ molecular weight characteristics, as measured by GPC, were: M_n = 10700 g mol^{-1} (theoretically expected molecular weight = 6900 g mol^{-1}) and $Đ$ = 1.34. Afterwards, 1.45 mL of THPMA (1.51 g, 8.85 mmol) and 1.69 mL of PyEMA (1.69 g, 8.85 mmol) were added to the active diblock copolymer BzMA$_{20}$-*b*-THPMA$_{20}$. Monomer conversion, measured by ^{1}H NMR spectroscopy, was 100% for THPMA and 88% for PyEMA, whereas the BzMA$_{20}$-*b*-THPMA$_{20}$-*b*-(THPMA$_{20}$-*co*-PyEMA$_{20}$) molecular weight characteristics, as measured by GPC, were: M_n = 16200 g mol^{-1} (theoretically expected molecular weight = 13300 g mol^{-1}) and $Đ$ = 1.31. The polymer was purified by precipitation in *n*-hexane and dried *in vacuo* for 48 hours.

2.3.3 Synthesis of Linear (Co)Polymers and End-linked Homopolymer Networks Using PyDEDBrMeP Initiator by ATRP.

Below is described the synthesis of one linear MMA homopolymer bearing the PyDEDBrMeP initiator and one linear amphiphilic MMA-DMAEMA triblock copolymer bearing the PyDEDBrMeP initiator. Additionally, is described the synthesis of a series of end-linked homopolymer networks using PyDEDBrMeP bifunctional initiator, with overall total nominal (targeted) degree of polymerization of MMA equal to 100, whereas the

EGDMA-to-initiator molar ratio varied at the values 1.0, 2.0 and 4.0. When the molar ratio of EGDMA-to-initiator was equal to 1.0, no network was formed, but, a (soluble) hyperbranched polymer was obtained. The same procedure followed for the preparation of linear MMA homopolymers, end-linked homopolymer networks and amphiphilic ABA diblock copolymers using the more stable PyDMDBrMeP bifunctional ATRP initiator.

2.3.3.1 Synthesis of linear MMA_{100}-b-PyDEDBrMeP-b-MMA_{100} Homopolymer by ATRP. To a 50-mL round-bottomed flask, fitted with a glass valve, were transferred PyDMDBrMeP (0.0204 g, 0.0467 mmol), CuCl (0.0046 g, 0.0467 mmol), HMTETA (12.71 μL, 0.0108 g, 0.0467 mmol), MMA (1.0 mL, 0.936 g, 9.3478 mmol) and anisole (1.0 mL). The system was degassed by three freeze-pump-thaw cycles. During every cycle, the flask was filled with argon. Finally, the flask was placed in an oil bath thermostated at 26 °C for 22 h. Monomer conversion as determined using ^{1}H NMR spectroscopy was 90.0%, while the M_n and $Đ$ values, as determined using GPC, were 11200 g mol^{-1} and 1.55, respectively. Finally, the polymer was passed through a neutral alumina column to remove the CuCl catalyst, precipitated in *n*-hexane, and dried *in vacuo* for 2 days.

2.3.3.2 Synthesis of linear amphiphilic $DMAEMA_{50}$-b-MMA_{50}-b-PyDEDBrMeP-b-MMA_{50}-b-$DMAEMA_{50}$ triblock copolymer by ATRP. The preparation of the amphiphilic $DMAEMA_{50}$-*b*-MMA_{50}-*b*-PyDEDBrMeP-*b*-MMA_{50}-*b*-$DMAEMA_{50}$ triblock copolymer was accomplished by the growth of DMAEMA off the ends of the MMA_{50}-*b*-PyDEDBrMeP-*b*-MMA_{50} linear homopolymer. The latter was prepared in a similar fashion to MMA_{100}-*b*-PyDEDBrMeP-*b*-MMA_{100} described in a previous paragraph. In particular, to a 50-mL round-bottomed flask, fitted with a glass valve, were transferred 0.3 g of the MMA_{50}-*b*-PyDEDBrMeP-*b*-MMA_{50} linear homopolymer (0.0341 mmol), CuCl (0.0067 g, 0.0681 mmol), HMTETA (18.54 μL, 0.0157 g, 0.0681 mmol), DMAEMA (0.5744 mL, 0.5359 g, 3.4091 mmol) and anisole (0.3 mL). The system was degassed by three freeze-pump-thaw cycles. During every cycle, the flask was filled with argon. Finally, the flask was placed in an oil bath thermostated at 26 °C for 16 h. The M_n and $Đ$ values of the resulting copolymer as determined using GPC were 13600 g mol^{-1} and 1.60, respectively, while the M_n and $Đ$ values for the precursor homopolymer, MMA_{50}-*b*-PyDEDBrMeP-*b*-MMA_{50}, were 8800 g mol^{-1} and 1.63, respectively. The conversion of the DMAEMA monomer to polymer, as measured using ^{1}H NMR spectroscopy, was 77.0% and the DMAEMA content in the copolymer was 39.5 mol%. Finally, the copolymer was passed through a neutral alumina column to remove the CuCl catalyst, precipitated in *n*-hexane, and dried *in vacuo* for 2 days. Following similar procedures, three further triblock

copolymers with the inverse architecture, BAB instead of ABA, and different compositions were also prepared: MMA_5-*b*-$DMAEMA_{50}$-*b*-PyDEDBrMeP-*b*-$DMAEMA_{50}$-*b*-MMA_5, MMA_{10}-*b*-$DMAEMA_{50}$-*b*-PyDEDBrMeP-*b*-$DMAEMA_{50}$-*b*-MMA_{10}, and MMA_{50}-*b*-$DMAEMA_{50}$-*b*-PyDEDBrMeP-*b*-$DMAEMA_{50}$-*b*-MMA_{50}.

2.3.3.3 Synthesis of the Linear Amphiphilic $DMAEMA_{50}$-b-MMA_{50}-b-PyDMDBrMeP-b-MMA_{50}-b-$DMAEMA_{50}$ triblock copolymer by ATRP. The preparation of the amphiphilic $DMAEMA_{50}$-*b*-MMA_{50}-*b*-PyDMDBrMeP-*b*-MMA_{50}-*b*-$DMAEMA_{50}$ triblock copolymer was accomplished by the growth of DMAEMA off the ends of the MMA_{50}-*b*-PyDMDBrMeP-*b*-MMA_{50} linear homopolymer. The latter was prepared in a similar fashion to MMA_{100}-*b*-PyDMDBrMeP-*b*-MMA_{100} described in a previous paragraph. In particular, to a 50-mL round-bottomed flask, fitted with a glass valve, were transferred 0.3 g of the MMA_{50}-*b*-PyDMDBrMeP-*b*-MMA_{50} linear homopolymer (0.0305 mmol), CuCl (0.0060 g, 0.0609 mmol), HMTETA (16.58 μL, 0.0140 g, 0.0609 mmol), DMAEMA (0.5137 mL, 0.4793 g, 3.0488 mmol) and anisole (0.3 mL). The system was degassed by three freeze-pump-thaw cycles. During every cycle, the flask was filled with argon. Finally, the flask was placed in an oil bath thermostated at 26 °C for 1 day. The M_n and $Đ$ values of the resulting copolymer as determined using GPC were 14300 g mol^{-1} and 1.62, respectively, while the M_n and $Đ$ values for the precursor homopolymer MMA_{50}-*b*-PyDMDBrMeP-*b*-MMA_{50} were 9840 g mol^{-1} and 1.48, respectively. The conversion of the DMAEMA monomer to polymer, as measured using ^{1}H NMR spectroscopy, was 88.8%, while the DMAEMA content in the copolymer was 50.2 mol%. Finally, the copolymer was passed through a neutral alumina column to remove the CuCl catalyst, precipitated in *n*-hexane, and dried *in vacuo* for 2 days.

2.3.3.4 Synthesis of the $EGDMA_{1.0}$-b-MMA_{50}-b-PyDEDBrMeP-b-MMA_{50}-b-$EGDMA_{1.0}$ end-linked homopolymer network. The network synthesis was achieved by the addition of EGDMA cross-linker off the ends of the MMA_{50}-*b*-PyDEDBrMeP-*b*-MMA_{50} linear homopolymer. The latter was prepared in a fashion similar to the synthesis of MMA_{100}-*b*-PyDEDBrMeP-*b*-MMA_{100} described in a previous paragraph. The synthesis of the $EGDMA_{1.0}$-*b*-MMA_{50}-*b*-PyDEDBrMeP-*b*-MMA_{50}-*b*-$EGDMA_{1.0}$ end-linked homopolymer network is detailed below. To a 50-mL round-bottomed flask, fitted with a glass valve, were transferred 0.3 g of the MMA_{50}-*b*-PyDEDBrMeP-*b*-MMA_{50} linear homopolymer (0.0341 mmol), CuCl (0.0067 g, 0.0682 mmol), HMTETA (18.54 μL, 0.0157 g, 0.0682 mmol), EGDMA (25.72 μL, 0.0270 g, 0.1363 mmol) and anisole (0.3 mL). The system

was degassed by three freeze-pump-thaw cycles. During every cycle, the flask was filled with argon. Finally, the flask was placed in an oil bath thermostated at 26 °C for 1 day.

In the case of the more stable PyDMDBrMeP bifunctional initiator, $EGDMA_{1.0}$-*b*-MMA_{50}-*b*-PyDMDBrMeP-*b*-MMA_{50}-*b*-$EGDMA_{1.0}$ end-linked homopolymer network is described below: 0.3 g of MMA_{50}-*b*-PyDMDBrMeP-*b*-MMA_{50} (0.0504 mmol), CuCl (0.0050 g, 0.0504 mmol), HMTETA (13.71 μL, 0.0116 g, 0.0504 mmol), and EGDMA (19.02 μL, 0.0199 g, 0.1008 mmol) were dissolved in anisole (0.3 mL). The system was degassed by three freeze-pump-thaw cycles. During every cycle, the flask was filled with argon. Finally, the flask was placed in an oil bath thermostated at 26 °C for 22 h.

2.3.4 Synthesis of Randomly Hyperbranched or Network Polymers Using the PyDMA Cross-linker by RAFT Polymerization.

PyDMA cross-linker was homopolymerized (composed only of cross-linker) at two different concentrations, to obtain a hyperbranched homopolymer at low concentration (0.8 M), and a homopolymer network at higher concentration (2.5 M). Additionally, a series of five randomly cross-linked MMA_{100}-*co*-PyDMA polymers with variable molar ratio of PyDMA to CTA (1, 2, 3, 4 and 8) was synthesized. In the case of the molar ratio of PyDMA to CTA equal to 8, a copolymer network was formed, while in the other four cases an MMA_{100}-*co*-PyDMA hyperbranched copolymer was formed.

2.3.4.1 Synthesis of the $PyDMA_{10}$ hyperbranched homopolymer. AIBN (0.0067 g, 0.0412 mmol) and CPDB (0.0145 g, 0.0659 mmol) were dissolved in 1,4-dioxane (0.8 mL), and the resulting solution was transferred to a 50-mL round-bottomed flask, fitted with a glass valve, containing PyDMA (0.2 g, 0.6593 mmol) and a magnetic stirring bar. The system was degassed by three freeze-pump-thaw cycles and was subsequently placed in an oil bath thermostated at 65 °C for 24 h.

2.3.4.2 Synthesis of the $PyDMA_{10}$ homopolymer network. AIBN (0.0101 g, 0.0618 mmol) and CPDB (0.0218 g, 0.0989 mmol) were dissolved in 1,4-dioxane (0.1 mL), and the resulting solution was transferred to a 50-mL round-bottomed flask, fitted with a glass valve, containing PyDMA (0.3 g, 0.9889 mmol) and a magnetic stirring bar. The system was degassed by three freeze-pump-thaw cycles and was subsequently placed in an oil bath thermostated at 65 °C for 24 h.

2.3.4.3 Synthesis of the MMA_{100}-co-$PyDMA_4$ hyperbranched polymer. AIBN (0.0096 g, 0.0584 mmol) and CPDB (0.0207 g, 0.09356 mmol) were dissolved in 1,4-dioxane (2.1

mL), and the resulting solution was transferred to a 50-mL round-bottomed flask, fitted with a glass valve, containing PyDMA (0.1134 g, 0.3739 mmol), MMA (0.9360 g, 1.00 mL, 9.3488 mmol) and a magnetic stirring bar. The system was degassed by three freeze-pump-thaw cycles and was subsequently placed in an oil bath thermostated at 65 °C for 24 h.

2.3.4.4 Synthesis of the MMA_{100}-co-$PyDMA_8$ polymer network. AIBN (0.0126 g, 0.0771 mmol) and CPDB (0.0273 g, 0.1234 mmol) were dissolved in 1,4-dioxane (2.8 mL), and the resulting solution was transferred to a 50-mL round-bottomed flask, fitted with a glass valve, containing PyDMA (0.3 g, 0.9889 mmol), MMA (1.2355 g, 1.32 mL, 12.3404 mmol) and a magnetic stirring bar. The system was degassed by three freeze-pump-thaw cycles and it was, subsequently, placed in an oil bath thermostated at 65 °C for 24 h.

2.3.5 Synthesis of Randomly Hyperbranched (Co)Polymers Using the PyDEBrMA Inimer by ATRP.

The ATRP *inimer* PyDEBrMA was used for the preparation of two MMA hyperbranched homopolymers with nominal degree of polymerization equal to 50 and 100. Furthermore, the same *inimer* was also used for the preparation of two MMA-DMAEMA amphiphilic hyperbranched diblock copolymers of molar content of DMAEMA equal to 25% and 50%.

2.3.5.1 Synthesis of the MMA_{50}-co-PyDEBrMA hyperbranched homopolymer. To a 50-mL round-bottomed flask, fitted with a glass valve, were transferred PyDEBrMA (0.1443 g, 0.3755 mmol), CuCl (0.0371 g, 0.3755 mmol), HMTETA (102.15 μL, 0.0865 g, 0.3727 mmol), MMA (2.0 mL, 1.88 g, 18.7774 mmol) and anisole (2.0 mL). The system was degassed by three freeze-pump-thaw cycles. During every cycle, the flask was filled with high purity argon. Finally, the flask was placed in an oil bath thermostated at 26 °C for 20 h. The monomer to polymer conversion was determined using ^{1}H NMR spectroscopy and found 96%, while the M_n and $Đ$ values, were measured using GPC, and were found 22800 g mol^{-1} and 2.70, respectively. Finally, the polymer was passed through a neutral alumina column to remove the CuCl catalyst, precipitated in *n*-hexane, and dried *in vacuo* for 2 days.

2.3.5.2 Synthesis of the [MMA_{50}-PyDEBrMA]-b-DMAEMA amphiphilic hyperbranched diblock copolymer. The synthesis of the hyperbranched amphiphilic [MMA_{50}-PyDEBrMA]-*b*-DMA_{17} diblock copolymer was achieved by the sequential polymerization of the MMA monomer followed by that of the DMA monomer. In particular, to a 50-mL round-bottomed flask, fitted with a glass valve, were transferred PyDEBrMA (0.0721 g,

0.1877 mmol), CuCl (0.0186 g, 0.1877 mmol), HMTETA (51.07 μL, 0.0433 g, 0.1886 mmol), MMA (1.0 mL, 0.94 g, 9.3887 mmol) and anisole (1.0 mL). The system was degassed by three freeze-pump-thaw cycles. During every cycle, the flask was filled with highly pure argon. Finally, the flask was placed in an oil bath thermostated at 26 °C for 16 h at which point monomer conversion was determined using ^{1}H NMR spectroscopy and found 99%, while M_n and $Đ$ values were found 9860 g mol^{-1} and 2.58, respectively. Then, 0.54 mL degassed DMA monomer (0.50 g, 3.1922 mmol) was added sequentially (without stopping the polymerization reaction) to the polymerization flask and was left to polymerize for 24 h. At that moment, DMA monomer conversion to polymer was determined using ^{1}H NMR spectroscopy and found 88%, while the values of M_n and $Đ$ were found 14100 g mol^{-1} and 2.45, respectively. Finally, the polymer was passed through a neutral alumina column to remove the CuCl catalyst, precipitated in *n*-hexane, and dried *in vacuo* for 2 days. Additionally, a hyperbranched amphiphilic [MMA_{50}-PyDEBrMA]-*b*-DMA_{50} diblock copolymer was also sequentially synthesized, where M_n and $Đ$ values of the first block were found 8430 g mol^{-1} and 1.99, while monomer conversion was found 95%.

2.3.6 Synthesis of Randomly 2PyMMA-2PyEMA Linear Copolymer or Cross-linked Network by RAFT Polymerization.

The synthesis of the randomly 2PyMMA-2PyEMA linear copolymers or cross-linked networks was accomplished by RAFT polymerization in the presence of EGDMA as cross-linker, 2-CPBD as CTA, AIBN as initiator and 1,4-dioxane as solvent.

2.3.6.1 Synthesis of the randomly 2PyMMA$_{50}$-co-2PyEMA$_{50}$ linear copolymer. 38.5 mg 2-CPBD (0.174 mmol), 17.8 mg AIBN (0.108 mmol), 1.6 mL PyMMA (1.6 g, 9.0 mmol), 1.6 mL PyEMA (1.6 g, 8.4 mmol), and 2.6 mL 1,4-dioxane were placed in a 25 mL Schlenk flask containing a magnetic stirring bar. The contents of the tube were, subsequently, degassed by three freeze-vacuum-thaw cycles, were placed under an inert argon atmosphere, and were heated in an oil bath at 65 °C for 24 h.

2.3.6.2 Synthesis of the randomly cross-linked 2PyMMA$_{52}$-co-2PyEMA$_{48}$-co-EGDMA$_6$ network. A 25 mL Schlenk tube containing a magnetic stirring bar was loaded with 38.5 mg 2-CPBD (0.174 mmol), 17.8 mg AIBN (0.108 mmol), 1.6 mL PyMMA (1.6 g, 9.0 mmol), 1.6 mL PyEMA (1.6 g, 8.4 mmol), 0.2 mL EGDMA (0.210 g, 1.060 mmol), and 2.6 mL 1,4-dioxane. The contents of the tube were, subsequently, degassed by three

freeze-vacuum-thaw cycles, were placed under an inert argon atmosphere, and were heated in an oil bath at 65 °C for 24 h.

2.4 Polymer Degradation-Deprotection

All polymers (linear and hyperbranched (co)polymers and (co)polymer networks) were subjected to thermolysis as well as to alkaline or acidic hydrolysis conditions to determine the hydrolytic and thermal stability.

2.4.1 Alkaline hydrolysis

All polymers were submitted to alkaline hydrolysis conditions using sodium hydroxide (or sodium deuteroxide) in DMSO (or in d_6-DMSO) at room temperature.

2.4.1.1 Alkaline hydrolysis of linear pyridinylalkyl methacrylate homopolymers. All linear homologues, as well all homopolymers based on different monomers, were subjected to alkaline hydrolysis conditions in d_6-DMSO in the presence of sodium deuteroxide, at room temperature. To this end, 0.02 g polymer (~0.10 meq of pyridine groups) was dissolved in 0.8 mL d_6-DMSO and, to the resulting polymer solution, 40 μL NaOD 40% (0.39 meq) in D_2O was added. The mixture was left to react for a few hours or a few days (for slower reactions), and the progress of the reaction was monitored using ^{1}H NMR spectroscopy.

2.4.1.2 Alkaline hydrolysis of the 2PyEMA units in the ABC triblock terpolymers. The $BzMA_{20}$-*b*-$THPMA_{20}$-*b*-($THPMA_{20}$-*co*-$2PyEMA_{20}$) triblock terpolymer was hydrolyzed selectively in a DMSO/MeOH (5:3 v/v) mixture in the presence of sodium hydroxide, at room temperature. In particular, 0.5 g of the original ABC triblock terpolymer (0.72 meq of 2PyEMA units) was dissolved in 8 mL DMSO/MeOH (5:3 v/v) and to the resulting solution was added 0.2 g solid NaOH (5 mmol). After 24 hours, DMSO, MeOH and the produced 2-vinyl pyridine were distilled off in the vacuum line. The product was purified from NaOH by dialysis against water for 3 days, using a dialysis tube with a 3000 g mol^{-1} molecular weight cut-off. The water was changed twice a day. Then, the purified $BzMA_{20}$-*b*-$THPMA_{20}$-*b*-($THPMA_{20}$-*co*-MAA_{20}) was isolated by freeze-drying from water.

2.4.1.3 Alkaline hydrolysis of the PyDEDBrMeP residue in (co)polymers. The PyDEDBrMeP initiator residues in the linear polyMMAs were subjected to hydrolysis in d_6-DMSO in the presence of sodium deuteroxide, at room temperature. For instance, a sample of the MMA_{50}-*b*-PyDEDBrMeP-*b*-MMA_{50} homopolymer (0.02 g, 0.0021 mmol) was dissolved in 1.0 mL d_6-DMSO, and, to the resulting solution, 40 μL of a 40% w/w (10

M) NaOD solution (0.390 mmol) in D_2O was added. The cleavage of the PyDEDBrMeP residue was confirmed by analysis using ^{1}H NMR spectroscopy 24 h after the mixing of the reagents.

All polymers were also subjected to alkaline hydrolysis in non-deuterated environments, i.e., using sodium hydroxide in DMSO, followed by precipitation and drying of the products. For example, 0.10 g of the MMA_{50}-*b*-PyDEDBrMeP-*b*-MMA_{50} homopolymer (0.0105 mmol) was dissolved in 5.0 mL DMSO, and, to the resulting solution, 0.2 mL of a 40% w/w (10 M) NaOH solution (1.950 mmol) in H_2O was added. The polymer was subsequently precipitated in water, dried *in vacuo* for 48 h, and analyzed using GPC. The same procedure was also followed for the other linear MMA homopolymers prepared using PyDEDBrMeP, and the ones prepared using the more stable PyDMDBrMeP as well. Furthermore, the procedure was also applied to the linear amphiphilic ABA and BAB triblock copolymers and the end-linked MMA homopolymer networks. After the alkaline hydrolysis and before the GPC analysis, the amphiphilic triblock copolymers were purified by dialysis against water for 1 week, using dialysis tubing with a 3000 g mol^{-1} molecular weight cut-off, followed by lyophilization.

In the case of the end-linked MMA homopolymer networks, alkaline hydrolysis of the initiator residue led to the conversion of the insoluble network to a polymer solution, which was characterized using ^{1}H NMR spectroscopy and GPC. In the case of the alkaline hydrolysis of the linear amphiphilic ABA triblock copolymers, the products were purified by dialysis against water for 1 week, using a dialysis tube with a 3000 g mol^{-1} molecular weight cut-off, followed by lyophilization in order to isolate the polymer.

2.4.1.4 Alkaline hydrolysis of the PyDMA units. The PyDMA units in the PyDMA hyperbranched homopolymer were hydrolyzed selectively in d_6-DMSO in the presence of sodium deuteroxide at room temperature. To this end, 0.1 g of the dried hyperbranched homopolymer was dissolved in 1.0 mL d_6-DMSO, and to the resulting solution 40 μL NaOD 40% in D_2O was added. The conversion of the PyDMA units to MAA units and 2,6-divinylpyridine was determined using ^{1}H NMR spectroscopy. The alkaline hydrolysis of the PyDMA units in the $PyDMA_{10}$ homopolymer network and the MMA_{100}-*co*-$PyDMA_8$ polymer network was performed by transferring 0.1 g of dried network in 1.0 mL d_6-DMSO containing 40 μL NaOD 40% in D_2O. The conversion of the PyDMA units to MAA units and 2,6-divinylpyridine was determined by analyzing the supernatant using ^{1}H NMR spectroscopy. In the case of the $PyDMA_{10}$ homopolymer network, alkaline

hydrolysis of the PyDMA units led to the formation of MAA homopolymer, while in the case of the MMA_{100}-*co*-$PyDMA_8$ polymer network, alkaline hydrolysis of the PyDMA units led to the formation of MMA_{100}-*co*-MAA_{16} statistical copolymer.

2.4.1.5 Alkaline hydrolysis of the PyDEBrMA residue in hyperbranched (co)polymers. The PyDEBrMA residues in the hyperbranched MMA homopolymers and the hyperbranched amphiphilic MMA-DMAEMA diblock copolymers were hydrolyzed using sodium deuteroxide in d_6-DMSO at room temperature. To this end, 0.020 g of the hyperbranched MMA_{50} homopolymer (M_n = 22800 g mol^{-1}) (0.003 mmol of PyDEBrMA residues) was dissolved in 1.0 mL d_6-DMSO, and to the resulting solution 40 μL of a 40% w/w (10 M) NaOD solution (0.390 mmol) in D_2O was added. The cleavage of the PyDEBrMA residues was confirmed using ^{1}H NMR spectroscopy. All polymers were also subjected to alkaline hydrolysis using (non-deuterated) sodium hydroxide in DMSO followed by purification and isolation of the products. To this end, 0.10 g of the hyperbranched MMA_{50} homopolymer (M_n = 22800 g mol^{-1}) (0.015 mmol of PyDEBrMA residues) was dissolved in 5.0 mL DMSO, and, to the resulting solution, 0.2 mL of a 40% w/w (10 M) NaOH solution (1.950 mmol) in H_2O was added. The polymer was subsequently precipitated in water, dried *in vacuo* for 48 h, and finally, was analyzed using GPC and ^{1}H NMR spectroscopy. The products of the alkaline hydrolysis of the hyperbranched amphiphilic MMA-DMA diblock copolymers were purified by dialysis against water for 1 week, with daily change of the water, using a dialysis tubing with a 3000 g mol^{-1} molecular weight cut-off, followed by lyophilization.

2.4.2 Thermolysis

Thermolysis of the polymers was accomplished either in the bulk (in a vacuum oven) or in solution (DMSO or DMF).

2.4.2.1 Thermolysis of linear pyridinylalkyl methacrylate homopolymers. Pyridinylalkyl methacrylates homologues thermolysis was pursued both in solution and in the bulk. Regarding the former, 0.05 g of polymer (~0.25 meq) was dissolved in 1 mL d_6-DMSO and the resulting solution was transferred into a 10 mL round-bottomed flask, fitted with a reflux condenser, and containing a magnetic stirring bar. The system was placed in an oil bath, thermostated at 130 °C, and left for 24 h. Samples were extracted and analyzed in d_6-DMSO using ^{1}H NMR spectroscopy. In the case of the polymer homologues, bulk thermolysis was also pursued at 130 °C in a vacuum oven. To this end, a small (capacity of 2 mL) glass vial, containing 20-30 mg of the polymer, was placed in the vacuum oven.

Vacuum was applied and the temperature was adjusted to 110 °C. The same procedure was also repeated in a similar way at the higher temperatures of 120 and 130 °C. After 24 hours, the heating in the vacuum oven was stopped, the vial was allowed to cool down in the vacuum oven, and its contents were analyzed in d_6-DMSO using ^{1}H NMR spectroscopy.

2.4.2.2 Thermolysis of the 2PyEMA and the THPMA units in the ABC triblock terpolymers. The $BzMA_5$-*b*-$PyEMA_5$-*b*-$THPMA_5$ and the $BzMA_{20}$-*b*-$THPMA_{20}$-*b*-($THPMA_{20}$-*co*-$PyEMA_{20}$) triblock terpolymers were thermolyzed at 130 °C. To this end, ~20 mg of each ABC triblock terpolymer was transferred in to a small (capacity of 2 mL) glass vial which was placed in a vacuum oven at 130 °C. After 6 hours, the heating in the vacuum oven was stopped, the vial was allowed to cool down in the vaccum oven and its contents were analyzed using ^{1}H NMR spectroscopy in d_6-DMSO.

2.4.2.3 Thermolysis of the PyDEDBrMeP residue in (co)polymers. The linear MMA homopolymers and the end-linked polymer networks were subjected to thermolysis conditions *in vacuo* at 150 °C. To this end, ~20 mg of each polymer was transferred in to a small (capacity of 2 mL) glass vial which was placed in a vacuum oven maintained at 150 °C. After 6 hours, the heating in the vacuum oven was stopped, the vial was allowed to cool down in the vacuum oven, and its contents were analyzed using ^{1}H NMR spectroscopy (in $CDCl_3$ or d_6-DMSO) and GPC. In the case of the MMA networks, it was observed that the thermolysis product became soluble in the NMR and the GPC solvents. The same procedure was followed for the study of the thermal stability of the PyDMDBrMeP residue. In this case, however, it was observed that the corresponding thermally treated polymer networks remained insoluble.

In the case of the linear amphiphilic ABA triblock copolymers, thermolysis was accomplished in DMSO at 135 °C for 12 h. To this end, 150 mg of the amphiphilic ABA triblock copolymer and 2.0 mL of DMSO were transferred to a 25-mL round-bottomed flask fitted with a condenser and containing a magnetic stirring bar. The whole set-up was placed in an oil bath thermostated at 135 °C for 12 h. After this time, DMSO was removed by evaporation in a vacuum line, and the resulting semi-dried polymer was dissolved in 4 mL THF and precipitated in 30 mL *n*-hexane.

2.4.2.4 Thermolysis of the PyDMA units. The hyperbranched polymers and the polymer gels were thermolyzed at 130 °C in d_6-DMSO for 12 h. To this end, a small amount of the hyperbranched homopolymer or of each gel was transferred to a 50-mL flask containing a

magnetic stirring bar and 1.0 mL d_6-DMSO. The temperature was raised to 130 °C and the mixture was left to react overnight. The cleavage of the PyDMA units was confirmed using ^{1}H NMR spectroscopy and GPC.

2.4.2.5 Thermolysis of the PyDEBrMA residue in hyperbranched (co)polymers. The hyperbranched MMA homopolymers were thermolyzed *in vacuo* at 150 °C. To this end, ~20 mg of each polymer was transferred in to a small (capacity of 2 mL) glass vial which was placed in a vacuum oven maintained at 150 °C. After 6 hours, the heating in the vacuum oven was stopped, the vial was allowed to cool down in the vacuum oven, and its contents were analyzed using ^{1}H NMR spectroscopy (in $CDCl_3$ or d_6-DMSO) and GPC. In the case of the hyperbranched amphiphilic MMA-DMAEMA diblock copolymers, thermolysis was accomplished in DMSO at 135 °C for 12 h. To this end, 150 mg of the hyperbranched amphiphilic MMA-DMAEMA diblock copolymers and 2.0 mL of DMSO were transferred to a 25-mL round-bottomed flask fitted with a condenser and containing a magnetic stirring bar. The whole set-up was placed in an oil bath thermostated at 135 °C for 12 h. The products were purified by dialysis against water for 1 week, using a dialysis tube with a 3000 g mol^{-1} molecular weight cut-off, followed by lyophilization in order to isolate the polymer.

The hyperbranched MMA homopolymers were thermolyzed *in vacuo* at 150 °C for 8 h. To this end, ~20 mg of each hyperbranched homopolymer was transferred into a small (capacity of 2 mL) glass vial which was placed in a vacuum oven maintained at 150 °C for 8 h and the contents of the vials were analyzed using ^{1}H NMR spectroscopy and GPC. The hyperbranched amphiphilic MMA-DMA diblock copolymers were thermolyzed at 130 °C in DMSO for 12 h. To this end, a small amount of each hyperbranched amphiphilic diblock copolymer was transferred into a 50-mL flask containing a magnetic stirring bar and 1.0 mL d_6-DMSO. The temperature of the mixture was raised to 130 °C where it was maintained for 12 h. After the thermal treatment, all copolymers were analyzed using GPC and ^{1}H NMR spectroscopy (only in the case of the hyperbranched MMA_{50} homopolymer).

2.4.3 Acid Hydrolysis

Acid hydrolysis was performed using hydrogen chloride (or deuterium chloride) in DMSO (or in d_6-DMSO) at room temperature.

2.4.3.1 Acidic hydrolysis of linear pyridinylalkyl methacrylate homopolymers. All linear homopolymers were subjected to acidic hydrolysis conditions in d_6-DMSO at room temperature by the addition of deuterium chloride. In particular, 0.02 g of polymer (~0.10

meq of pyridine groups) was dissolved in 0.8 mL d_6-DMSO and, to the resulting polymer solution, 40 μL DCl 10 M (0.37 meq) in D_2O was added. The mixture was left to react for 1 week, and the progress of the reaction was monitored using ^{1}H NMR spectroscopy.

2.4.3.2 Acid hydrolysis of the THPMA units in the ABC triblock terpolymers. The $BzMA_{20}$-*b*-$THPMA_{20}$-*b*-($THPMA_{20}$-*co*-$PyEMA_{20}$) triblock terpolymer was hydrolyzed selectively in a DMSO/MeOH (1:1 v/v) mixture in the presence of hydrochloric acid, at room temperature. In particular, 0.5 g of the original ABC triblock terpolymer (1.32 meq of THPMA units) was dissolved in 10 mL DMSO/MeOH (1:1 v/v) and to the resulting solution were added 5 drops of HCl (35%, 6.7 mmol). After 24 hours, DMSO, MeOH and the produced 3,4-dihydro-2*H*-pyran were distilled off in the vacuum line. The product was purified from HCl by dialysis against water for 3 days, using a dialysis tube with a 3000 g mol^{-1} molecular weight cut-off. The water was changed twice a day. Then, the purified $BzMA_{20}$-*b*-MAA_{20}-*b*-(MAA_{20}-*co*-$PyEMA_{20}$) was isolated by freeze-drying from water.

2.5 Polymer Characterization

The linear or hyperbranched (co)polymers synthesized in this PhD Thesis were characterized using gel permeation chromatography (GPC) and nuclear magnetic resonance (NMR) Spectroscopy. Additionally, the products obtained after alkaline or thermal treatment were also analyzed using GPC and NMR spectroscopy. Polymer thermal analysis was investigated by differential scanning calorimetry (DSC) και thermogravimetric analysis (TGA). The micellar solution self-assembly characterization was accomplished using dynamic/static light scattering (DLS/SLS) and atomic force microscopy (AFM).

2.5.1 GPC. The molecular weight distributions (MWDs) of all the polymers were recorded using gel permeation chromatography (GPC), from which the number-average molecular weights, M_n, the weight-average molecular weights, M_w, and the molecular weight dispersities ($Đ = M_w/M_n$) were calculated. A single Polymer Laboratories PL-Mixed "D" column (bead size = 5 μm; pore sizes = 100, 500, 10^3 and 10^4 Å) was used for sample analysis. The mobile phase was THF, delivered using a Waters 515 isocratic pump at a flow rate of 1 mL min^{-1}. The refractive index (RI) signal was measured using a Polymer Laboratories ERC-7515A RI detector. The calibration curve was based on nine narrow MW (800, 2220, 6400, 12600, 23500, 41400, 84300, 201000 and 342000 g mol^{-1}) linear polyMMA standards also supplied by Polymer Laboratories.

2.5.2 NMR Spectroscopy. A 300 and a 500 MHz Avance Bruker NMR spectrometers, equipped with Ultrashield magnets, were used to acquire the ^{1}H and ^{13}C NMR spectra of all the synthesized monomers in $CDCl_3$ and the ^{1}H NMR spectra of all the polymers in $CDCl_3$ or d_6-DMSO.

2.5.3 DSC. DSC was performed using a Thermal Instruments (TA) differential scanning calorimeter model Q1000. Sample amounts of 0.5 – 2.0 mg were prepared in hermetically-sealed DSC pans. The temperature range covered was from 40 to 275 °C.

2.5.4 TGA. TGA was performed on a TA thermogravimetric analyzer model Q500 using ceramic pans. The temperature range from 40 to 600 °C was covered, whereas sample amounts of around 10 mg were loaded.

2.5.5 Hydrogen Ion Titration. Aqueous solutions of the ABC triblock terpolymers (7 mL of a 1% w/w solution) were titrated within the pH range from 1 to 12 using a 0.5 M NaOH standard solution. The pH of the solution was measured using a Corning PS30 portable pH-meter. The effective p*K* values of the PyEMA and the MAA monomer repeating units were calculated as the pH corresponding to 50% ionization. The pH at which polymer precipitation was first observed during the titration was also noted.

2.5.6 DLS/SLS. DLS experiments were performed at room temperature using an ALV/CGS-3 Compact Goniometer System equipped with 22 mW He-Ne laser operating at 632.8 nm. The scattered light was detected at 90° for the DLS measurements, while for the SLS measurements the scattered light was detected at the angles of 30° - 150°, with rate of 10° per measurement. 50 mg of the amphiphilic ABA triblock copolymers were dispersed in 5.0 g of deionized water (1% w/w). To afford full copolymer dissolution small amount of a 0.5 M aqueous solution were added to the dispersion. For the DLS measurements only one concentration of the amphiphilic ABA triblock copolymers was employed (1.0% w/w), while for the SLS measurement a range of concentrations of the amphiphilic ABA triblock copolymer were used (1.0%, 0.66% and 0.33% w/w). Prior to the light scattering measurements, the samples were filtered using PTFE syringe filters with a pore size of 0.45 μm.

2.5.7 AFM. AFM experiments were performed using an Asylum Research Cypher ES AFM in AC mode in air at room temperature, using ACT silicon tips from Applied Nanostructures (frequency 300 kHz, tip radius <10 nm, spring contrast 37 N/m). The upper layer of the mica slide was removed using a sticky tape, and 1 drop of the sample (0.01% w/w H_2O solution) was spin coating on the mica

2.5.8 Determination of the Sol Fraction (Extractables). After the synthesis, the $PyDMA_{10}$ (co)polymer networks were characterized in term of the sol fraction (extractables). In particular, the networks were placed in a glass-jar containing THF, and left there for 2 days to equilibrate and also to release its extractables. Subsequently, the THF solution of the extractables was transferred in to a pre-weighed round-bottomed flask, followed by the removal of the THF solvent using a rotary evaporator and further drying in a vacuum oven at room temperature for 24 h. The remaining dried mass was weighed, and the sol fraction was calculated as the ratio of the dried mass divided by the theoretical mass of the gel which was estimated as the sum of the masses of the monomer and the cross-linker (and the CTA or initiator). Finally, sample from the extractable was analyzed GPC and ^{1}H NMR spectroscopy to determine the molecular weight and composition, respectively.

2.5.9 Measurement of the Degree of Swelling (DS) in THF. After the extraction of the sol fraction, the (co)polymer networks were also characterized in terms of the degree of swelling (DS) in THF. Three pieces from the network were placed in small vials and were weighed to determine their THF-swollen mass, followed by their drying in a vacuum oven at room temperature for 48 h. Subsequently, the dried pieces were re-weighed to determine the dry mass, and, finally, the DS in THF was calculated as the ratio of the average swollen network mass (determined three times) divided by the dry network mass.

2.5.10 Measurement of the DSs in Water. All electrolytic or ampholytic dry copolymer networks were characterized in terms of their DSs in water as a function of pH within the pH range from ~1.5 to ~12.5. In the case of the double-cationic polyelectrolytic networks (i.e. before thermolysis), several dried network pieces were transferred in to glass vials each containing a volume of 5 mL of water where the precalculated volume of a 0.5 M HCl standard solution had been added in order to adjust the PyMMA and the PyEMA units to the desired degrees of ionization (DI), leading to pH values of the supernatant solutions in the range from 1.4 to 8.5. The number of moles of HCl required for each sample was calculated as the product of the desired DI (same as the degree of protonation in this case) times the total number of moles of the PyMMA plus the PyEMA units contained in the sample. The latter was calculated from the network dry mass and the polymerization stoichiometry, divided by the appropriate average PyMMA-PyEMA monomer molecular weight (184.2 g mol^{-1} in the case of the equimolar network). In addition to the acidified network samples, three more samples were prepared for each different network. The first two samples were made alkaline by the addition of small volumes of a 0.5 M NaOH standard solution, while the third sample remained neutral (without any addition of HCl or

NaOH). The samples were equilibrated for three weeks and the swollen masses were measured. The DSs of the samples were again calculated by dividing the swollen by the dry masses.

In the case of the ampholytic networks (i.e. after thermolysis), several dried pieces were transferred in to glass vials containing water (5 mL) where the appropriate volume of a 0.5 M HCl (pH range from 1.4 to 8.0) or a 0.5 M NaOH (pH range from 8.0 to 12.3) standard solutions had been added. The number of moles of NaOH or HCl required for each sample was calculated as the product of the desired degree of deprotonation or protonation times the total number of moles of MAA or PyMMA units contained in the sample. The latter was calculated from the conetwork dry mass, and the polymerization stoichiometry. For these calculations, a linear hydrogen ion titration curve was assumed, in which the targeted degree of protonation or deprotonation was varied from 0 to 1 within the pH range from 1.5 to 12.5. The samples were again equilibrated for three weeks and the swollen masses were measured. The DSs of all samples were again found by dividing the average values of the swollen by the dry masses for the different samples of each network.

2.5.11 Determination of the Isoelectric pH (pI) of the Polyampholyte Hydrogels. The p*I* of the polyampholyte hydrogels was estimated as the pH at the middle point of the swelling minimum plateau formed in the swelling profile (DS *vs.* pH curve) of the networks.

Chapter 3 – Results and Discussion

This Ph.D. Thesis deals with the synthesis of polymers bearing pyridinylalkyl ester moieties either in their side group or along their main chain, and investigates and exploits the lability of these moieties under thermolysis and alkaline hydrolysis conditions. The directions in this Thesis are based on our initial observation of the great lability, both thermolytic and alkaline hydrolytic, of the pyridinylethyl ester group, shown in the center (higher portion of the ellipsoid) of Figure 3.1. We proved that this lability is also displayed by the pyridinyldiethyl diester group illustrated below the mono-ester structure mentioned above. The sub-projects of this PhD Thesis were built around the behavior of these mono- and di-esters.

Starting with the mono-esters, a major sub-project, shown in a table on the top of the figure, is the preparation and study of homopolymers of the three isomeric 2-(pyridinyl)ethyl methacrylates, with the nitrogen atom placed at the three possible positions in the pyridine ring, together with homopolymers of the six homologous pyridinylalkyl methacrylates, with methyl and propyl, instead of ethyl, spacers, and again the three pyridine *N*-position isomers.

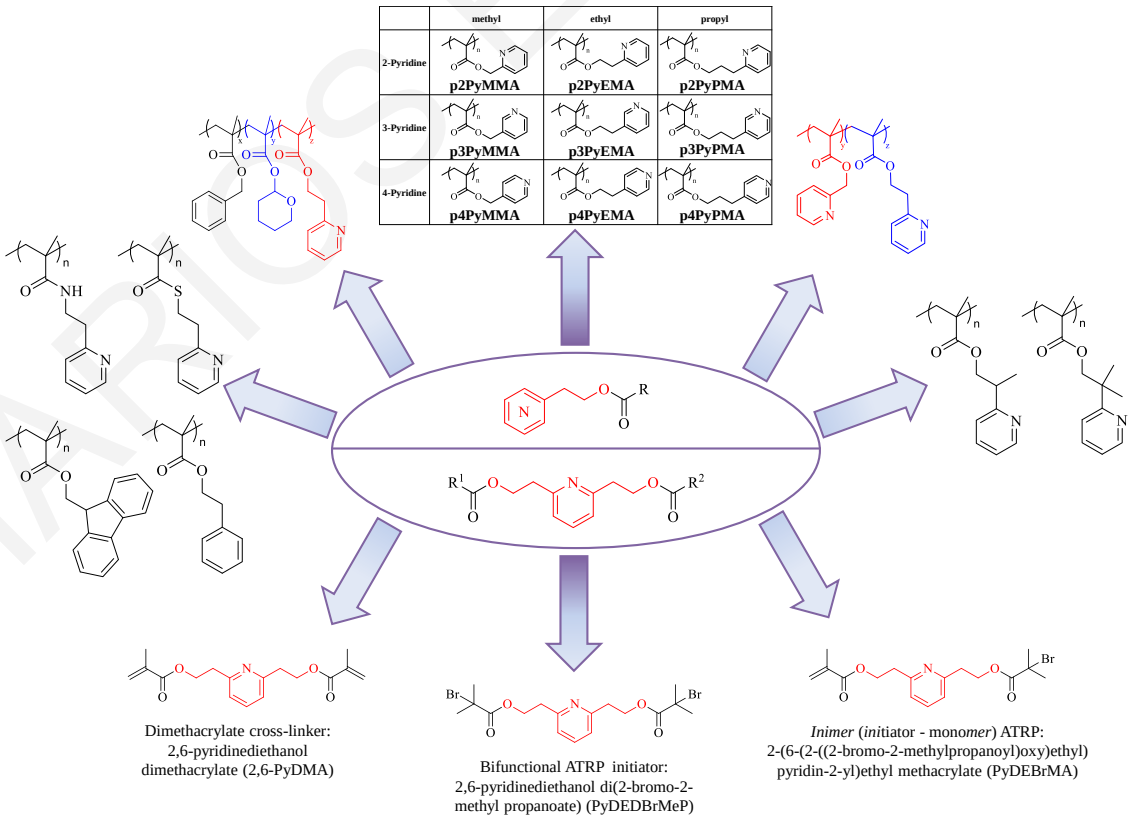

Figure 3.1. Overview of the pyridinylalkyl ester and related structures prepared in this PhD Thesis.

The next sub-project aimed at the introduction of the labile 2-(pyridin-2-yl)ethyl methacrylate (2PyEMA) unit in terpolymers with two other labile, under different conditions, monomer repeating units, 2-tetrahydropyranyl methacrylate (THPMA) and benzyl methacrylate (BzMA) in order to prove the orthogonality in their cleavage, with the terpolymer structure displayed on the top – left corner of Figure 3.1. Another sub-project involved the combination of two of the nine homologous monomers in copolymers, one with ethyl and the other with methyl spacers, both bearing the 2-pyridine moiety, whose structure is drawn on the top – right corner of Figure 3.1. The following sub-projects targeted the preparation and study of variants of poly2PyEMA ("related" polymers), either by introducing one or two methyl groups at the 2-position in the pendant (right side of the figure), or by replacing the ester linkage in the pendant for amide or thioester, or replacing the 2-(pyridin-2-yl)ethyl ester group in the pendant for 2-phenylethyl or 9-fluorenylmethyl (left side of the figure).

Proceeding with the pyridinyldiethyl diesters, three novel degradable molecules were synthesized, a cross-linker, an ATRP inimer and a bifunctional ATRP initiator, shown on the bottom of the figure.

3.1 Poly(Pyridinylalkyl Methacrylate)s: A Class of Addition Polymers With Rich Chemical Properties

This Section will focus on the synthesis and polymerization of nine homologous pyridinylalkyl methacrylates differing in the position of the nitrogen atom in the pyridine ring (2-, 3- or 4-pyridine) or/and in the length of the spacer (from methyl to propyl) between the ester moiety and the pyridine ring is presented, and the stability of the resulting polymers to thermolysis and hydrolysis is investigated. It was found that all polymers were stable under acidic hydrolysis conditions, but they presented partial or complete lability under alkaline hydrolysis conditions or thermally, leading to the cleavage of the pyridinylalkyl side-group. The polymer homologues bearing the ethyl spacer, [poly(2-pyridinyl)ethyl methacrylates] (pPyEMA), could be most readily hydrolyzed under alkaline conditions *via* an elimination reaction, yielding poly(methacrylic acid) (pMAA) and the corresponding vinylpyridine. The other six homologues underwent only partial alkaline hydrolysis even after two weeks of reaction, leading to the formation of pMAA and the corresponding hydroxyalkylpyridine. The pPyEMAs were also subjected to thermolysis at 200 ºC, with the pyridin-2-yl and pyridin-4-yl isomers being quantitatively converted to pMAA and the corresponding vinylpyridine, and the pyridin-3-yl isomer remaining stable. The other six polymer homologues were thermally stable up to 250 ºC, with the most stable being poly(3-(pyridin-3-yl)propyl methacrylate) (p3PyPMA) whose cleavage temperature exceeded 350 ºC, as measured using differential scanning calorimetry and thermogravimetric analysis. Additionally, some related homopolymers were also synthesized, whose structure was similar to that of 2PyEMA, but having a non-pyridine aromatic group (phenyl, PheMA or fluorenyl, FMMA), or a non-ester side-group (amide, 2PyEMAAm or thioester, 2PyESMA), or a substituted ethyl ester spacer (2-methylethyl, 2PyEmeMA or 2,2-dimethyl ethyl, 2PyEdimeMA). These polymers were subjected to thermolysis or acidic or alkaline hydrolysis conditions, and similar to the homologous pyridine polymers, the related pyridine polymers also presented stability to acidic conditions, but some of them exhibited partial or complete lability to thermolysis or alkaline hydrolysis conditions. The polymeric thioester p2PyESMA presented similar lability to thermolysis or alkaline hydrolysis conditions to p2PyEMA, while the polymeric amide p2PyEMAAm was stable. pPheMA and pFMMA were thermally stable up to ~300 ºC and presented partial and complete cleavage under alkaline hydrolysis conditions, respectively. The p2PyEmeMA, bearing a methyl group attached on the α-carbon next to pyridine ring, was partially cleaved under alkaline hydrolysis conditions and was slightly

thermally more stable than p2PyEMA, while, p2PyEdimeMA, being steric hindrance with two methyl groups on the α-carbon next to pyridine ring, was stable under these conditions.

3.1.1 Synthesis of Methacrylate Monomers.

In total, nine pyridinylalkyl methacrylate monomers and six related monomers were synthesized from the esterification of the corresponding alcohol with a slight excess of methacryloyl chloride in absolute THF and in the presence of a large excess of triethylamine or pyridine, in order to capture the hydrochloric acid formed and drive the reaction to completion. Figure 3.2 shows the chemical reaction involving the preparation of the pyridinylalkyl methacrylate monomers and their subsequent homopolymerization using GTP, ATRP or RAFT polymerization.

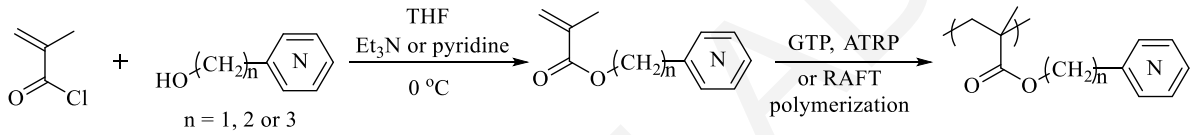

Figure 3.2 Chemical reactions for the synthesis of the pyridinylalkyl methacrylate monomers by the esterification of the hydroxyalkylpyridines with methacryloyl chloride, and their subsequent homopolymerization using GTP, ATRP or RAFT polymerization.

In the case of the esterification for the preparation of 2-(pyridin-4-yl)ethyl methacrylate (4PyEMA), when triethylamine was used as base, a spontaneous *in situ* hydrolysis of the ester moiety of the newly formed 4PyEMA was observed. In contrast, when pyridine was used as base, no hydrolysis of the ester moiety of 4PyEMA took place. This behavior may be due to the high basicity of triethylamine (pK_α = 10.75) as compared to that of pyridine (pK_a = 5.22).[294,295] Figure 3.3 shows the chemical structures, names and abbreviations of the pyridinylalkyl methacrylate monomers, differing either in the length of the alkyl spacer or/and in the position of the nitrogen atom in the pyridine ring, together with those of related monomers, *S*-(2-(pyridin-2-yl)ethyl) methacrylthioate (2PyESMA), *N*-(2-(pyridin-2-yl)ethyl) methacrylamide (2PyEMAAm), 2-phenethyl methacrylate (2PheMA), 9*H*-fluoren-9-yl)methyl methacrylate (FMMA), 2-(pyridin-2-yl)propyl methacrylate **(**2PyEmeMA), and 2-methyl-2-(pyridin-2-yl)propyl methacrylate (2PyEdimeMA).

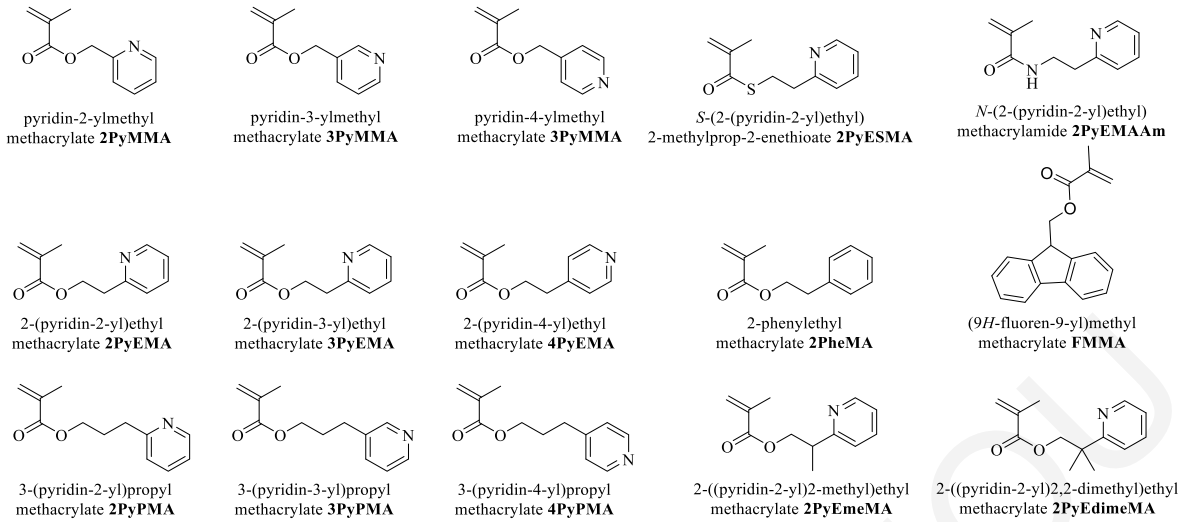

Figure 3.3 Chemical structures of the nine homologous pyridinylalkyl methacrylate monomers, together with those of related monomers 2PheMA, 2PyEMAAm, 2PyESMA, 2PyEmeMA and 2PyEdimeMA.

Below is presented the chemical reactions followed for the synthesis of each monomer, along with their ^{1}H and ^{13}C NMR spectra. Additionally, in the case where the precursor alcohol was synthesized in our laboratory, its ^{1}H and ^{13}C NMR spectra are also presented.

3.1.1.1 Synthesis of pyridin-2-ylmethyl methacrylate (2PyMMA). 2PyMMA was synthesized by the esterification of 2-pyridinemethanol with a 25% molar excess of methacryloyl chloride in dry THF in the presence of a large excess of triethylamine base at 0 °C.

Scheme 3.1 Esterification Reaction of 2-pyridinemethanol for the Synthesis of 2PyMMA, Together with its ^{1}H and ^{13}C NMR Spectra.

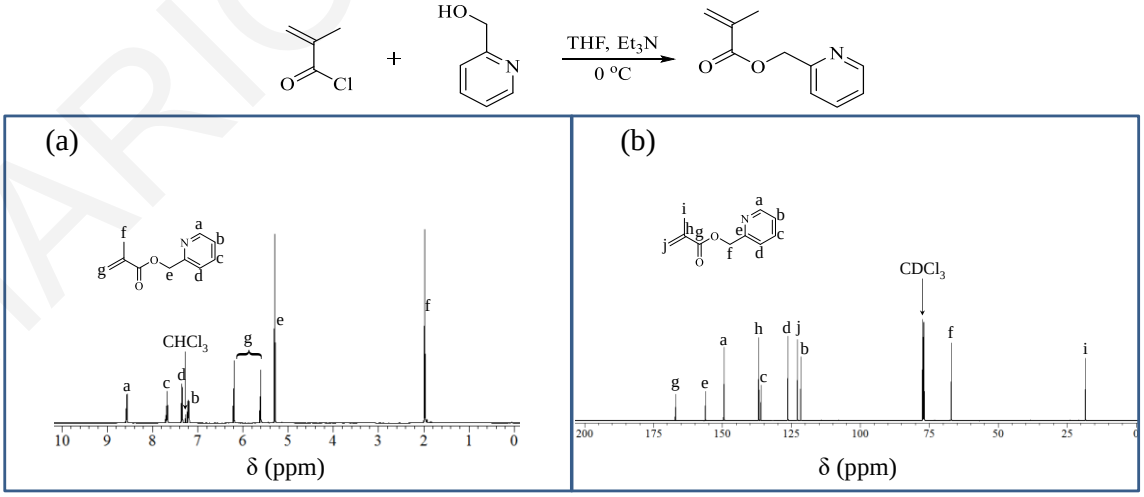

3.1.1.2 Synthesis of 2-(pyridin-2-yl)ethyl methacrylate (2PyEMA). 2PyEMA was synthesized by the esterification of 2-pyridineethanol with a 25% molar excess of methacryloyl chloride in dry THF in the presence of a large excess of triethylamine base at 0 °C.

Scheme 3.2 Esterification Reaction of 2-pyridineethanol for the Synthesis of 2PyEMA, Together with its ^{1}H and ^{13}C NMR Spectra.

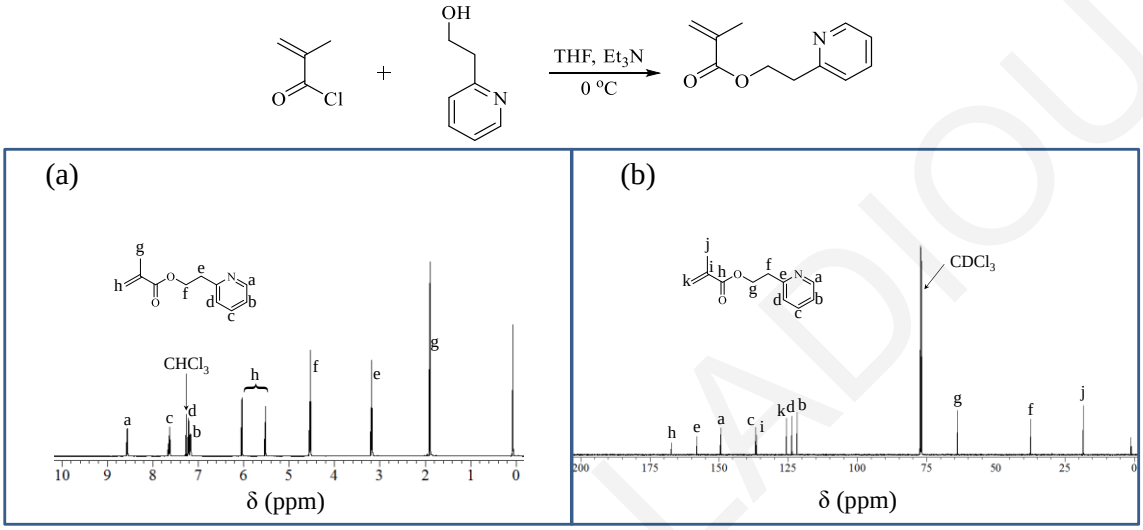

3.1.1.3 Synthesis of 3-(pyridin-2-yl)propyl methacrylate (2PyPMA). 2PyPMA was synthesized by the esterification of 2-pyridinepropanol with a 25% molar excess of methacryloyl chloride in dry THF in the presence of a large excess of triethylamine base at 0 °C.

Scheme 3.3 Esterification Reaction of 2-pyridinepropanol for the Synthesis of 2PyPMA, Together with its ^{1}H and ^{13}C NMR Spectra.

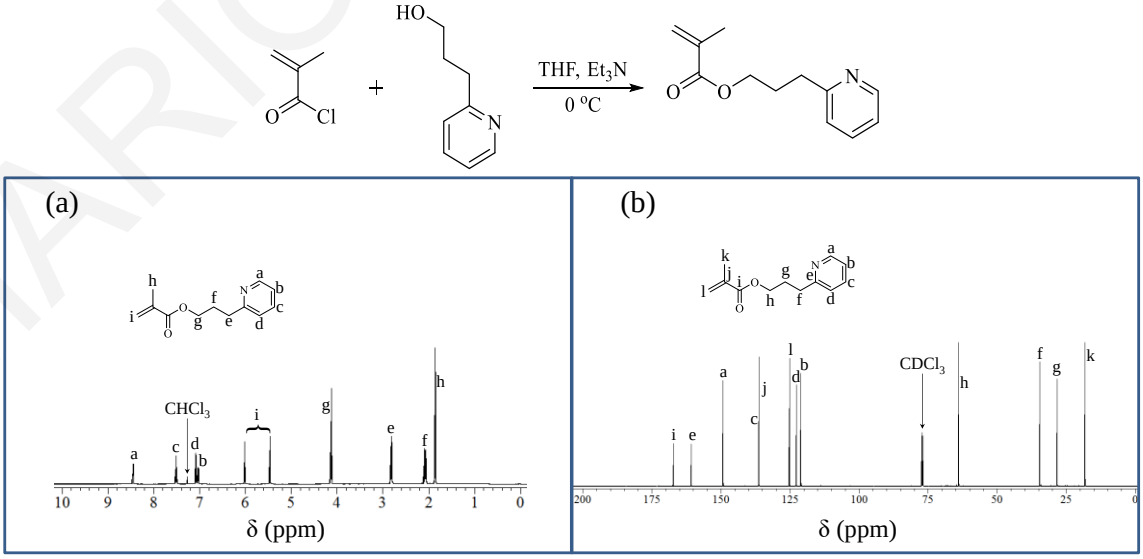

3.1.1.4 Synthesis of pyridin-3-ylmethyl methacrylate (3PyMMA). 3PyMMA was synthesized by the esterification of 3-pyridinemethanol with a 25% molar excess of methacryloyl chloride in dry THF in the presence of a large excess of triethylamine base at 0 °C.

Scheme 3.4 Esterification Reaction of 3-pyridinemethanol for the Synthesis of 3PyMMA, Together with its ^{1}H and ^{13}C NMR Spectra.

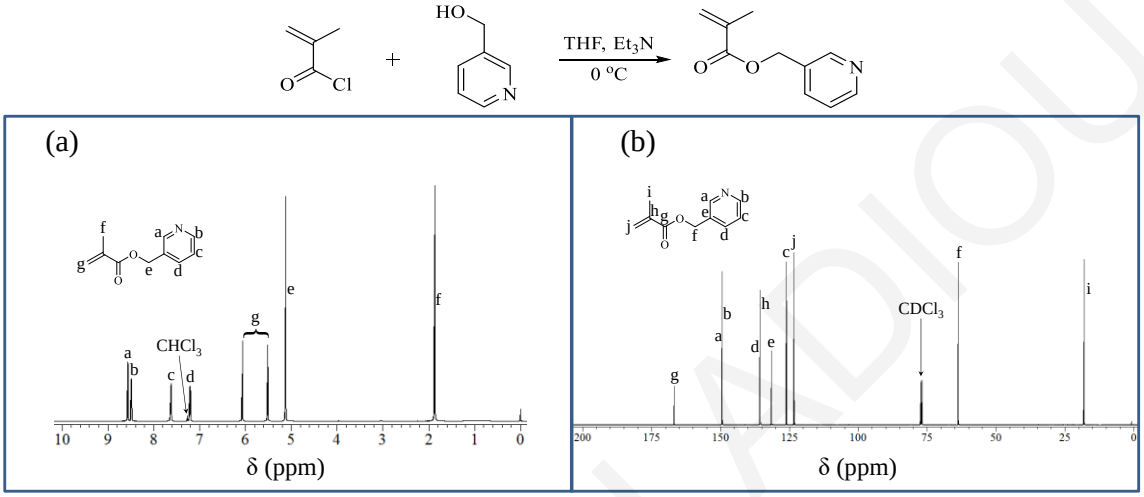

3.1.1.5 Synthesis of 2-(pyridin-3-yl)ethyl methacrylate (3PyEMA). 3PyEMA was synthesized by the esterification of 3-pyridineethanol with a 25% molar excess of methacryloyl chloride in dry THF in the presence of a large excess of triethylamine base at 0 °C. Due to the commercial unavailability of 3-pyridineethanol, 3-pyridineethanol was prepared according to the procedure of Almond et al.[284] which followed the modification of the method of Barnden,[285] by the reduction of ethyl 3-pyridylacetate using lithium aluminum hydride in tetrahydrofuran (THF).

Scheme 3.5 Chemical Reactions Performed for the Synthesis of 3-pyridineethanol and 3PyEMA, Together with their ^{1}H and ^{13}C NMR Spectra.

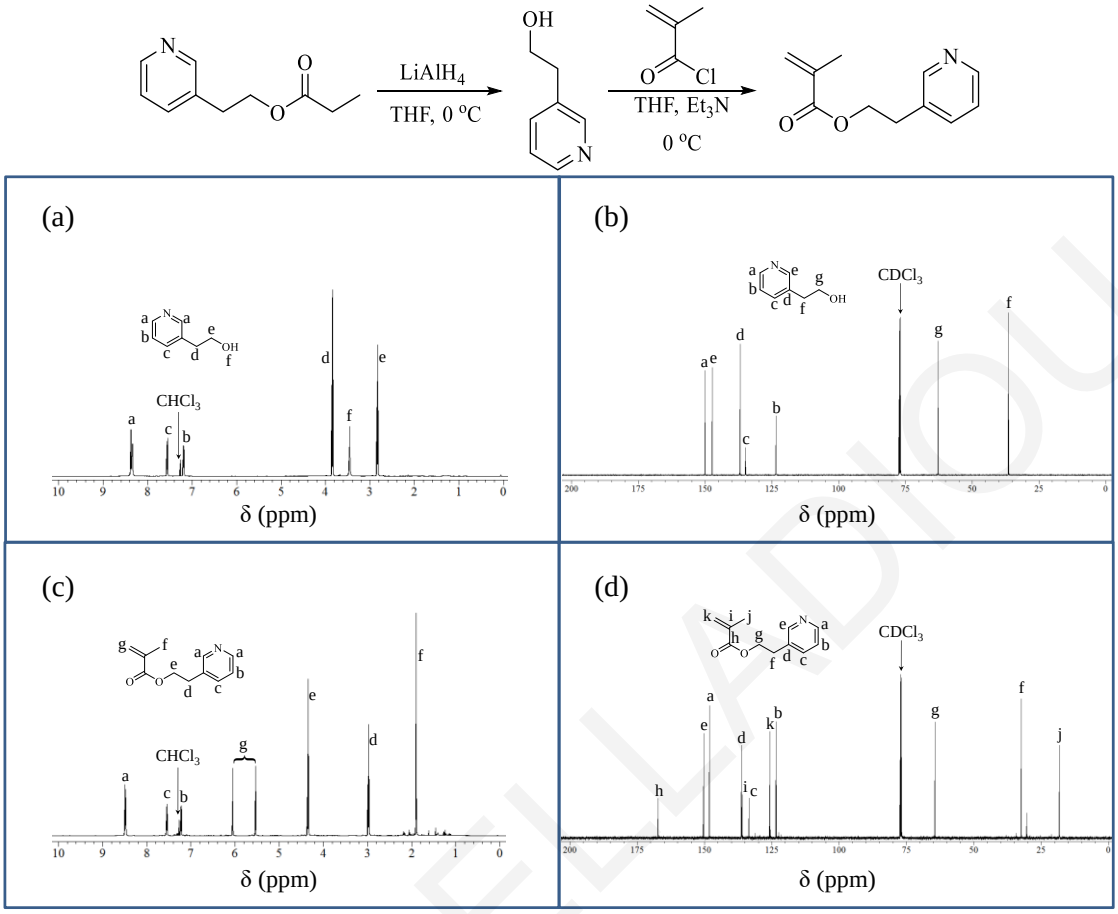

3.1.1.6 Synthesis of 3-(pyridin-3-yl)propyl methacrylate (3PyPMA). 3PyPMA was synthesized by the esterification of 3-pyridinepropanol with a 25% molar excess of methacryloyl chloride in dry THF in the presence of a large excess of triethylamine base at 0 °C.

Scheme 3.6 Esterification Reaction of 3-pyridinepropanol for the Synthesis of 3PyPMA, Together with its ^{1}H and ^{13}C NMR Spectra.

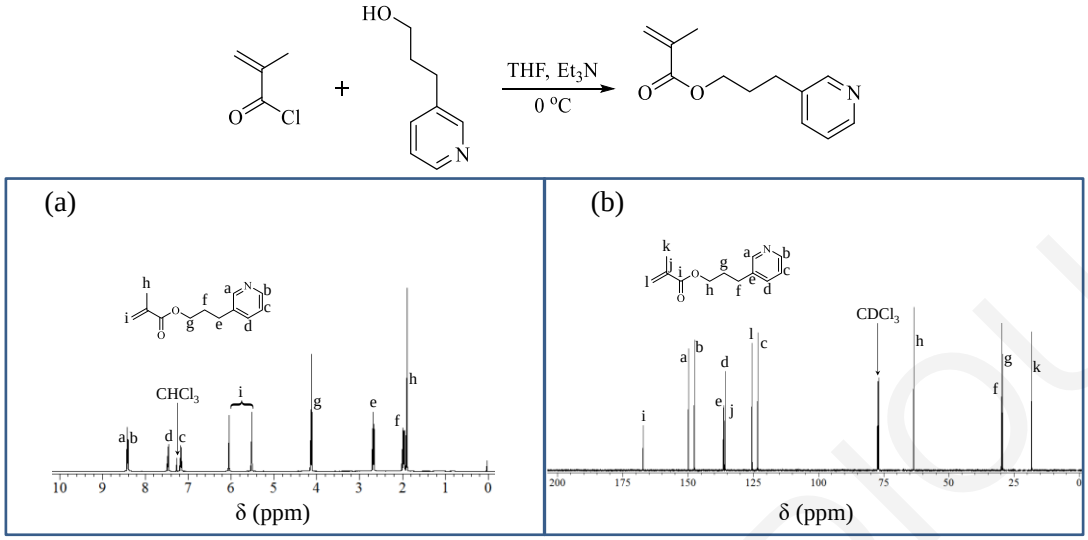

3.1.1.7 Synthesis of pyridin-4-ylmethyl methacrylate (4PyMMA). 4PyMMA was synthesized by the esterification of 4-pyridinemethanol with a 25% molar excess of methacryloyl chloride in dry THF in the presence of a large excess of triethylamine base at 0 °C.

Scheme 3.7 Esterification Reaction of 4-pyridinemethanol for the Synthesis of 4PyMMA, Together with its ^{1}H and ^{13}C NMR Spectra.

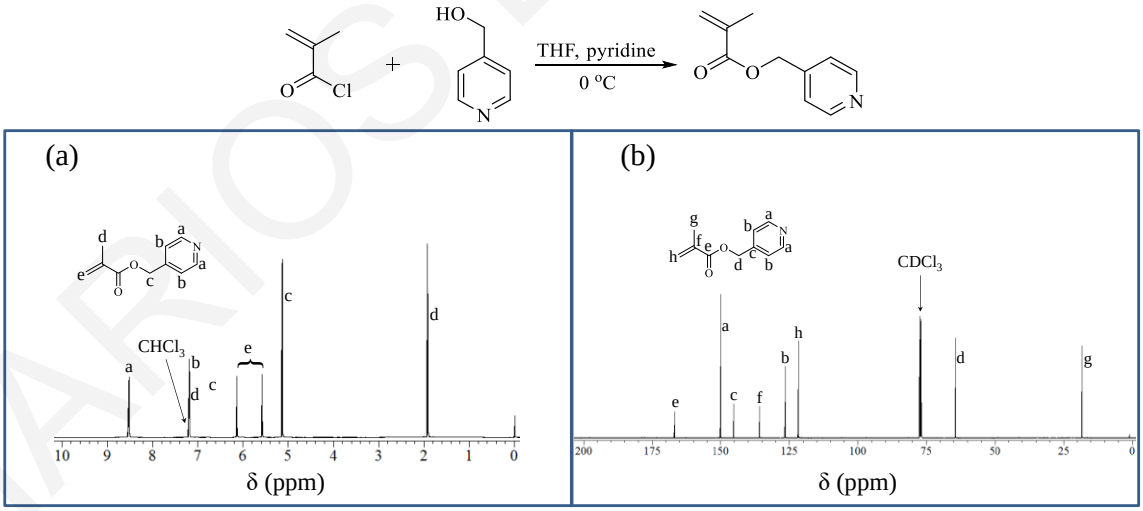

3.1.1.8 Synthesis of 2-(pyridin-4-yl)ethyl methacrylate (4PyEMA). 4PyEMA was synthesized by the esterification of 4-pyridineethanol with a 25% molar excess of methacryloyl chloride in dry $CHCl_3$ in the presence of a large excess of pyridine base at 0 °C. Due to the commercial unavailability of 4-pyridineethanol, 4-pyridineethanol was

prepared according to the procedure of Vaganova et al.[286] from the reaction of 4-methylpyridine (4-picoline) with formaldehyde under reflux.

Scheme 3.8 Chemical Reactions Performed for the Synthesis of 4-pyridineethanol and 4PyEMA, Together with their ^{1}H and ^{13}C NMR Spectra.

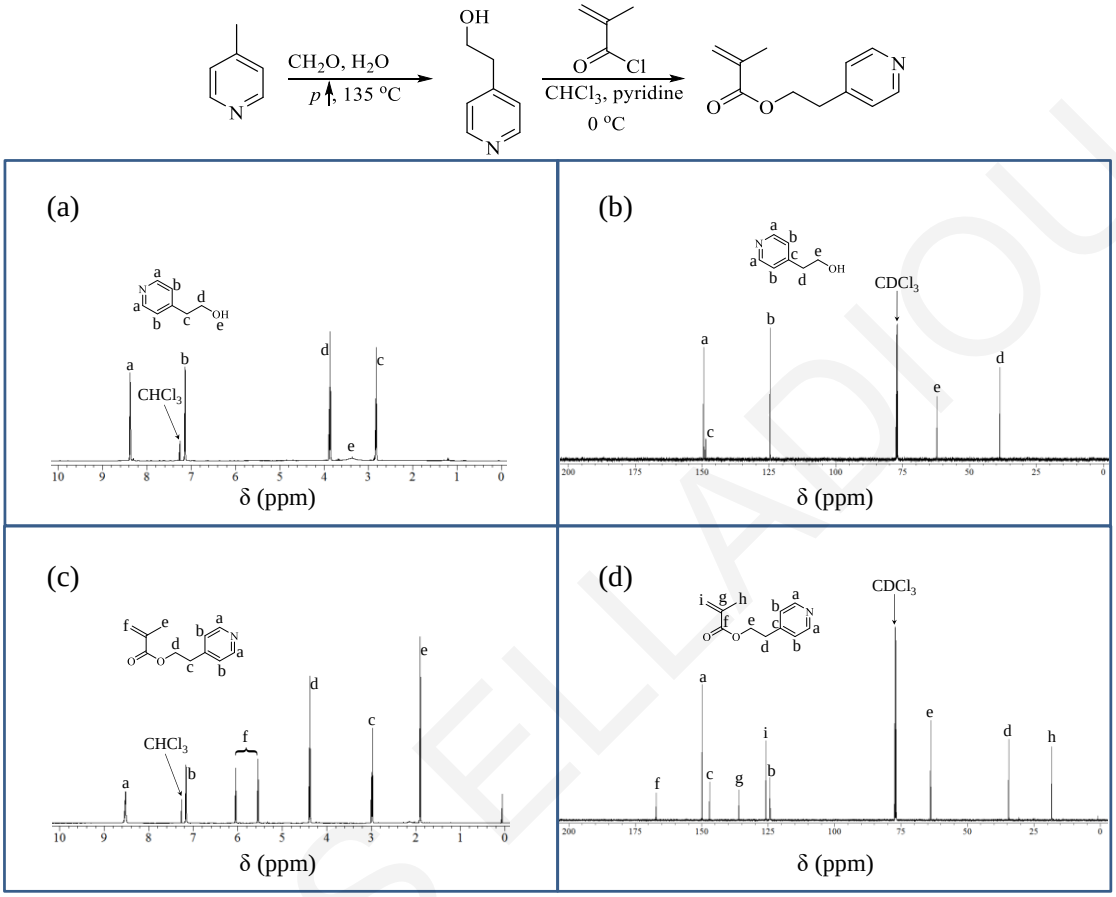

3.1.1.9 Synthesis of 3-(pyridin-4-yl)propyl methacrylate (4PyPMA). 4PyPMA was synthesized by the esterification of 4-pyridinepropanol with a 25% molar excess of methacryloyl chloride in dry THF in the presence of a large excess of triethylamine base at 0 °C.

Scheme 3.9 Esterification Reaction of 4-pyridinepropanol for the Synthesis of 4PyPMA, Together with its ^{1}H and ^{13}C NMR Spectra.

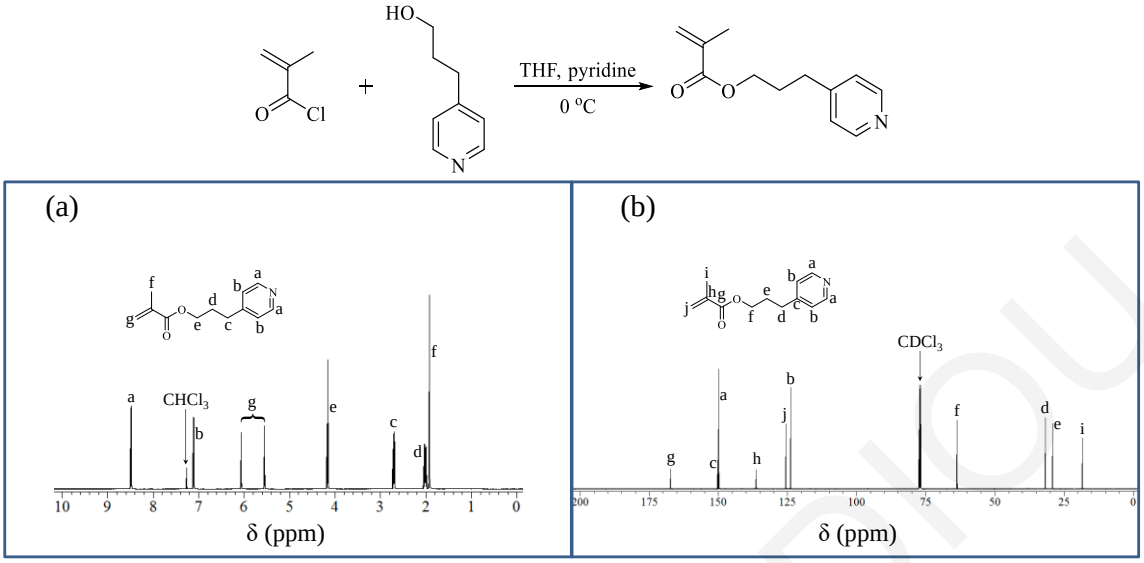

3.1.1.10 Synthesis of 2-phenethyl methacrylate (2PheMA). PheMA was synthesized by the esterification of 2-phenylethanol with a 25% molar excess of methacryloyl chloride in dry THF in the presence of a large excess of triethylamine base at 0 °C.

Scheme 3.10 Esterification Reaction of 2-phenylethanol for the Synthesis of 2PheMA, Together with its ^{1}H and ^{13}C NMR Spectra.

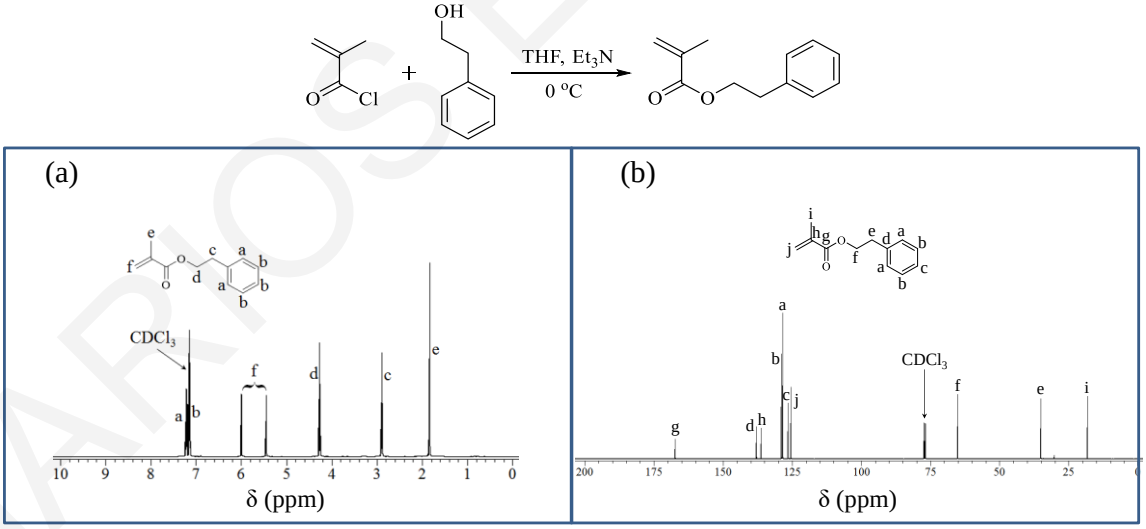

3.1.1.11 Synthesis of N-(2-(pyridin-2-yl)ethyl) methacrylamide (2PyEMAAm). **2**PyEMAAm was synthesized by the esterification of 2-pyridineethylamine with a 25% molar excess of methacryloyl chloride in dry THF in the presence of a large excess of triethylamine base at 0 °C.

Scheme 3.11 Esterification Reaction of 2-pyridineethylamine for the Synthesis of 2PyEMAAm, Together with its ^{1}H and ^{13}C NMR Spectra.

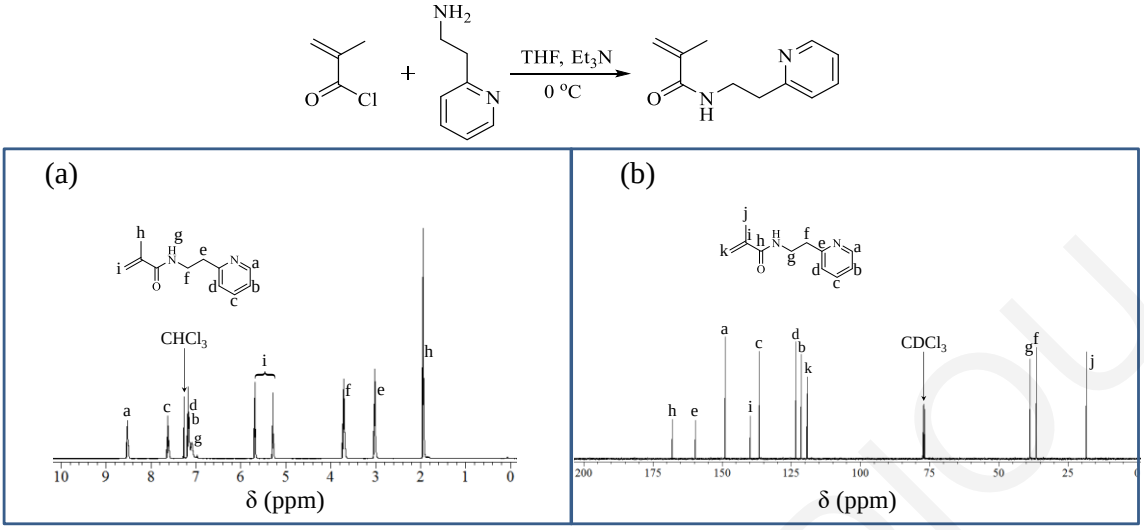

3.1.1.12 Synthesis of (9H-fluoren-9-yl)methyl methacrylate (FMMA). FMMA was synthesized by the esterification of 9-fluorenemethanol with a 25% molar excess of methacryloyl chloride in dry THF in the presence of a large excess of triethylamine base at 0 °C.

Scheme 3.12 Esterification Reaction of 9-fluorenemethanol for the Synthesis of FMMA, Together with its ^{1}H and ^{13}C NMR Spectra.

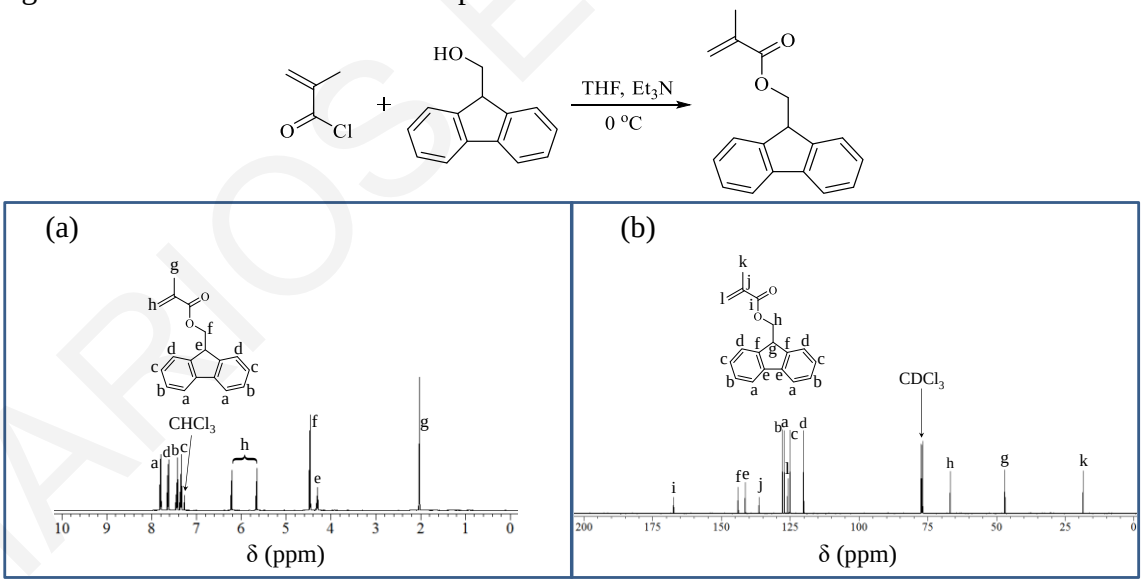

3.1.1.13 Synthesis of S-(2-(pyridin-2-yl)ethyl) methacrylthioate (2PyESMA). The synthesis of 2PyESMA was performed in two stages. The first stage involved the synthesis of precursor 2-pyridineethanethiol, while in the second stage followed the esterification of 2-pyridineethanethiol with a slightly excess of methacryloyl chloride.

Scheme 3.13 Chemical Reactions Performed for the Synthesis of 2-pyridineethanthiol and 2PyESMA, Together with their ^{1}H and ^{13}C NMR Spectra.

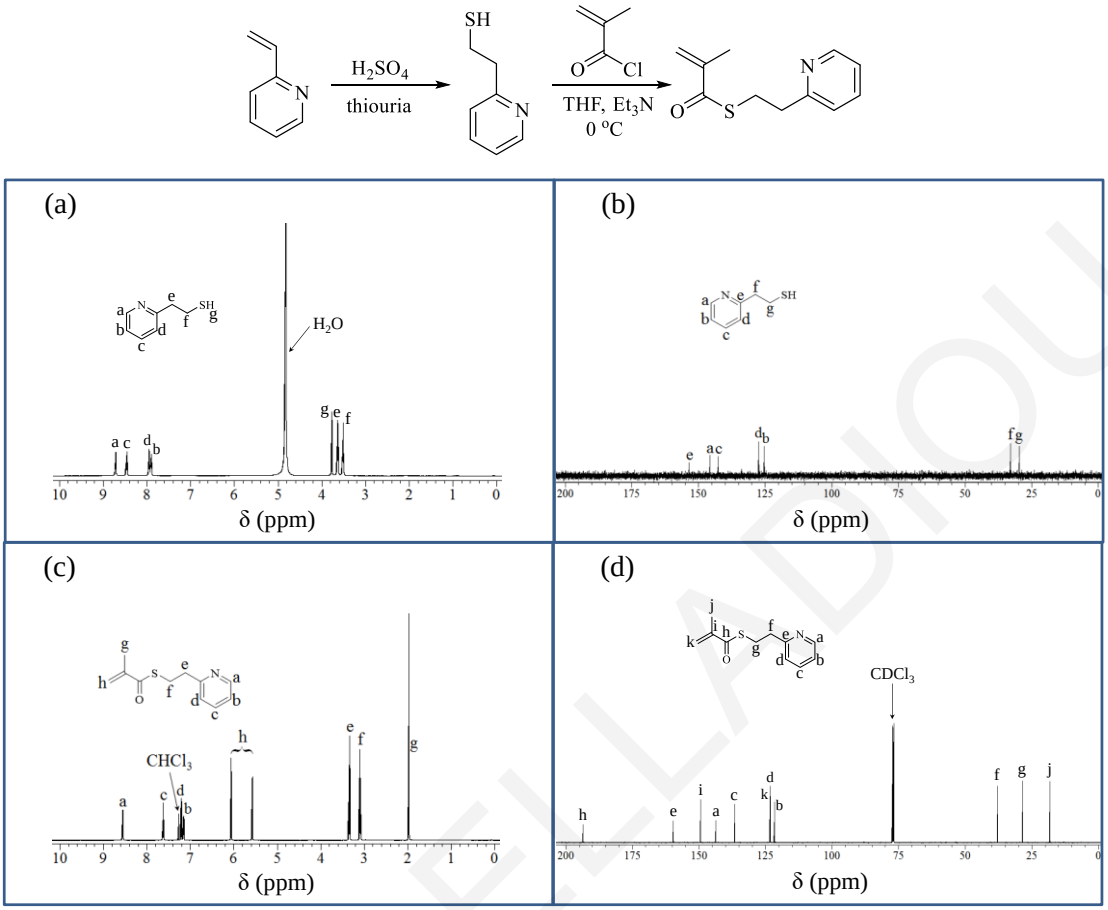

3.1.1.14 Synthesis of 2-((pyridin-2-yl)2-methyl)ethyl methacrylate (2PyEmeMA). 2PyEmeMA was synthesized by the esterification of 2-(pyridin-1-methyl)ethan-2-ol with 30% molar excess of methacryloyl chloride. 2-(Pyridin-1-methyl)ethan-2-ol was synthesized according to Gade et al.[288] by the reaction of 2-ethylpyridine with formaldehyde in water under high pressure and temperature. Scheme 3.14 shows the chemical reaction leading to the synthesis of 2-(pyridin-1-methyl)ethan-2-ol and 2PyEmeMA, along with their ^{1}H and ^{13}C NMR spectra.

Scheme 3.14 Chemical Reactions Performed for the Synthesis of 2-(pyridin-1-methyl)ethan-2-ol and 2PyESMA, Together with their ^{1}H and ^{13}C NMR Spectra.

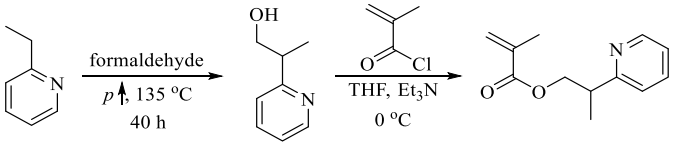

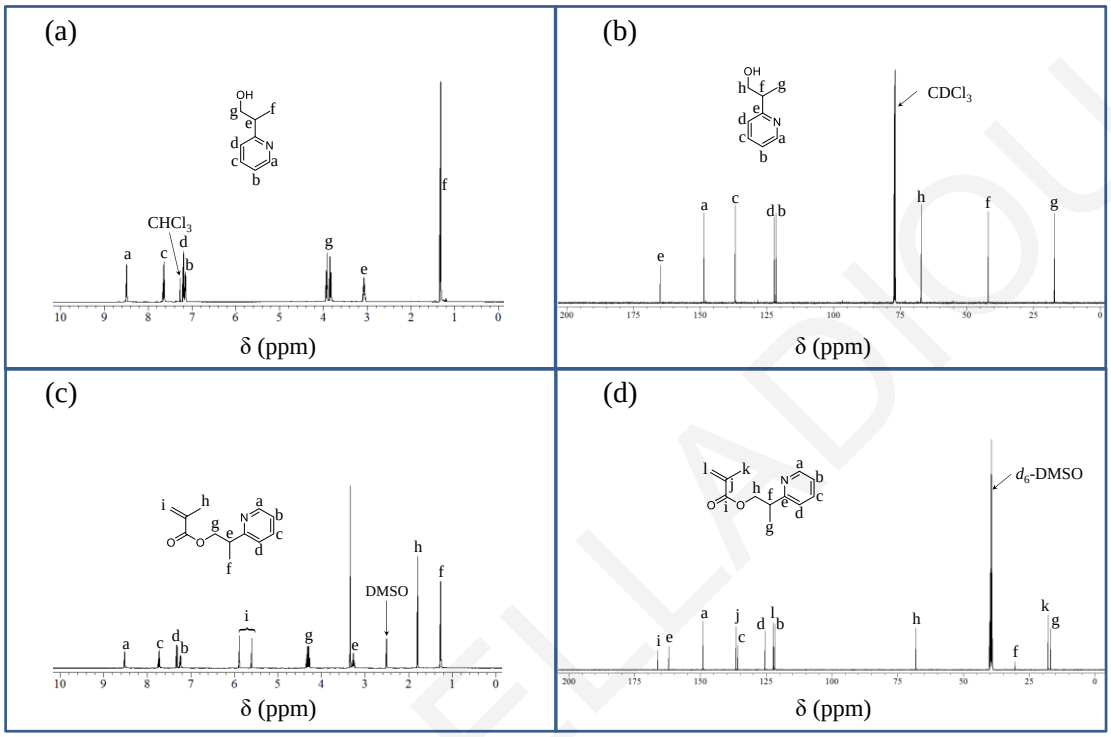

3.1.1.15 Synthesis of 2-((pyridin-2-yl)2,2-dimethyl)ethyl methacrylate (2PyEdimeMA). The synthesis of 2PyEdimeMA was accomplished by the esterification of 2-(pyridin-1,1-dimethyl)ethan-2-ol with 30% molar excess of methacryloyl chloride. 2-(Pyridin-1,1-dimethyl)ethan-2-ol was synthesized according to Fraenkel et al.[289] by the reaction of 2-isopropylpyridine with paraformaldehyde in water under high pressure and temperature. 2-Isopropylpyridine was prepared by the alkylation using iodomethane of deprotonated (using n-BuLi) of 2-ethylpyridine.[290]

Scheme 3.15 Chemical Reactions Performed for the Synthesis of 2-isopropylpyridine, 2-(pyridin-1,1-dimethyl)ethan-2-ol and 2PyEdimeMA, Together with their ^{1}H and ^{13}C NMR Spectra.

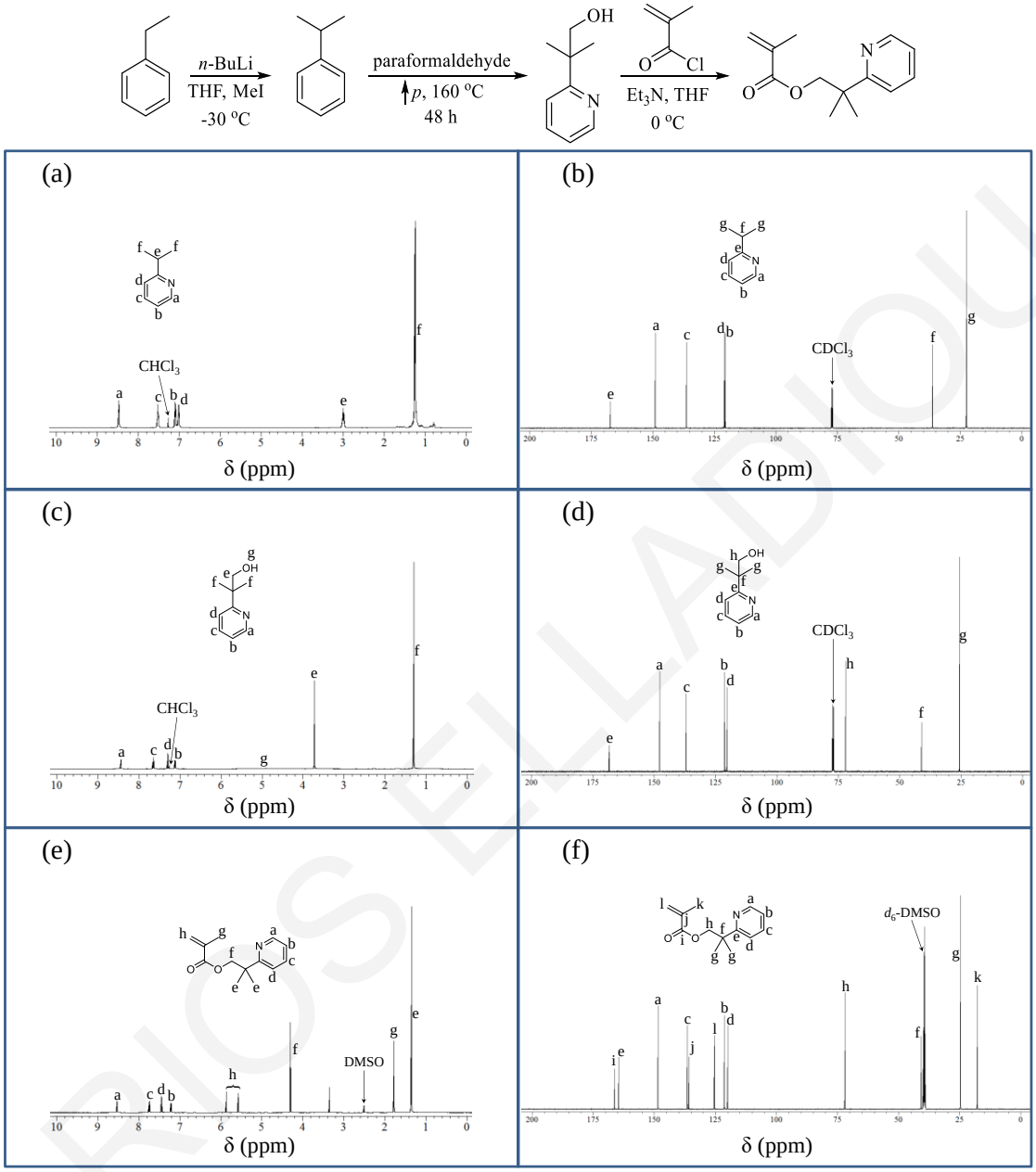

3.1.2 Polymer Syntheses. After their successful syntheses, the pyridinylalkyl methacrylates and the related monomers were homopolymerized using one of three different controlled polymerization methods, GTP, ATRP or RAFT polymerization. The majority of the pyridinylalkyl methacrylates were homopolymerized using GTP and RAFT polymerization, while the most sensitive 4PyEMA was polymerized using ATRP at 26 °C. All related monomers were homopolymerized using RAFT polymerization. Figure 3.4 illustrates the chemical structures, names and abbreviations of the main reagents used for polymer syntheses, except of the monomers.

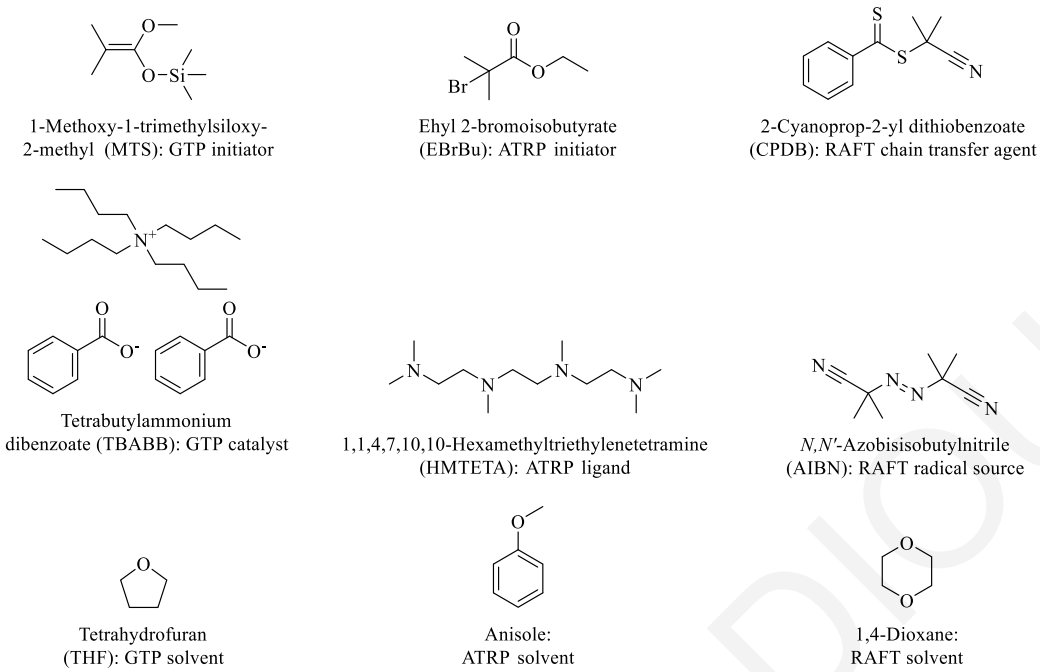

Figure 3.4 Chemical structures, names and abbreviations of the initiators and solvents used for polymer synthesis: the ATRP ligand (HMTETA), the GTP initiator (MTS), the RAFT chain transfer agent (CPDB), the GTP catalyst (TBABB), the RAFT initiator (AIBN), and the solvent THF, anisole and 1,4-dioxane, for GTP, ATRP and RAFT polymerization, respectively.

Table 3.1 lists the structures of all homopolymers synthesized, together with monomer-to-polymer conversion, theoretical and experimental molecular weights, molecular weight dispersities, and stability characteristics toward hydrolysis and thermolysis. The table is divided in two parts: the upper part concerns the homopolymers of the pyridinylalklyl methacrylate homologues, while the lower part contains the homopolymers of the related monomers. These related polymers were p2PheMA, pFMMA, p2PyEMAAm, p2PyESMA, p2PyEmeMA and p2PyEdimeMA, whose structure was similar to that of 2PyEMA, most of them (exception is pFMMA) also having an ethyl spacer, but having a non-pyridine aromatic group (phenyl or fluorenyl), or a non-ester side-group (amide or thioester), or a substituted ethyl ester spacer (2-methylethyl or 2,2-dimethyl ethyl). In most cases, the M_n values agree well with the theoretical molecular weights, while most $Đ$ values ranged between 1.3 and 1.7, indicating reasonable control of the polymerizations. The relatively higher $Đ$ values of the homopolymers prepared using GTP can be attributed their low DPs, 5 and 10. The rather high $Đ$ value of 2.13 for the linear 4PyPMA homopolymer may be due to the high reactivity of the 4-pyridine substituted ester, leading to the formation of several side reactions.[21,22] All poly(pyridinylalkyl methacrylate)s were practically stable under acidic hydrolysis conditions. In contrast, under alkaline hydrolysis conditions, these

polymers underwent partial or, in three cases, total loss of their pyridinylalkyl side group. The polymers that completely lost their side groups were the **poly(pyridinylethyl methacrylate)** (**pPyEMA**) isomers. The products of this reaction were poly(methacrylic acid) (pMAA) and the corresponding vinylpyridine as low-molecular weight side-product. The other six homologues of the upper part of Table 3.1 underwent only partial alkaline hydrolysis of the ester moiety, after 2 weeks of hydrolysis, and were converted to MAA units and the corresponding hydroxyalkylpyridine. Thus, the homopolymers of the pyridinylalkyl methacrylate homologues exhibited two different routes of alkaline hydrolysis, the first one involving the complete cleavage of the PyEMA units and their conversion to MAA units and vinylpyridine, and the second involving only partial cleavage and formation of MAA units and an alcohol rather than an olefin, as illustrated in Figure 3.5. Furthermore, p2PyEMA and p4PyEMA could also be cleaved thermally at 180 and 160 °C, respectively, again being converted to MAA units and the corresponding vinylpyridine. In contrast, p3PyEMA was thermally more stable than the other two pPyEMA isomers, undergoing only partial thermal removal of the pyridinylethyl side group up to around 200 °C, being converted to MAA units and 3-vinylpyridine.

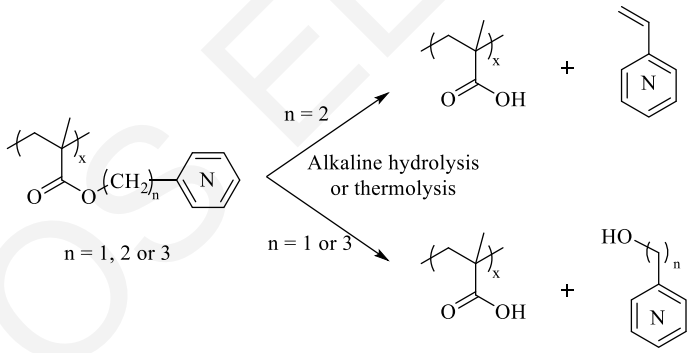

Figure 3.5. Cleavage of homologous poly(pyridinylalkyl methacrylate)s upon treatment under alkaline hydrolysis conditions or thermolysis. The cleavage followed two different routes, one for the three pPyEMA homologues (β-elimination), and the other for the remaining six homologues (addition/elimination).

Table 3.1 Polymer Structures, Monomer Conversions, Molecular Weights, Molecular Weight Dispersities, and Hydrolytic and Thermal Stability Characteristics of the Homopolymers of the Pyridinylalkyl Methacrylates and Related Monomers.

Polymer Structure	$MW^{theor.}$ (g mol^{-1})	^1H NMR	GPC		% Hydrolysis [d]		Cleavage Temp. (°C)		DSC
		Conversion (%)	M_n (g mol^{-1})	*Đ*	*Alkaline*	*Acidic*	*DSC*	*TGA*	Δ*H* (kJ/mol)
$2PyMMA_5$ [a]	990	100.0	1150	1.84	44.44	0	325	330	12.75
$2PyEMA_{55}$ [a]	9660	91.0	11800	1.51	100.00	0	180	200	61.34
$2PyPMA_{10}$ [a]	2150	100.0	1140	1.43	16.67	0	250	250	10.97
$3PyMMA_5$ [a]	990	100.0	1040	1.66	58.33	7	310	330	6.48
$3PyEMA_{50}$ [b]	9780	100.0	4080	1.29	100.00	0	180, 300	180, 300	33.52
$3PyPMA_5$ [a]	1130	100.0	860	1.66	33.33	5	>360	370	6.30
$4PyMMA_{50}$ [b]	9080	100.0	4640	1.31	67.74	10	275	270	22.06
$4PyEMA_{50}$ [c]	6080	61.5	3710	1.30	100.00	0	160	170	61.35
$4PyPMA_{50}$ [b]	10500	100.0	6040	2.13	60.00	10	325	320	12.38
$2PheMA_{50}$ [b]	9730	100.0	11700	1.17	47.00	0	330	320	45.79
$FMMA_{50}$ [b]	11900	88.4	6100	1.39	100.00	0	280	275	11.40
$2PyEMAAm_{50}$ [b]	6570	66.8	----[e]	----[e]	0	0	330	310	64.69
$2PyESMA_{50}$ [b]	10200	96.3	13300	1.46	100.00	0	250	240	64.81
$2PyEmeMA_{50}$ [b]	10500	100.0	7980	1.27	45.00	0	210	200	61.88
$2PyEdimeMA_{50}$ [b]	11200	100.0	7920	1.28	0	0	200, **350**	195, 330	15.99

[a] Synthesized using GTP. [b] Synthesized using RAFT polymerization. [c] Synthesized using ATRP. [d] Determined using ^1H NMR spectroscopy. [e] GPC results unavailable as the polymer was insoluble in THF, the GPC solvent.

The fact that in the case of the three isomeric pPyEMA the hydrolysis side-product was vinylpyridine indicated that an E2 elimination reaction took place from the *β*-substituted ethyl ester, as shown in Figure 3.6,[296,297] while in the case of the other six homologues, a nucleophilic addition/elimination took place.

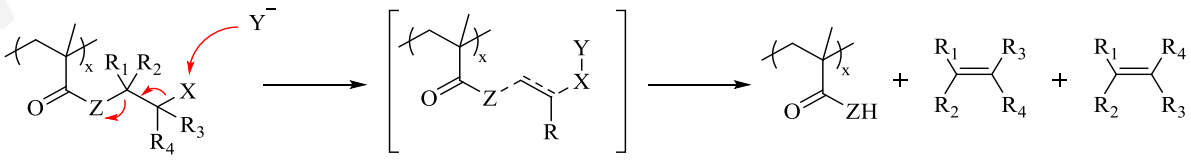

Figure 3.6 Elimination mechanism for the alkaline hydrolysis of the polymeric homologues bearing pyridylethyl ester side groups.[296]

The β-elimination of esters can also take place thermally and occurs by way of a six-membered ring transition state, where the carbonyl oxygen is approximately cis-coplanar,[298-301] as shown in Figure 3.7, known as β-scission.

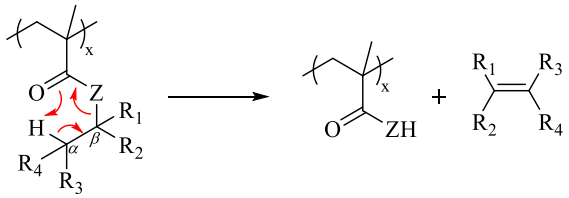

Figure 3.7 β-Scission mechanism for the thermal cleavage of the pyridinylethyl ester side groups of the polymeric homologues.[298]

The ability of β-substituted ethyl esters to cleave under thermolysis or under alkaline hydrolysis conditions via an elimination reaction is affected by several factors including the electron supply to the β-carbon of ethyl spacer between the ester moiety and pyridine ring (or α-carbon relative to the pyridine ring), the polarity of the C-Z bond (increased electronegativity in the Z group assists in the elimination and the reactivity therefore decreases: acetates > thioacetates), the acidity and the number of the hydrogen atoms attached on the α-carbon relative to the pyridine ring and the thermodynamic stability of the alkene product arising from both electronic and steric effects. Additionally, the ability of an aryl substituent to stabilize an adjacent carbonium ion decreases in the order Ph>>3Py>>2Py>4Py,[302] due to the presence of the electronegative nitrogen atom to position 2 or 4, and, therefore, the 4-pyridyl-ethyl substituted acetate is the least stable, followed by the 2-pyridyl-ethyl substituted acetate, and the 3-pyridyl-ethyl acetate.

3.1.3 Thermal and Hydrolytic Stability of Homologues: All pyridinylalkyl methacrylate homologues and related homopolymes were subjected under alkaline and/or acidic hydrolysis and thermolysis conditions, in order to investigate their stability. Alkaline hydrolysis was accomplished using sodium deuteroxide in d_6-DMSO at room temperature, while acidic hydrolysis was performed using deuterium chloride, also in d_6-DMSO at room temperature. Thermal properties of pyridinylalkyl methacrylate homologues were investigated using DSC and TGA. Table 3.1 summarizes the main results of this study, which are the percentage of the cleavage of each homologue after treatment under alkaline / acidic hydrolysis conditions and thermally.

^{1}H NMR Spectroscopic Evidence for Hydrolytic and Thermal Stability of the Polymers. In the following, we provide the ^{1}H NMR spectra of the polymers after hydrolytic

3.1.3.1 Alkaline Hydrolysis and Thermolysis Cleavage of p2PyEMA. Figure 3.8 shows the ^{1}H NMR spectrum of the original 2PyEMA$_{55}$ homopolymer in d_6-DMSO (a, black), along with the ^{1}H NMR spectra obtained after its treatment under alkaline hydrolysis conditions using sodium deuteroxide in d_6-DMSO (b, red), or after thermolysis in DMSO at 130 °C under reflux for 6 h (removal of 2-vinylpyridine and DMSO by evaporation under reduced pressure) in d_6-DMSO (c, blue). Peaks "d" and "e" are characteristic of the 2PyEMA monomer repeating units in the original polymer, corresponding to the oxyethylene protons, and appearing at 4.30 and 3.10 ppm (black cycles), respectively, in the ^{1}H NMR spectrum. These peaks are absent from the ^{1}H NMR spectra of the products obtained after alkaline hydrolysis or thermolysis. In both of these cleavage methods, the removal of the 2-pyridinylethyl moieties from the polymer was complete, as no polymeric pyridine signals were visible in the ^{1}H NMR spectra of the cleavage product. In contrast, all expected signals from 2-vinylpyridine were identified in the ^{1}H NMR spectrum of the alkaline hydrolysis product. Due to its removal by evaporation prior to analysis by ^{1}H NMR spectroscopy, no signal from 2-vinylpyridine was present in the ^{1}H NMR spectrum of the thermolysis product; however, the carboxylic acid proton "c" at 12.40 ppm of the MAA unit was clearly visible in this spectrum.

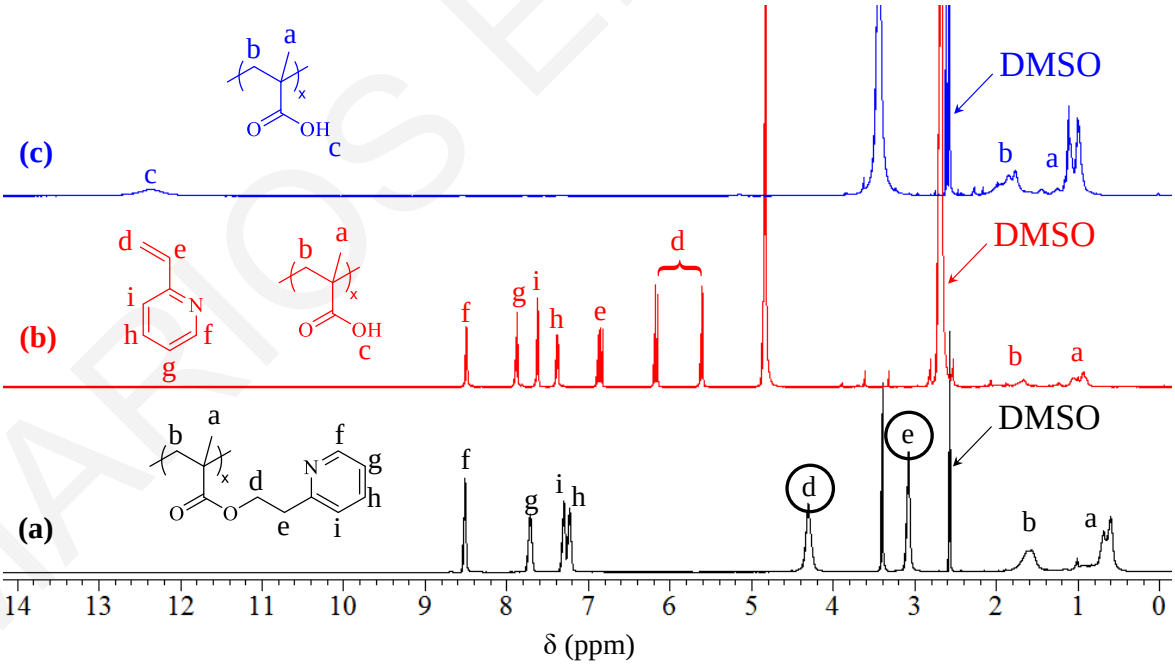

Figure 3.8 ^{1}H NMR spectra in d_6-DMSO of (a) the original 2PyEMA$_{55}$ homopolymer (black), (b) the 2PyEMA$_{55}$ homopolymer after alkaline hydrolysis using NaOD in d_6-DMSO (red), and (c) the 2PyEMA$_{55}$ homopolymer after thermolysis at 200 °C in the bulk in DSC (blue).

3.1.3.2 Alkaline Hydrolysis and Thermolysis Cleavage of p4PyEMA. The homopolymer of 4PyEMA was also quantitatively cleaved under both thermolysis and alkaline hydrolysis conditions. Figure 3.9 shows the ^{1}H NMR spectrum of the original 4PyEMA$_{50}$ homopolymer in d_6-DMSO (a, black), along with the ^{1}H NMR spectra obtained after its treatment under alkaline hydrolysis conditions using sodium deuteroxide in d_6-DMSO (b, red), and after thermolysis *via* DSC up to 200 °C in d_6-DMSO (c, blue). Similar to Figure 3.8 concerning p2PyEMA, the ^{1}H NMR spectra of alkaline-hydrolyzed and thermolyzed p4PyEMA in Figure 3.9 lacked the signals from the polymeric oxyethylene protons while they both exhibited olefinic signals from 4-vinylpyridine (4-vinylpyridine was retained in the thermolysis product here, as no evaporation was applied). Furthermore, the presence of the carboxylic acid proton of the MAA unit was again evident in the ^{1}H NMR spectrum of the thermolysis product.

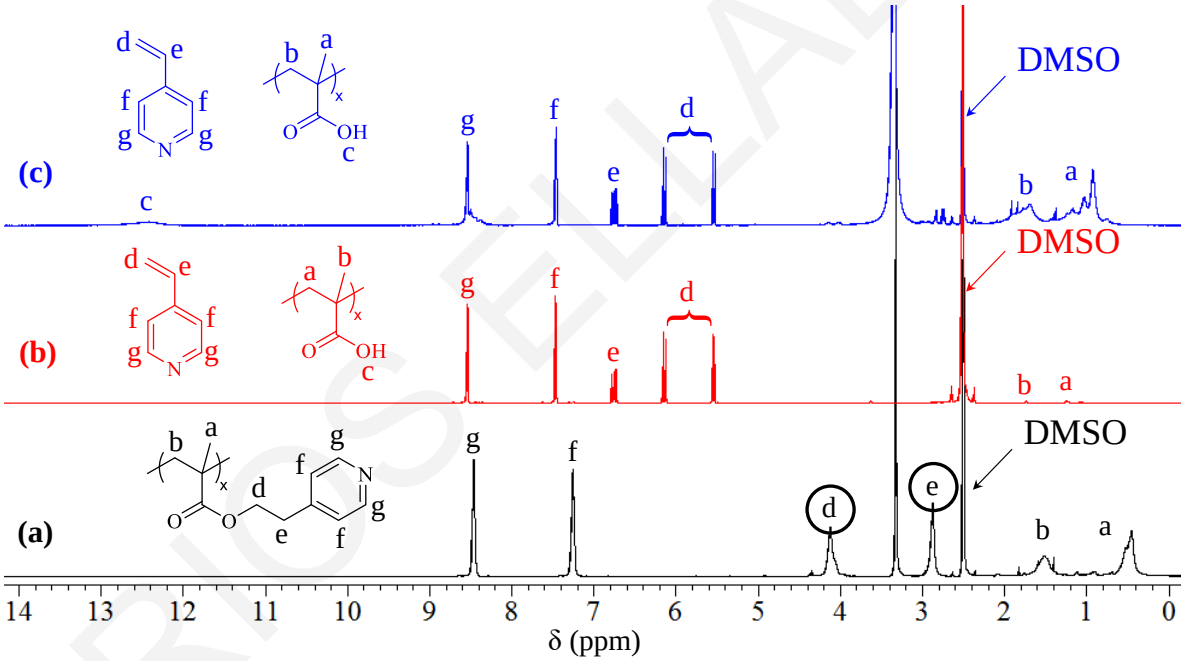

Figure 3.9 ^{1}H NMR spectra in d_6-DMSO of (a) the original 4PyEMA$_{50}$ homopolymer (black), (b) the 4PyEMA$_{50}$ homopolymer after alkaline hydrolysis using NaOD in d_6-DMSO (red), and (c) the 4PyEMA$_{50}$ homopolymer after thermolysis at 200 °C in the bulk in DSC (blue).

3.1.3.3 Alkaline Hydrolysis and Thermolysis Cleavage of p3PyEMA. Figure 3.10 shows the ^{1}H NMR spectrum in d_6-DMSO of the original 3PyEMA$_{50}$ homopolymer (a, black), and also the ^{1}H NMR spectra in d_6-DMSO too of the same polymer after subjecting it to alkaline hydrolysis (b, red), or thermolysis conditions through DSC up to 220 °C (c, blue). Examining first the ^{1}H NMR spectrum of the polymer treated in alkaline conditions, we may conclude that alkaline hydrolysis quantitatively cleaved off the 2-(pyridin-3-yl)ethyl

group as evidenced by the complete absence of the oxyethylene protons in the polymer product and the appearance of olefinic signals. Examining next the ^{1}H NMR spectrum of the polymer sample heated up to 220 °C, it appears that the polymer largely remained unchanged, exhibiting only a small (~10%) cleavage of the 3PyEMA units and conversion to MAA units and 3-vinylyridine. This is in sharp contrast to the thermal behavior of p2PyEMA and p4PyEMA and their quantitative cleavage to MAA units and the corresponding vinylpyridine already from 200 °C. This can be attributed to the reduced acidity of the hydrogen atoms attached on the *α*-carbon next to the pyridine ring in the 3PyEMA units, rendering the removal of their side – group *via β*-scission less favourable than those of the more acidic 2PyEMA and 4PyEMA units.[296,303]

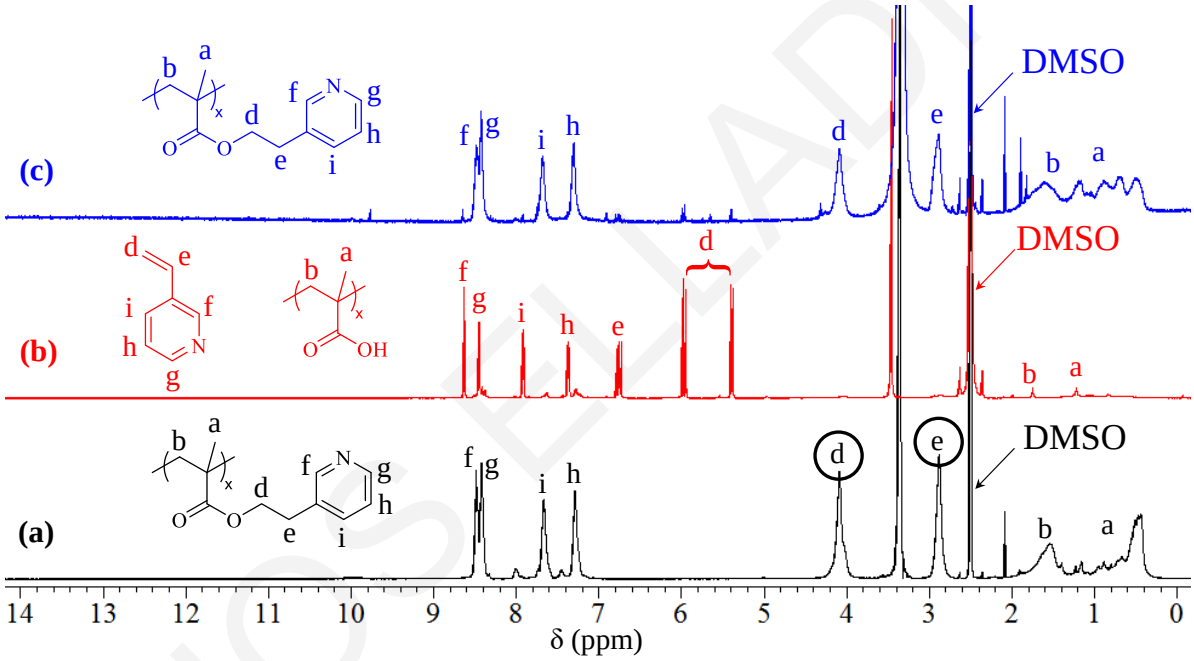

Figure 3.10 ^{1}H NMR spectra in d_6-DMSO of (a) the original 3PyEMA$_{50}$ homopolymer (black), (b) the 3PyEMA$_{50}$ homopolymer after alkaline hydrolysis using NaOD in d_6-DMSO (red), and (c) the 3PyEMA$_{50}$ homopolymer after being subjected to thermolysis (up to 220 °C) conditions (blue).

3.1.3.4 Alkaline Hydrolysis and Thermolysis Cleavage of Related Polymers. All related homopolymers were stable under acidic hydrolysis conditions, but they all very much differentiated their behavior toward alkaline hydrolysis conditions. In particular, the homopolymers of 2PyEMAAm and 2PyEdimeMA remained intact when subjected to alkaline hydrolysis conditions, while those of 2PheMA and 2PyEmeMA were partially hydrolyzed under the same conditions. The homopolymer of 2PheMA was hydrolyzed to an extent of 47 mol%, forming pMAA and a mixture of two different low-molecular-weight side-products, styrene (87 mol%) and 2-phenylethanol (13 mol%), indicating a

competition between E2 elimination and ester nucleophilic addition / elimination. The fact that 2PheMA cleaved approximately half, may be due to the decreased acidity of hydrogens attached on the *β*-carbon of ethyl spacer compared to that of 2PyEMA, due to the absence of pyridine which enhance the acidity. The partial cleavage of p2PyEmeMA was to a similar extent, 50%, forming pMAA and only 2-(prop-1-en-2-yl)pyridine, showing that only an E2 elimination mechanism took place. The half cleavage of the p2PyEmeMA units compared with that of p2PyEMA can be attributed to steric hindrance of the *β*-carbon of the ethyl spacer. Under alkaline hydrolysis conditions, pFMMA was fully hydrolyzed, giving pMAA and the low-molecular-weight olefinic side-product 9-methylene-9*H*-fluorene; the 9-fluorenylmethyl group is a well-known carboxylic acid-protecting group readily removable under basic conditions. p2PyESMA was also quantitatively cleaved and formed pMAA and a mixture of two side-products, 71 mol% of 2-vinylpyridine and 29 mol% of 2-(pyridin-2-yl)ethane-1-thiol, due to the presenceof less electronegative sulfur, something that promotes the production of a thiol, the ester nucleophilic addition / elimination product. The thermally most stable related homopolymers were those of 2PyEdimeMA, 2PheMA and 2PyEMAAm, all three with cleavage temperatures above 300 °C. pFMMA was thermally cleaved at 280 °C, while the homopolymers of 2PyEmeMA and 2PyESMA were less stable, with cleavage temperatures around 200 and 250 °C, respectively.

The formation, in some cases, of two different low-molecular-weight side-products indicates either the simultaneous hydrolysis by two different mechanisms, or the occurrence of two consecutive reactions, such as first production of only the alcohol, followed by its dehydration. We ruled out the second possibility by performing a control experiment in which 2-pyridineethanol was treated with the same concentration of NaOD as in the polymer alkaline hydrolysis experiments and observed no formation of 2-vinylpyridine that would result from the dehydration of the alcohol. The result of this experiment is displayed in Figure 3.11, which shows the ^{1}H NMR spectra of the original 2-pyridineethanol in d_6-DMSO (a, black), along with the ^{1}H NMR spectrum obtained after its treatment under alkaline hydrolysis conditions using sodium deuteroxide in d_6-DMSO (b, red). The hydoxyethylene protons “e” and “f” at 2.85 and 3.78 ppm, respectively, were fully preserved after the treatment (b, red), and no vinyl protons were observed. The only difference between the original spectrum and that obtained after treatment under alkaline hydrolysis conditions was the deprotonation of the acidic alcohol proton “g” at 4.69 ppm.

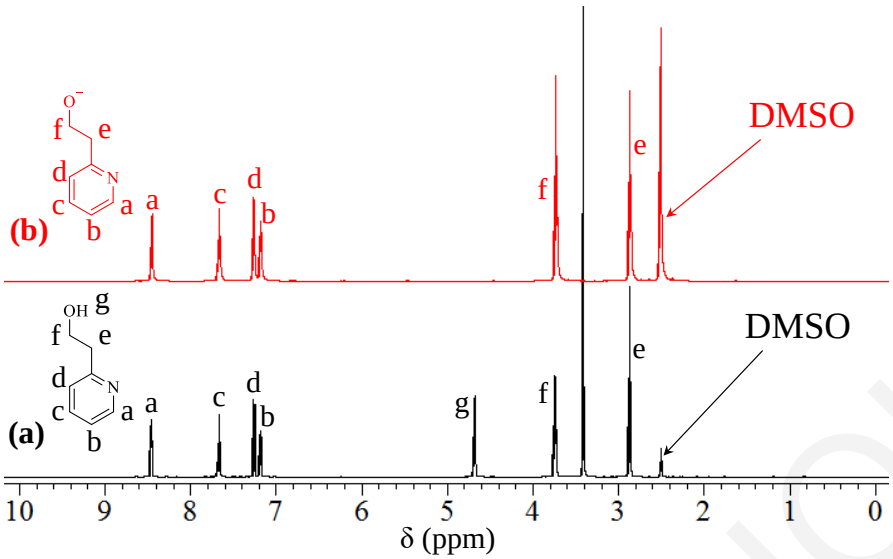

Figure 3.11 ^{1}H NMR spectra in d_6-DMSO of (a) 2-pyridineethanol (black), (b) 2-pyridineethanol after alkaline treatment (red).

Figure 3.12 shows the ^{1}H NMR spectrum of the original 2PheMA$_{50}$ homopolymer in d_6-DMSO (a, black), along with the ^{1}H NMR spectra obtained after its treatment under alkaline hydrolysis conditions using sodium deuteroxide in d_6-DMSO (b, red), or thermolysis using DSC until 250 °C in d_6-DMSO (c, blue). As already mentioned, the formation of two low-molecular-weight side-products after treatment under alkaline hydrolysis conditions, styrene and 2-phenylethanol, is due to the competition of two different mechanistic routes, where an elimination reaction gives a vinyl-product, while a nucleophilic substitution of ester gives an alcohol. The ^{1}H NMR spectrum in Figure 10 (c) indicated that thermolysis from DSC up to 250 °C affected only partially the 2PheMA$_{50}$ homopolymer, depolymerizing it back to the 2PheMA monomer to an extent of 10%; monomer formation was concluded from the appearance of the peaks due to the olefinic protons at 5.60 and 6.00 ppm and the oxymethylene protons at 4.30 ppm. The presence of pyridine in the side-chain of ethyl esters plays an important role in the rate of hydrolysis due to the increased acidity of the hydrogen atoms attached on the β-carbon of the ethyl spacer. Thus, the lability under alkaline hydrolysis conditions follows the order: 2PyEMA > 2PheMA.

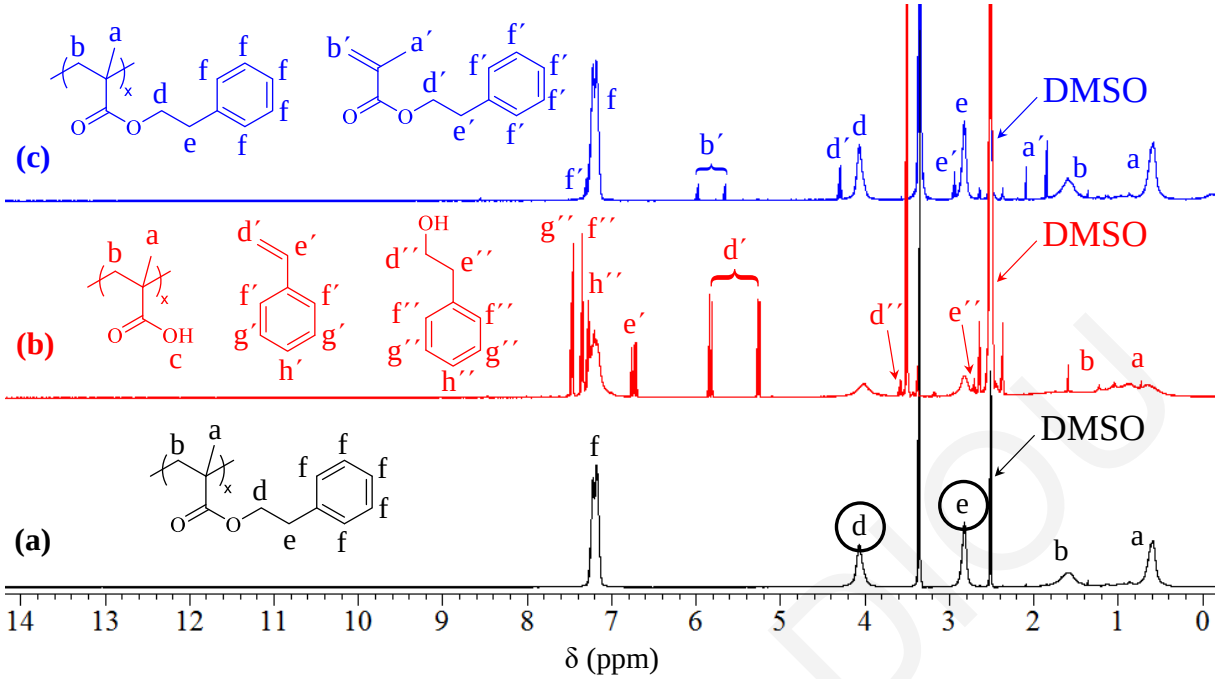

Figure 3.12 ^{1}H NMR spectra in d_6-DMSO of (a) the original 2PheMA$_{50}$ homopolymer (black), (b) the 2PheMA$_{50}$ homopolymer after alkaline hydrolysis using NaOD in d_6-DMSO (red), and (c) the 2PheMA$_{50}$ homopolymer after thermolysis in the bulk in DSC up to 250 °C (blue).

Figure 3.13 shows the ^{1}H NMR spectrum in d_6-DMSO of the original 2PyEmeMA$_{50}$ homopolymer (a, black), along with the ^{1}H NMR spectra also in d_6-DMSO obtained after its treatment under alkaline hydrolysis conditions (b, red), or thermally by subjecting it to DSC analysis up to 250 °C (c, blue). The oxymethylene protons "d" at ~4.0 ppm of the 2PyEmeMA repeating units appear in the ^{1}H NMR spectrum of the original polymer, while the intensity of these protons is decreased after alkaline hydrolysis, and, at the same time, the peak of vinyl protons "e′" at 5.95 and 5.35 ppm of 2-(prop-1-en-2-yl)pyridine appear in the same spectrum. The extent of cleavage of the 2PyEmeMA units under alkaline hydrolysis conditions was 45 mol%, while that by thermolysis was 100 mol%, as shown in parts (b) and (c) of Figure 3.13, respectively.

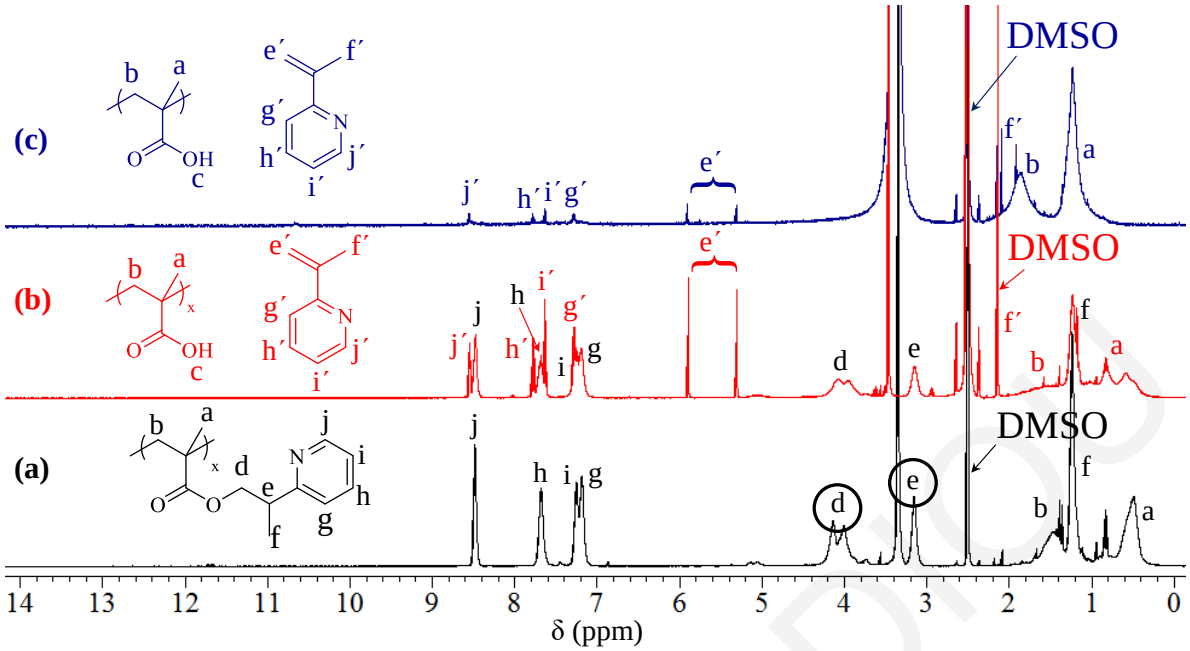

Figure 3.13 ^{1}H NMR spectra in d_6-DMSO of (a) the original 2PyEmeMA$_{50}$ homopolymer (black), (b) the 2PyEmeMA$_{50}$ homopolymer after alkaline hydrolysis using NaOD in d_6-DMSO (red), and (c) the 2PyEmeMA$_{50}$ homopolymer after thermolysis in the bulk in DSC up to 250 °C (blue).

Hydrolytic Stability of p2PyEMA, p2PyEmeMA and p2PyEdimeMA

The hydrolyzability under alkaline conditions of p2PyEMA, p2PyEmeMA and p2PyEdimeMA was examined and compared to each other and helped elucidate the effect of substitution on the position of the α-carbon relative to the pyridine ring in these polymers with 2-(pyridin-2-yl)ethyl group in the pendant. The lability under alkaline hydrolysis conditions for these three homologous polymers follows the order: 2PyEMA > 2PyEmeMA >> 2PyEdimeMA. This order can be attributed to the steric hindrance imparted by the methyl group on the α-carbon relative to the pyridine ring in the 2PyEmeMA units. p2PyEdimeMA totally resisted alkaline hydrolysis due to the lack of hydrogens attached on the α-carbon next to the pyridine ring. Thus, the number of hydrogen atoms attached on the α-carbon next to the pyridine ring, and its steric hindrance on the α-carbon are important rate-determined factors in the hydrolysis of the poly(pyridinylalkyl methacrylate) homologues.

Hydrolytic Stability of p2PyEMA, p2PyESMA and p2PyEMAAm

The hydrolyzability of p2PyEMA, p2PyESMA and p2PyEMAAm was examined and compared to each other, and helped elucidate the effect of the nature of the group connecting the 2-(pyridin-2-yl)ethyl group in the pendant onto the main chain, whether

ester, thioester or amide, on polymer stability. Although p2PyEMA was completely converted to MAA units and 2-vinylpyridine within 90 minutes under alkaline hydrolysis conditions, p2PyESMA required almost 1 day for the full cleavage of the pendant in the 2PyESMA repeating unit into two different low-molecular-weight side-products, 2-vinylpyridine at 67 mol% and 2-(pyridin-2-yl)ethanethiol at 33 mol%. On the other extreme, p2PyEMAAm was totally stable under these conditions,[264] due to the delocalization of the lone pair of electrons in the nitrogen into the carbonyl group forming a partial double bond between nitrogen and the carbonyl carbon. Thus, the lability under alkaline hydrolysis conditions follows the order: 2PyEMA > 2PyESMA >> 2PyEMAAm. The order between 2PyEMA and 2PyESMA can be attributed to the electronegativity of O and S, which follows the order O > S, and facilitates cleavage by elimination in the same order. Thus, the exchange of the etheric oxygen atom of the ester moiety in the 2PyEMA unit for sulfur or nitrogen atoms leads to an increase in hydrolytic stability.

3.1.4 Thermal Stability of Homologues. Table 3.1 also illustrates the results of the thermal stability of the homopolymers of the pyridinylalkyl methacrylate homologues along with those of the related homopolymers, expressed as side-group cleavage temperature, as determined using DSC and TGA. Figure 3.14 shows the cleavage temperature, obtained from DSC, for the poly(pyridinylalkyl methacrylate)s plotted against the number of carbon atoms in the spacer between the ester moiety and pyridine, and also against the position of the N atom in the pyridine ring. As already mentioned, the homopolymers of 4PyEMA and 2PyEMA were the most thermally labile, exhibiting the lowest cleavage temperatures, 160 and 180 °C, respectively, with complete removal of the pyridinylethyl groups. The homopolymer of 3PyEMA was also completely cleaved, but at a much higher temperature, 310 °C, exhibiting only a small (~10%) cleavage of the 3PyEMA units to MAA and 3-vinylpyridine. Comparing 2PyEMA and 4PyEMA cleavage temperature with that of 3PyEMA, it seems that the reduced acidity of hydrogen atoms attached on β-carbon of ethyl spacer of 3PyEMA has a significant impact to its thermal stability, being the most stable of pPyEMA. The most stable homologue was p3PyPMA, whose cleavage temperature exceeded 350 °C. Cleavage temperatures that exceeded 300 °C were also displayed by the homopolymers of 2PyMMA, 3PyMMA and 4PyPMA. The higher cleavage temperature of poly(pyridinylmethyl methacrylate)s (pPyMMAs) compare to that of pPyEMAs, can be attributed to the fact that no β-scission mechanism took place, due to methyl spacer between the ester moiety and pyridine, and therefore the six-membered ring transition state could not be formed. Comparing now the thermal stability of pPyEMAs

with that of poly(pyridinylpropyl methacrylate)s (pPyPMAs), where the spacer between the ester moiety and pyridine is a propyl group, a β-scission mechanism could also took place, but doesn't occur the reduced acidity of hydrogen atoms of the β-carbon of the propyl spacer.

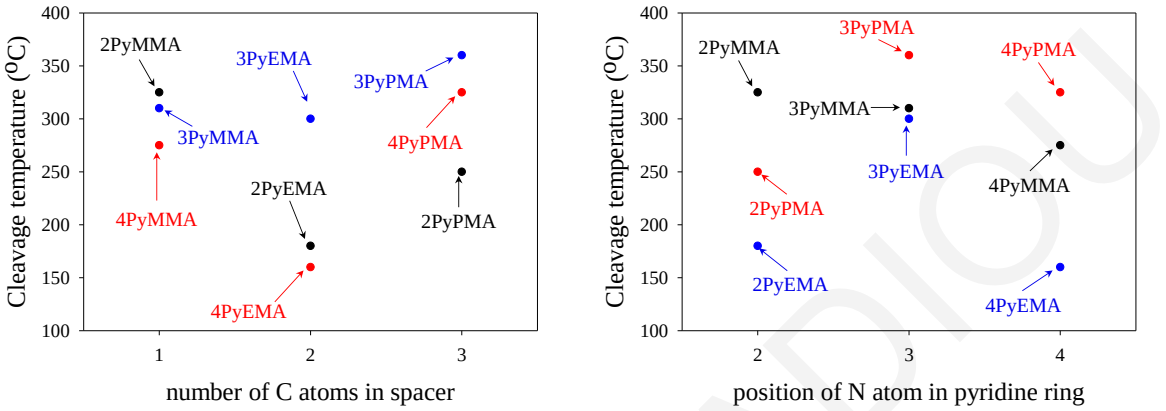

Figure 3.14 Cleavage temperature from DSC for the homopolymers of the pyridinylalkyl methacrylate homologues as a function of (a) depending on the number of carbon atoms in the spacer between the ester moiety and pyridine, and (b) the position of nitrogen in the pyridine ring.

Figure 3.15 shows the DSC and TGA thermograms of the three isomeric homopolymers with ethyl spacers, p2PyEMA, p3PyEMA and p4PyEMA. The DSC thermograms of the homopolymers of 4PyEMA and 2PyEMA exhibited major endothermic and irreversible peaks at 160 and 180 °C, respectively, followed by less intense endothermic peaks at ~200 °C, most likely due to anhydride formation. The TGA thermograms of the same homopolymers showed a weight loss at ~200 °C, manifesting side-group removal, consistent with DSC. The side-group removal was complete for both homopolymers as it exactly corresponded to that expected on the basis of the relative weight of the side-group (dashed line labeled "theory" in Figure 3.15 (b)). However, the weight loss was more gradual between 150 and 350 °C in the case of $4PyEMA_{50}$. This may be due to spontaneous polymerization of the very reactive 4-vinylpyridine being released during side-group removal. Final weight loss was observed between 400 and 450 °C for all three homopolymers due to complete backbone decomposition. In the case of the 3PyEMA homopolymer, there was a small endothermic peak in the DSC trace at 190 °C, indicating a small percentage of cleavage of the 3PyEMA units, something corroborated by the ^{1}H NMR spectrum in Figure 3.10, and a large (main) endothermic peak right above 300 °C (^{1}H NMR spectroscopic analysis of the DSC pan at 2020 °C of p3PyEMA showed partial

cleavage of the 3PyEMA units (~10%), and their conversion to MAA units and 3-vinylyridine, leaving most of the polymer unchanged). The TGA thermogram of poly3PyEMA showed a small weight loss at ~180 °C, followed by a greater weight loss at ~290 °C, again in agreement with DSC. The final weight loss in the TGA for p3PyEMA takes place at 400 °C, probably due to backbone decomposition.

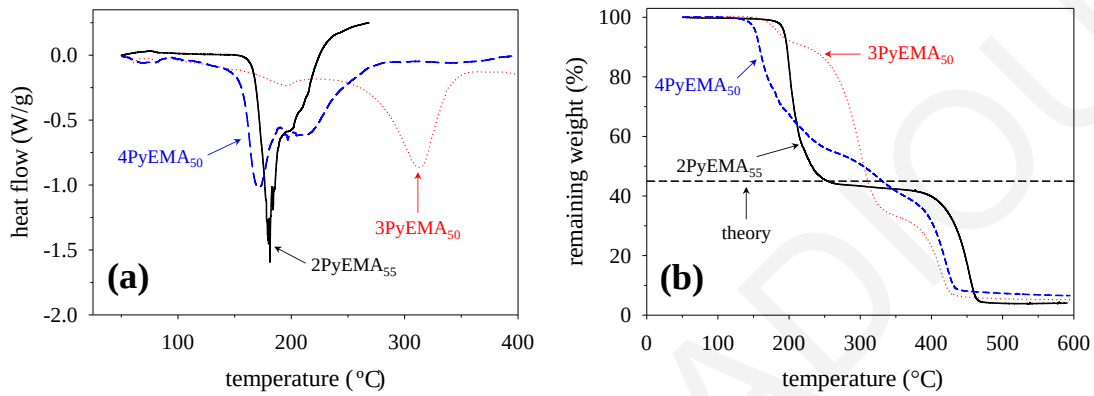

Figure 3.15 (a) DSC, and (b) TGA thermograms for p2PyEMA (black continuous lines), p3PyEMA (red dotted lines) and p4PyEMA (blue dashed lines). The black dashed horizontal line labelled "theory" in part (b) indicates the expected remaining weight upon complete side-group removal.

Figure 3.16 shows the DSC and TGA thermograms for p2PyEMA, p2PyEmeMA and p2PyEdimeMA. p2PyEmeMA exhibited a strong thermal response in DSC at ~210 °C, a temperature slightly higher than that where the DSC thermal response of p2PyEMA took place at 180 °C. In contrast, p2PyEdimeMA displayed a small endothermic peak at 195 °C, which corresponded to its partial depolymerization as inferred from the analysis of the DSC sample using ^{1}H NMR spectroscopy. The main peak for the DSC thermal response of p2PyEdimeMA was located at around ~350 °C, and was also endothermic. Thus, comparing p2PyEmeMA and p2PyEMA, we may conclude that the introduction of a methyl group to the α-carbon next to the pyridine ring increased the cleavage temperature by 30 °C. Comparing now p2PyEdimeMA and p2PyEMA, we may infer that the attachment of two methyl groups onto the same position rendered p2PyEdimeMA thermally much more stable. The black dashed and red dotted horizontal lines indicate the weight percentages expected to remain after the complete removal of the pyridine side groups (2-vinylpyridine and 2-(prop-1-en-2-yl)pyridine), and they agree well with the experimental results from TGA.

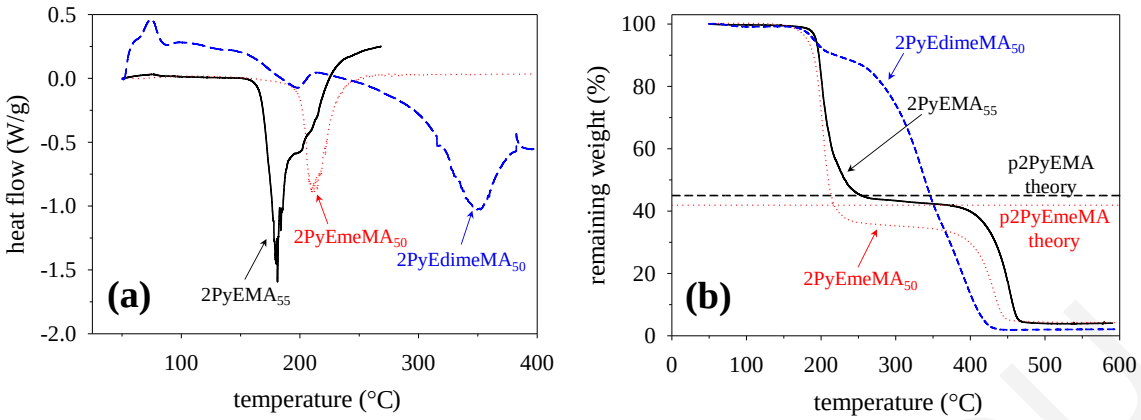

Figure 3.16 (a) DSC, and (b) TGA thermograms for p2PyEMA (black continuous lines), p2PyEmeMA (red dotted lines) and p2PyEdimeMA (blue dashed lines). The black dashed horizontal dotted lines labelled "theory" indicate the expected remaining weight upon complete removal of the side-group of p2PyEMA and p2PyEmeMA, respectively.

3.1.5 Hydrolytic and Thermal Stability Between the Homologues

Poly2PyEMA, poly3PyEMA and poly4PyEMA:

Figure 3.17 shows the percentage of alkaline hydrolysis in the homopolymers of the pyridinylalkyl methacrylate homologues after treatment with ~0.2 M NaOD for 7 days, plotted against the number of carbon atoms in the spacer between the ester moiety and pyridine, and also against the position of nitrogen in the pyridine ring. The homopolymers of the isomeric 2PyEMA, 3PyEMA and 4PyEMA were fully converted to MAA units and the corresponding vinylpyridine upon subjecting them to the above-mentioned alkaline hydrolysis conditions, while the homopolymers of the other six pyridinylalkyl methacrylate homologues were only partially cleaved under the same conditions, producing pMAA and the corresponding pyridinealcohol. As already noted, in the case of the three isomeric pPyEMA, an E2 elimination reaction took place from the β-substituted ethyl ester due to the presence of β-hydrogen atoms attached to the α-carbon relative to pyridine ring,[296,297,304] while in the case of the other six homologues, a nucleophilic substitution of ester took place. Figure 3.17 shows that the extent of cleavage under alkaline hydrolysis conditions is higher when the spacer between the ester moiety and the pyridine ring is a methyl than a propyl group, for all positions of nitrogen in the pyridine ring. Additionally, the extent of cleavage under alkaline hydrolysis conditions of the 4-pyridine methyl- and propyl-substituted homologues is higher than those of the 2- or 3-pyridine methyl- and propyl-substituted homologues. This may be due to the increased reactivity of 4-substituted pyridine. The percentage of the alkaline hydrolysis of

pPyMMAs was higher than that of pPyPMAs. This can be attributed to the stability of the alkoxy anion, which increases in the order PyMMAs > PyPMAs, due to the delocalization of the anion. Comparing Figures 3.14 and 3.17, one may conclude that there is good agreement between the cleavage temperatures and the extent of cleavage under alkaline hydrolysis conditions for most poly(pyridinylalkyl methacrylate)s, suggesting similar cleavage mechanisms.

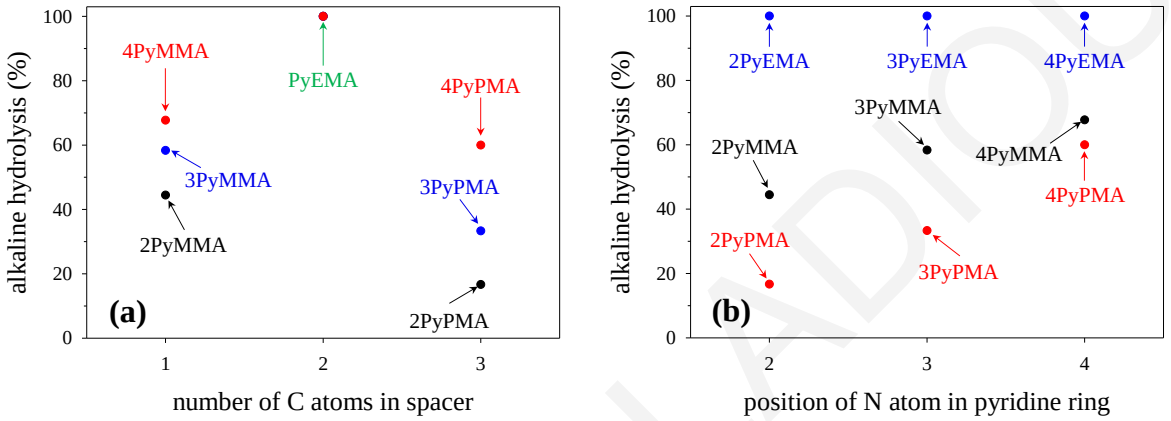

Figure 3.17 Percentage of alkaline hydrolysis in the homopolymers of the pyridinylalkyl methacrylate homologues, as a function of (a) the length of the spacer between the ester moiety and the pyridine ring, and (b) the position of nitrogen in the pyridine ring.

As already mentioned, the three pPyEMA isomers were fully hydrolyzed under alkaline conditions. However, hydrolysis took place at different rates. Figure 3.18 illustrates the temporal evolution of the extent of hydrolysis for the three homopolymers, as recorded using ^{1}H NMR spectroscopy. p4PyEMA was completely hydrolyzed within 30 minutes, while p2PyEMA required 90 minutes for full hydrolysis, and, finally, complete side-group removal from p3PyEMA took 24 h. Thus, the rate of hydrolysis for p4PyEMA was slightly faster than that for p2PyEMA, whereas that for p3PyEMA was the slowest. The first order plot for the later stages of hydrolysis of p3PyEMA was not linear, indicating change in the hydrolysis mechanism. The lability of the three pPyEMA isomers under alkaline hydrolysis conditions follows the order: poly4PyEMA (k= 0.130 min^{-1}) > poly2PyEMA (k=0.028 min^{-1}) >> poly3PyEMA (k=0.005 min^{-1}). This difference in the hydrolysis rate for the three isomeric homopolymers can be attributed to the acidity of the α-methylene group relative to pyridine ring. These acidities can be obtained from the pK_a values of model compounds. For this case, the relevant model compounds are 2-methylpyridine (2-picoline), 3-methylpyridine (3-picoline) and 4-methylpyridine (4-picoline), having pK_a values of 34.0, 37.7 and 32.2, respectively.[296,303] These values indicate that the protons of

the α-methylene group of 4PyEMA are more acidic than those of 2PyEMA, which are, in turn, more acidic than those of 3PyEMA. In line with the above, Katritzky et al.[305] observed the complete cleavage of (pyridin-4-yl)ethyl substituted esters after quaternization, and only partial cleavage of the quaternized (pyridin-2-yl)ethyl substituted esters.

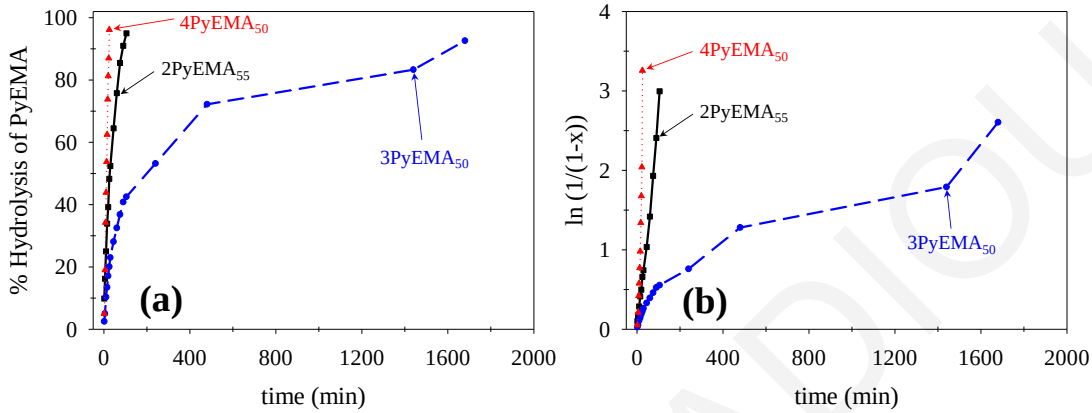

Figure 3.18 (a) Temporal evolution of the extent of alkaline hydrolysis and (b) first order plots for the alkaline hydrolysis of p2PyEMA (black continuous lines), p3PyEMA (blue dashed lines) and p4PyEMA (red dotted lines).

The above observations imply that there are some similarities and differences between the hydrolysis and thermolysis behavior of the pPyEMA homologues and the related polymers. In the case of alkaline hydrolysis, elimination from β-substituted ethyl esters takes place, while in the case of thermolysis, a β-scission mechanism takes place. Additionally, all factors affecting the hydrolytic stability also affect the thermal stability.

3.1.6 Alkaline Hydrolysis of the Monomers.

After confirming the degradability under alkaline hydrolysis conditions of the p2PyEMA and p4PyEMA isomers, we decided to also subject the starting monomers to alkaline hydrolysis. Furthermore, the 2PyEMAAm, 2PyESMA, 2PyEmeMA and 2PyEdimeMA monomers were also subjected to alkaline hydrolysis conditions, and the main results obtained are summarized in Table 3.2. As already mentioned, pyridinylalkyl methacrylate homologues can be hydrolyzed via two different routes; the first involves an E2 elimination where an olefin is produced, while the second involves a nucleophilic substitution of esters and produces an alcohol.

The alkaline hydrolysis behavior of the monomers was somewhat different from that of their corresponding homopolymers. All these results are summarized in Table 3.2. Upon being subjected to alkaline hydrolysis conditions, the 2PyEMA monomer was fully cleaved

and converted to MAA units and a mixture of two low-molecular-weight products, 2-pyridineethanol (88 mol%) and 2-vinylpyridine (12 mol%), indicating the competition between two different mechanistic routes, E2 elimination which led to the olefinic product and nucleophilic addition/elimination which led to the formation of the alcohol. The competition between the two mechanisms can be attributed to the different local environment, where the steric hindrance, in the case of polymers, of the ester moiety prevents its nucleophilic attack. The same results were observed in the case of the alkaline hydrolysis of the 4PyEMA monomer, but in this case the percentage of the olefinic-product was higher than the alcohol (61 mol% 4-vinylpyridine and 39 mol% 4-pyridineethanol). Comparing the alkaline hydrolysis of 4PyEMA monomer with that of 2PyEMA monomer, the olefinic product in the case of 4PyEMA was higher due to its increased acidity of the β-hydrogen, favoring the E2 elimination reaction.[305]

The 2PyEmeMA monomer was completely converted to MAA and 2-(pyridin-2-yl)propan-1-ol after treatment under alkaline hydrolysis conditions, while p2PyEmeMA was only 45% cleaved and converted to MAA units and only 2-isopropenylpyridine as low-molecular-weight product. 2PyESMA monomer was completely cleaved and converted to a mixture of two low-molecular-weight products, 59% 2-vinylpyridine and 41% 2-pyridin-2-ylethanethiol, indicating again the action of two hydrolysis mechanisms. The same behavior was observed in the case of the alkaline hydrolysis of the p2PyESMA. The 2PyEdimeMA monomer was completely cleaved and converted to MAA and 2-methyl-2-(pyridin-2-yl)propan-1-ol, while p2PyEdimeMA was stable under alkaline hydrolysis conditions. Finally, both the 2PyEMAAm monomer and the 2PyEMAAm monomer repeating unit in the respective homopolymer were stable under alkaline hydrolysis conditions, consistent with the greater stability of the amide groups. The above observations imply that there are some similarities and differences between the hydrolysis and thermolysis behavior of the pPyEMA homologues and the related polymers.

Table 3.2 Results of alkaline hydrolysis of the 2-(pyridin-2-yl)ethyl ester monomers and the corresponding homopolymers.

Name of Monomer or Repeating Unit	Alkaline Hydrolysis of Monomer [a]			Alkaline Hydrolysis of Polymer [a]		
	% Conversion	Products (mol%)		% Conversion	Products (mol%)	
		olefin	alcohol		olefin	alcohol
2PyEMA	100	12	88	100	100	0
4PyEMA	100	61	39	100	100	0
2PyESMA	100	59	41	100	67	33
2PyEMAAm	0	0	0	0	0	0
2PyEmeMA	100	0	100	45	100	0
2PyEdimeMA	100	0	100	0	0	0

a. Analyzed using ^{1}H NMR spectroscopy.

Scheme 3.16 shows the chemical reaction for the alkaline hydrolysis of the 2PyEMA monomer using sodium deuteroxide in d_6-DMSO, along with its ^{1}H NMR spectra before (a, black) and after alkaline hydrolysis (b, red). The absence of the oxyethylene protons “d” and “e” at 4.45 and 3.10 ppm, respectively, of the starting 2PyEMA monomer from the ^{1}H NMR spectrum of the hydrolysis products indicated the full cleavage of the ester moiety in 2PyEMA. Careful examination of the ^{1}H NMR spectrum of the hydrolysis products led to the conclusion that the original oxyethylene protons “d” and “e” were converted to hydroxyethylene protons “d′” and “e′” (88%) and to olefinic protons “d′′” and “e′′” (12%).

Scheme 3.16 Chemical reaction for the alkaline hydrolysis of the 2PyEMA monomer, along with its ^{1}H NMR spectra before (a, black) and after alkaline hydrolysis (b, red), both in d_6-DMSO.

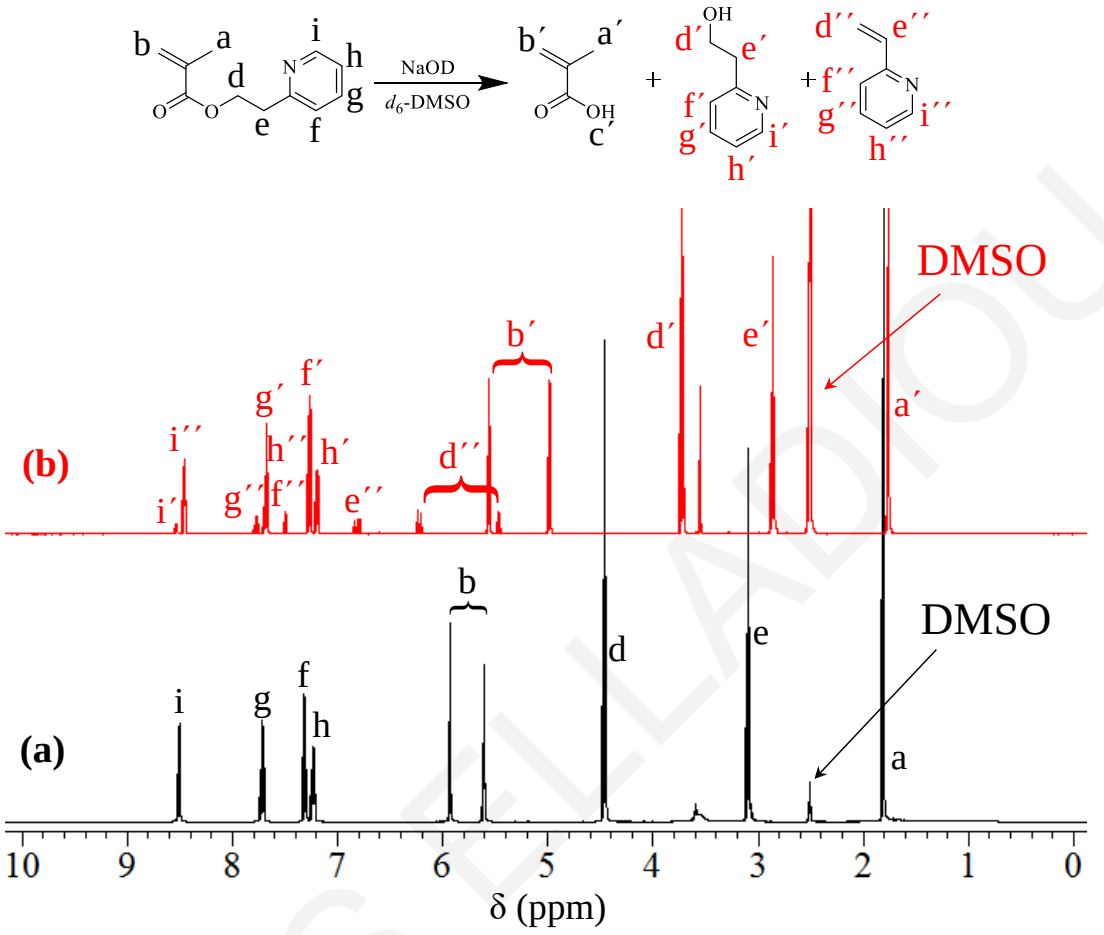

The alkaline hydrolysis of the 4PyEMA monomer also led to full cleavage of the ester moiety and its conversion to MAA and a mixture of 4-vinylpyridine (61%) and 4-pyridineethanol (39%), according to ^{1}H NMR spectroscopy as illustrated in Scheme 3.17, which also displays the relevant chemical reaction. The ^{1}H NMR spectrum of the hydrolysis products indicated the full cleavage of the ester moiety in 4PyEMA (absence of the oxyethylene protons "d" and "e" at 4.35 and 2.95 ppm, respectively), and its conversion to MAA (methacrylate protons "b′" at 5.00 and 5.60 ppm), 4-vinylpyridine (vinyl protons "d′′" at 5.50 and 6.15 ppm) and 4-pyridineethanol (hydroxymethylene protons "d′" at 3.60 ppm). The difference between the alkaline hydrolysis of the 4PyEMA monomer and that of the 2PyEMA monomer is that, in the case of 4PyEMA, the olefin is the main product, whereas in the case of 2PyEMA, the alcohol is the main product.

Scheme 3.17 Chemical reaction for the alkaline hydrolysis of the 4PyEMA monomer, along with its ^{1}H NMR spectra before (a, black) and after alkaline hydrolysis (b, red), both in d_6-DMSO.

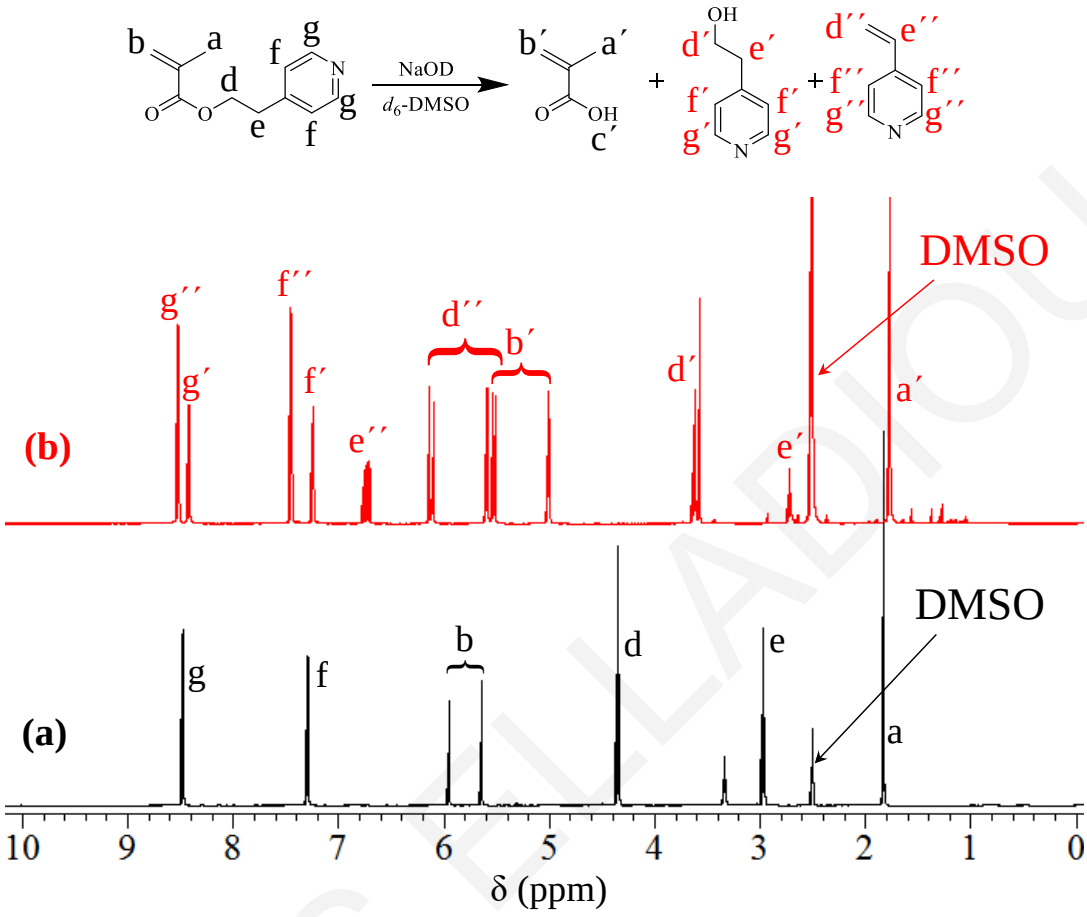

3.1.7 2-Pyridineethanol as Protecting Group for Carboxylic Acids. From previous observations 2-pyridineethanol could be characterized as a good protecting group for MAA, which can be selectively removed, after polymerization, either chemically under alkaline conditions or thermally at or above 110 °C, while it is stable under acidic conditions and it resists catalytic hydrogenolysis. The 2-pyridineethanol protecting group is one of the very few moieties that can be hydrolyzed under alkaline conditions.

Scheme 3.18 shows the controlled (co)polymerization and chemical and thermal deprotection of 2PyEMA. As already noted, 2PyEMA monomer was synthesized by the esterification of 2-pyridineethanol with slightly excess of methacryloyl chloride in THF in the presence of excess (8-folf) triethylamine base at 0 °C. 2PyEMA monomer could also be synthesized at ~30% yield prepared by in bulk reaction of MAA with 2-vinylpyridine at 60 °C for 12 h, in the presence of small amount of DPPH free-radical inhibitor. 2PyEMA was homo- and co-polymerized with methyl methacrylate (MMA) and styrene (Sty) using

GTP and RAFT polymerization, respectively, and their molecular weight and composition characteristics are summarized in Table 3.3.

Scheme 3.18 (Co)polymerization of 2PyEMA, and Polymer Chemical and Thermal Deprotection.

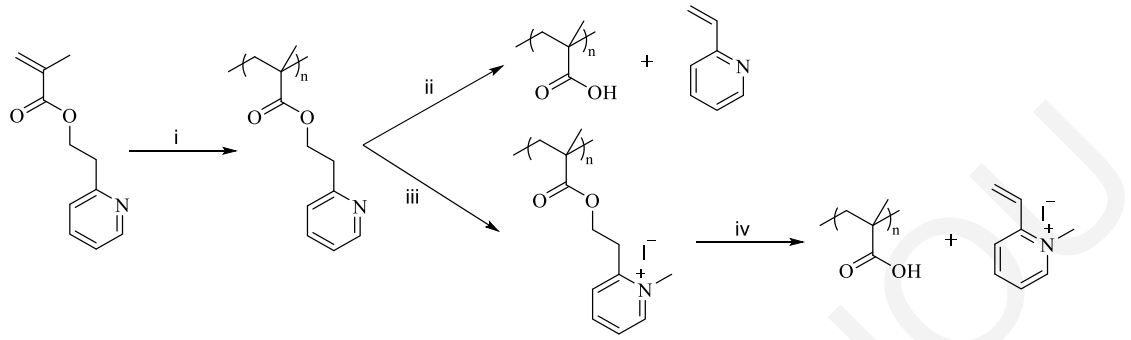

i. GTP or RAFT polymerization, ii. NaOH (aq) in DMSO at room temperature (RT), or at 110 °C in bulk, in DMSO or in DMF, iii. excess methyl iodide in DMSO, RT, 1 h, iv. excess K_2CO_3 in water, RT, 12 h.

Table 3.3 Molecular Weight and Composition Characteristics of the 2PyEMA-containing (Co)polymers Obtained by GTP and RAFT Polymerization.

Polymer Structure	$MW^{theor.}$ (g mol^{-1})	GPC			^{1}H NMR	
		M_p (g mol^{-1})	M_n (g mol^{-1})	*Đ*	*% Monomer Conversion*	*% mol 2PyEMA*
$2PyEMA_5$ [a]	1057	1350	1164	1.22	100.0	100.0
$2PyEMA_{55}$ [a]	9662	13200	11800	1.51	91.0	100.0
$2PyEMA_{10}$-*b*-MMA_{50} [a]	7022	16600	4200	1.10	100.0	13.7
$2PyEMA_{100}$ [b]	19344	26000	12000	2.37	100.0	100.0
$2PyEMA_{100}$-*b*-Sty_{500} [a]	63100	82300	42500	2.04	84.0	16.1

a. Synthesized using GTP, b. Synthesized using RAFT polymerization.

Although the 2PyEMA-based (co)polymers made by GTP were rather homogeneous in terms of their molecular weights, with polydispersity indices (PDIs) equal to or lower than 1.5, those prepared by RAFT polymerization presented broader molecular weight distributions and PDIs of 2.0 and 2.4. This can be attributed to the thermal lability of the 2PyEMA monomer and its monomer repeating units in the (co)polymers, leading to partial deprotection even at the moderately high temperature of 65 °C used for the polymerization. Thus, most of the following deprotection studies involved the largest homopolymer prepared by GTP, $2PyEMA_{55}$.

2PyEMA$_{55}$ was converted to pMAA and (monomeric) 2-vinylpyridine, either by alkaline hydrolysis in dimethyl sulfoxide (DMSO) at room temperature, or by thermolysis at or above 110 °C in the bulk or in solution (DMSO or dimethyl formamide, DMF) without the addition of external base or acid (ii). In both of these deprotection methods, the removal of the 2-pyridinyl moieties from the polymer was complete, as no polymeric pyridine signals were visible in the spectra. Worthy of note was that similar thermolyses [306] and alkaline hydrolyses [307] have been reported in the organic chemistry and the medicinal chemistry literature to remove 2-hydroxyethyl-2-pyridine from low-molecular-weight compounds, but, to our knowledge, these processes have not been applied to synthetic polymers. Another route explored for the conversion of the 2PyEMA units to MAA units was via quarternization of the pyridine ring, first reported in the peptide literature.[308-310] Thus, excess methyl iodide was used to iodomethylate PyEMA$_{55}$ in DMSO, followed by treatment with excess K_2CO_3 base in water overnight, resulting in pMAA at ~85% yield and iodomethylated 2-vinylpyridine.

The facile removal of the 2-hydroxyethyl-2-pyridine group in solution at room temperature using a hydroxide (quantitative deprotection) or a carbonate salt (after methylation, near-quantitative deprotection) renders 2PyEMA a very attractive monomer as a precursor to pMAA, when initial stability to neutral or acidic conditions is required. Another monomer with similar tolerance to acidic and neutral conditions and sensitivity to hydroxides and primary and secondary amines is pentafluorophenyl (meth)acrylate, whose polymers are used as activated polyesters to mediate their quantitative conversion to polyamides, recently developed by Théato and co-workers.[144-146]

The thermal behavior of the 2PyEMA$_{55}$ homopolymer and the two diblock copolymers, 2PyEMA$_{10}$-*b*-MMA$_{50}$ and 2PyEMA$_{100}$-*b*-Sty$_{500}$, was further explored using DSC and TGA. Figure 3.19 (a) displays the DSC thermograms of 2PyEMA$_{55}$, 2PyEMA$_{10}$-*b*-MMA$_{50}$ and 2PyEMA$_{100}$-*b*-Sty$_{500}$. All three thermograms exhibited strong endotherms initiated at 160 °C, with that of the homopolymer being the most pronounced. These endotherms were not reproduced upon the second heating, suggestive of irreversibility, due to a chemical reaction. This was confirmed by analyzing, using ^{1}H NMR spectroscopy, the product of the treatment of 2PyEMA$_{55}$ to one heating cycle (sample retrieved from the DSC pan); the analysis showed that the product consisted of pMAA and 2-vinyl pyridine. 2PyEMA$_{55}$, 2PyEMA$_{10}$-*b*-MMA$_{50}$ and 2PyEMA$_{100}$-*b*-Sty$_{500}$, were also studied using TGA and the obtained thermograms are shown in Figure 3.19 (b). All three (co)polymers exhibited an

initial weight loss at ~170 °C, and further weight losses at ~400 °C and higher. The 2PyEMA homopolymer exhibited the most pronounced weight loss at the lower temperature, and that corresponded exactly to the weight percentage of 2-vinylpyridine.

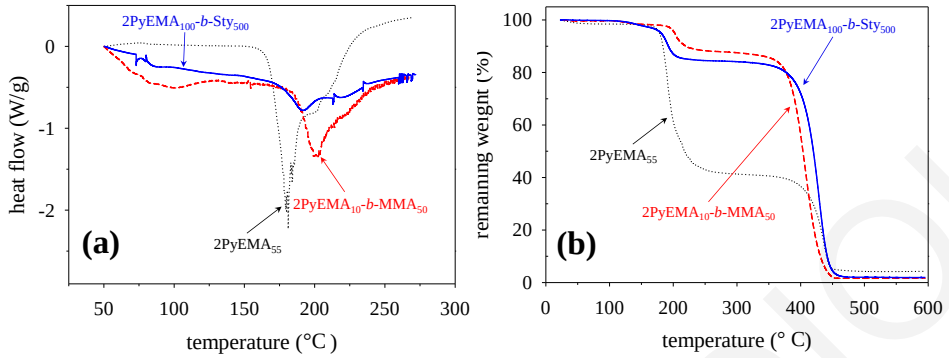

Figure 3.19 (a) DSC and (b) TGA thermograms of the 2PyEMA homopolymer and its diblock copolymers with MMA and Sty, exhibiting endotherms at 160 °C, indicative of release of 2-vinylpyridine.

Subsequently, isothermal TGA on $2PyEMA_{55}$ at 160 °C was performed. The obtained TGA thermogram is displayed in Figure 3.20. The dashed horizontal line in the figure indicates the theoretical weight percent, calculated on the basis of the complete removal of 2-vinylpyridine. The thermogram suggests that after 120 min of heating at 160 °C, the sample lost more than 85% of the weight due to 2-vinylpyridine, whereas the reaction was nearing completion at 400 min, without any indication for anhydride formation.

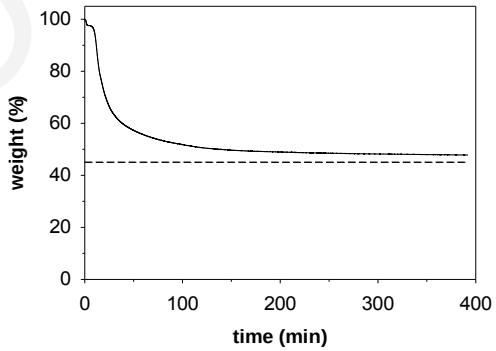

Figure 3.20 TGA thermogram of $2PyEMA_{55}$ at constant temperature of 160 °C. The dashed horizontal line indicates the final polymer weight when all pyridine side-groups are removed.

3.2 ABC Triblock Terpolymers With Orthogonally Deprotectable Blocks: Synthesis, Characterization and Deprotection

The development and availability of new protecting groups is vital for all branches of synthetic chemistry. Equally vital is the facile and selective removal of these groups, leaving intact other protecting groups which are to be cleaved later. This concept of orthogonal deprotection by combining three different forms of protected methacrylic acid (MAA) in the same terpolymers was exploited in this section. One of these protected monomers was the 2PyEMA whose units can be readily converted to MAA units either under alkaline hydrolysis conditions or thermally. The second monomer was tetrahydro-2*H*-pyran-2-yl methacrylate (THPMA) which is cleaved either via acidic hydrolysis or by thermolysis, and the third form of protected MAA was the hydrogenolyzable benzyl methacrylate (BzMA). Two ABC triblock terpolymers based on all three of these monomers were synthesized, one by RAFT polymerization, and the other by GTP. Subsequently, the two ABC triblock terpolymers were sequentially subjected to conditions of alkaline hydrolysis, acidic hydrolysis and hydrogenolysis, leading to the selective cleavage of the 2PyEMA, the THPMA and the BzMA units, respectively, without affecting the remaining types of protecting groups, according to analysis using ^{1}H NMR spectroscopy. Similarly selective was the acidic hydrolysis followed by alkaline hydrolysis. Thermal treatment at 130 °C of the terpolymers led to the conversion of both the PyEMA and the THPMA units to MAA units, without affecting the BzMA units, yielding amphiphilic diblock copolymers, whose self-assembly properties in water were investigated.

3.2.1 Monomers syntheses. For the purposes of this work, were used three monomers, the 2PyEMA and THPMA monomers and the commercially available BzMA monomer. The synthesis of the 2PyEMA has already discussed. Bellow follows the synthesis for the THPMA monomer.

3.2.1.1 Synthesis of THPMA. The THPMA monomer was prepared by the reaction of MAA with a 100% excess of 3,4-dihydro-2*H*-pyran.[291] Scheme 3.19 shows the reaction leading to the THPMA formation, along with its ^{1}H and ^{13}C NMR spectra of the THPMA.

Scheme 3.19 Synthesis of THPMA monomer, along with its ^{1}H and ^{13}C NMR spectra.

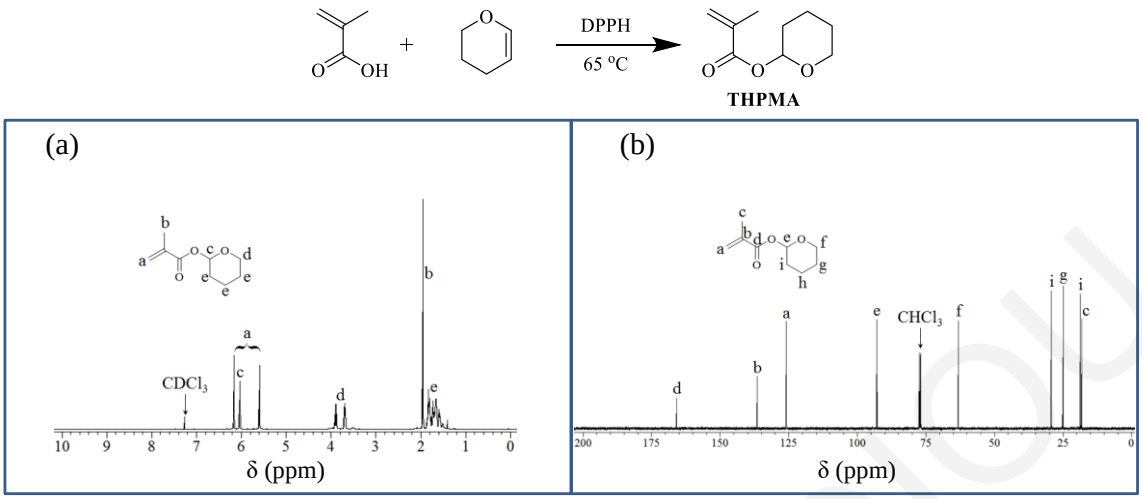

3.2.2 Polymer Design and Synthesis. Polymer preparation in the present study was performed using two controlled polymerization methods, GTP and RAFT polymerization. GTP was used to synthesize a rather small ABC triblock terpolymer with short blocks comprising 5 units each, while RAFT polymerization allowed the synthesis of a larger terpolymer with 20 or more units in each block. The most stable BzMA was introduced as the first block in both terpolymers. Since 2PyEMA has a large tendency to thermolyze, it was introduced as the last block, mixed with a further equimolar amount of THPMA, in the terpolymer made by RAFT polymerization (polymerization temperature was 65 °C). In contrast, THPMA was chosen to be polymerized last in GTP, based on the large tendency of this monomer to hydrolyze even at room temperature, yielding carboxylic acid protons which would lead to GTP termination. Scheme 3.20 illustrates the addition sequences followed for the syntheses of the two ABC triblock terpolymers via the two polymerization methods.

Scheme 3.20 Addition Sequences Followed for the Preparation of the Two ABC Triblock Terpolymers.

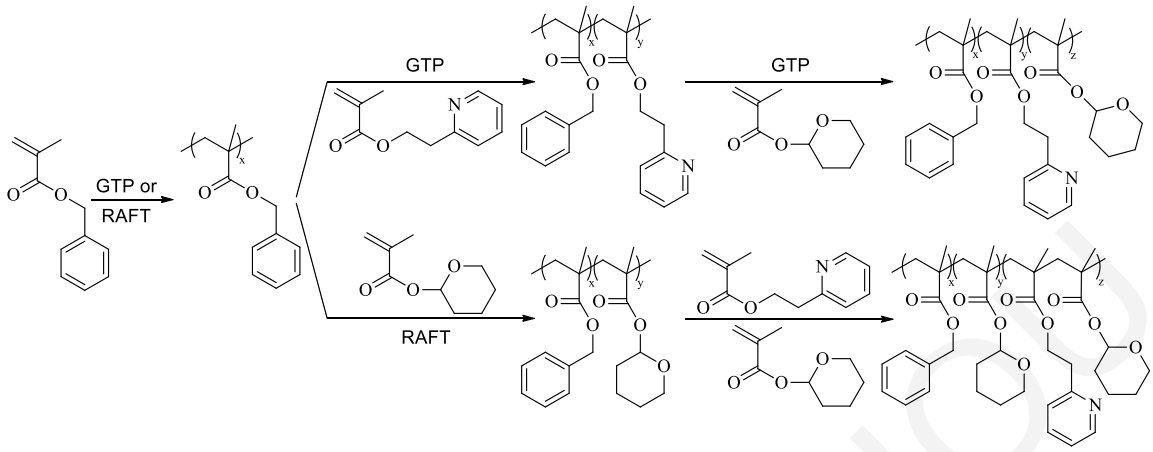

Figure 3.21 shows the GPC traces of the terpolymers and their precursors, while Table 3.4 summarizes the results calculated from these GPC traces. These results were the M_n, M_p, and the $Đ$ values. The theoretical molecular weights, calculated from the monomer–to–initiator ratio in the polymerization feed and taking into account monomer conversion as determined using ^{1}H NMR spectroscopy, are also listed in the table. Furthermore, the content in each type of unit in the terpolymers and their precursors, also calculated from the ^{1}H NMR spectra, are also listed in the table. The table shows that monomer conversion was quantitative or near-quantitative in all cases, the polymer composition and molecular weights were close to the expected, and the molecular weight dispersities were reasonably low, 1.40 or lower.

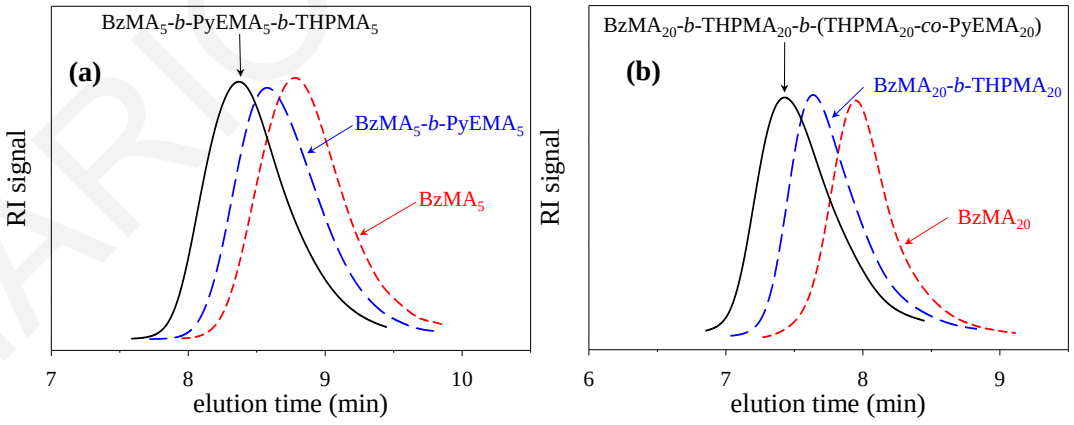

Figure 3.21 GPC traces of (a) the $BzMA_5$-*b*-$PyEMA_5$-*b*-$THPMA_5$ and (b) the $BzMA_{20}$-*b*-$THPMA_{20}$-*b*-($THPMA_{20}$-*co*-$PyEMA_{20}$) triblock terpolymers along with those of their precursors.

Table 3.4 Molecular Weight and Composition Characteristics of the Polymers Synthesized Using GTP and RAFT Polymerization.

Polymer Structure	$MW^{theor.}$ (g mol^{-1})	M_p (g mol^{-1})	M_n (g mol^{-1})	$Đ$	% Monomer Conversion [c]	Polymer Composition (mol%) [c]	
						BzMA	PyEMA
$BzMA_5$ [a]	980	2170	1570	1.37	100	100.0	0.0
$BzMA_5$-*b*-$PyEMA_5$ [a]	1940	3090	2060	1.40	100	50.0	50.0
$BzMA_5$-*b*-$PyEMA_5$-*b*-$THPMA_5$ [a]	2790	3800	3700	1.29	100	33.3	33.3
$BzMA_{20}$ [b]	3500	9500	6880	1.30	100	100.0	0.0
$BzMA_{20}$-*b*-$THPMA_{20}$ [b]	6900	16700	10700	1.34	100	50	0.0
$BzMA_{20}$-*b*-$THPMA_{20}$-*b*-($THPMA_{20}$-*co*-$PyEMA_{20}$) [b]	13700	21100	13600	1.38	94 [d]	33.5	20.2

a. Synthesized using GTP, b. Synthesized using RAFT polymerization, c. Determined using ^{1}H NMR spectroscopy.

3.2.3 Step–wise Removal of the Protecting Groups. Scheme 3.21 shows the various routes followed for the sequential and selective deprotection of $BzMA_{20}$-*b*-$THPMA_{20}$-*b*-($THPMA_{20}$-*co*-$2PyEMA_{20}$). The 2PyEMA units are labile in an alkaline environment, whereas the THPMA units are labile under acidic conditions. pBzMA can be converted to pMAA via catalytic hydrogenolysis using a palladium catalyst. According to Scheme 3.21, first, by exposing the terpolymer to acidic conditions (i), its THPMA units would be converted to MAA units, while the 2PyEMA and the BzMA units are preserved. If the resulting terpolymer is now subjected to alkaline hydrolysis conditions (ii), the 2PyEMA units would be cleaved to MAA units, leading to the formation of a BzMA-MAA diblock copolymer. If this copolymer is hydrogenolyzed (iv), it would be converted to an MAA homopolymer. Alternatively, the terpolymer could be first exposed to alkaline hydrolysis conditions (ii), which would convert its 2PyEMA units to MAA units, without affecting the THPMA or the BzMA units. Then, the resulting terpolymer can be subjected to acidic hydrolysis conditions (i), which would convert the THPMA units to MAA units, yielding again the BzMA-MAA diblock copolymer which could be hydrogenolyzed (iv) to polyMAA. The 2PyEMA and the THPMA units in the original terpolymer can also be simultaneously (and non–selectively) converted to MAA units thermally (iii), without affecting the BzMA units.

Scheme 3.21 Cleavage Sequences Followed for the Step-wise and Selective Deprotection of the $BzMA_{20}$-*b*-$THPMA_{20}$-*b*-($THPMA_{20}$-*co*-$PyEMA_{20}$) Triblock Terpolymer All the Way to MAA_{80}.

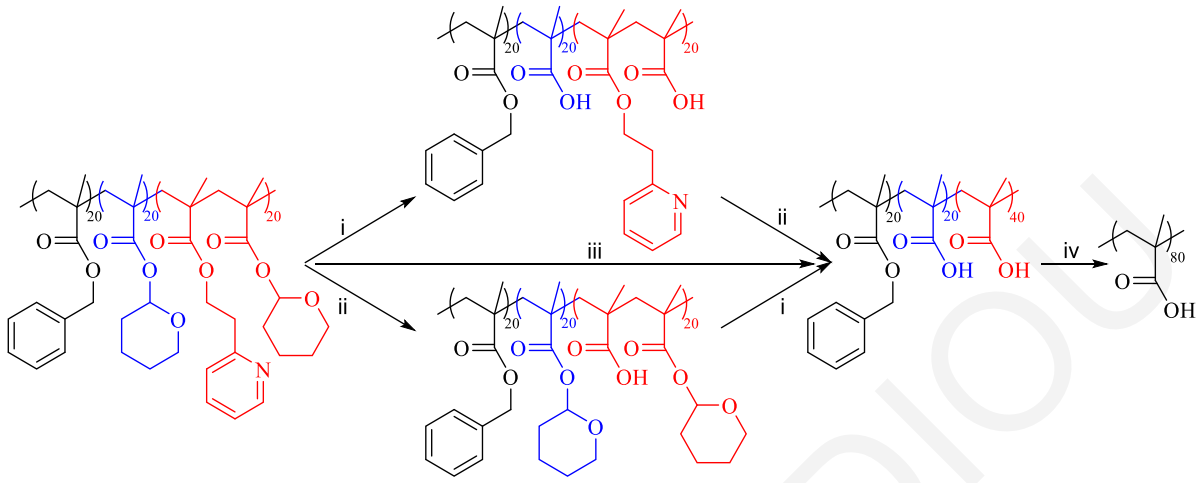

i. HCl in DMSO/MeOH (1:1 v/v); ii. NaOH (s) in DMSO/MeOH (5:3 v/v); iii. vacuum oven at 130 °C for 6 h; iv. H_2 in ethyl acetate/MeOH (9:1 v/v) and Pd/C catalyst.

3.2.3.1 Sequential Application of Hydrolyses and Hydrogenolysis. Figure 3.22 shows the ^{1}H NMR spectra of the polymer products obtained by subjecting the original terpolymer first to acidic hydrolysis conditions and then to alkaline. The ^{1}H NMR spectrum of the original $BzMA_{20}$-*b*-$THPMA_{20}$-*b*-($THPMA_{20}$-*co*-$2PyEMA_{20}$) triblock terpolymer is also presented in Figure 3.22. Comparing spectra (a) and (b) in the figure, it can be seen that upon treatment with acid, the methine proton "e" of the THPMA unit at 5.8 ppm disappeared in spectrum (b), due to the removal of the tetrahydropyranyl ring. This did not affect the 2PyEMA units as their characteristic oxymethylene protons "j" at 4.3 ppm and the adjacent methylene protons "k" at 3.0 ppm of the 2PyEMA unit were preserved in spectrum (b). Subsequent treatment of this acidic hydrolysis product with NaOH resulted in the removal of the side–groups of the 2PyEMA units as evidenced by the absence of their "j" and "k" protons (blue circle) in the ^{1}H NMR spectrum in Figure 3.22 (c).

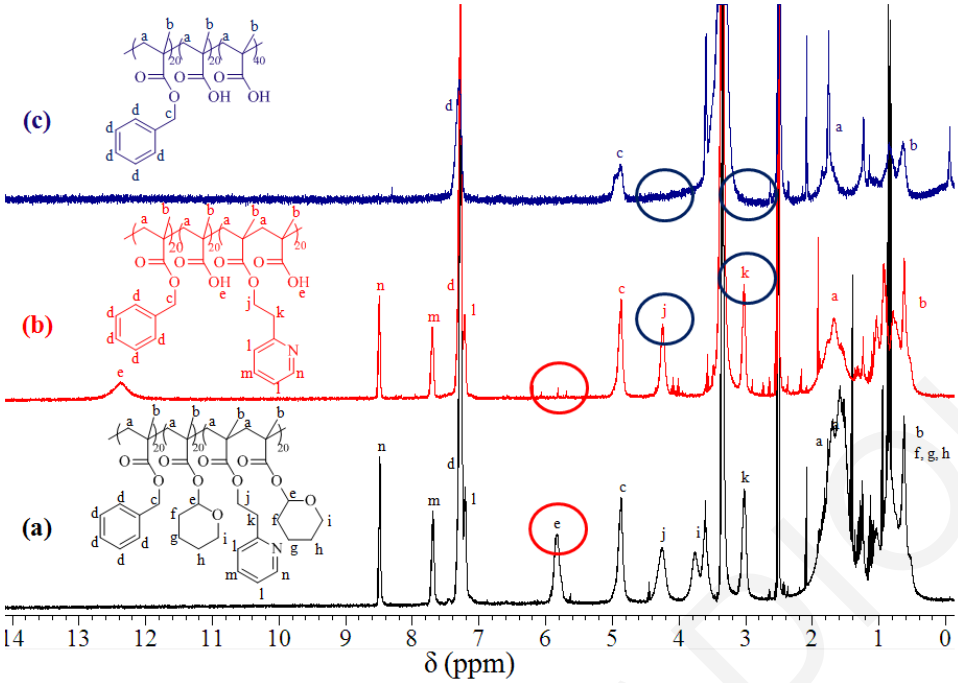

Figure 3.22 ^{1}H NMR spectra in d_6-DMSO of (a) the original BzMA$_{20}$-*b*-THPMA$_{20}$-*b*-(THPMA$_{20}$-*co*-2PyEMA$_{20}$) triblock terpolymer (black), (b) the same terpolymer after acidic hydrolysis (red), and (c) after acidic and alkaline hydrolyses (blue).

Similarly, Figure 3.23 displays the ^{1}H NMR spectra of the polymer products obtained by processing the original triblock terpolymer now first under alkaline hydrolysis conditions, then under acidic hydrolysis conditions, and finally, under hydrogenolysis conditions. The ^{1}H NMR spectrum of the original BzMA$_{20}$-*b*-THPMA$_{20}$-*b*-(THPMA$_{20}$-*co*-2PyEMA$_{20}$) triblock terpolymer is shown in the figure too. By examining ^{1}H NMR spectra (a) and (b) in Figure 3.23, the result of subjecting to alkaline hydrolysis conditions can be inferred. Compared to spectrum (a), spectrum (b) lacks the peak of the oxymethylene protons "j" at 4.3 ppm and the peak of the adjacent methylene protons "k" at 3.0 ppm in the side-group of the 2PyEMA unit (blue circles). At the same time the peak of the vinyl protons "o" at 5.5 ppm and "p" at 6.2 ppm of 2-vinylpyridine appeared in the spectrum (b), due to the conversion of the 2PyEMA unit to a MAA unit and 2-vinylpyridine. By subsequently subjecting the thus-obtained terpolymer to acidic hydrolysis conditions, this led to the disappearance of the methine proton "e" (red circle) due to the hydrolysis of the THPMA units and their conversion to MAA units. Finally, catalytic hydrogenolysis of this hydrolysis product resulted in the removal of the benzylic protons "c" at 4.9 ppm (green circle) and the conversion of the BzMA units to MAA units.

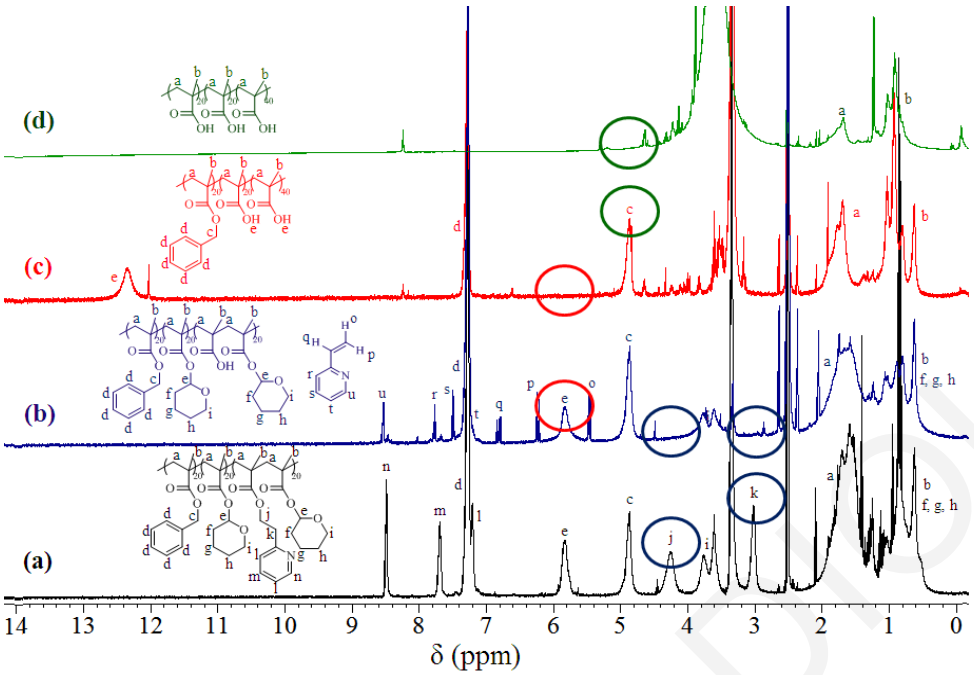

Figure 3.23 ^{1}H NMR spectra in d_6-DMSO of (a) the original BzMA$_{20}$-*b*-THPMA$_{20}$-*b*-(THPMA$_{20}$-*co*-2PyEMA$_{20}$) triblock terpolymer (black), (b) the same terpolymer after alkaline hydrolysis (blue), (c) the same terpolymer after alkaline and acidic hydrolyses (red), and (d) after alkaline and acidic hydrolyses as well as catalytic hydrogenolysis (green).

The BzMA$_5$-*b*-2PyEMA$_5$-*b*-THPMA$_5$ triblock terpolymer, obtained by GTP, was also subjected to alkaline and acidic hydrolyses. The product obtained after alkaline or acidic treatment, was subsequently subjected to acidic or alkaline treatment, respectively, converting the original BzMA$_5$-*b*-2PyEMA$_5$-*b*-THPMA$_5$ triblock terpolymer to a BzMA$_5$-*b*-MAA$_{10}$ diblock copolymer. However, due to the low molecular weight of this polymer, purification after each processing step using dialysis was impossible. Thus, the hydrogenolysis of the BzMA units in the BzMA-MAA diblock copolymer was not attempted. Figure 3.24 shows the ^{1}H NMR spectrum of the original BzMA$_5$-*b*-2PyEMA$_5$-*b*-THPMA$_5$ triblock terpolymer (a, in black), the same terpolymer after acidic hydrolysis (b, in red), the same terpolymer after alkaline hydrolysis (c, in blue), and also after alkaline and acidic hydrolyses (d, in green). Upon treatment with acid, the methine proton of the THPMA unit at 5.8 ppm disappeared (red circle), due to the acidic hydrolysis of the THPMA units. This did not affect the 2PyEMA units as their characteristic "e" protons at 4.3 ppm were preserved in the spectrum. After alkaline hydrolysis, the peak at 4.3 ppm of the 2PyEMA unit disappeared (blue circle), due to the conversion of the 2PyEMA units to MAA units. However, subsequent treatment with HCl resulted in the cleavage of the THPMA side–groups as evidenced by the disappearance of their "j" protons (green circle).

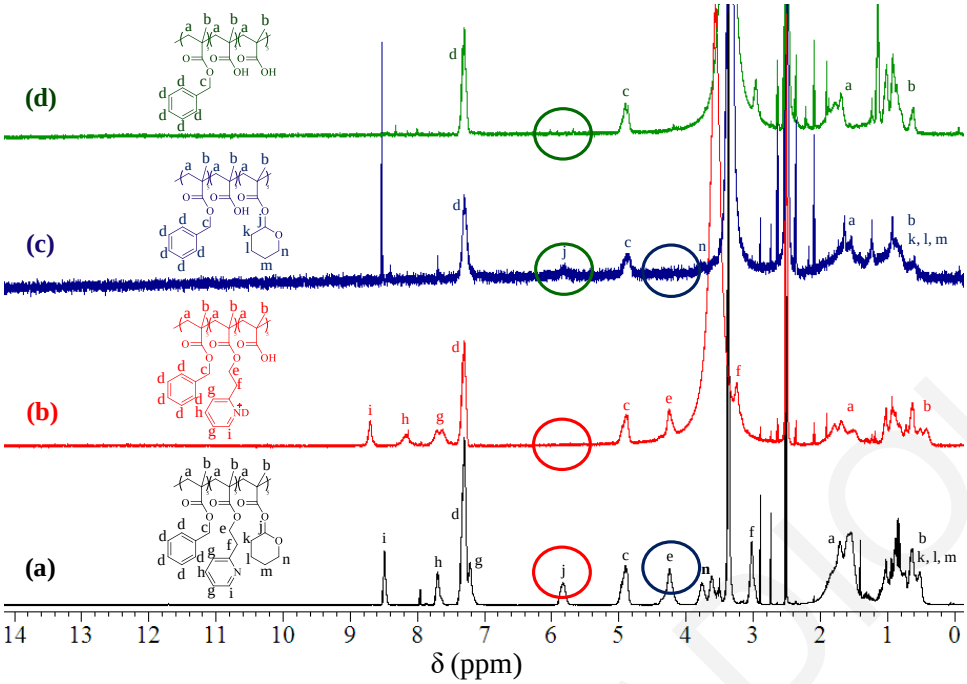

Figure 3.24 ^{1}H NMR spectra in d_6-DMSO of (a) the original $BzMA_5$-*b*-$2PyEMA_5$-*b*-$THPMA_5$ triblock terpolymer (black), (b) the same terpolymer after acidic hydrolysis (red), (c) the same terpolymer after alkaline hydrolysis (blue), and (d) after alkaline and acidic hydrolyses (green).

3.2.4 Thermal Deprotection of 2PyEMA and THPMA. Figure 3.25 shows the DSC thermograms of the 2PyEMA, the THPMA and the BzMA homopolymers, and those of the two ABC triblock terpolymers. All major peaks were endothermic and irreversible (not reproduced upon the second heating cycle), suggestive of their origin in chemical reactions, and took place between 150 and 250 °C. In the case of the 2PyEMA homopolymer, the main endothermic peak was located at 180 °C, followed by a shoulder at 210 °C, both of which were related to the cleavage of the 2PyEMA unit. In the case of the THPMA homopolymer, the main peak was at 160 °C, at slightly lower temperature than that of the 2PyEMA homopolymer but of much higher intensity (enthalpy of reaction) than that of 2PyEMA, and followed by a less intense peak at 220 °C, manifesting the conversion of the THPMA to MAA units. In the case of the BzMA homopolymer, no thermal response was observed up to 250 °C, but an endotherm was initiated at 270 °C. This was interestingly due to the depolymerization of pBzMA,[311] inferred from the analysis of the material recovered from the DSC pan using ^{1}H NMR spectroscopy. The DSC thermograms of the two ABC triblock terpolymers were very similar to each other and exhibited all endothermic peaks displayed by the 2PyEMA and the THPMA homopolymers between 150 and 250 °C. However, these thermograms were dominated by

the more intense main peak of the thermolysis of polyTHPMA at 160 °C, with the main peak of poly2PyEMA thermolysis appearing as a much weaker endotherm at 180 °C.

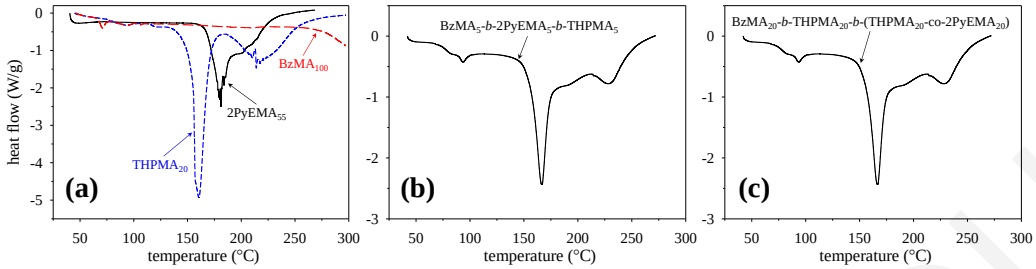

Figure 3.25 DSC thermograms of (a) the homopolymers of 2PyEMA, THPMA and BzMA, (b) the $BzMA_5$-*b*-$2PyEMA_5$-*b*-$THPMA_5$ triblock terpolymer and (c) the $BzMA_{20}$-*b*-$THPMA_{20}$-*b*-($THPMA_{20}$-*co*-$2PyEMA_{20}$) triblock terpolymer.

Figure 3.26 shows the ^{1}H NMR spectra of the BzMA homopolymer before and after DSC (reached 275 °C); the latter spectrum indicates the presence of BzMA monomer, suggesting the thermal depolymerization of the homopolymer.

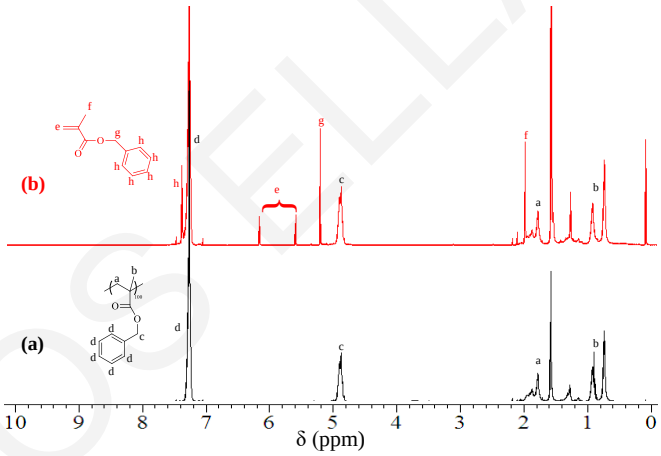

Figure 3.26 ^{1}H NMR spectra of $BzMA_{100}$ (a) before and (b) after DSC (up to 275 °C) in $CDCl_3$.

Figure 3.27 shows the TGA thermograms of the 2PyEMA, the THPMA and the BzMA homopolymers, and those of the two ABC triblock terpolymers. In the case of the 2PyEMA homopolymer, the weight loss started at ~170 °C, manifesting side group removal, consistent with DSC, followed by a further weight loss at ~400 °C and higher temperature due to complete backbone decomposition. In the case of the THPMA homopolymer, the weight loss started at ~140 °C, again in agreement with DSC, followed by a further weight loss at ~400 °C and higher temperature owing to backbone destruction. In the case of the BzMA homopolymer, the weight loss was due to the depolymerization of the BzMA units. This change started at ~250 °C, also in agreement with the DSC data, and

was completed just below ~400 °C. The TGA thermograms of the two ABC triblock terpolymers were similar to each other, and, as the DSC thermograms, they seemed to result from linear superpositions of the TGA thermograms of the three constituting homopolymers. In particular, the TGA thermograms of the terpolymers showed initial weight losses due to the cleavage of the side groups of the 2PyEMA and the THPMA units between 150 and 200 °C, with complete weight loss occurring between 350 and 450 °C due to backbone decomposition. The dashed horizontal lines indicate the theoretical weight percent remaining after complete side group removal, and calculated on the basis of thorough loss of 2-vinylpyridine and 3,4-dihydro-2*H*-pyran from the ABC triblock terpolymers. For both terpolymers, there is good agreement between experimental and theoretical weight percentage of polymer left following thermal side group removal at ~200 °C.

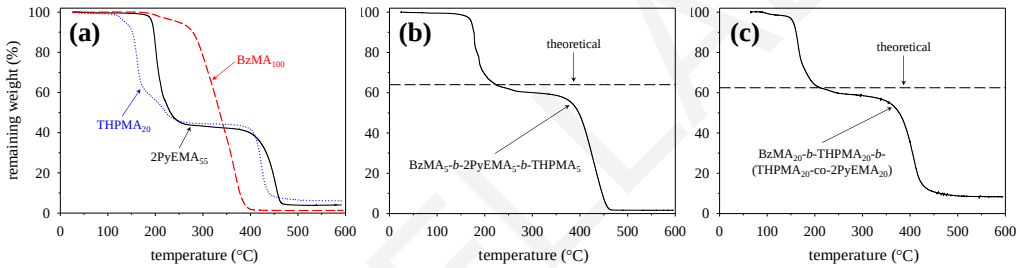

Figure 3.27 TGA thermograms of (a) the homopolymers of 2PyEMA, THPMA and BzMA, (b) the $BzMA_5$-*b*-$2PyEMA_5$-*b*-$THPMA_5$ triblock terpolymer and (c) the $BzMA_{20}$-*b*-$THPMA_{20}$-*b*-($THPMA_{20}$-*co*-$2PyEMA_{20}$) triblock terpolymer.

Figure 3.28 shows the ^1H NMR spectrum of the thermally deprotected $BzMA_5$-*b*-$2PyEMA_5$-*b*-$THPMA_5$ triblock terpolymer (Figure 3.28(b)), along with that of the original terpolymer (Figure 3.28(a)). In this case, thermal deprotection was performed in a vacuum oven at 130 °C for 6 h. The peaks due to the side groups of the 2PyEMA and the THPMA units at 4.3 and 5.8 ppm, respectively, (red circles) are totally absent from the spectrum of the thermolyzed sample, confirming the completeness of side group removal.

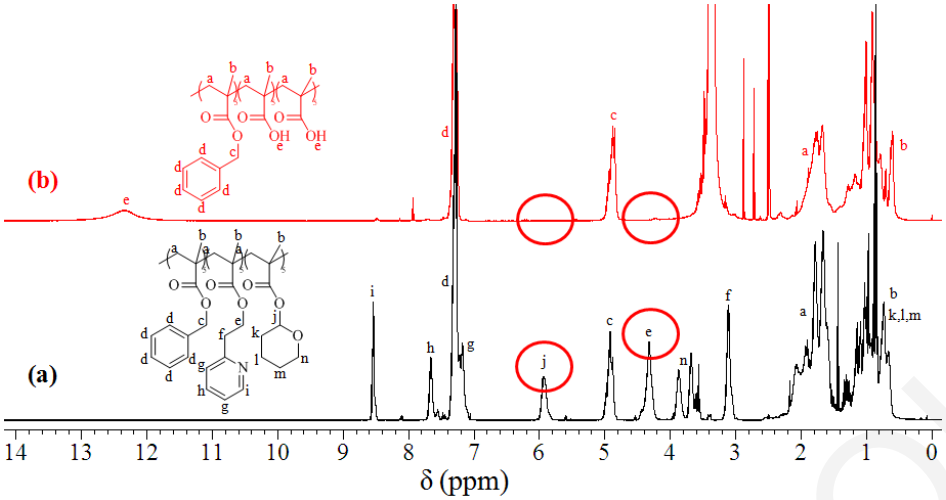

Figure 3.28 ^{1}H NMR spectra of (a) the original BzMA$_5$-*b*-2PyEMA$_5$-*b*-THPMA$_5$ triblock terpolymer in $CDCl_3$ (black) and (b) the same terpolymer in d_6-DMSO after thermolysis at 130 °C in vacuum (red).

3.2.5 Micelle Formation in Water. The BzMA-MAA diblock copolymers obtained after the thermolysis of the two ABC triblock terpolymers were amphiphilic and, therefore, formed micelles in aqueous solution. Preliminary characterization of the size of these micelles was performed using light scattering and AFM. AFM images of the micelles formed by the two copolymers are displayed in Figure 3.29, whereas a summary of all results, both from AFM and light scattering, is provided in Table 3.5. Figure 3.29 shows that the micelles formed were spherical and rather monodisperse. Furthermore, the micelles formed by the larger copolymer were clearly larger than those formed by the smaller, as expected.

Table 3.5 Micellar Characteristics of the Linear Amphiphilic BzMA-MAA Diblock Copolymers Determined Using Light Scattering and AFM.

Polymer Structure	M_n^{unimer} (g mol^{-1})	SLS		DLS	AFM	Max. Theor. Diam. (nm)
		M_w (g mol^{-1})	$N = M_w/M_n$	D_h (nm)	D (nm)	
BzMA$_5$-*b*-MAA$_{10}$	1840	2.151×10^4	12	29	47	7.56
BzMA$_{20}$-*b*-MAA$_{60}$	8470	2.684×10^6	320	154	67	40.32

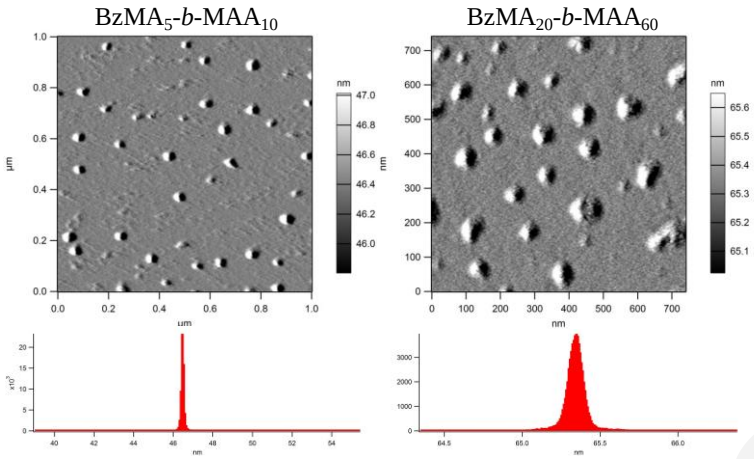

Figure 3.29 AFM images and distributions of the diameters of the spherical micelles formed by the $BzMA_5$-*b*-MAA_{10} and the $BzMA_{20}$-*b*-MAA_{60} amphiphilic diblock copolymers in water.

Table 3.5 lists the average diameters of the adsorbed micelles formed by the two copolymers, determined using AFM. Both diameters were larger than the diameters calculated from the chain dimensions, listed in the last column of the table. This can be attributed to micellar widening due to flattening upon adsorption, and also to the "tip effect" (tip diameter, ~10 nm, included in the determined size), particularly in the case of the smaller micelles. Furthermore, formation of multi-micellar aggregates cannot be totally excluded. Table 3.5 also presents the results from light scattering, which are consistent with those from AFM. The hydrodynamic diameters, D_h, the absolute weight-average molecular weights, M_w, and the micellar aggregation numbers, N, calculated by dividing M_w by the single-chain M_n, were consistently larger for the micelles formed by the larger copolymer, as expected.

3.3 "Inverse Polyampholyte" Hydrogels From Double-Cationic Hydrogels: Synthesis by RAFT Polymerization and Characterization

Synthetic polyampholytes comprise both weakly acidic and weakly basic monomer repeating units, and provide a simple physicochemical model for proteins. The preparation of synthetic polyampholytes is most usually accomplished via the conventional free radical copolymerization of unsaturated acids and bases, leading to copolymers with poorly-controlled structure. The synthesis of well-defined polyampholytes has also been reported in a smaller number of studies as it is more demanding, requiring use of controlled copolymerization of the two comonomers, with the acidic monomer introduced in a protected form to avoid interference with the polymerization. In this section, two homologous, pyridine-based monomers, 2PyEMA and 2PyMMA, were used, which, despite their structural similarity, the former can be readily thermolyzed to methacrylic acid, while the latter remains intact under the same conditions. This was most dramatically demonstrated in the present work, where 2PyEMA and 2PyMMA were randomly terpolymerized with a dimethacrylate cross-linker using RAFT polymerization to yield weakly double-basic polyelectrolyte hydrogels of three different compositions which, upon thermal treatment, they were readily converted to polyampholyte hydrogels. While the parent double-cationic polyelectrolyte hydrogels exhibited a swelling response only to low-pH conditions, the daughter polyampholyte hydrogels presented swelling responses to both high and low pH conditions. Owing to the relative values of the effective pK_a's of the weakly acidic and weakly basic units, with the latter being lower than the former ("inverse polyampholyte" behavior), the swelling profiles of the daughter hydrogels were insensitive to polyampholyte composition.

3.3.1 Polymer Design and Synthesis. In literature, many polyampholyte hydrogels were prepared using controlled polymerization methods, as GTP and RAFT polymerization,[312,313] based on a tertiary-amine monomer DMAEMA, whose pK_a value is higher than that of the MAA units. Three polyampholyte hydrogels with different ratios of the weakly acidic MAA units and the very weakly basic 2PyMMA units were prepared. The basic monomer was pyridine-based, possessing a very low pK_a value, lower than that of DMAEMA and also even lower than that of MAA. Thus, the 2PyMMA-MAA combination constitutes an extraordinary monomer pair, where the very weakly basic 2PyMMA units are more acidic than the weakly acidic MAA units. This leads to the formation of a particular type of polyelectrolyte, named "inverse polyampholyte", to

signify the fact that the extremely low basicity of the basic units results in materials where positive and negative charges cannot coexist at any pH. This is in marked contrast to regular polyampholytes which present a large pH window (in between the two pK_a values) where both types of units are simultaneously oppositely charged. For the present polymer synthesis, controlled RAFT polymerization was used, while random cross-linking rather than end-linking was chosen for the preparation due to its simplicity employing one synthetic step without intermediate product isolations.

3.3.2 Linear Copolymer. Before the network synthesis, a linear, near-equimolar 2PyMMA-2PyEMA statistical copolymer with an overall DP of 100, 2PyMMA$_{52}$-*co*-2PyEMA$_{48}$, (GPC: number-average MW = M_n = 24700, $Đ$ = 1.58, ^{1}H NMR spectroscopy: 2PyMMA = 52 mol%, monomer conversion = 100%) was synthesized also by RAFT polymerization, and studied. As analyses of solutions of linear polymers are more straightforward than the analyses of the solid-like hydrogels, the investigation of this linear copolymer before and after thermolysis by ^{1}H NMR spectroscopy and hydrogen ion titration provided a convenient means for confirming the completeness and selectivity of thermolysis in the 2PyMMA-2PyEMA comonomer system. The procedures for the synthesis and thermolysis of this copolymer are displayed in Figure 3.30.

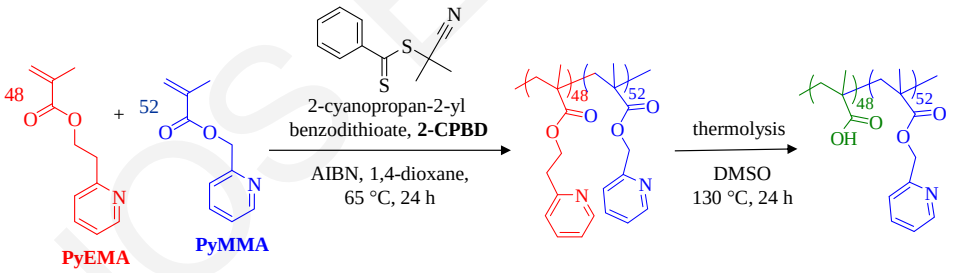

Figure 3.30 Synthetic procedure followed for the preparation of the linear near-equimolar statistical polyampholyte. The 2PyMMA units are shown in blue, the 2PyEMA units are painted red, and the MAA units are displayed in green.

Figures 3.31 (a) and 3.31 (b) show the ^{1}H NMR spectra of the linear copolymer before and after its thermolysis, respectively. The ^{1}H NMR spectrum of the original copolymer in Figure 3.31 (a) bears all the signals with the correct intensity according to the copolymer structure. The ^{1}H NMR spectrum of the thermolyzed copolymer in Figure 3.31 (b) also confirms the expected structure as the signals from the 2-(pyridin-2-yl)ethyl group completely disappeared (most characteristic being peaks “c” and “d” at 4.3 and 3.2 ppm, respectively), while a new peak “n” appeared at 12.5 ppm, corresponding to the carboxylic acid proton (-COO*H*) of the MAA unit.

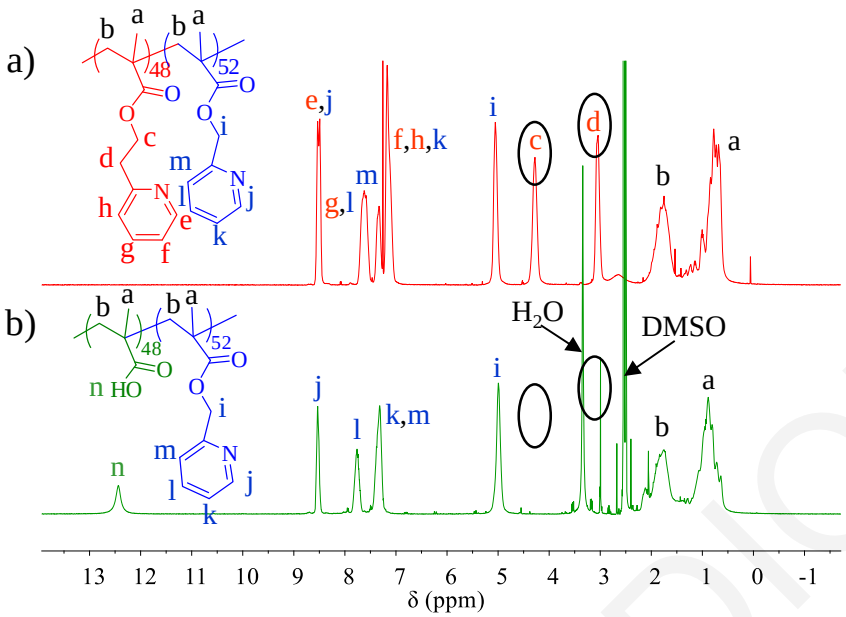

Figure 3.31 ^{1}H NMR spectra of (a) 2PyMMA$_{52}$-*co*-2PyEMA$_{48}$ (before thermolysis) in $CDCl_3$, and (b) 2PyMMA$_{52}$-*co*-MAA$_{48}$ (after thermolysis) in d_6-DMSO.

The successful formation of the polyampholyte copolymer was also confirmed using hydrogen ion titration. The hydrogen ion titration curves of both the original double-cationic polyelectrolytic copolymer (2PyMMA-2PyEMA) and the final polyampholytic copolymer (2PyMMA-MAA) are plotted in Figure 3.32, in which the effective pK_a values of the various protonable groups were determined and indicated with arrows. Unlike the hydrogen ion titration curve of the original copolymer in which the protonable groups exhibited very low pK_a values, 2.0 and 2.6, corresponding to the PyMMA and the PyEMA units, respectively, the hydrogen ion titration curve of the polyampholytic copolymer also presented a protonable group with a higher pK_a value, of 6.5, corresponding to the newly-formed MAA units. It is noteworthy that the linear polyampholyte solution was cloudy within the pH range from 2 to 7, due to the lack of charges (and consequently zero overall charge too) in this range. Similarly, the linear double-cationic polyelectrolyte solution was cloudy above pH 2.5 due to the deprotonation of its weakly basic monomer repeating units.

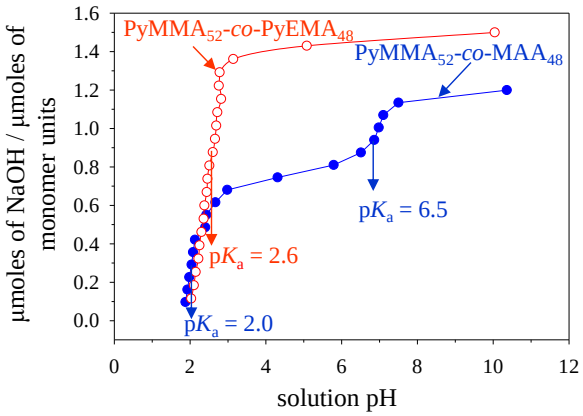

Figure 3.32 Hydrogen ion titration curves of the linear double-cationic polyelectrolyte PyMMA$_{52}$-*co*-PyEMA$_{48}$ and the linear polyampholyte PyMMA$_{52}$-*co*-MAA$_{48}$.

The deprotection of the 2PyEMA units in the linear copolymer was also explored using DSC and TGA. Figure 3.33 (a) presents the DSC traces of the linear statistical copolymer 2PyMMA$_{52}$-*co*-2PyEMA$_{48}$ and the linear homopolymer 2PyEMA$_{55}$, while Figure 3.33 (b) shows the corresponding TGA traces. Figure 3.31 also displays the DSC and TGA traces of networks 2PyMMA$_{30}$-*co*-2PyEMA$_{70}$-*co*-EGDMA$_6$ and 2PyMMA$_{52}$-*co*-2PyEMA$_{48}$-*co*-EGDMA$_6$. The DSC thermograms in Figure 3.31 (a) display a clear endothermic peak at approximately 185 °C for all three polymers, corresponding to the cleavage of the 2PyEMA units. This was also confirmed by the TGA thermograms in Figure 3.33 (b) where an initial weight loss took place at ~200 °C, corresponding exactly to the mass percentage of 2-vinyl pyridine in the 2PyEMA units. Further weight loss at ~400 °C and higher was also observed due to the cleavage of the backbone of the polymers.

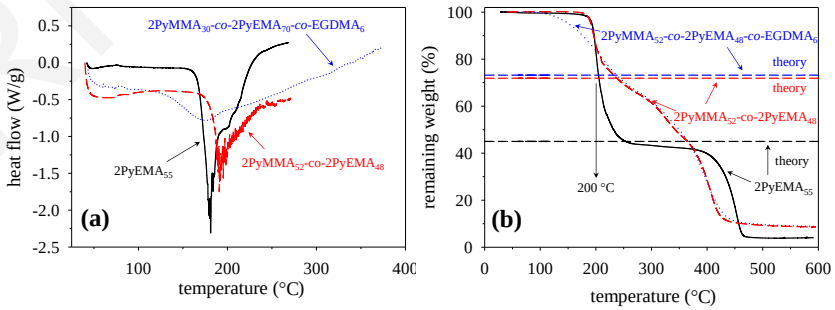

Figure 3.33 (a) DSC and (b) TGA thermograms of the linear 2PyEMA$_{55}$ homopolymer, the linear 2PyMMA$_{52}$-*co*-2PyEMA$_{48}$ copolymer and networks 2PyMMA$_{30}$-*co*-2PyEMA$_{70}$-*co*-EGDMA$_6$ and 2PyMMA$_{52}$-*co*-2PyEMA$_{48}$-*co*-EGDMA$_6$.

3.3.3 Networks. The syntheses of the polymer networks were performed in the same way as for the linear copolymer, but with the extra addition of EGDMA cross-linker. In

particular, RAFT polymerization was again the method of synthesis, with 2-CPBD as the CTA, AIBN as the initiator (radical source), and 1,4-dioxane as the polymerization solvent. The loading of the EGDMA cross-linking agent was such that its molar ratio to the 2-CPBD CTA was 6 : 1, identified as optimal. Comparable cross-linker to CTA active site loadings, ranging from 3 to 5, have been employed in previous studies on network formation using RAFT polymerization.[313-317] The polymerizations took place at 65 °C for 24 h. After the polymerizations, the 2PyEMA units were thermolyzed in a vacuum oven at 130 °C for 24 h, giving MAA units. Figure 3.34 illustrates the polymerization and the thermolysis procedures employed for the preparation of the polyampholyte networks by the simultaneous terpolymerization of the two comonomers (2PyMMA and 2PyEMA) and the cross-linker (EGDMA), followed by the thermal treatment of the resulting double-cationic polyelectrolyte networks.

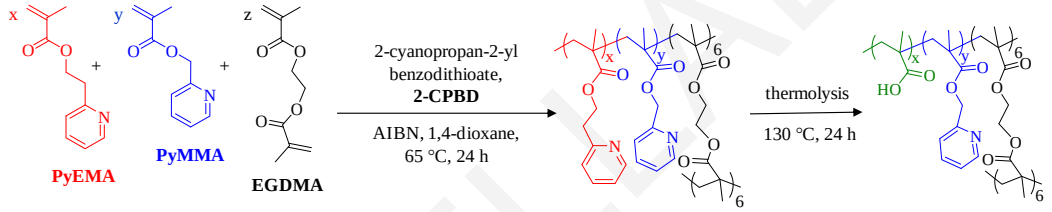

Figure 3.34 Synthetic procedure followed for the preparation of the randomly cross-linked polyampholyte networks. The 2PyMMA units are shown in blue, the 2PyEMA units are painted red, the MAA units are displayed in green, and the EGDMA cross-linker units are presented in black.

The sol fraction (extractables) of the three polyelectrolyte networks was determined and characterized using GPC and ^{1}H NMR spectroscopy analyses. Table 3.6 presents the percentage (w/w) of the extractables, their composition, and their MW (peak MW, M_p, and number-average MW, M_n) and $Đ$ values. The percentage of the extractables was very low, indicating successful and efficient network formation, also indicating the adequacy of the EGDMA cross-linker at the chosen EGDMA : CTA molar ratio of 6 : 1 used for cross-linking. From the ^{1}H NMR spectra, it was observed that the extractables mainly consisted of 2PyMMA and 2PyEMA monomers, as well as of 2PyMMA-*co*-2PyEMA hyperbranched chains which had not been incorporated in the network. The 2PyMMA$_{30}$-*co*-2PyEMA$_{70}$-*co*-EGDMA$_6$ network presented the highest percentage of free hyperbranched chains, followed by 2PyMMA$_{70}$-*co*-2PyEMA$_{30}$-*co*-EGDMA$_6$ and 2PyMMA$_{52}$-*co*-2PyEMA$_{48}$-*co*-EGDMA$_6$. The GPC traces of the extractables from the three networks presented two peaks, a high-MW and broad one corresponding to the hyperbranched copolymer, and a low-MW and narrow one due to the unreacted

comonomers (2PyMMA and 2PyEMA). The effective pK_a values of the three weakly basic polyelectrolyte hydrogels were determined from the plots of DI *vs* solution pH in Figure 3.35 as the pH at 50% ionization, and they are listed in Table 3.6. The effective pK_a values were between 1.9 and 2.4, being close to (but lower than) the effective pK_a values of the corresponding 2PyMMA and 2PyEMA monomer repeating units in the linear statistical copolymer of 2.0 and 2.6, respectively.

Table 3.6 Percentage, compositions, molecular weights of the extractables and the effective pKa values of the pyridinyl units from the three polyelectrolyte networks.

Network Structure	% w/w Extracta.	^{1}H NMR Results (mol%)			GPC Results			Eff. pK_a
		2PyMMA	*2PyEMA*	*2PyMMA-co-2PyEMA*	M_p (g mol^{-1})	M_n (g mol^{-1})	*Đ*	
2PyMMA$_{30}$-*co*-2PyEMA$_{70}$-*co*-EGDMA$_6$	4.5	40.3	25.7	34.0	4270 133	3600 143	1.84 1.04	1.9
2PyMMA$_{52}$-*co*-2PyEMA$_{48}$-*co*-EGDMA$_6$	10.6	27.6	57.5	14.9	766 133	1410 153	2.12 1.06	2.1
2PyMMA$_{70}$-*co*-2PyEMA$_{30}$-*co*-EGDMA$_6$	5.4	40.3	34.0	25.7	5990 129	5190 139	1.62 1.04	2.4

3.3.3.1 pH-Dependence of the DSs of the double-cationic polyelectrolyte hydrogel. The three double-cationic polyelectrolyte (i.e. before thermolysis) networks were characterized in terms of their aqueous DSs (along with their 95% confidence intervals) as a function of pH. The measured DSs and calculated DIs (from the amounts of HCl and polymer network) of the three polyelectrolyte hydrogels are plotted against pH in Figure 3.35. In these graphs, the DS *vs* pH curve followed the corresponding DI *vs* pH curve, confirming the importance of charge in hydrogel swelling. All networks began to swell below pH ∼2 due to the ionization of the 2PyEMA and the 2PyMMA monomer repeating units. The ionization of these units resulted in electrostatic repulsions between the positively charged chains, and the build-up of an osmotic pressure created by the chloride counteranions to the charges within the network. In all cases, the DS maximum (pH between 1.8 and 2.1) was followed by a decrease at lower pH values (pH < 1.8). This can be attributed to the increase in ionic strength effected by the relatively high concentration of HCl under these rather extremely acidic conditions.

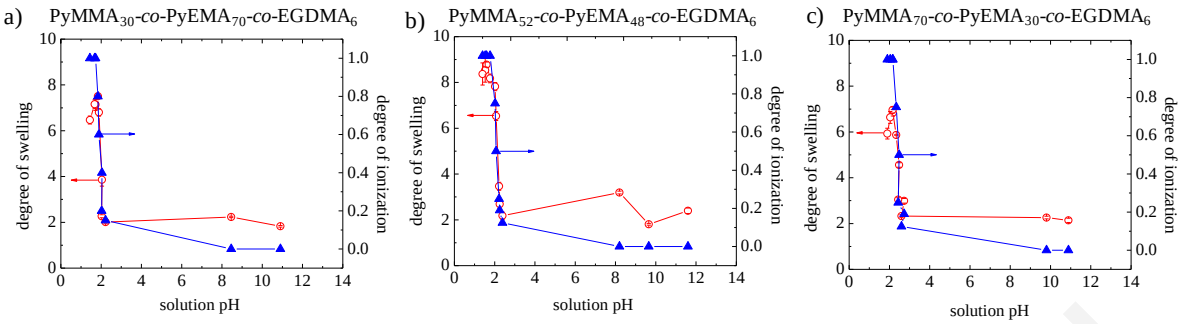

Figure 3.35 Aqueous degrees of swelling and degrees of ionization as a function of the supernatant solution pH for the three weakly basic double-cationic polyelectrolyte hydrogels.

3.3.3.2 Composition-dependence of the DSs of the double-cationic polyelectrolyte hydrogels. The DSs in pure water (pH ~ 8.5) and in acidic water (pH ~2), both taken from Figure 3.35, as well as the DSs in THF of the three double-cationic polyelectrolyte hydrogels are plotted in Figure 3.36 as a function of hydrogel composition (percentage of 2PyEMA units). The highest DSs were presented in acidic water, as expected, due to the full ionization of the 2PyMMA and the 2PyEMA monomer repeating units, and ranged from 7.0 to 8.8. In contrast, the DSs in pure water and in THF for the three hydrogels acquired much lower values, between 2 and 3. The low DSs in pure water are consistent with the hydrophobicity of the two comonomers and the cross-linker. The insensitivity of the DSs, especially those in acidic water which were the highest, to hydrogel composition is due to the similarity between the two homologous comonomers, differing only by one methylene group.

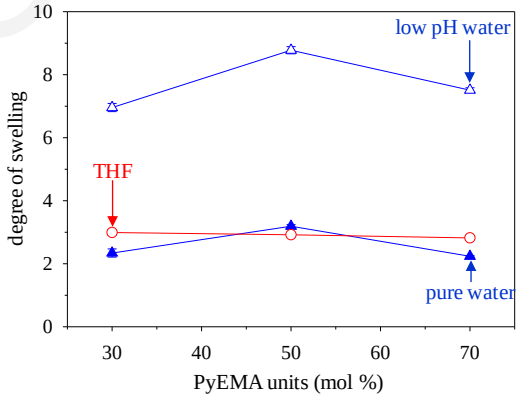

Figure 3.36 Degrees of swelling in THF, and in acidic (pH ~ 2) and in pure (pH ~ 8.5) water as a function of the composition of the weakly basic double-cationic polyelectrolyte hydrogels.

3.3.3.3 pH-Dependence of the DSs of the polyampholyte hydrogels. After thermolysis, the resulting polyampholyte hydrogels were also studied in terms of their aqueous DSs as a function of the solution pH. Figure 3.37 shows the aqueous swelling curves (along with the 95% confidence intervals of the DSs) for the three hydrogels, displaying a characteristic minimum at intermediate pH values, flanked by higher DS values at acidic and basic pHs. This behavior is typical of polyampholyte hydrogels,[318,319] due to the existence of the isoelectric point, p*I*, which is the pH of zero net charge. At and around the p*I*, the net repulsive forces are zero, while the van der Waals and hydrophobic attractive forces dominate, leading to a reduced extension of the polyampholyte chains, and also a trend for coalescence among them.

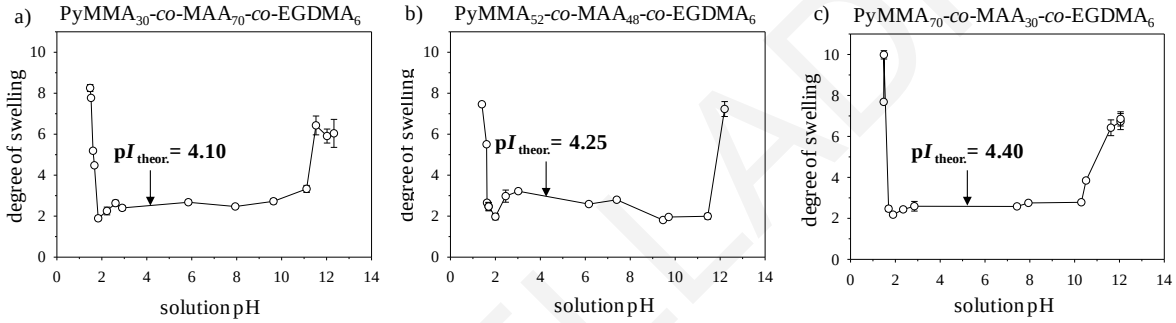

Figure 3.37 Aqueous degrees of swelling as a function of the supernatant solution pH for the three polyampholyte hydrogels.

The pH range of the swelling minimum was very broad, from ~2 to ~11, and insensitive to hydrogel composition. This was probably due to the relative values of the effective pK_a's of the 2PyMMA and the MAA monomer repeating units, with that of the basic units being lower than that of the acidic units, leading to uncharged units within the pH range between the two pK_a values, and insensitivity of the p*I* to composition. Using the experimentally determined values of the effective pK_a's of the 2PyMMA and the MAA monomer repeating units of 2.0 and 6.5, p*I* calculation [320,321] led to values close to 4.2 for all three polyampholyte hydrogels, listed in Table 3.7 and indicated in the graphs of Figure 3.37. These values should be compared with the pH values at the middle of the swelling minimum, also listed in Table 3.7. These latter values ranged between 6 and 7, and were, therefore, higher than the theoretical p*I*s. This can be attributed to the different hydrophobicities of the 2PyMMA and the MAA units. In particular, the 2PyMMA units are more hydrophobic than the MAA units. Thus, at high pH, when the 2PyMMA units are uncharged, a greater degree of ionization of the MAA units is required before the hydrogel starts to swell again.

Table 3.7 Theoretical and experimental isoelectric points of the three polyampholyte hydrolgels.

Network Structure	Theoretical p*I*	Middle of pH range of collapse
$2PyMMA_{30}$-*co*-$2PyEMA_{70}$-*co*-$EGDMA_6$	4.10	6.4 ± 0.5
$2PyMMA_{52}$-*co*-$2PyEMA_{48}$-*co*-$EGDMA_6$	4.25	7.1 ± 0.5
$2PyMMA_{70}$-*co*-$2PyEMA_{30}$-*co*-$EGDMA_6$	4.40	5.8 ± 0.5

3.3.3.4 Effect of polymer composition on the DSs of the polyampholyte hydrogels. Figure 3.38 presents the effect of polymer composition (percentage of MAA units) on the aqueous DSs of the polyampholyte hydrogels at three characteristic pH values, taken from Figure 3.37. These characteristic pH values were the p*I* (pH ~4.2), basic pH (~12) and acidic pH (~1.5). The Figure shows that the aqueous DSs of the polyampholyte hydrogels around the p*I* were low and constant at approximately 2, indicating that the hydrogels were in a less expanded state due to the absence of counterions and repulsive forces. The low and the high pH aqueous DSs of the three polyampholyte hydrogels were high due to the ionization of the 2PyMMA and the MAA units, respectively. The low pH aqueous DS of the 2PyMMA-rich network was higher than that at high pH due to the excess of basic over acidic units, ionizable at low pH. The near-equimolar hydrogel presented almost the same aqueous DSs at low and high pH.

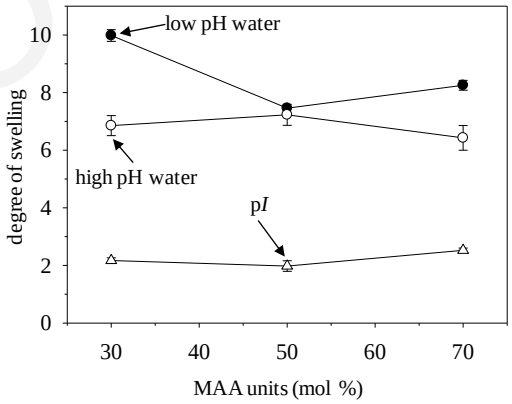

Figure 3.38 Aqueous degrees of swelling of the polyampholyte hydrogels at alkaline, acidic and isoelectric pH as a function of the MAA content.

3.4 A dimethacrylate Cross-linker Cleavable Under Alkaline Hydrolysis Conditions or Thermally: Synthesis, Polymerization and Degradation

2,6-Pyridinediethanol dimethacrylate (PyDMA) was developed as a new labile cross-linker, degradable thermally and also under alkaline hydrolysis conditions, with the latter property being rare among cross-linkers. PyDMA was prepared from the esterification of 2,6-pyridinediethanol with methacryloyl chloride in absolute tetrahydrofuran in the presence of excess triethylamine base. 2,6-Pyridinediethanol was synthesized via the high-pressure, high-temperature, aqueous hydroxymethylation of 2,6-lutidine using paraformaldehyde. RAFT polymerization was subsequently employed to homopolymerize PyDMA both at relatively low and at higher concentrations to produce a hyperbranched soluble polymer and an insoluble polymer network, respectively. Furthermore, PyDMA was randomly RAFT copolymerized with MMA to obtain again an insoluble polymer network. All three polymeric materials synthesized were shown to be cleavable both thermally (either in the bulk or in solution) and under alkaline hydrolysis conditions at room temperature, resulting in the expected linear degradation polymeric products.

3.4.1 Synthesis of PyDMA Cross-linker. PyDMA cross-linker was synthesized by the esterification of 2,6-pyridinediethanol with methacryloyl in the presence excess triethylamine base in absolute THF at 0 °C. 2,6-Pyridinediethanol was synthesized by the reaction of 2,6-dimethylpyridine (2,6-lutidine) with paraformaldehyde in water under elevated pressure and temperature (135 °C).

3.4.1.1 Synthesis of 2,6-pyridinediethanol preparation and purification. 2,6-Pyridinediethanol was prepared following the procedure of Kelly et al.[292] which is based on the method of Löffler and Thiel,[293] as illustrated in Scheme 3.22. Although the procedure is of low yield, it uses readily available, low-cost and recyclable reagents. 2,6-Lutidine was reacted in water with paraformaldehyde in a pressure glass vial at 135 °C for 16 h, leading to three hydroxymethylation products: the desired 2,6-pyridinediethanol (1.6% yield), its isomeric 2-(6-methylpyridin-2-yl)propane-1,3-diol (6.5% yield), and the monosubstituted 2-(6-methylpyridin-2-yl)ethanol (30% yield). The unreacted 2,6-lutidine was removed by steam distillation, whereas 2-(6-methylpyridin-2-yl)ethanol was removed on the vacuum line at 80 °C. The two diols were separated in a subsequent step by column chromatography using an acetone – *n*-hexane eluent of variable composition (increasing in acetone content).

Scheme 3.22 Chemical Reaction of hydroxymethylation od 2,6-lutidine leading to synthesis of 2,6-pyridinediethanol, along with its (a) ^{1}H and (b) ^{13}C NMR Spectra.

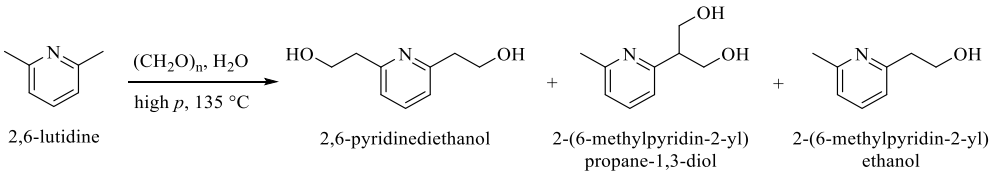

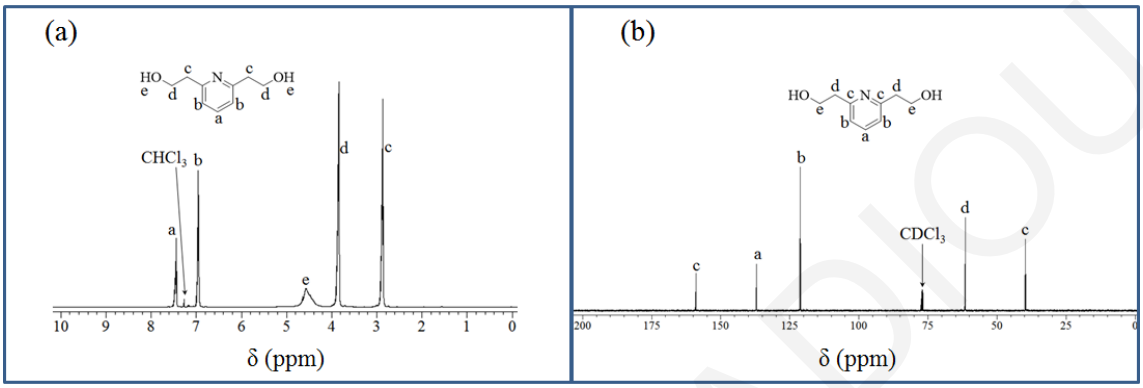

3.4.1.2 Cross-linker preparation. Subsequently, the symmetrical diol was esterified using an excess (40%) of methacryloyl chloride in absolute tetrahydrofuran and a large excess of triethylamine base (7-fold to minimize product loss via the action of product as base) to obtain PyDMA. PyDMA was purified by passage through basic alumina columns to neutralize the excess of methacryloyl chloride or/and its hydrolysis product methacrylic acid.

Scheme 3.23 shows the esterification reaction of 2,6-pyridinediethanol with methacryloyl chloride, leading to the formation of PyDMA. The scheme also presents the ^{1}H and ^{13}C NMR spectra of PyDMA in d_6-DMSO. One can see the three characteristic pyridine aromatic protons at 7.0 and 7.6 ppm, and the characteristic oxymethylene protons at 4.5 ppm in the ^{1}H NMR spectrum of PyDMA.

Scheme 3.23 Chemical Reaction for the Synthesis of the PyDMA Cross-linker, Along with its (a) ^{1}H and (b) ^{13}C NMR Spectra.

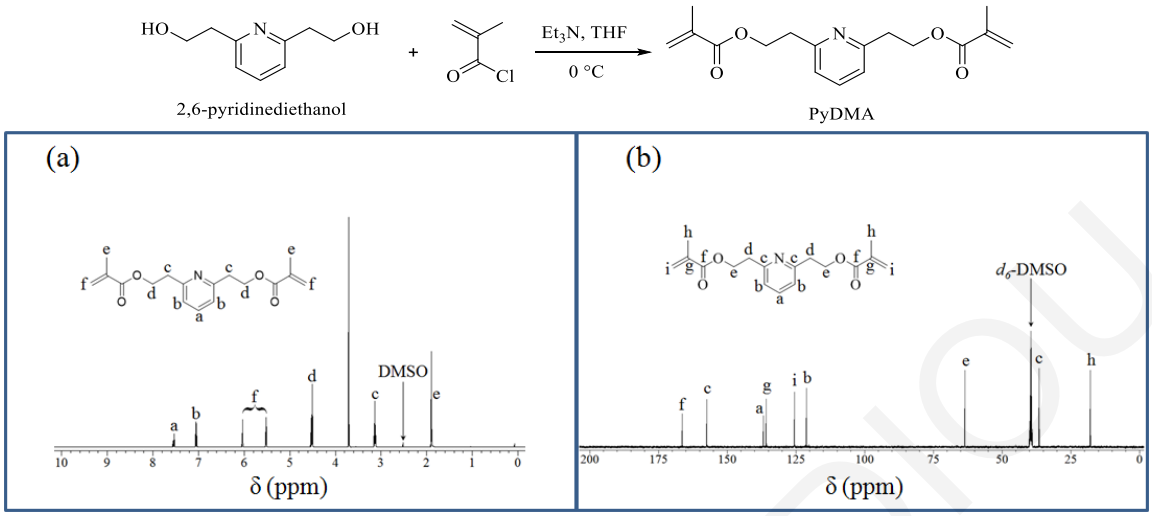

3.4.2 Polymer Syntheses of PyDMA Cross-linker. Following the synthesis and purification of PyDMA, this was polymerized in a controlled way. In particular, RAFT polymerization was employed to homopolymerize PyDMA at two different concentrations, and also to copolymerize it with MMA, as illustrated in Scheme 3.24. Scheme 3.24 also illustrates the cleavage of the PyDMA units in the (co)polymers thermally or via alkaline hydrolysis at room temperature. In all cases, 2-CPDB, AIBN and 1,4-dioxane served as the CTA, the radical source and the solvent for the polymerization, respectively. PyDMA concentrations of 0.66 and 2.50 M were used for the homo-polymerizations (DP = 10), leading to a hyperbranched polymer and a polymer network respectively. Additionally, a series of five randomly cross-linked MMA_{100}-*co*-PyDMA polymers with variable molar ratio of PyDMA to CTA (1, 2, 3, 4 and 8) was synthesized. In the case of the molar ratio of PyDMA to CTA equal to 8, a copolymer network was formed, while in the other four cases, MMA_{100}-*co*-$PyDMA_x$ hyperbranched copolymers were obtained. After their characterization, the PyDMA-containing polymeric products were evaluated for their degradability by being subjected to thermal and alkaline-hydrolysis treatment. These tests proved the full cleavage of the PyDMA repeating units and their concomitant conversion to MAA units and 2,6-divinylpyridine. First, the results from the solution cleavage (alkaline hydrolysis at room temperature and thermolysis in solution) of the hyperbranched homopolymer of PyDMA are presented and discussed.

Scheme 3.24 RAFT (Co)Polymerization of the PyDMA Cross-Linker, and the Thermal and the Alkaline Hydrolysis Treatments of the Resulting Polymers.

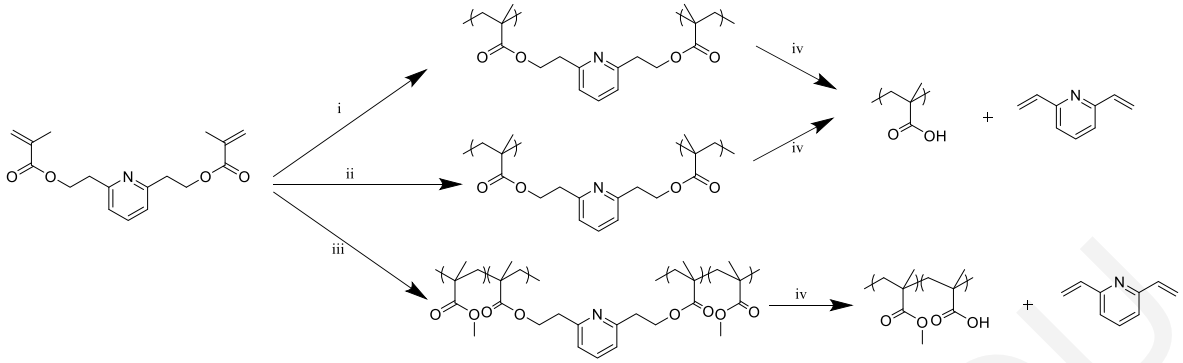

i. RAFT homopolymerization of PyDMA (2.50 M); ii, RAFT homopolymerization of PyDMA (0.66 M); iii. RAFT copolymerization of MMA plus PyDMA (total concentration 3.0 M); iv. NaOH (aq) in DMSO at RT overnight or 130 °C in a vacuum oven for 6 h.

The hyperbranched (co)polymers were characterized using GPC to determine their M_n and $Đ$ values, and ^{1}H NMR spectroscopy to calculate the MMA monomer and the PyDMA cross-linker conversions. In all cases, full conversion of the MMA and PyDMA was observed. Table 3.8 summarizes the molecular weight characteristics and the percentage (w/w) of extractables and their composition for the (seven) (co)polymers prepared. The DS in THF of both networks were determined, and found to be 1.3 and 3.1 for the homopolymer and the copolymer networks, respectively, with the lower DS value in the former case reflecting its higher cross-linking density. Although the sol fraction in the homopolymer network (25.9%) was higher than in the copolymer network (6.0%), the former sol fraction did not comprise monomeric or polymeric material, just catalyst. Table 3.8 also shows the molecular weight characteristics of the (co)polymers prepared using the PyDMA cross-linker, after the cleavage of the PyDMA residue under alkaline hydrolysis conditions or thermally. In the case of the alkaline hydrolysis or thermolysis products of the hyperbranched homopolymer and homopolymer network, no GPC data recorded due to the insolubility of these compounds in THF, the GPC solvent. In the case of the MMA_{100}-*co*-PyDMA hyperbranched copolymers, the GPC traces of the alkaline hydrolysis or thermolysis products are given in Figure 3.39, together with those of the parent material. The GPC traces of the cleavage products were shifted to longer elution times compared to the original MMA_{100}-*co*-PyDMA hyperbranched copolymers, indicating a reduction in their molecular weight, as a result of the cleavage of the cross-linker residue and the formation of the MMA-*co*-MAA linear copolymers and the low molecular weight side-product, 2,6-divinylpyridine, as already illustrated in Scheme 3.8. The $Đ$ values of the MMA_{100}-*co*-$PyDMA_x$ (x = 2, 3 and 4) hyperbranched copolymers are larger than the $Đ$

values of the MMA_{100}-*co*-$PyDMA_1$ hyperbranched copolymer, maybe due to the increased cross-linking concentration, while the *Đ* values of the cleavage products of the MMA_{100}-*co*-PyDMA hyperbranched copolymers are around 1.50, much lower than the *Đ* values of parent materials.

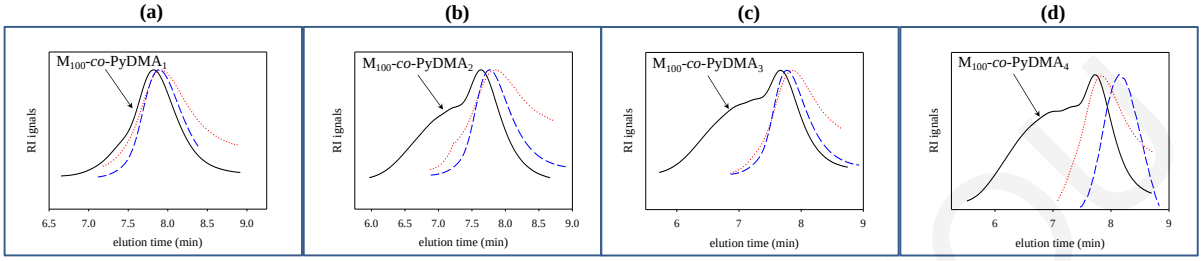

Figure 3.39 GPC traces of the hyperbranched copolymers before (black continuous line) and after thermolysis (red dotted line) or alkaline hydrolysis (blue dashed line). (a) MMA_{100}-*co*-$PyDMA_1$, (b) MMA_{100}-*co*-$PyDMA_2$, (c) MMA_{100}-*co*-$PyDMA_3$, and (d) MMA_{100}-*co*-$PyDMA_4$.

Table 3.8 Degree of Swelling in THF, % w/w extractables and molecular weights and molecular weight dispersities of the randomly cross-linked (co)polymers before and after treatment under alkaline hydrolysis or thermolysis conditions.

Polymer Structure	DS in THF	% w/w Extract.	M_n (g mol^{-1})	*Đ*	After Thermolysis [b]		After Alkaline Hydrolysis [c]	
					M_n (g mol^{-1})	*Đ*	M_n (g mol^{-1})	*Đ*
$PyDMA_{10}$	---	100	5580	2.13	----	----	----	----
$PyDMA_{10}$ [a]	1.3	25.9	1500	1.05	----	----	----	----
MMA_{100}-*co*-$PyDMA_1$	---	100	7850	1.53	6130	1.36	5320	1.52
MMA_{100}-*co*-$PyDMA_2$	---	100	15700	2.08	6900	1.51	6010	1.47
MMA_{100}-*co*-$PyDMA_3$	---	100	14300	3.17	6700	1.57	6510	1.42
MMA_{100}-*co*-$PyDMA_4$	---	100	15400	3.94	5480	1.58	6400	1.47
MMA_{100}-*co*-$PyDMA_8$ [a]	3.1	6.0	1820	1.16	4700	1.25	6460	1.99

a. Network formation.
b. Vacuum oven at 130 °C for 6 h.
c. NaOH (0.48 M) in DMSO at RT.

3.4.2.1 Cleavage in Solution. The hyperbranched PyDMA homopolymer was successfully hydrolyzed in d_6-DMSO containing 0.4 M NaOD at room temperature, as proven by ^{1}H NMR spectroscopy. Upon hydrolysis, a two-phase system was formed, with a d_6-DMSO solution top phase, and a precipitate bottom phase soluble in D_2O. ^{1}H NMR spectroscopy analysis of the two phases in the respective deuterated solvents indicated that the bottom phase was poly(sodium methacrylate), whereas the top phase was 2,6-divinylpyridine. These ^{1}H NMR spectra are given in Figure 3.38, together with that of the starting

hyperbranched homopolymer in d_6-DMSO before the addition of NaOD. The small sharp signals at 8.0 ppm correspond to the 2-CPDB residue.

The hyperbranched PyDMA homopolymer was also thermolyzed in d_6-DMSO solution (without the addition of NaOD) at 130 °C for 8 h. The ^{1}H NMR spectrum of the thermolysis product (in d_6-DMSO) is also shown in Figure 3.40, and it displays broad polymeric peaks due to the polyMAA units (including the carboxylic acid protons at 12.5 ppm) and sharp peaks due to the newly-formed 2,6-divinylpyridine.

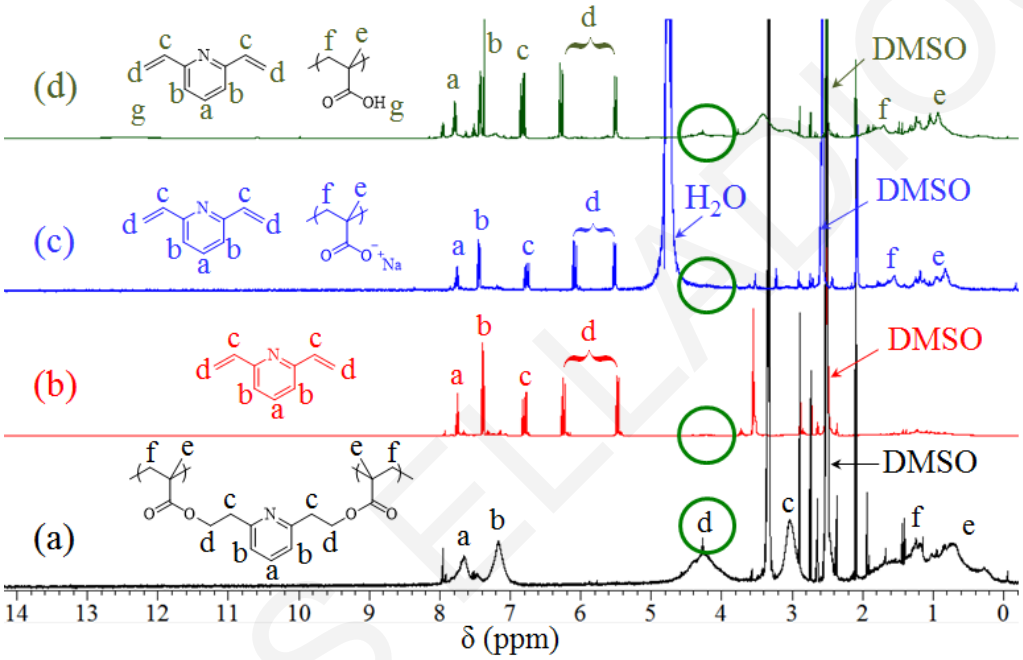

Figure 3.40 ^{1}H NMR spectra of the hyperbranched PyDMA homopolymer (a) before any treatment in d_6-DMSO (black), (b) after alkaline hydrolysis using NaOD in d_6-DMSO (red), (c) after alkaline hydrolysis using NaOD in D_2O (blue), and (d) after thermolysis in a vacuum oven at 130 °C for 6 hours in d_6-DMSO (green).

The PyDMA homopolymer network was also successfully cleaved both by solution thermolysis and by alkaline hydrolysis at room temperature. Here, the cleavage was most dramatically demonstrated by the conversion of the insoluble network to a polymer solution. Furthermore, the ^{1}H NMR spectra of the cleavage products (via thermolysis or hydrolysis) in d_6-DMSO show the appearance of the olefinic protons of 2,6-divinylpyridine and the disappearance of the α- and β- (relative to the ring) methylene protons. In the thermolysis product, a weak signal due to the polyMAA carboxylic acid protons was also visible.

The cleavage of the PyDMA-MMA network was also performed both thermally and hydrolytically, and the results are shown in Figure 3.41. The degradation products here were a linear MMA-MAA random copolymer plus 2,6-divinylpyridine. The ^{1}H NMR spectra were consistent with the expected degradation products.

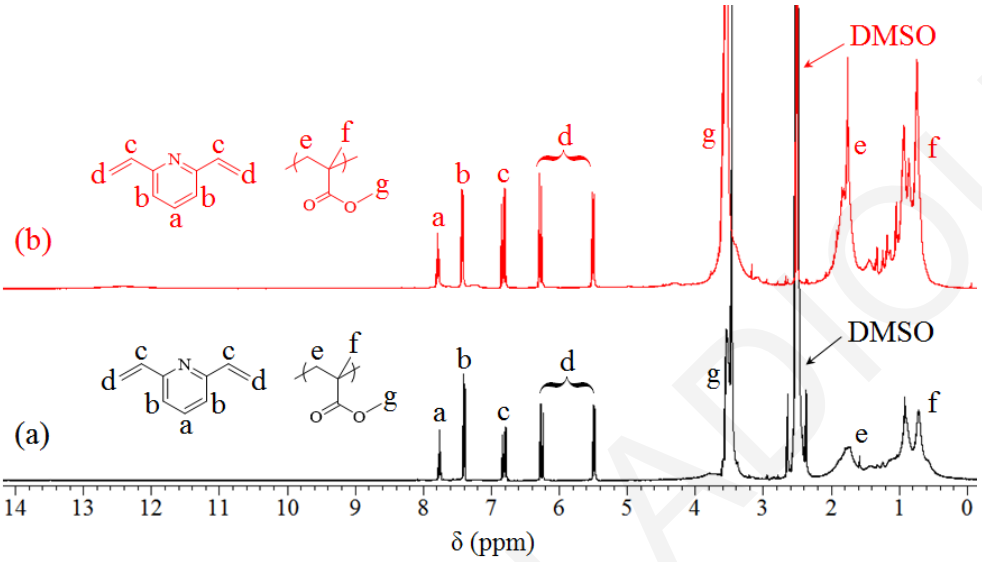

Figure 3.41 ^{1}H NMR spectra of (a) the cleavage product of the PyDMA-MMA network after alkaline hydrolysis using NaOD in d_6-DMSO (black), and (b) after thermolysis in a vacuum oven at 130 °C for 6 hours in d_6-DMSO (red).

3.4.2.2 Thermal Properties. The bulk thermolysis of the PyDMA-containing polymers was also investigated using DSC and TGA. Figure 3.42 (a) shows an overlay of all the DSC traces and Figure 3.42 (b) an overlay of all the TGA traces of the three PyDMA-bearing polymeric materials. In all three cases, there is an endotherm at around 200 °C, corresponding to the cleavage of the 2-(pyridin-2-yl)ethyl ester group. The highest degradation temperature was exhibited by the MMA-*co*-PyDMA network, probably a result of the protection offered to the PyDMA units by the MMA units. Note that the temperature of cleavage using DSC for polyPyEMA was lower, at 160 °C. The enthalpies of the cleavage endotherms of the three PyDMA-containing polymers were calculated and found to be ΔH = 171.7 J g^{-1}, ΔH = 149.1 J g^{-1} and ΔH = 18.93 J g^{-1} for the PyDMA hyperbranched homopolymer, the PyDMA homopolymer network, and the PyDMA$_8$-*co*-MMA$_{100}$ copolymer network, respectively. Taking into account the PyDMA content in each sample, the molar enthalpies for the cleavage of the PyDMA units become ΔH = 52.08 kJ mol^{-1}, ΔH = 45.23 kJ mol^{-1} and ΔH = 45.94 kJ mol^{-1}, values very close to each other, and lower than that for the PyEMA units in their homopolymers of ~70 kJ mol^{-1}.

The weak exotherm in the DSC trace of the PyDMA homopolymer network at 120 °C was due to a small percentage of unreacted methacrylate groups, identified in the ATR-FTIR spectrum of dried sample from a weak signal at 1630 cm^{-1}. Such a signal was absent from the ATR-FTIR spectrum of dried MMA_{100}-*co*-$PyDMA_8$ copolymer network. Similarly, complete vinyl group conversion was also accomplished in the PyDMA hyperbranched homopolymer, as signals from such groups were absent from its ^1H NMR spectrum.

Overlays of the TGA traces showed a first mass loss at 200 °C, in agreement with DSC, and a second mass loss at 400 °C due to backbone destruction. The horizontal continuous black line corresponds to the theoretical weight loss of 2,6-divinylpyridine for the hyperbranched PyDMA homopolymer and the PyDMA homopolymer network, while the horizontal dashed blue line corresponds to the theoretical weight loss of 2,6-divinylpyridine for the MMA_{100}-*co*-$PyDMA_8$ copolymer network. In the case of the hyperbranched PyDMA homopolymer, the weight loss agreed well with the mass loss calculated for complete removal of 2,6-divinylpyridine, while, in the case of the copolymer network, the experimental weight loss was exceeded the expected possibly due to solvent loss.

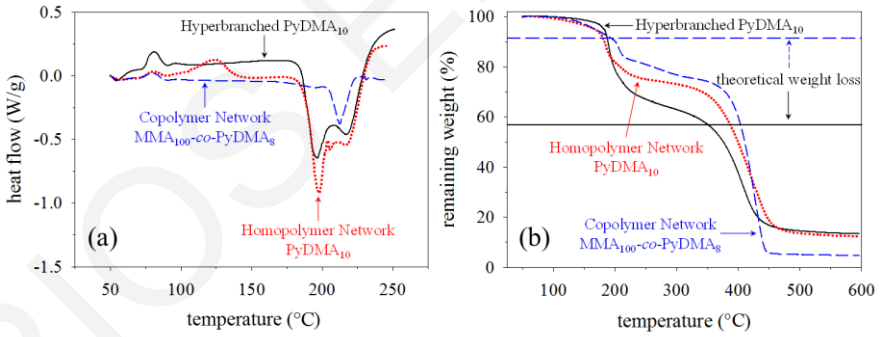

Figure 3.42 (a) DSC and (b) TGA traces of the PyDMA hyperbranched homopolymer (black, ontinuous line), PyDMA homopolymer network (red, dotted line), and MMA_{100}-*co*-$PyDMA_8$ copolymer network (blue, dashed line).

3.5 Symmetrical Polymer Systems Prepared Using a Degradable Bifunctional ATRP Initiator: Synthesis, Characterization and Cleavage

Linear (co)polymers and dimethacrylate-end-linked polymer networks of MMA with 2-(dimethylamino)ethyl methacrylate, cleavable in the middle of the polymer chain, either under thermolysis or alkaline hydrolysis conditions, were prepared *via* ATRP using a specially designed bifunctional degradable initiator. This initiator was PyDEDBrMeP, bearing two 2-(pyridin-2-yl)ethyl ester moieties, known for their thermal and hydrolytic (alkaline conditions) lability. As a control, a more stable bifunctional ATRP initiator, PyDMDBrMeP, was also synthesized together with the corresponding linear polymers and polymer networks prepared from it. Thermal or hydrolytic treatment of the polymers prepared using PyDEDBrMeP led to a reduction of the molecular weights of the linear polymers by a factor of two, and to the conversion of the polymer networks to soluble branched (star) structures, consistent with the expected cleavage of the initiator residue located in the middle of the polymer chain. Thermal treatment of the polymers prepared using PyDMDBrMeP did not affect their molecular weight due to the thermal stability of the (pyridin-2-yl)methyl ester group, while treatment under alkaline hydrolysis conditions resulted in complete cleavage, similar to the PyDEDBrMeP-prepared polymers.

3.5.1 Synthesis of the Labile and the More Stable Bifunctional ATRP Initiators. The degradable bifunctional initiator for ATRP, PyDEDBrMeP, and the more stable bifunctional initiator for ATRP, PyDMDBrMeP, were synthesized by the esterification reaction of 2,6-pyridinediethanol or and 2,6-pyridinedimethanol, respectively, with α-bromoisobutyryl bromide. Whereas 2,6-pyridinedimethanol is commercially available, 2,6-pyridinediethanol is not, and it was prepared in our laboratory from 2,6-lutidine. Scheme 3.25 shows the chemical reaction leading to the synthesis of 2,6-pyridinediethanol, followed by its esterification reaction to PyDEDBrMeP, along with the ^{1}H NMR spectra of 2,6-pyridinediethanol and PyDEDBrRMeP. The most characteristic peaks of 2,6-pyridinediethanol are those of the hydroxymethylene protons “d” at 3.85 ppm, while the most characteristic peaks of PyDEDBrMeP are those of oxymethylene protons “d” at 4.48 ppm.

The degradable bifunctional initiator for ATRP, PyDEDBrMeP, and the more stable bifunctional initiator for ATRP, PyDMDBrMeP, were synthesized by the esterification reaction of 2,6-pyridinediethanol or 2,6-pyridinedimethanol, respectively, with α-bromoisobutyryl bromide. Whereas 2,6-pyridinedimethanol is commercially available, 2,6-

pyridinediethanol is not, and it was therefore prepared in our laboratory from 2,6-lutidine. Scheme 3.25 shows the chemical reaction leading to the synthesis of 2,6-pyridinediethanol, followed by its esterification reaction to PyDEDBrMeP, along with the ^{1}H NMR spectra of 2,6-pyridinediethanol and PyDEDBrRMeP. The most characteristic peak of 2,6-pyridinediethanol is that of the hydroxymethylene protons “d” at 3.90 ppm, while the most characteristic peak of PyDEDBrMeP is that of the oxymethylene protons “d” at 4.53 ppm.

Scheme 3.25 Chemical reactions performed for the synthesis of 2,6-pyridinediethanol and the PyDEDBrMeP degradable bifunctional ATRP initiator, together with their ^{1}H NMR spectra.

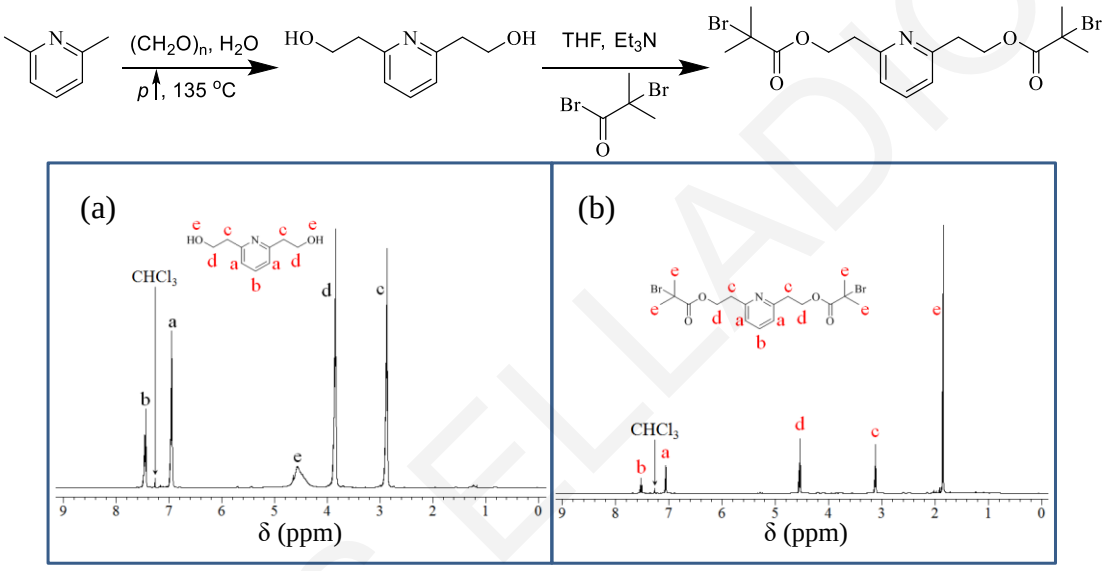

Scheme 3.26 displays the esterification reaction of 2,6-pyridinedimethanol leading to the formation of the more stable bifunctional ATRP initiator PyDMDBrMeP, along with the ^{1}H NMR spectra of 2,6-pyridinedimethanol and PyDMDBrMeP. The most characteristic peaks of 2,6-pyridinedimethanol are those of the hydroxymethylene protons “c” at 4.72 ppm, while the most characteristic peaks of PyDMDBrMeP are those of the oxymethylene protons “c” at 5.30 ppm.

Scheme 3.26 Esterification reaction of 2,6-pyridinedimethanol for the synthesis of the PyDMDBrMeP more stable bifunctional ATRP initiator, and their ^{1}H NMR spectra.

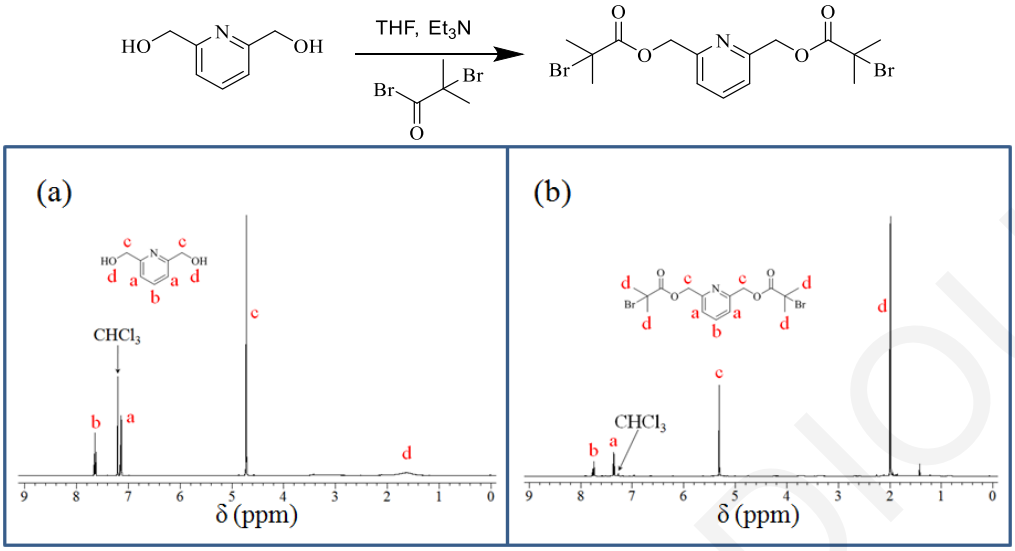

3.5.2 Polymer Syntheses. Subsequently, the two newly-synthesized bifunctional ATRP initiators were used to prepare the polymers of this study, which were linear homopolymers and copolymers, and dimethacrylate-end-linked homopolymer networks.

3.5.2.1 Linear MMA homopolymers. Four linear MMA homopolymers, with nominal degrees of polymerization (DP) equal to 50, 100, 200 and 500, were synthesized using each of the two bifunctional ATRP initiators, PyDEDBrMeP and PyDMDBrMeP. Figure 3.43 displays the GPC traces of the eight (parent) linear MMA homopolymers prepared, along with the GPC traces of the products obtained after thermal treatment or treatment under alkaline hydrolysis conditions of the eight parent linear polymers, while Table 3.9 summarizes the molecular weight results (M_p, M_n, and $Đ$ values) calculated on the basis of these GPC traces. All GPC traces, whether belonging to processed or parent polymer, were monomodal, indicating reasonable size homogeneity (given the use of bifunctional initiators) for all samples. Regarding the thermally processed samples, the GPC traces of the ones prepared using PyDEDBrMeP were shifted to longer elution times compared to those of the parent materials, whereas the GPC traces of the ones prepared using PyDMDBrMeP were at the same position as their parent materials. These observations suggested molecular weight reduction in the case of the PyDEDBrMeP-based polymers, consistent with the thermal cleavage of the PyDEDBrMeP residue, and molecular weight preservation for the PyDMDBrMeP-based polymers, indicating the thermal stability of the PyDMDBrMeP residue. Regarding the polymers processed under alkaline hydrolysis conditions, the GPC traces of all polymers, prepared using either of the two bifunctional

initiators, were shifted to longer elution times compared to those of the parent polymers, suggesting molecular weight reduction *via* cleavage of the initiator residues. It is noteworthy that the position of the GPC traces of three out of the four polymers prepared using the PyDEDBrMeP bifunctional initiator were the same irrespective of the type of processing, whether thermal or hydrolytic. This indicated that the two cleavage methods effected the same extent of cleavage upon these polymers, most likely *via* destruction of the initiator residue. Exception was M_{100}-I_d-M_{100}, whose thermolysis product had higher molecular weight than the corresponding hydrolysis product. This may be attributed to partial adventitious (due to higher local temperature in the vacuum oven) recombination (possibly via anhydride formation) of the thermolysis product. Note, however, that both the thermolysis and hydrolysis products displayed M_n values much lower than that of the parent sample.

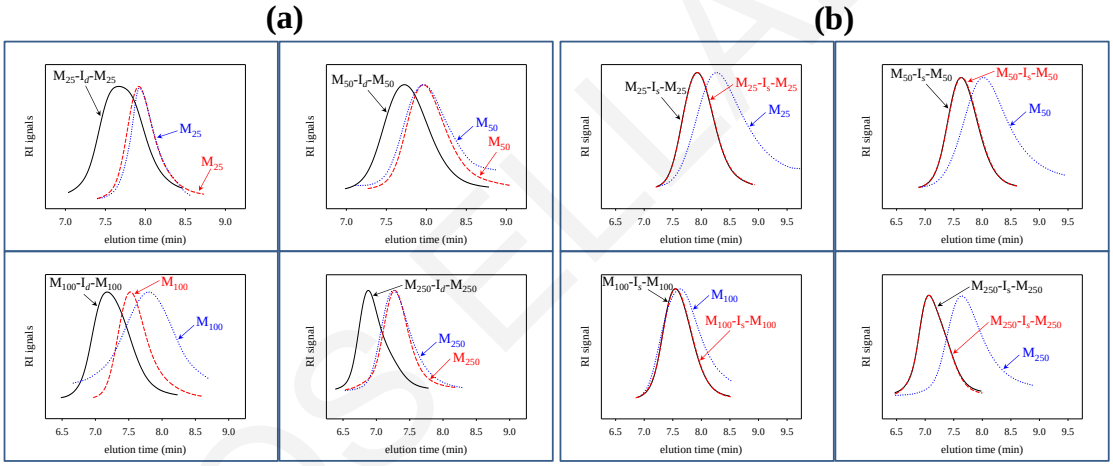

Figure 3.43 GPC traces of the linear MMA homopolymers before (black continuous line) and after thermolysis (red dashed line) or alkaline hydrolysis (blue dotted line). (a) Polymers prepared using the labile PyDEDBrMeP bifunctional ATRP initiator, and (b) polymers prepared using the more stable PyDMDBrMeP bifunctional ATRP initiator.

As mentioned, Table 3.9 summarizes the MW and the *Đ* values of the produced polymers both before and after cleavage (thermal or hydrolytic treatment). Upon treatment under alkaline hydrolysis conditions, or thermolysis, the size of the PyDEDBrMeP polymers was expected to be lowered to one half of the original, a result of the cleavage of the initiator residue in the middle of the chain. Thus, MMA_{50}-*b*-PyDEDBrMeP-*b*-MMA_{50} is expected to be converted to MMA_{50}-*b*-iBuA, with the latter having half the molecular weight of the former and a carboxylic acid group from the isobutyric acid (iBuA) unit at the end of the newly-formed macromolecular chain, as illustrated in Figure 3.44. In contrast, in the case of the PyDMDBrMeP initiator, the corresponding polymers were expected to show better

thermal and hydrolytic stability. In the case of the thermally treated MMA homopolymers prepared using the PyDMDBrMeP bifunctional initiator, no MW reduction was observed after the treatment, indicating the thermal stability of the PyDMDBrMeP residue. In contrast, when subjected to alkaline hydrolysis conditions, the same polymers underwent a substantial reduction in MW, suggesting lability of this initiator residue too under these conditions.

As already mentioned, Table 3.9 summarizes the molecular weight results for the produced linear homopolymers both before and after cleavage (thermal or hydrolytic). The data in the table show that almost all original linear MMA homopolymers exhibited M_n values, close to the theoretical values calculated on the basis of the polymerization stoichiometry and monomer conversion. Homopolymer M_{25}-I_d-M_{25} exhibited a higher, by a factor of two, molecular weight than the theoretically expected, most likely due to a lower (~50%) initiator efficiency. In all cases, the monomer conversion to polymer was higher than 80%, as calculated using ^{1}H NMR spectroscopy. The M_n values of the original linear MMA homopolymers ranged between 5590 and 39100 g mol^{-1}, whereas the $Đ$ values varied from 1.35 to 1.63. These $Đ$ values are rather high for ATRP, but justifiable on the basis of the bifunctionality of the initiator where the final $Đ$ value is the result of the compounding of the size heterogeneity on both sides of the polymer chain. This argument is supported by the measured reduction in the $Đ$ values of the thermolysis products. Upon treatment under alkaline hydrolysis conditions or thermolysis, the size of the PyDEDBrMeP polymers was expected to be lowered to one half of the original, a result of the cleavage of the initiator residue in the middle of the chain. This implied that MMA_{50}-*b*-PyDEDBrMeP-*b*-MMA_{50} should be converted to MMA_{50}-*b*-iBuA, with the latter having one half the molecular weight of the former and a carboxylic acid group from the isobutyric acid (iBuA) unit at the end of the newly-formed macromolecular chain, as illustrated in Figure 3.44. Indeed, the M_n values of the products obtained after thermal or hydrolytic cleavage of the PyDEDBrMeP residue in the linear MMA homopolymers were approximately one half of those of the original linear MMA homopolymers. For instance, the original linear MMA_{50}-*b*-PyDEDBrMeP-*b*-MMA_{50} homopolymer had an M_n value equal to 8800 g mol^{-1}, while after hydrolytic or thermal treatment, that value was lowered to 5360 or 5850 g mol^{-1}, respectively. In contrast, in the case of the PyDMDBrMeP initiator, the corresponding polymers were expected to show better thermal and hydrolytic stability. In the case of the thermally treated MMA homopolymers prepared using the PyDMDBrMeP bifunctional initiator, no molecular weight reduction was observed after the treatment, as can be judged

from the M_n values in the table, indicating the thermal stability of the PyDMDBrMeP residue. In contrast, when subjected to alkaline hydrolysis conditions, the same polymers underwent a substantial reduction in molecular weight, suggesting lability of this initiator residue too under these conditions. For instance, the original linear MMA_{50}-*b*-PyDMDBrMeP-*b*-MMA_{50} homopolymer had an M_n value of 9840 g mol^{-1}, which, after hydrolytic or thermal processing, that value was converted to 3490 or 12600 g mol^{-1}, respectively.

Table 3.9 Molecular weights and molecular weight dispersities of all the linear MMA homopolymers before and after treatment under thermolysis or alkaline hydrolysis conditions.

Polymer Structure [a]	Original				After Thermolysis [b]			After Alkaline Hydrolysis [c]		
	$MW^{theor.}$ (g mol^{-1})	M_p (g mol^{-1})	M_n (g mol^{-1})	*Đ*	M_p (g mol^{-1})	M_n (g mol^{-1})	*Đ*	M_p (g mol^{-1})	M_n (g mol^{-1})	*Đ*
M_{25}-I_d-M_{25}	4470	13600	9610	1.49	9210	5720	1.39	7470	5860	1.16
M_{50}-I_d-M_{50}	8470	13200	8800	1.63	9210	5850	1.43	7700	5360	1.92
M_{100}-I_d-M_{100}	17200	33300	19500	1.62	18900	12500	1.39	10400	6750	1.96
M_{250}-I_d-M_{250}	32500	60600	39100	1.35	29600	21600	1.29	27900	20000	1.29
M_{25}-I_s-M_{25}	4500	8680	5590	1.62	8680	6440	1.40	4490	2050	2.16
M_{50}-I_s-M_{50}	8540	14900	9840	1.48	17300	12600	1.35	7040	3490	2.07
M_{100}-I_s-M_{100}	18500	17300	11200	1.55	12100	8700	1.77	14400	9680	1.49
M_{250}-I_s-M_{250}	40500	41100	24800	1.50	41100	29400	1.30	14000	8010	1.68

[a] M: MMA, I_d: PyDEDBrMeP and I_s: PyDMDBrMeP. [b] Vacuum oven at 150 °C for 6 h. [c] NaOH (0.48 M) in DMSO at RT.

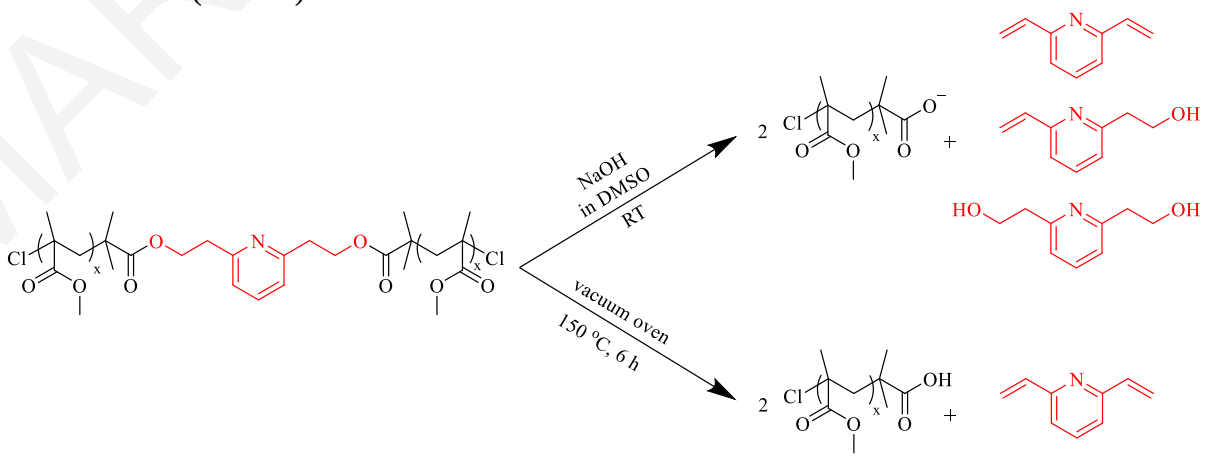

Figure 3.44 Chemical reaction presenting the cleavage of the PyDEDBrMeP residue in the linear MMA homopolymers under thermolysis or alkaline hydrolysis conditions.

Figure 3.45 shows the ^{1}H NMR spectra in d_6-DMSO of the linear MMA_{25}-*b*-PyDEDBrMeP-*b*-MMA_{25} homopolymer (Figure 3.45a), along with those obtained after its treatment under alkaline hydrolysis conditions (Figure 3.45b) and thermally (Figure 3.45c). The ^{1}H NMR spectrum of the original linear homopolymer (Figure 3.45a) exhibited peak "d" at 4.35 ppm, corresponding to the oxymethylene protons of the PyDEDBrMeP residue. This peak is absent from the ^{1}H NMR spectra (black circle) of the products obtained after alkaline hydrolysis or thermolysis of this polymer, confirming the cleavage and removal of the PyDEDBrMeP residue. As already mentioned, the removal of the PyDEDBrMeP residue from the middle of the linear MMA homopolymer converted it to two linear MMA homopolymers each having one half the molecular weight of the starting homopolymer. In addition to the polymeric cleavage products, some low-molecular-weight side-products were also obtained. The latter originated from the removed PyDEDBrMeP residue. The ^{1}H NMR spectrum of the thermolysis products indicated the formation of just one low-molecular-weight cleavage side-product, 2,6-divinylpyridine. In contrast, the ^{1}H NMR spectrum of the alkaline hydrolysis products showed the formation of a mixture of side-products, 2,6-divinylpyridine (34.6 mol%), 2-(6-vinylpyridin-2-yl)ethan-1-ol (38.5 mol%), and 2,6-pyridinediethanol (26.9 mol%). Thus, the two cleavage methods, alkaline hydrolysis and thermolysis, do not give exactly the same low-molecular-weight side-products. It appears that thermolysis is selective, exclusively favoring the β-elimination of ethyl esters, leading to the formation of only one low-molecular-weight cleavage side-product, the divinylpyridine compound. In contrast, in alkaline hydrolysis, both nucleophilic substitution and ethyl ester β-elimination were simultaneously in action, resulting in the diol and the divinyl products, respectively, as well as the alcohol-vinyl mixed product.

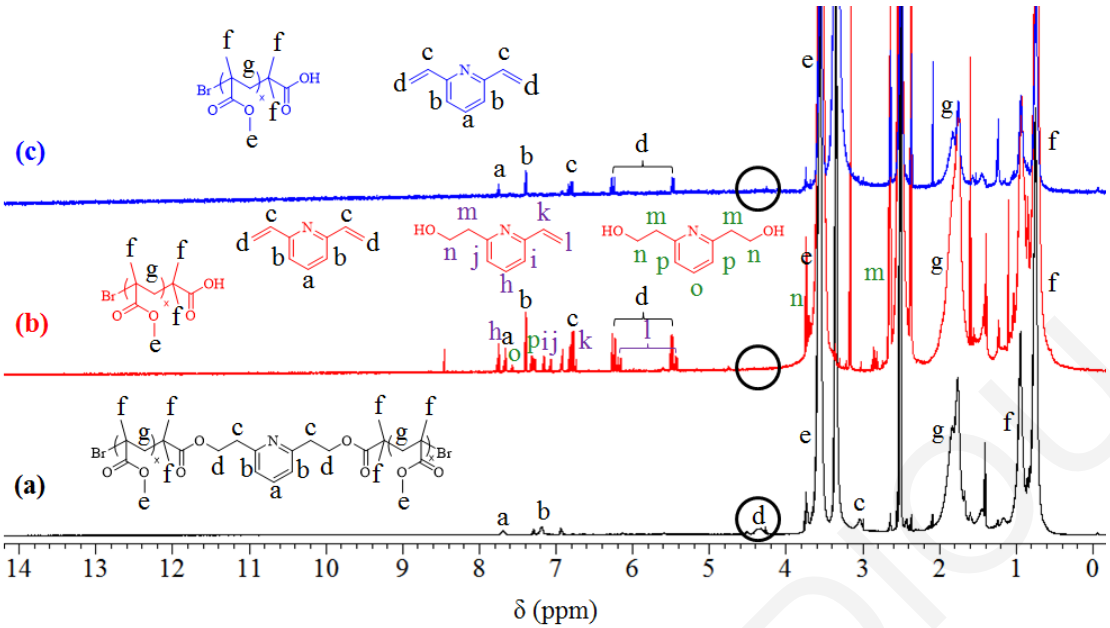

Figure 3.45 ^{1}H NMR spectra in d_6-DMSO of the linear MMA_{25}-*b*-PyDEDBrMeP-*b*-MMA_{25} homopolymer. (a) Original polymer (black). (b) Polymer after alkaline hydrolysis (red). (c) Polymer after thermolysis in the DSC pan up to 240 °C (blue).

Figure 3.46 shows the ^{1}H NMR spectra in d_6-DMSO of the linear MMA_{25}-*b*-PyDMDBrMeP-*b*-MMA_{25} homopolymer (Figure 3.46a), along with those obtained after its treatment under alkaline hydrolysis (Figure 3.46b) and thermolysis (Figure 3.46c) conditions. The characteristic PyDMDBrMeP oxymethylene proton peak "c" at 5.15 ppm is preserved after thermal treatment in Figure S2c, indicating the thermal stability of this residue. In contrast, this peak disappears after alkaline treatment (Figure 3.46b), the result of the sensitivity of the PyDMDBrMeP residue to basic conditions. However, unlike the three-component low-molecular-weight side-products resulting from the alkaline hydrolysis of the PyDEDBrMeP-bearing polymer presented in Figure 4b, no olefin is produced here due to the inability of the (pyridine-2-yl)*methyl* ester to undergo *β*-elimination, leading to the release of only the starting diol.

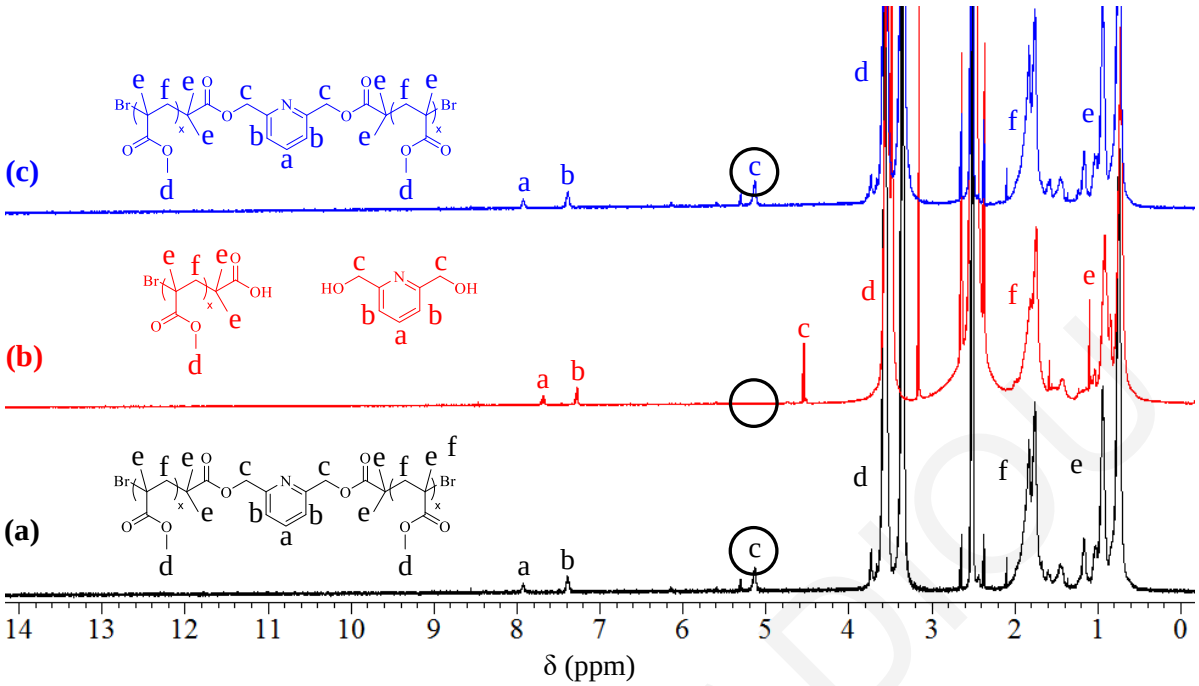

Figure 3.46 ^{1}H NMR spectra in d_6-DMSO of the linear MMA_{25}-*b*-PyDMDBrMeP-*b*-MMA_{25} homopolymer. (a) Original polymer (black). (b) Polymer after alkaline hydrolysis (red). (c) Polymer after thermal treatment in the DSC pan up to 240 °C (blue).

3.5.2.2 Linear amphiphilic ABA triblock copolymers. The degradable bifunctional initiator, PyDEDBrMeP, was used for the preparation of four linear amphiphilic ABA triblock copolymers. Three of the four ABA triblock copolymers had a DMAEMA central block with the same DP and equal to 100, and MMA end-blocks of various lengths corresponding to copolymer MMA contents of 10, 20 and 50 mol%. The fourth ABA triblock copolymer prepared using the PyDEDBrMeP initiator was equimolar and had an MMA midblock with a DP equal to 100 and DMAEMA end-blocks. Furthermore, the more stable bifunctional initiator, PyDMDBrMeP, was also used for the preparation of one linear equimolar amphiphilic ABA triblock copolymer with an MMA midblock of DP equal to 100 and DMAEMA end-blocks. Table 3.10 summarizes the molecular weight and composition characteristics of the produced ABA triblock copolymers both before and after their treatment under alkaline hydrolysis conditions, whereas Figure 3.47 presents all relevant GPC traces. Upon treatment under alkaline hydrolysis conditions, the linear amphiphilic ABA triblock copolymers were converted to amphiphilic diblock copolymers, with the latter having approximately one half the molecular weight of the original copolymers. These include the original triblock copolymers prepared using either of the bifunctional ATRP initiators, PyDEDBrMeP or PyDMDBrMeP, their homopolymer precursors, and the alkaline hydrolysis products of the triblock copolymers.

Table 3.10 Molecular weights and composition characteristics of the linear amphiphilic ABA triblock copolymers before and after alkaline hydrolysis.

Polymer Structure [a]	$MW^{theor.}$ (g mol^{-1})	Original				After Alkaline Hydrolysis [b]		
		M_p (g mol^{-1})	M_n (g mol^{-1})	$Đ$	% mol MMA	M_p (g mol^{-1})	M_n (g mol^{-1})	$Đ$
M_5-*b*-D_{50}-I_d-D_{50}-*b*-M_5	17000	17300	15300	1.48	11.8	7530	6540	1.25
M_{10}-*b*-D_{50}-I_d-D_{50}-*b*-M_{10}	18000	20000	17200	1.50	19.4	9590	6850	1.70
M_{50}-*b*-D_{50}-I_d-D_{50}-*b*-M_{50}	21100	24700	19000	1.42	53.8	12200	7690	1.88
D_{50}-*b*-M_{50}-I_d-M_{50}-*b*-D_{50}	23700	20400	16600	1.38	53.7	13000	7790	1.39
D_{50}-*b*-M_{50}-I_s-M_{50}-*b*-D_{50}	21200	25500	16200	1.62	49.8	21000	10900	1.59

[a] M: MMA, D: DMAEMA, I_d: PyDEDBrMeP, and I_s: PyDMDBrMeP, [b] NaOH (0.48 M) in DMSO at RT.

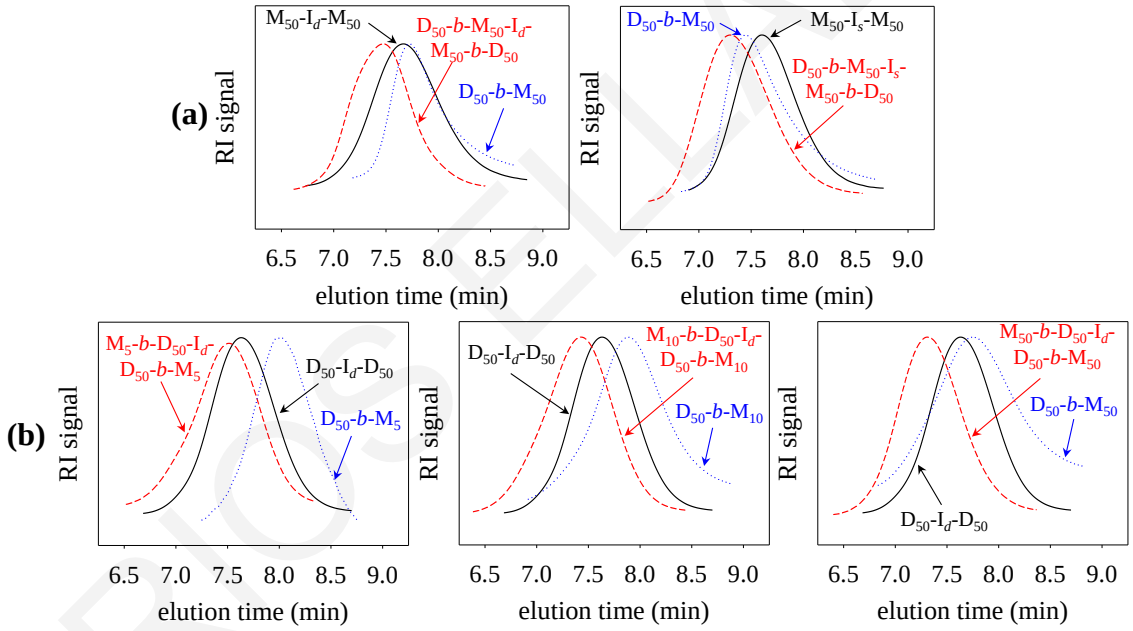

Figure 3.47 GPC traces of the linear DMAEMA-*b*-MMA-*b*-DMAEMA and MMA-*b*-DMAEMA-*b*-MMA triblock copolymers prepared using the two bifunctional ATRP initiators, PyDEDBrMeP (I_d) and PyDMDBrMeP (I_s). Triblock copolymer: red dashed line; homopolymer precursor: black continuous line; diblock copolymer obtained after alkaline hydrolysis: blue dotted line.

3.5.2.3 End-linked MMA homopolymer networks. Dimethacrylate-end-linked MMA homopolymer networks were prepared using the two initiators, PyDEDBrMeP or PyDMDBrMeP, to synthesize first linear MMA homopolymers, followed by their end-linking by the addition of EGDMA cross-linker off the ends of the linear homopolymer. The overall nominal (targeted) degree of polymerization of MMA was equal to 100,

whereas the EGDMA-to-initiator molar ratio was varied at the values 1.0, 2.0 and 4.0. When the molar ratio of EGDMA-to-initiator was equal to 1.0, no network was formed. Instead, a (soluble) hyperbranched polymer was obtained, because the amount of EGDMA cross-linker was apparently not sufficient to interconnect all polymer chains to a network.[40-42,86,249,252] However, when the EGDMA-to-initiator molar ratio was equal to 2.0 or 4.0, a network was formed. Table 3.11 summarizes the main characteristics of all end-linked MMA networks, i.e., their degree of swelling (DS) in THF, and the molecular weight characteristics and the percentage (w/w) of their extractables, and also the molecular weight characteristics of the thermolysis products together with those of the linear precursors to the original networks. Figure 3.48 displays all relevant GPC traces. In the case of the PyDEDBrMeP-based networks, the DSs were equal to 35.4 and 6.7 for EGDMA-to-initiator molar ratios equal to 2.0 and 4.0, respectively, while in the case of the PyDMDBrMeP-based networks, the DSs were found to be 25.9 and 43.0 for EGDMA-to-initiator molar ratios of 2.0 and 4.0, respectively. The very high DS value in THF of 43.0 for the last polymer network may be related to its high percentage of extractables (= 60.0% w/w) in which most of the EGDMA cross-linker may have partitioned, as is also supported by the particularly high $Đ$ value for these extractables of 6.7. In all cases, the percentage of the extractables was above 20.0%; these extractables consisted of hyperbranched polymers, comprising polyMMA segments interconnected with EGDMA cross-linker, which had not been incorporated in the network, and possessing relatively high $Đ$ values, ranging from 1.6 to 6.7. Furthermore, the molecular weight characteristics of the hyperbranched polymers, synthesized using the degradable PyDEDBrMeP and the more stable PyDMDBrMeP bifunctional initiators, are also listed in the table. These two hyperbranched polymers exhibited high $Đ$ values of 4.7 and 5.0.

Table 3.11 DS in THF, percentage of the extractables, and molecular weights characteristics of the linear precursors and the thermolysis products of the end-linked MMA homopolymer networks.

Network Structure [a]	DS in THF	% w/w Extractables	Lin. Precursors		Extractables			After Thermolysis [c]		
			M_n (g mol^{-1})	$Đ$	M_p (g mol^{-1})	M_n (g mol^{-1})	$Đ$	M_p (g mol^{-1})	M_n (g mol^{-1})	$Đ$
$E_{0.5}$-M_{50}-I_d-M_{50}-$E_{0.5}$ [a]	----	100	8800	1.63	17500	25100	4.95	10400	9580	2.16
$E_{1.0}$-M_{50}-I_d-M_{50}-$E_{1.0}$	35.4	39.8	8800	1.63	11500	9700	1.60	46100 8800	71500 6000	6.02 1.36
$E_{2.0}$-M_{50}-I_d-M_{50}-$E_{2.0}$	6.7	21.2	8800	1.63	13000	16400	3.91	92200 8420	88700 6180	1.37 1.33
$E_{0.5}$-M_{50}-I_s-M_{50}-$E_{0.5}$ [b]	----	100	9840	1.48	86800	42900	4.68	16000	24800	7.40
$E_{1.0}$-M_{50}-I_s-M_{50}-$E_{1.0}$	25.9	64.0	9840	1.48	13400	16600	4.01	11800	10500	1.85
$E_{2.0}$-M_{50}-I_s-M_{50}-$E_{2.0}$	43.0	60.0	9840	1.48	14200	19200	6.67	11500	10800	1.12

[a] M: MMA, E: EGDMA, I_d: PyDEDBrMeP, and I_s: PyDMDBrMeP. [b] Hyperbranched homopolymer. [c] Vacuum oven at 150 °C for 6 h.

Table 3.11 also presents the molecular weight characteristics of the products obtained after the thermolysis in a vacuum oven at 150 °C for 6 h of the dimethacrylate-end-linked polymer networks and hyperbranched polymers. The thermolysis product of the hyperbranched MMA homopolymer based on the degradable bifunctional initiator exhibited a monomodal molecular weight distribution with a molecular weight much lower than the original and just above that of its linear precursor. This was due to the cleavage of the initiator residue in the middle of the linear polymer segments constituting the hyperbranched polymer, and the formation of smaller MMA homopolymers, probably of a star architecture. In the case of the dimethacrylate-end-linked MMA homopolymer networks based on the degradable bifunctional initiator, thermolysis converted the insoluble polymer networks to soluble products, whose GPC analysis revealed a bimodal molecular weight distribution. The population in the distribution with higher molecular weight corresponded to MMA star homopolymers formed upon the cleavage of the PyDEDBrMeP residue in the middle of the polyMMA chain between the cross-links. The lower molecular weight population corresponded to linear MMA homopolymers formed again upon the cleavage of the initiator residue in the middle of chains, in this case connected to the network only from one end (dangling chains).

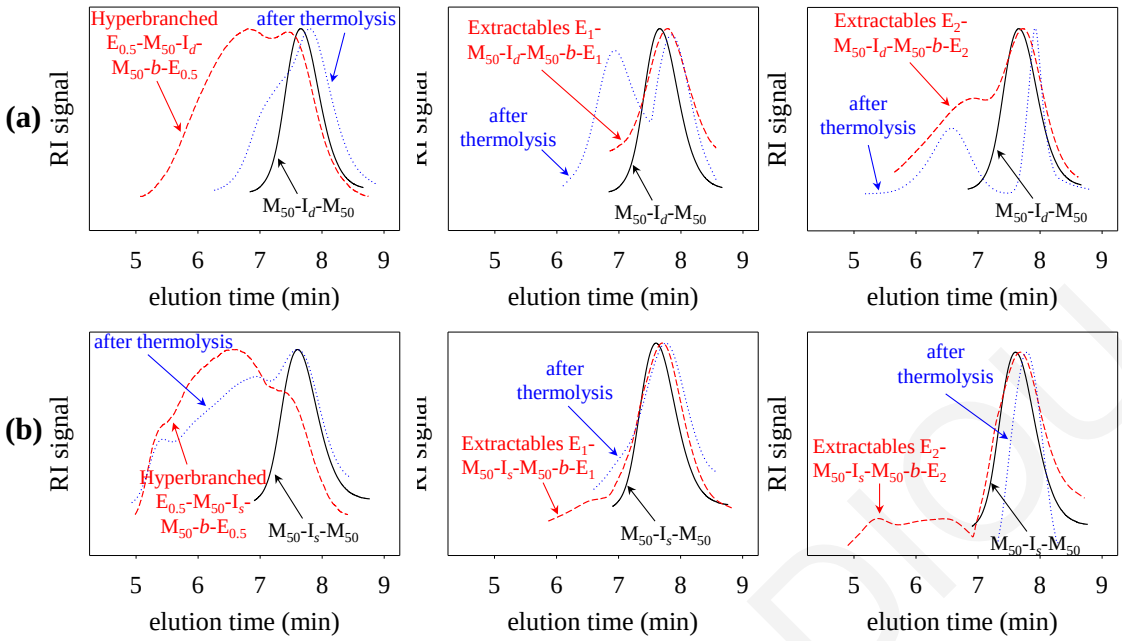

Figure 3.48 GPC traces of the polymers concerning the dimethacrylate-end-linked pMMA networks and the hyperbranched polymers prepared using the two bifunctional ATRP initiators, (a) PyDEDBrMeP (I_d), and (b) PyDMDBrMeP (I_s). Hyperbranched polymer or network extractables: red dashed line; linear homopolymer precursor: black continuous line; thermolysis product: blue dotted line.

3.5.3 Thermal Stability. The thermal of the PyDEDBrMeP and PyDMDBrMeP residue in the polymers was also investigated using DSC and TGA. Figure 3.49a shows the DSC thermograms of two linear MMA homopolymers containing the degradable bifunctional initiator PyDEDBrMeP (residue: I_d) and the more stable bifunctional initiator PyDMDBrMeP (residue: I_s), while Figure 3.49b shows the DSC thermograms of two hyperbranched MMA homopolymers, one based on the degradable PyDEDBrMeP bifunctional initiator, and the other on the more stable PyDMDBrMeP bifunctional initiator. The DSC thermograms of the linear MMA homopolymer and the hyperbranched MMA homopolymer bearing the PyDEDBrMeP residue showed an endothermic and irreversible (absence of DSC endothermic peak upon a second DSC cycle) cleavage of the initiator residue at around ~200 °C, identical to that of the PyDMA homopolymers [279] and higher than that of the PyEMA units of 160 °C.[275] In contrast, the DSC thermograms of the linear and the hyperbranched homopolymers of MMA carrying the PyDMDBrMeP residue displayed thermal stability up to at least 250 °C, right above which much less intense endotherms appeared. This higher thermal stability is comparable to that of the PyMMA units (stable up to 300 °C) which also bore a (pyridin-2-yl)methyl ester moiety.

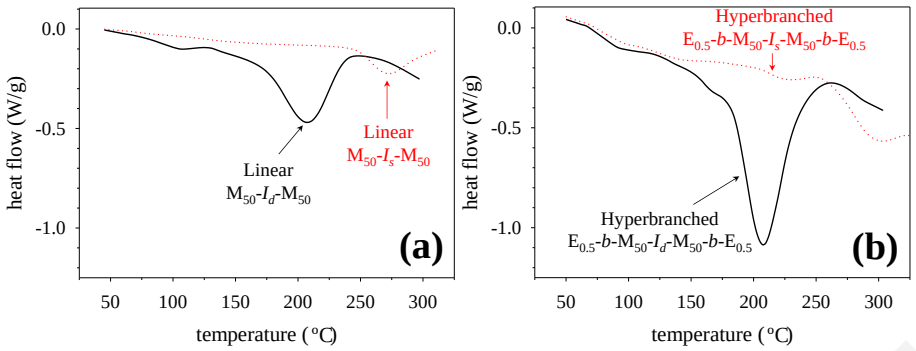

Figure 3.49 DSC thermograms of (a) the linear MMA homopolymers, and (b) the hyperbranched MMA homopolymers prepared using the degradable PyDEDBeMeP (black continuous line) or the more stable PyDMDBeMeP (red dotted line) bifunctional initiators. M: MMA, I_d: PyDEDBrMeP, I_s: PyDMDBrMeP, and E: EGDMA.

Figure 3.50a shows the TGA thermograms of two linear MMA homopolymers, one based on the degradable PyDEDBrMeP bifunctional initiator, and the other on the more stable PyDMDBrMeP bifunctional initiator, while Figure 3.50b shows the TGA thermograms of two hyperbranched MMA homopolymers based again on these two initiators. Given the low molecular weight of the 2,6-divinylpyridine moiety (131 g mol^{-1}) relative to that of the polymer segments (5000 – 10 000 g mol^{-1}), we did not expect to observe in the TGA traces any weight loss due to the cleavage of the initiator residues. Yet, large weight losses (15 – 30%) appeared in the TGA thermograms at ~200 and ~260 °C, the temperatures at which the DSC traces in Figure 3.49 indicated irreversible chemical endothermic reactions for the PyDEDBrMeP and the PyDMDBrMeP residues, respectively. Thus, the main origin of these weight losses should not be the cleavage of the initiator residues, but solvent removal or / and the destruction of weak linkages within pMMA.[322] In all cases, the large weight loss at ~400 °C and above corresponded to backbone decomposition.

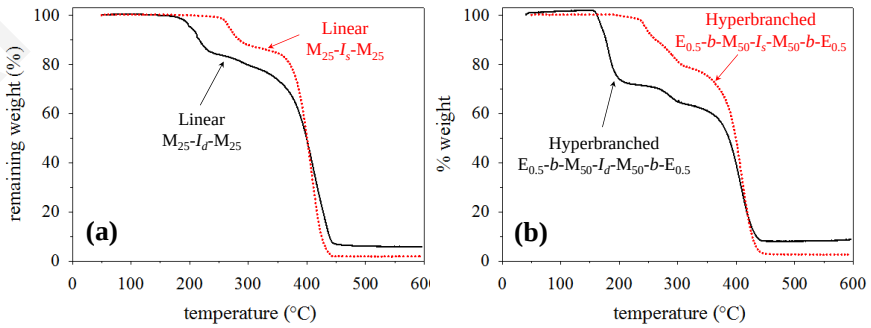

Figure 3.50 TGA thermograms of (a) the linear MMA homopolymers, and (b) the hyperbranched MMA homopolymers prepared using the two bifunctional ATRP initiators. M: MMA, I_d: PyDEDBrMeP, I_s: PyDMDBrMeP and E: EGDMA.

3.5.4 Alkaline Hydrolysis of the Starting PyDEDBrMeP Initiator. After confirming the degradability under alkaline hydrolysis conditions of the PyDEDBrMeP initiator residue within the polymers, we decided to also subject the starting PyDEDBrMeP initiator itself to alkaline hydrolysis. PyDEDBrMeP indeed hydrolyzed, but the main hydrolysis product was just 2,6-pyridinediethanol, rather than the mixture of three pyridine compounds, diol, divinyl and mixed alcohol-vinyl, obtained from the alkaline hydrolysis of the PyDEDBrMeP residue in the MMA homopolymer. Scheme 3.27 shows the chemical reaction for the alkaline hydrolysis of the PyDEDBrMeP bifunctional ATRP initiator using sodium deuteroxide in d_6-DMSO, along with its ^{1}H NMR spectra before (a, black) and after alkaline hydrolysis (b, red). The most characteristic peaks in the ^{1}H NMR spectrum of PyDEDBrMeP are those of the oxymethylene protons "d" at 4.53 ppm and the adjacent methylene protons "c" at 3.11 ppm. In the ^{1}H NMR spectrum of the hydrolysis products, one can see the hydroxymethylene protons "d" at 3.70 ppm and the adjacent methylene protons "c" at 2.80 ppm of the released 2,6-pyridinediethanol.

The difference in the alkaline hydrolysis behavior of the starting PyDEDBrMeP from that of its residue in the polymers arises from the proximity of the two terminal bromine atoms to the two carbonyl groups in the starting initiator. Via the inductive effect, each bromine atom renders its adjacent carbonyl carbon more electron deficient, and, therefore, more prone to nucleophilic addition of the OH^- anion, leading to purely ester hydrolysis and production of the pyridinediol. In contrast, in the polymer, the two pyridine carbonyl groups have adjacent C – C bonds, as the two bromines are now only at the two polymer ends. Because carbon is a weak inductive donor, the carbonyl carbon is less prone to nucleophilic addition of the hydroxyl anion, thereby favoring now an E2 elimination mechanism, resulting in the (partial) production of the bis- and mono-olefin. The fact that a mixture of three products (diol, bisolefin and alcohol-olefin) rather than pure divinylpyridine, was obtained can be attributed to steric hindrances associated with the hydroxyl attack onto the carbonyl carbon in the initiator residue in the middle of the polymer chain. These hindrances lead to the simultaneous operation of both mechanisms, the nucleophilic addition/elimination mechanism favoring alcohol production, and the E2 elimination mechanism favoring olefin production. It is noteworthy that, contrary to the alkaline hydrolysis of the PyDEDBrMeP residue, the alkaline hydrolysis of the PyEMA unit in polymers of PyEMA produces an olefin (2-vinylpyridine) rather than the mixture of three pyridine compounds. In this case, the 2-(pyridin-2-yl)ethyl group is less sterically

crowded (carbonyl carbons here have only a pyridineethanol group on the side), alkaline hydrolysis leads exclusively to the production of olefin (2-vinylpyridine).

Scheme 3.27 Chemical reaction for the alkaline hydrolysis of the PyDEDBrMeP degradable bifunctional ATRP initiator, its ^{1}H NMR spectrum (a, black) in $CDCl_3$ and the ^{1}H NMR spectrum after alkaline hydrolysis (b, red) in d_6-DMSO.

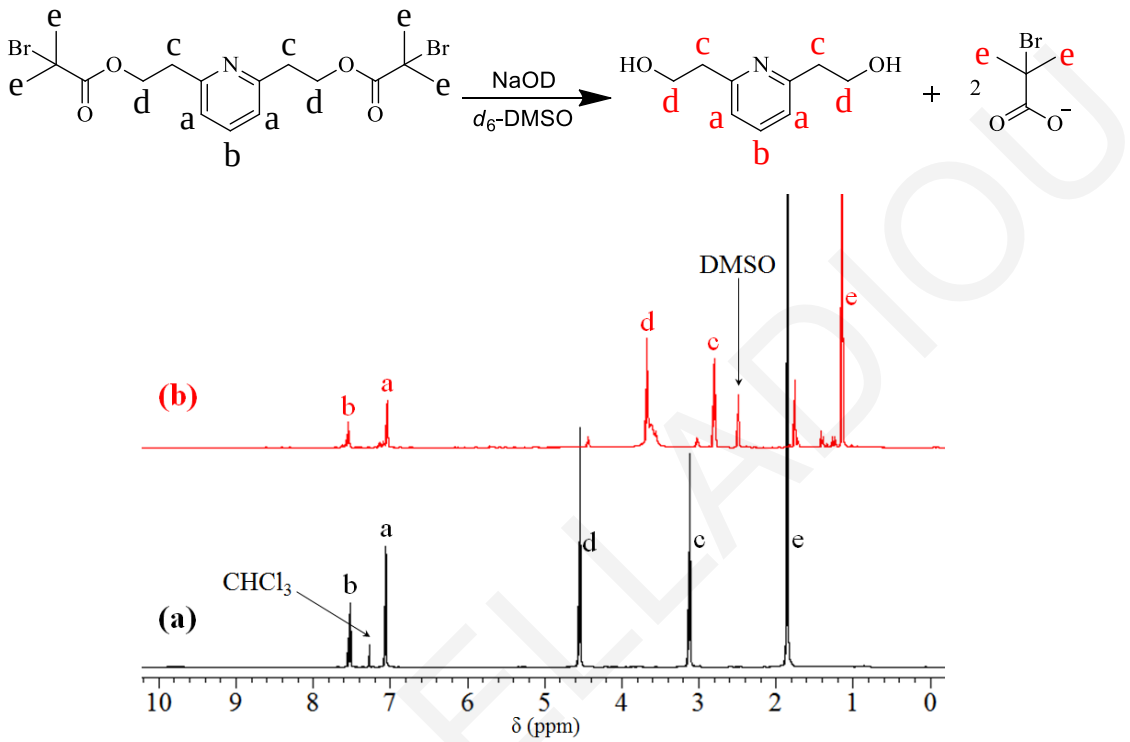

3.5.5 Properties of the Micelles Formed in Water. DLS and AFM study were conducted to probe the micellization behavior (hydrodynamic diameters, D_h, and adsorption diameters, D_{AFM}) of the linear amphiphilic ABA triblock copolymers before and after treatment under alkaline hydrolysis conditions. The DLS and AFM measurements were performed in acidified water, where the amphiphilic copolymers were fully dissolved. Figure 3.51 shows the AFM images of the spherical micelles, while Table 3.12 shows all results, both from AFM and DLS. As illustrated in Figure 3.46, the spherical micelles formed were monodisperse.

Table 3.12 shows the D_h values, the D_{AFM} values of the formed micelles and the theoretical micellar diameters, as calculated by multiplying twice the total degree of polymerization of the copolymers times 0.252 nm, which is the contribution of one monomer repeating to the contour length. As illustrated in Table 3.12, in all cases, D_h values agree well with D_{AFM} values, but are slightly higher than the theoretical values. The novelty of this work is that

using a degradable bifunctional initiator should not affect the size of the formed micelles before and after cleavage of the initiator residue.

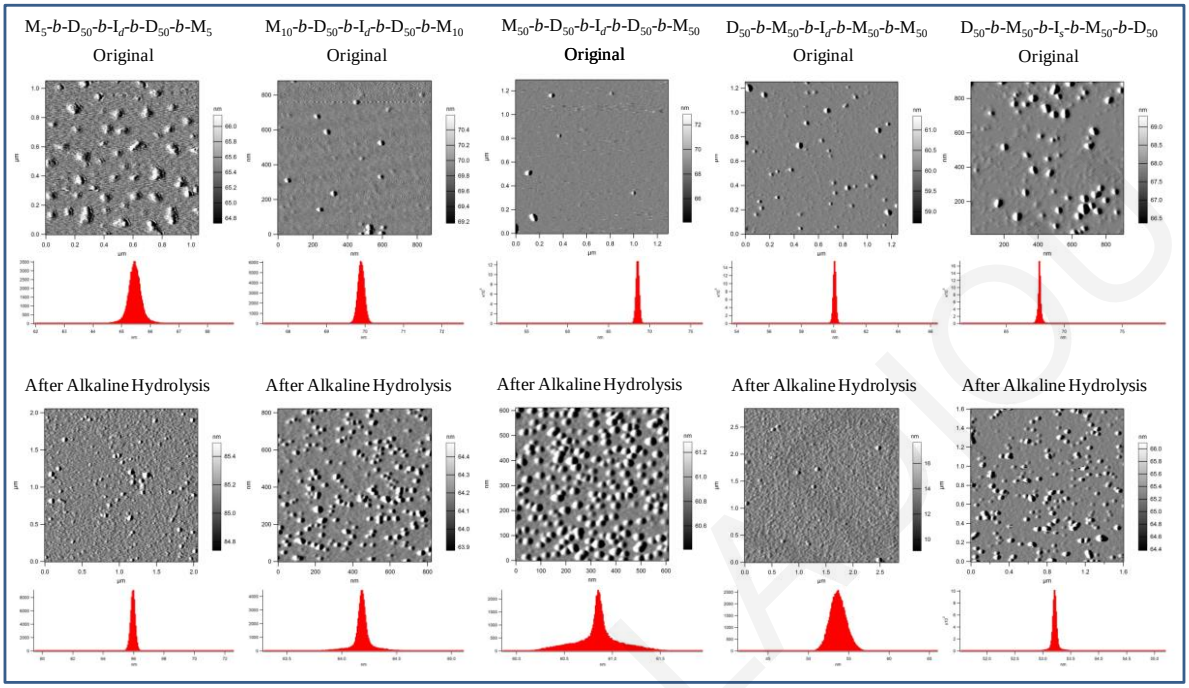

Figure 3.51 AFM images and distributions of the diameters of the micelles formed by the ABA triblock copolymers in water before and after cleavage of the initiator residue under alkaline hydrolysis conditions.

Table 3.12 Micellar hydrodynamic radius of the linear original amphiphilic ABA triblock copolymers and those obtained after alkaline hydrolysis as determined by DLS and AFM.

Polymer Structure	Original			After Alkaline Hydrolysis		
	DLS D_h (nm)	AFM D (nm)	Theor. D (nm)	DLS D_h (nm)	AFM D (nm)	Theor. D (nm)
M_5-*b*-D_{50}-*I_d*-D_{50}-*b*-M_5	68.06	65.40	27.94	100.64	65.95	27.94
M_{10}-*b*-D_{50}-*I_d*-D_{50}-*b*-M_{10}	56.32	69.90	30.48	26.36	64.25	30.48
M_{50}-*b*-D_{50}-*I_d*-D_{50}-*b*-M_{50}	54.20	68.70	50.80	27.60	60.80	50.80
D_{50}-*b*-M_{50}-*I_d*-M_{50}-*b*-D_{50}	63.40	60.05	50.80	65.56	54.10	50.80
D_{50}-*b*-M_{50}-*I_s*-M_{50}-*b*-D_{50}	66.36	67.80	50.80	71.82	53.15	50.80

M: MMA, D: DMAEMA, I_d: PyDEDBrMeP and I_s: PyDMDBrMeP.

3.6 A Degradable ATRP Inimer Cleavable Under Alkaline Hydrolysis Conditions or Thermally: Synthesis, Polymerization and Cleavage

Inimer provide a facile route to hyperbranched polymers, whereas degradable inimers render these hyperbranched polymers convertible to linear polymers. A small number of degradable ATRP inimers have been developed, the majority of them degraded in the presence of reducing agent and to acidic conditions. A novel degradable inimer for ATRP, 2-(6-(2-((2-bromo-2-methylpropanoyl)oxy)ethyl)pyridin-2-yl)ethyl methacrylate (PyDEBrMA), was synthesized by the two-step esterification of 2,6-pyridinediethanol, first with α-bromoisobutyryl bromide in order to introduce the initiating moiety, and then with methacryloyl chloride in order to introduce the monomer moiety. The present labile PyDEBrMA inimer, bearing one polymerizable and one initiator moieties, could be considered a hybrid of the 2,6-PyDMA cross-linker [279] and the PyDEDBrMeP ATRP bifunctional initiator.[280] The degradability of the PyDEBrMA inimer under thermolysis or alkaline hydrolysis conditions arises from the presence in its structure of two 2-(pyridin-2-yl)ethyl ester moieties. PyDEBrMA was used to initiate the self-condensing ATRP of two hyperbranched methyl methacrylate (MMA) homopolymers with different MMA to inimer molar ratios, 50 and 100. Furthermore, two hyperbranched amphiphilic diblock copolymers were also synthesized using as macroinitiator the smallest hyperbranched MMA homopolymer (hydrophobic core) and the hydrophilic 2-(dimethylamino)ethyl methacrylate (DMA) at compositions in the copolymer of 25 and 50 mol%. Alkaline hydrolysis, using sodium deuteroxide in d_6-DMSO, or thermolysis, at or above 130 °C, of these polymeric materials, led to a reduction in their molecular weight and conversion of their architecture from hyperbranched (high molecular weight dispersity) to linear (near monodisperse). The hyperbranched amphiphilic diblock copolymers and their cleavage products were analyzed in organic or aqueous solution using dynamic light scattering and atomic force microscopy, which indicated that the latter copolymers formed micelles of smaller sizes compared with those formed by the parent hyperbranched amphiphilic diblock copolymers.

The original hyperbranched MMA_x-PyDEBrMA homopolymer is expected to be cleaved and converted to a linear polymer with the structure iBuA-*b*-(MMA_x-*co*-MAA)-Br, while the original hyperbranched MMA_x-*b*-DMA_y-PyDEBrMA copolymer is expected to be cleaved and converted to a linear diblock copolymer with the structure iBuA-*b*-(MMA_x-*co*-MAA)-*b*-DMA_y-Br, possessing a clearly lower molecular weight than the original polymer

and one (on average) carboxylic acid group randomly dispersed along the linear polymer chain, as shown in Scheme 3.28.

Scheme 3.28 Synthesis of the Hyperbranched MMA Homopolymers and the Hyperbranched Amphiphilic MMA-DMA Diblock Copolymers and the Products Obtained after Thermolysis or Alkaline Hydrolysis of the PyDEBrMA Residues.

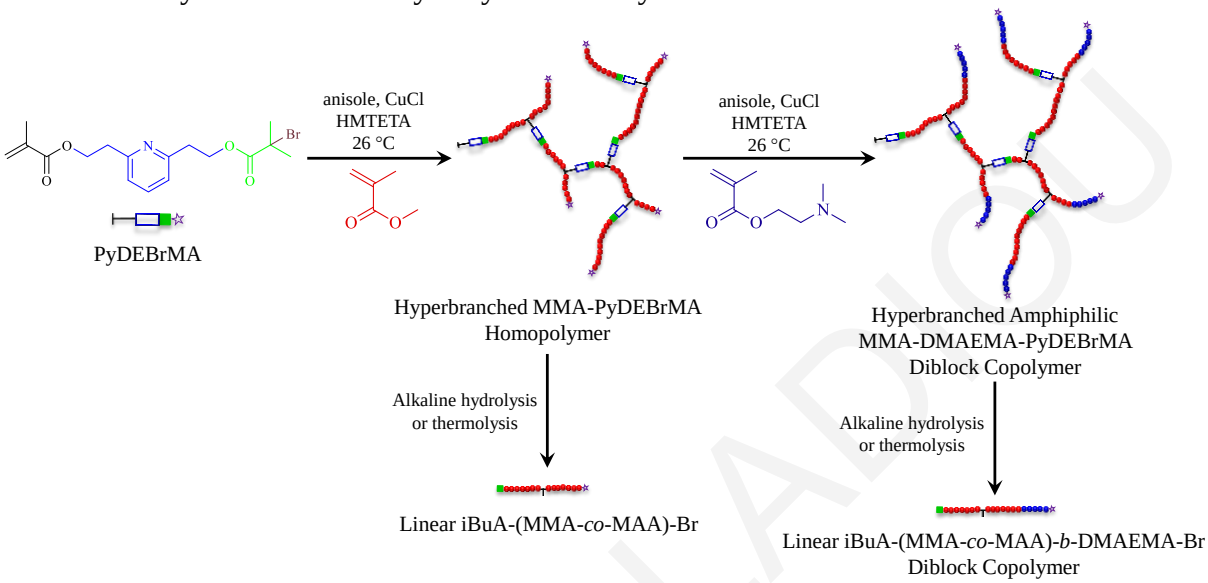

3.6.1 Synthesis of the PyDEBrMA Degradable ATRP Inimer. The labile PyDEBrMA ATRP inimer was synthesized by the two step bisesterification of 2,6-pyridinediethanol, first with *a*-bromoisobutyryl bromide, and, subsequently, with methacryloyl chloride. Although the reverse bisesterification sequence is also possible and it would lead to the same final product, the chosen sequence has the advantage of lower risk for undesired thermal polymerization of the inimer as the methacrylate moiety is attached only in the final step. Scheme 2 shows the chemical reaction leading to the synthesis of 2,6-pyridinediethanol, followed by the esterification with *a*-bromoisobutyryl bromide, resulting in the preparation of the intermediate monofunctional ATRP initiator, and then with methacryloyl chloride, yielding the desire PyDEBrMA inimer. Scheme 3.29 also presents the ^{1}H and ^{13}C NMR spectra of 2,6-pyridinediethanol in $CDCl_3$, the intermediate monofunctional ATRP initiator in $CDCl_3$, and the final product, the PyDEBrMA inimer, in d_6-DMSO.

Scheme 3.29 Synthesis of 2,6-pyridinediethanol, the intermediate monofunctional ATRP initiator, and the 2PyDEBrMA ATRP inimer, along with their ^{1}H and ^{13}C NMR spectra.

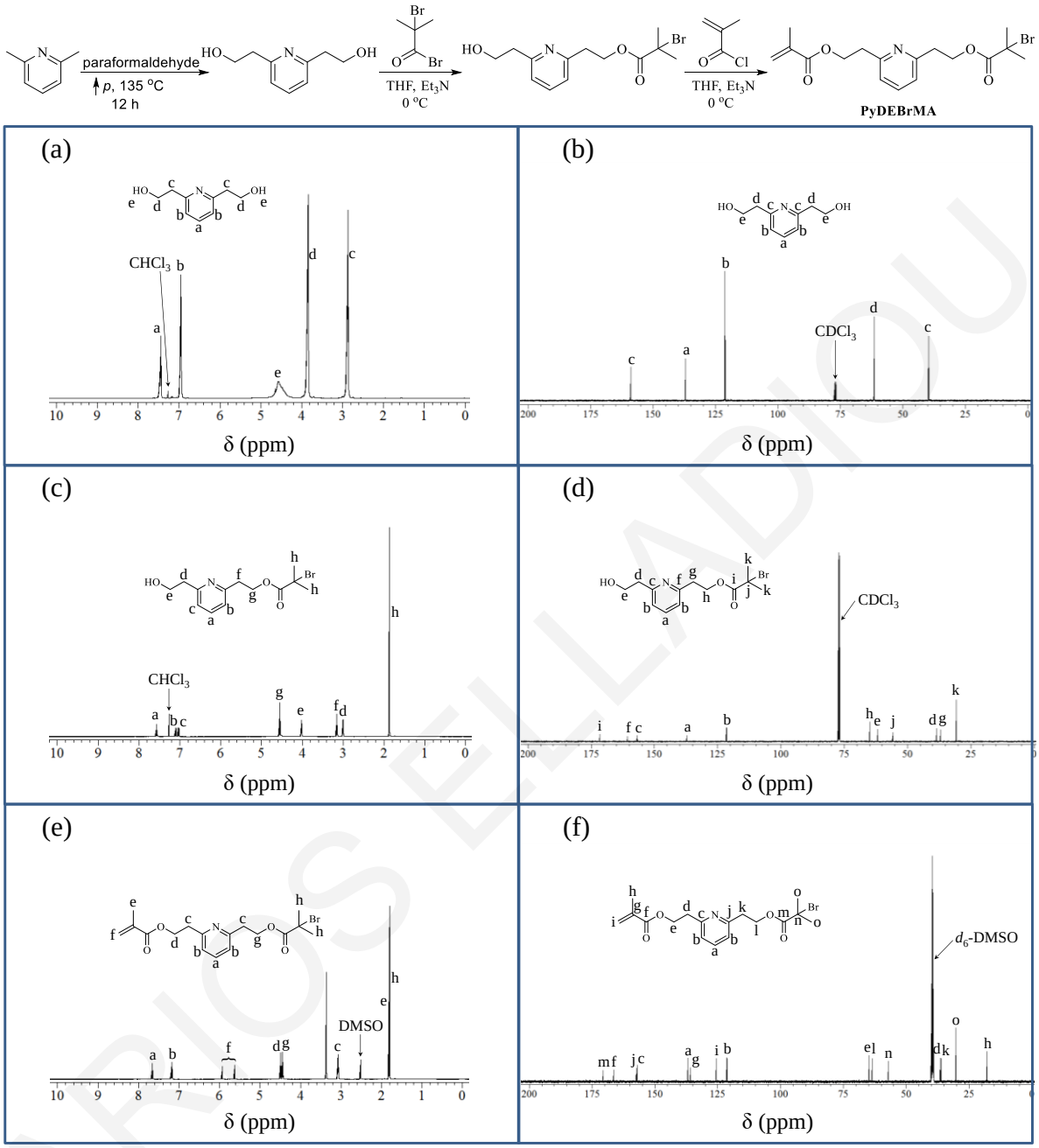

3.6.2 **Cleavage of the PyDEBrMA ATRP *Inimer by Alkaline Hydrolysis Before Polymerization*.** The PyDEBrMA residues in the hyperbranched (co)polymers are expected to degrade under thermolysis or alkaline hydrolysis conditions, causing a reduction in the molecular weight of the starting hyperbranched (co)polymers and converting their architecture from hyperbranched to linear. However, before exploring (co)polymer degradation, we decided to first investigate the lability of the PyDEBrMA inimer as a small organic molecule prior to its polymerization. Scheme 3.30 shows the chemical

reaction for the alkaline hydrolysis of the PyDEBrMA inimer using sodium deuteroxide in d_6-DMSO, leading to the formation of an equimolar mixture of MAA and *a*-bromoisobutyric acid, plus a mixture of 2,6-pyridinediethanol, 2-(6-vinylpyridin-2-yl)ethan-1-ol and 2,6-divinylpyridine in a ratio of 64/27/9, as inferred from the analysis of the relative peak areas in the ^{1}H NMR spectrum of the (mixture of) products obtained at the end of the reaction of its alkaline hydrolysis (b, red). The ^{1}H NMR spectrum of the inimer before its hydrolysis is also shown in Scheme 3.30 (a, black) for comparison. The complete hydrolysis of the PyDEBrMA inimer was confirmed by the complete disappearance of the peaks of the oxymethylene protons "d" and "g" at 4.50 and 4.42 ppm, respectively, in the ^{1}H NMR spectrum of the products. This was accompanied by the appearance of the peaks corresponding to an equimolar mixture of MAA (olefinic protons "f" at 5.00 and 5.60 ppm) and *a*-bromoisobutyric acid (methyl protons "h" at 1.10 ppm) mixture, and a mixture of 2,6-pyridinediethanol (hydroxymethylene protons "d" at 3.50 ppm), 2,6-divinylpyridine (vinyl protons protons "d*" at 5.43 and 6.20 ppm) and their hybrid 2-(6-vinylpyridin-2-yl)ethan-1-ol.

Scheme 3.30 Chemical Reaction of the Alkaline Hydrolysis of the PyDEBrMA *Inimer* in d_6-DMSO using NaOD, along with the ^{1}H NMR spectra before (black) and after (red) alkaline hydrolysis of the PyDEBrMA ATRP Inimer.

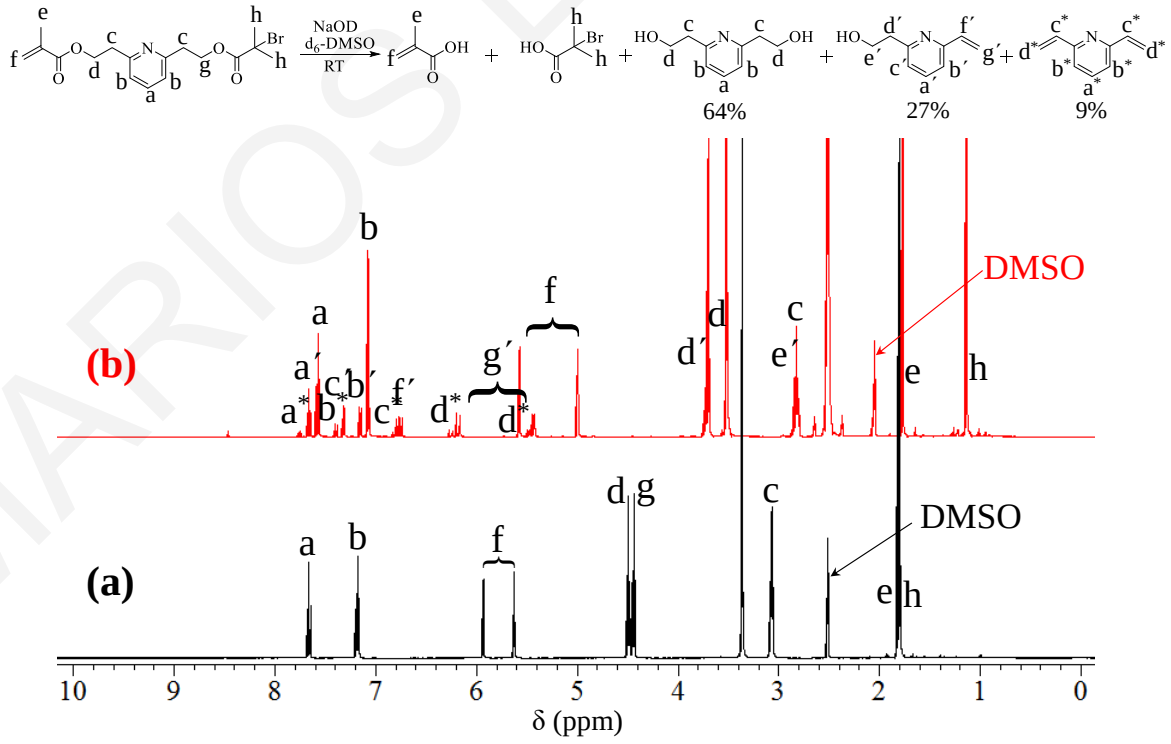

3.6.3 Copolymerization of the PyDEBrMA ATRP Inimer. The degradable PyDEBrMA ATRP inimer was used for the preparation of two hyperbranched MMA homopolymers

and two hyperbranched amphiphilic diblock copolymers, containing MMA as the hydrophobic segment and DMA as the hydrophilic segment.

3.6.3.1 Hyperbranched (co)polymers. Two hyperbranched MMA homopolymers with nominal degrees of polymerization equal to 50 and 100 were synthesized using the PyDEBrMA labile ATRP inimer. Furthermore, the same *inimer* was also used for the preparation of hyperbranched amphiphilic MMA-DMA diblock copolymers with DMA contents of 25 and 50 mol%. Figure 3.52 displays the GPC traces of the two hyperbranched MMA homopolymers and the two hyperbranched amphiphilic MMA-DMA diblock copolymers, along with the GPC traces of the products obtained after thermal treatment or treatment under alkaline hydrolysis conditions, while Table 3.13 summarizes the M_n and $Đ$ values of all the original and cleaved polymer samples. The GPC traces of the products obtained after treatment under alkaline hydrolysis conditions or thermolysis were shifted to longer elution times compared to those of the parent polymers, suggesting molecular weight reduction *via* cleavage of the inimer residue, and the conversion of the hyperbranched (co)polymer to linear (co)polymer. The M_n values of the cleaved polymer samples, either hydrolytically or thermally, were close to each other, as expected, due to the lability of the pyridinyldiethyl diester moiety under the above conditions, and therefore, the reduction of the molecular weight of the original hyperbranched polymers to linear polymers with lower and similar molecular weight.

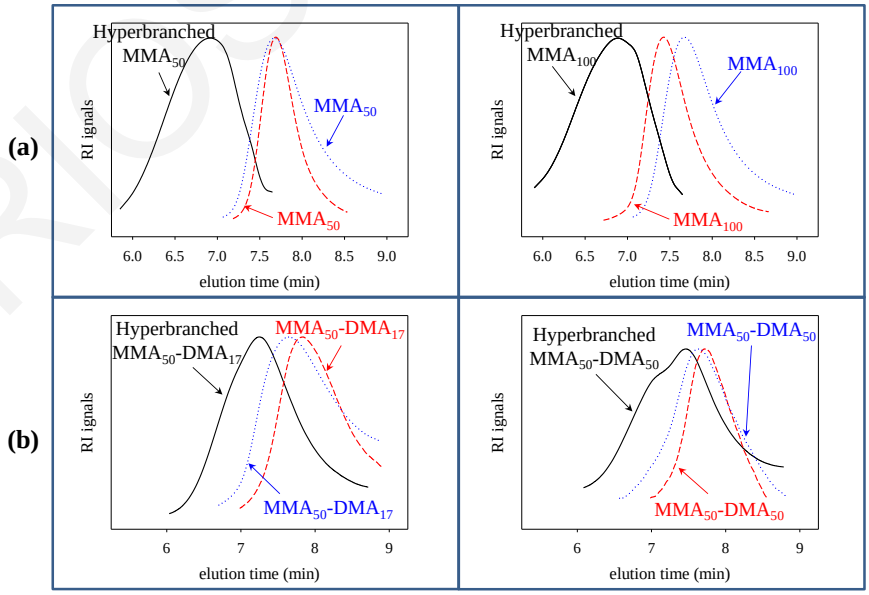

Figure 3.52 GPC traces of the hyperbranched MMA homopolymers before (black continuous line) and after thermolysis (red dashed line) or alkaline hydrolysis (blue dotted line). (a) Hyperbranched MMA-PyDEBrMA homopolymers, and (b) Hyperbranched amphiphilic MMA-DMA-PyDEBrMA diblock copolymers.

The high *Đ* values listed in the table for the original polymers, higher than 2.0 in most cases, are consistent with the highly branched nature of the polymers, conferred upon them by the successful action of the *inimer* as a branching agent. Table 3.13 also summarizes the M_n and *Đ* values of the polymers obtained after the cleavage of the *inimer* residues after treatment by thermolysis or alkaline hydrolysis. In the case of the hyperbranched MMA homopolymers, thermolysis was performed in the bulk in the vacuum oven at 150 °C for 8 h, while in the case of the hyperbranched amphiphilic MMA-DMA diblock copolymers, thermolysis was performed in DMSO at 130 °C for 12 h. When the hyperbranched amphiphilic MMA-DMA diblock copolymers were thermolyzed in the bulk in the vacuum oven at 130 °C or higher, an insoluble mass was obtained. Thermal or alkaline treatment of the hyperbranched (co)polymers led to the reduction of their size, as a result of the cleavage of the inimer residues due to the sensitivity of the 2-(pyridin-2-yl)ethyl ester group at elevated temperature or under alkaline hydrolysis conditions.

Table 3.13 Molecular weights and molecular weight dispersities of the hyperbranched MMA homopolymers and the hyperbranched amphiphilic MMA-DMA diblock copolymers, before and after treatment by thermolysis or alkaline hydrolysis.

Polymer Structure	Original				Cleavage	After Thermolysis			After Alkaline Hydrolysis [c]		
	M_p (g mol^{-1})	M_n (g mol^{-1})	*Đ*	%mol DMA	MW$^{theor.}$ (g mol^{-1})	M_p (g mol^{-1})	M_n (g mol^{-1})	*Đ*	M_p (g mol^{-1})	M_n (g mol^{-1})	*Đ*
M_{50} [a]	53800	22800	2.70	96	4800	14000	9070	1.33	12800	9610	1.72
M_{100} [a]	27900	28400	2.12	81	8100	23300	13400	1.48	15800	14900	1.80
M_{50}-D_{17} [b]	27900	14100	2.45	88	7360	9780	5660	1.65	14000	6370	2.04
M_{50}-D_{50} [b]	18900	12000	2.68	93	12300	11700	9170	1.28	13800	9320	1.67

[a] Thermolysis: vacuum oven at 150 °C for 8 h. [b] Thermolysis: in DMSO by reflux at 130 °C for 12 h. [c] NaOH (0.48 M) in DMSO at RT.

3.6.3.2 Cleavage of the PyDEBrMA residue in hyperbranched (co)polymers. The cleavage of the PyDEBrMA residue in the (co)polymers was also confirmed using ^{1}H NMR spectroscopy. Figure 3.53a shows the ^{1}H NMR spectrum of the original hyperbranched homopolymer MMA_{50}-PyDEBrMA in d_6-DMSO, while Figures 3.5.3b and 3.53c show the ^{1}H NMR spectra obtained after subjecting the polymer to alkaline hydrolysis using sodium deuteroxide in d_6-DMSO at room temperature, and to a brief heating up to 240 °C *via* DSC, respectively. The ^{1}H NMR spectrum of the hyperbranched MMA_{50}-PyDEBrMA homopolymer displays the peak of oxymethylene protons "d" of the PyDEBrMA residue at 4.35 ppm, while this peak is completely absent from the other two

^{1}H NMR spectra, due to the cleavage and removal of this residue after the hydrolytic and thermal treatments. The ^{1}H NMR spectrum of the hydrolyzed MMA$_{50}$-PyDEBrMA showed the formation of a mixture of two low-molecular-weight side-products, 2,6-divinylpyridine (vinyl protons "d" at 5.47 and 6.27 ppm) and 2-(6-vinylpyridin-2-yl)ethan-1-ol (vinyl protons "l" at 5.43 and 6.16 ppm) in a ratio of 80/20. This suggest that hydrolysis proceeds *via* two mechanisms, ethyl ester *β*-elimination leading to the olefinic moieties and nucleophilic addition/elimination yielding the alcohol moiety in the latter product. Comparing the alkaline hydrolysis of the PyDEBrMA residue in the MMA$_{50}$-PyDEBrMA hyperbranched polymer with that of the PyDEBrMA inimer, it seems that in the latter case nucleophilic addition/elimination predominates over ethyl ester *β*-elimination, probably due to the presence of the terminal bromine atom to the carbonyl end group, which through the inductive effect render the carbonyl carbon more electron deficient, and therefore, more capable for nucleophilic attack of the hydroxyl anion, leading to the formation of alcohol. Furthermore, carbonyl carbon of the PyDEBrMA residue in polymers is more steric hindrance against the hydroxyl attack, thereby leading to ethyl ester *β*-elimination and the olefinic product.

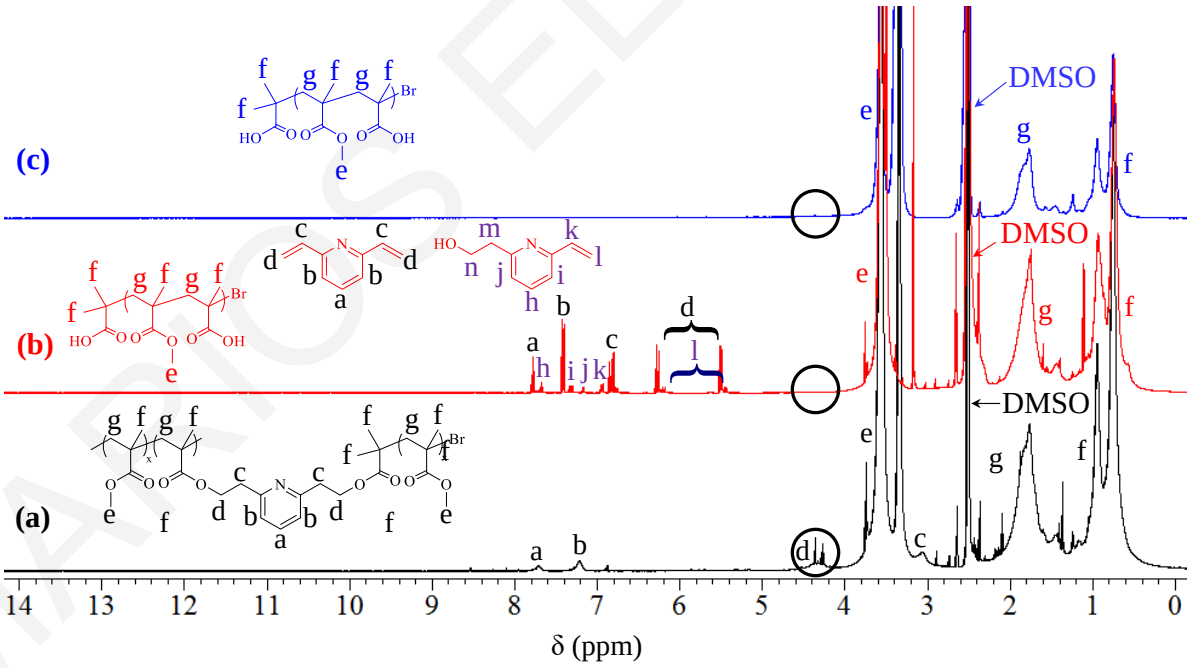

Figure 3.53 ^{1}H NMR spectra in d_6-DMSO of the hyperbranched MMA$_{50}$-PyDEBrMA homopolymer. (a) Original polymer (black), (b) after alkaline hydrolysis (red), and (c) after thermolysis *via* DSC up to 240 °C (blue).

3.6.4 Thermal Properties of the PyDEBrMA Containing Polymers. The thermal behavior of the MMA$_{50}$-PyDEBrMA hyperbranched homopolymer was studied using DSC, as

shown in Figure 3.54. The DSC thermogram of the hyperbranched MMA homopolymer bearing PyDEBrMA residues showed an endothermic peak at around 230 °C, corresponding to the cleavage of the PyDEBrMA residue, while a linear MMA homopolymer was stable at least up to 350 °C. This cleavage temperature of the PyDEBrMA residue is higher than that of the 2PyEMA units in their homopolymers of 160 °C, possibly due to the greater protection offered to the inimer residue by the two polyMMA segments flanking it. units by the MMA units. The enthalpy of the reaction for the cleavage of the PyDEBrMA residues in the hyperbranched MMA_{50}-PyDEBrMA homopolymer was found equal to 10.20 J g^{-1}. Taking into account the PyDEBrMA content in each sample, the molar enthalpy for the cleavage of the PyDEBrMA residue is calculated ΔH = 52.88 kJ mol^{-1}, lower than that for the 2PyEMA units in their homopolymers of ~70 kJ mol^{-1}, but in good agreement with that for the PyDMA residue in their (co)polymers of ~50 kJ mol^{-1}.[279]

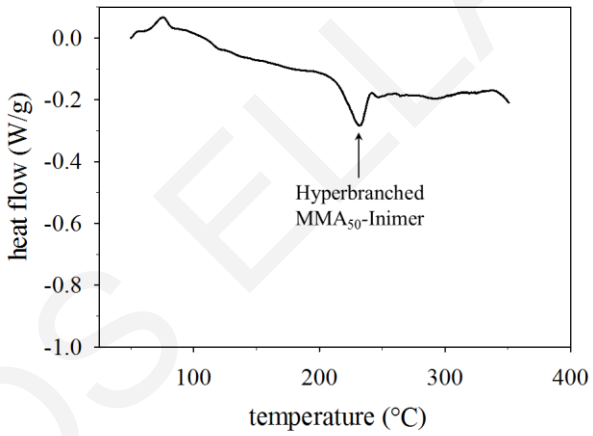

Figure 3.51 DSC thermograms of the hyperbranched MMA homopolymer containing the PyDEBrMA inimer.

3.6.5 Solution Self-Assembly. Toluene solutions of the hyperbranched amphiphilic [MMA-PyDEBrMA]-*b*-DMA diblock copolymers were characterized using DLS and AFM to determine the hydrodynamic diameter, D_h, and adsorbed diameter, D_{AFM}, of the formed entities. The DMA units were quaternized using methyl iodide in order to increase the incompatibility with MMA units in toluene. Additionally, the linear amphiphilic MMA-*b*-DMA diblock copolymers, obtained after the alkaline hydrolysis of the PyDEBrMA residues in the hyperbranched amphiphilic diblock copolymers, were also analyzed using AFM and DLS, both, in toluene (after quaternization of DMA units with methyl iodide) and in acidic water.

Figure 3.55 presents the AFM images of the original hyperbranched amphiphilic [MMA-*co*-Inimer]-*b*-DMA copolymers (first column), as well as those of the linear amphiphilic MMA-*b*-DMA diblock copolymers obtained by treatment of the former polymer under alkaline hydrolysis conditions, in toluene (second column) and in water (third column). AFM images indicated the formation of spherical and monodisperse micelles in all cases. Furthermore, the size of the original hyperbranched copolymers was higher than those of the products obtained after alkaline hydrolysis of the PyDEBrMA residue, as expected. Table 3.14 summarizes the results from AFM and DLS for both the original hyperbranched and linear amphiphilic MMA-*b*-DMAEMA copolymers (D_h and D_{AFM}). For all the copolymers in Table 3.14, there is a relative good agreement between the D_h and D_{AFM}, determined by DLS and AFM, respectively. The D_h values of the original hyperbranched amphiphilic [MMA-PyDEBrMA]-*b*-DMA diblock copolymers were larger than their D_{AFM} values, may be due to aggregate formation in their solutions. The D_h and D_{AFM} values of the linear amphiphilic MMA-*b*-DMA diblock copolymers, both in organic and aqueous solution, were similar to each other, both being smaller than these obtained of the formed micelles of the original hyperbranched amphiphilic [MMA-PyDEBrMA]-*b*-DMA diblock copolymers in toluene. The most important conclusion is that both D_h and D_{AFM} were reduced after the cleavage of the inimer residue under alkaline hydrolysis conditions.

Table 3.14 Micellar Characteristics of the hyperbranched amphiphilic [MMA-Inimer]-*b*-DMAEMA diblock copolymers and their products obtained after alkaline hydrolysis of the PyDEBrMA residue.

Polymer Structure	Original hyperbranched in toluene		After Cleavage of PyDEBrMA in water			
			in toluene		in water	
	D_h (nm)	D_{AFM} (nm)	D_h (nm)	D_{AFM} (nm)	D_h (nm)	D_{AFM} (nm)
MMA_{50}-*b*-DMA_{17}	279.60	79.70	39.02	49.50	55.40	49.30
MMA_{50}-*b*-DMA_{50}	219.80	80.00	38.38	35.55	51.46	39.00

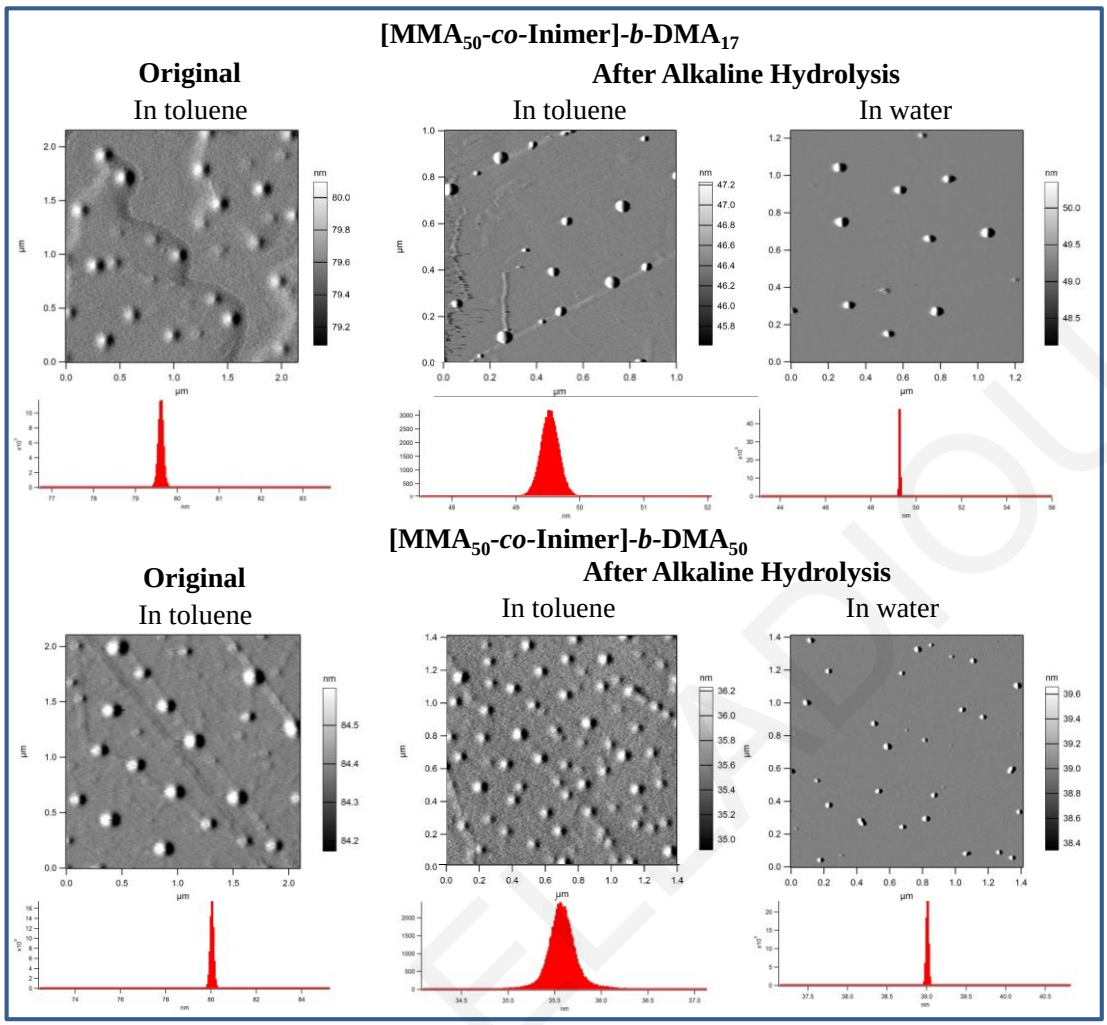

Figure 3.52 AFM images and distributions of the diameters of the spherical micelles formed by the original hyperbranched amphiphilic [MMA-*co*-PyDEBrMA]-*b*-DMAEMA copolymers (first column), and the linear amphiphilic MMA-*b*-DMAEMA diblock copolymers (after treatment of the hyperbranched copolymer under alkaline hydrolysis conditions) in toluene (second column) and in water (third column).

Chapter 4 – Conclusion and Future Work

This Ph.D. Thesis presented a new platform of polymers bearing the pyridinylalkyl ester moiety which was introduced through the monomer repeating unit, the cross-linker residue, the bifunctional initiator residue or the inimer residue. Regarding the introduction through the monomer, nine pyridinylalkyl methacrylate homologues, varying in the spacer length between the ester moiety and the pyridine ring, from methyl to propyl, and / or the position of nitrogen in the pyridine ring, were synthesized and polymerized. These polymer homologues were studied in terms of their stability under thermolysis, as well as to alkaline and acidic hydrolysis conditions, presenting stability under acidic conditions, but partial or complete lability to thermolysis or alkaline hydrolysis conditions, as manifested by the cleavage of the pyridinylalkyl side-group. The three isomeric homopolymers bearing the pyridinylethyl ester side-group were fully cleavable under alkaline hydrolysis conditions, yielding pMAA and the corresponding vinylpyridine through an E2 elimination reaction, while the other six poly(pyridinylalkyl methacrylate) homologues were only partially cleavable to pMAA and the corresponding hydroxyalkylpyridine through a nucleophilic addition/elimination reaction. Furthermore, the homopolymers possessing in the pendant pyridinylethyl esters with nitrogen placed at position 2 or 4 in the pyridine ring were also cleavable at around 200 ºC through a β-scission mechanism, being converted also to pMAA and 2-vinylpyridine or 4-vinylpyridine, respectively, whereas the 3-pyridine substituted ethyl ester polymeric homologue was thermally more stable, presenting only partial cleavage to MAA units and 3-vinylpyridine. In contrast, the other six polymer homologues were thermally more stable than these three previously-mentioned isomeric polymers, with the most thermally stable being poly(3-(pyridin-3-yl)propyl methacrylate) whose cleavage temperature exceeded 350 ºC.

Our study was expanded around poly(2-(pyridin-2-yl)ethyl methacrylate) (p2PyEMA), by preparing and characterizing the thermal and hydrolytic stability of its thioester and amide polymeric analogues. We determined that the thioester polymer analogue was more stable than p2PyEMA, whereas the amide polymer analogue was much more stable, in agreement with the expected stability which should increase with the electronegativities of oxygen, sulfur and nitrogen. The polymer of 2-phenylethyl methacrylate (PhEMA), where the phenyl group replaced pyridine, was also prepared and found to be more stable than p2PyEMA, due to the reduced electron supply to the β-carbon in the case of pPhEMA compared to p2PyEMA. Finally, the polymeric analogues of 2PyEMA with one or two

methyl groups attached onto the *β*-carbon of the ethyl spacer were more an much more stable than p2PyEMA, respectively, as a result of the steric hindrance conveyed by these methyl groups.

Next, the selectivity in the hydrolytic and thermal lability of the 2PyEMA units was examined in the copolymers of 2PyEMA with tetrahydro-2*H*-pyran-2-yl methacrylate (THPMA) or with (pyridin-2-yl)methyl methacrylate (2PyMMA). Being base-labile, the 2PyEMA units in the 2PyEMA-THPMA copolymers could be selectively hydrolyzed under alkaline conditions at room temperature, without affecting the THPMA units which are acid-labile. Conversely, the acid-labile THPMA units in these copolymers were hydrolyzed under acidic conditions at room temperature, with the 2PyEMA units remaining intact. Thus, the mutual orthogonality in the stability of the 2PyEMA and THPMA units was established. Upon the thermal treatment of the 2PyEMA-2PyMMA copolymers at 130 °C for 24 hours, the 2PyEMA units were converted to MAA units, whereas the 2PyMMA units were preserved. Thus, the 2PyEMA units can be selectively thermolyzed in the presence of the homologous 2PyMMA units in the same copolymer.

Finally, extending the finding of the great lability of pyridinylethyl monoesters to pyridinyldiethyl diesters, we prepared three novel, labile molecules: a cross-linker, a bifunctional ATRP initiator, and an ATRP inimer, all based on 2,6-pyridinediethanol. All three of these molecules were used for polymerizations, and the resulting polymers were examined for their stability. As expected, these polymers were labile because the residues of the three 2,6-pyridinediethanol molecules preserved their lability and were, therefore, cleavable under thermolysis or alkaline hydrolysis conditions. Upon cleavage, hyperbranched polymers, linear polymers, and end-linked networks were converted to linear polymers, linear polymers of half the molecular weight than the original, and star polymers, respectively.

The cleavability under (relatively mild) alkaline hydrolysis conditions of the pyridinylethyl monoesters in the side-groups of the monomer repeating units, and of the pyridinyldiethyl diesters in the residues of the cross-linker, the bifunctional initiator, and the inimer is significant, because most such esters are usually acid-cleavable. Of particular significance is the utility of the commercially-available and rather inexpensive 2-pyridineethanol as protective group for (meth)acrylic acid units, and removable under mildly basic conditions at room temperature.

As future work, we could further exploit the lability of both the pyridinylethyl monoester and the pyridinyldiethyl diester for the development of novel initiators and inimers. In particular, 2-pyridineethanol can be used to protect carboxylic acid functionalities on monofunctional initiators for GTP, ATRP and RAFT polymerization. The chemical structures of such compounds are shown on the upper part of Figure 4.1. Furthermore, 2,6-pyridinediethanol may be employed as the central, labile part of degradable bifunctional initiators or degradable inimers, for both RAFT polymerization and GTP. These structure appear in the lower part of Figure 4.1.

Some of the more stable polymers developed here, e.g., the homopolymer of 3PyPMA, may also find applications similar to those where poly(vinylpyridine)s are usually employed, such as for resins for CO_2 adsorption, or for manufacture of isoporous membranes (if in block copolymers) for water purification. Additionally, the 2,6-pyridinediethanol-based cross-linker could be combined with an acid-labile cross linker, and prepare polymers for controlled drug release in stomach where the pH is low (~3), and the intestine where the pH is slightly alkaline (~8).

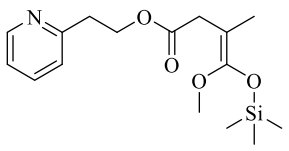

2-(pyridin-2-yl)ethyl (*E*)-4-methoxy-3-methyl-
4-((trimethylsilyl)oxy)but-3-enoate: GTP initiator

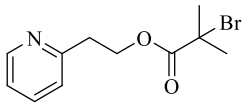

2-(pyridin-2-yl)ethyl 2-bromo-
2-methylpropanoate: ATRP initiator

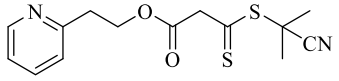

2-(pyridin-2-yl)ethyl 3-((2-cyanopropan-2-yl)thio)-
3-thioxopropanoate: RAFT chain transfer agent

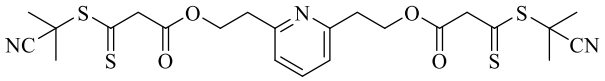

pyridine-2,6-diylbis(ethane-2,1-diyl) bis(3-((2-cyanopropan-2-yl)thio)-
3-thioxopropanoate): RAFT bifunctional chain transfer agent

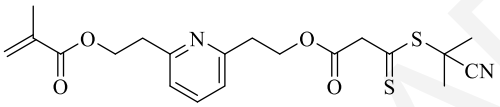

2-(6-(2-((3-((2-cyanopropan-2-yl)thio)-3-thioxopropanoyl)oxy)ethyl)
pyridin-2-yl)ethyl methacrylate: RAFT inimer

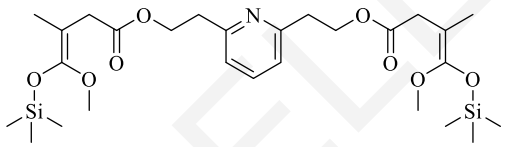

pyridine-2,6-diylbis(ethane-2,1-diyl) (3*E*,3'*E*)-bis(4-methoxy-3-methyl-
4-((trimethylsilyl)oxy)but-3-enoate): GTP bifunctional initiator

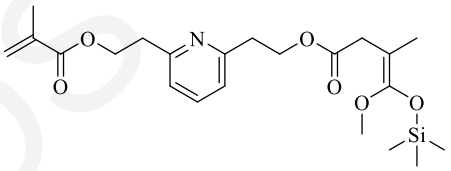

2-(6-(2-(methacryloyloxy)ethyl)pyridin-2-yl)ethyl (*E*)-4-methoxy-
3-methyl-4-((trimethylsilyl)oxy)but-3-enoate: GTP inimer

Figure 4.1 Chemical structures of molecules proposed to be investigated in future work.

Chapter 5 – Literature

1. Krishnamoorthly, S.; Pugin, R.; Brugger, J.; Heinzelmann, H.; Hinderling, C. *Adv. Funct. Mater.* **2006**, *16*, 1469−1475.
2. Cui, L.; Wang, H.; Ding, Y.; Han, Y. *Polymer* **2004**, *45*, 8139−8146.
3. Clarke, C. J.; Eisenberg, A.; La Scala, J.; Rafailovich, M. H.; Sokolov, J.; Li, Z.; Qu, S.; Nguyen, D.; Schwarz, S. A.; Strzhemechny, Y.; Sauer, B. B. *Macromolecules*, **1997**, *30*, 4184−4188.
4. Hahn, J.; Clodt, J. I.; Filiz, V.; Abetz, V. *RSC Adv.* **2014**, *4*, 10252−10260.
5. Murugan, R.; Scriven, E. F. V. "Pyridine: From Lab to Production," Elsevier, Amsterdam, 2013.
6. Anderson, T. *Liebigs Ann.* **1846**, *60*, 86−103.
7. Anderson, T. *Liebigs Ann.* **1851**, *80*, 44−65.
8. Ramsey, W. *Ber.* **1877**, *10*, 736.
9. Hantzsch, A. *Liebigs Ann.* **1882**, *215*, 72.
10. Chichibabin A. E. *Russ. J. Phys. Chem.* **1906**, *37*, 1229.
11. Frank, R. L.; Seven, R. P. *J. Am. Chem. Soc.* **1949**, *71*, 2629−2635.
12. Philips, A. P. *J. Am. Chem. Soc.* **1949**, *71*, 4003−4007.
13. Shimizu, S.; Watanabe, N.; Kataoka, T.; Shoji. T.; Abe, N.; Morishita, S.; Ichimura, H. *Ullmann's Encyclopedia of Industrial Chemistry* **2000**, *30*, 557−589.
14. Nguyen, V. Q.; Turecek, F. *J. Mass Spec.* **1997**, *32*, 55−63.
15. Blackmore, I. J.; Gibson, V. C.; Hitchcock, P. B.; Rees, C. W.; Williams, D. J.; White, A. J. P. *J. Am. Chem. Soc.* **2005**, *127*, 6012−6020.
16. Colabroy, K. L.; Begley, T. P. *J. Am. Chem. Soc.* **2005**, *127*, 840−841.
17. Robinson, D. J.; McMorn, P.; Bethell, D.; Bulman-Page, P. C.; Sly, C.; King, F.; Hancock, F. E.; Hutchings, G. J. *Catal. Lett.* **2001**, *72*, 233−234.
18. Xi, Z.; Liu, B.; Chen, W. *J. Org. Chem.* **2008**, *73*, 3954−3957.
19. Den Hertog, H. J.; Van der Does, L.; Lanheer, C. A. *Recueil* **1962**, *81*, 864−870.
20. Schmitz, F. P.; Hilgers, H.; Gemmel, B. *Macromol. Chem.* **1990**, *191*, 1033 – 1049
21. Kang, N.-G.; Changez, M.; Lee, J,-S. *Macromolecules* **2007**, *40*, 8553 – 8559.
22. Kang, B.-G.; Kang, N.-G.; Lee, J.-S. *Macromolecules* **2010**, *43*, 8400 – 8408.
23. Cui, L.; Lattermann, G. *Macromol. Chem. Phys.* **2002**, *203*, 2432 – 2437.
24. Pozharskii, A. F.; Soldatenkov, A.; Katritzky, A. R. "Heterocycles in Life and Society: An Introduction to Heterocyclic Chemistry, Bbiochemistry, and Applications," Wiley, 2nd edn, Wiltshire, 2011.
25. Joule, J. A.; Mills, K. "Heterocyclic Chemistry," Wiley, 5th edn, Singapore, 2010.
26. Newkome, G. R.; Strekowski, L. "Pyridine-Metal Complexes" John Wiley & Sons, N. York, 1985.
27. Metcalfe, C.; Tthomas, J. A. *Chem. Soc. Rev.* **2003**, *32*, 215−224.
28. Erkkila, K. E.; Odom, D. T.; Barton, J. K. *Chemical Reviews* **1999**, *99*, 2777−2795.
29. Demeunynck, M.; Baily, C.; Wilson, W. D., Eds., *DNA and RNA Binders: From SmallMolecules to Drugs*,Wiley-VCH, Weinheim, Germany, 2003.
30. Gielen, M.; Ttiekink, E. R. T., Eds., *Metallotherapeutic Drugs and Metal-Based Diagnostic Agents: The Use of Metals in Medicine*, JohnWiley & Sons, New York, NY, USA, 2005.
31. Cowan, J. A. *Current Opinion in Chemical Biology* **2001**, *5*, 634−642.
32. Ji, L.-N.; Zou, X.-H.; Liu, J.-G. *Coordination Chemistry Reviews* **2001**, *216*, 513–536.
33. Farrell, N.; Kelland, L. R.; Roberts, J. D.; Van Beusichem, M. *Cancer Research* **1992**, *52*, 5065–5072.

34. Nagababu, P.; Kumar, D. A.; Reddy, K. L.; Kumar, K. A.; Mustafa, M. B.; Shilpa, M.; Satyanarayana, S. *Metal-Based Drugs* Vol. **2008**, Article ID 275084, 8 pages.
35. Ali, K. A.; Abd-Elzaher, M. M.; Mahmoud, K. *Int. J. Med. Chem.* Vol. **2013**, Article ID 256836, 7 pages.
36. Cheng, Y.; Yang, S.; Hsu, C. Chemical Reviews 2009, 109, 5868.
37. Bernède, J. C. *J. of Chilean Chem. Soc.* **2008**, *53*, 149.
38. Jessop, I. A.; Zamora, P. P.; Diaz, F. R.; Valle M. A.; Leiva, A.; Cattin, L.; Makha, M.; Bernède, J. C. *Int. J. of Electroch. Sci.* **2012**, *7*, 9502.
39. Yoshikawa, M.; Ezaki, T.; Sanui, K.; Ogata, N. *J. Appl. Polym. Sci.* **1988**, *35*, 145−154.
40. Saxena,A.; Tripathi, B. P.; Kumar, M.; Shahi, V. K.; *Adv. Colloid Interface Sci.* **2009**, *145*, 1–22.
41. Van Reis, R.; Zydney, A. *Curr. Opin. Biotechnol.* **2001**, *12*, 208–211.
42. Geise, G. M.; Lee, H.-S.; Miller, D. J.; Freeman, B. D.; McGrath, J. E.; Paul, D. R. *J. Polym. Sci., Part B: Polym. Phys.* **2010**, *48*, 1685–1718.
43. Savage, N.; Diallo, M. *J. Nanopart. Res.* **2005**, *7*, 331–342.
44. Van Der Bruggen, B.; Vandecasteele, C.; Van Gestel, T.; Doyen, W.; Leysen, R. *Environ. Prog.* **2003**, *22*, 46–56.
45. Qiu, X.; Yu, H.; Karunakaran, M.; Pradeep, N.; Nunes, S. P.; Peinemann, K.-V. *ACSNano* **2013**, *7*, 768–776.
46. Torres, M. R.; Ramos, A. J.; Soriano, E. *Bioprocess. Eng.* **1998**, *19*, 213−215.
47. Pujar, N. S.; Zydney, A. L. J. *J. Chromatogr.* **1998**, *796*, 229−238.
48. Koehler, J. A.; Ulbricht, M.; Belfort, G. *Langmuir* **1997**, *13*, 4162−4171.
49. Saksena, S.; Zydney. A. L. *J. Membr. Sci.* **1997**, *125*, 93−108.
50. Changez, M.; Kang, N. G.; Lee, C. H.; Lee, J.-S. *Small* **2010**, *6*, 63−68.
51. Liu, R.; Liao, P.; Liu, J.; Feng, P. *Langmuir* **2011**, *27*, 3095−3099.
52. Nunes, S. P.; Behzad, A. R.; Hooghan, B.; Sougrat, R.; Karunakaran, M.; Pradeep, N.; Vainio, U.; Peinemann, K.-V. *ACSNano* **2011**, *5*, 3516–3522.
53. Yang, X.; Moosa, B. A.; Deng, L.; Zhao, L.; Khashab, N. M. *Polym. Chem.* **2011**, *2*, 2543−2547.
54. Yoshikawa, M.; Ogata, H.; Sanui, K.; Ogata, N. *Polym. J.* **1983**, *15*, 609–612.
55. Yoshikawa, M.; Yatsuzuka, Y.; Kohei, S.; Ogata, N. *Macromolecules* **1986**, *19*, 995–998.
56. Xiao, L.; Zhang, H.; Jana, T.; Scanlon, E.; Chen, R.; Choe, E.-W.; Ramanathan, L. S.; Yu, S.; Benicewicz, B. C. *Fuel Cells* **2005**, *5*, 287–295.
57. Shin, W. J.; Basarir, F.; Yoon, T. H.; Lee, J.-S. *Langmuir* **2009**, *25*, 3344−3348.
58. Koh, H. D.; Kang N. G.; Lee, J.-S. *Langmuir* **2007**, *23*, 12817−12820.
59. Kang, N. G.; Kang, B. G.; Koh, H. D.; Changez, M.; Lee, J.-S. *React. Funct. Polym.* **2009**, *69*, 470−479.
60. Arndt, K.-F.; Lechner, M. D. "Architecture of Polymers" Springer, Berlin, 2013.
61. Hult, A.; Johansson, M.; Malmstrom, E. *Adv. Polym. Sci.* **1999**, *143*, 1–34.
62. Yan, D.; Gao, C.; Frey, H.; *Hyperbranched Polymers: Synthesis, Properties and Applications*; J. Wiley and Sons: Hoboken, New Jersey, 2011.
63. Wang, D.; Zhao, T.; Zhu, X.; Yan, D.; Wang, W. *Chem. Soc. Rev.* **2015**, *44*, 4023–4071.
64. Chen, S.; Zhang, X.-Z.; Cheng, S.-X.; Zhuo R.-X.; Gu, Z.-W. *Biomacromolecules* **2008**, *9*, 2578–2585.
65. Van Benthem, R. A. T. M. *Progress in Organic Coatings* **2000**, *40*, 203–214.
66. Mańczyk, K.; Szewczyk, P. *Progress in Organic Coatings* **2002**, *44*, 99–109.
67. Zhang, Y.; Wang, L.; Wada, T.; Sasabe, H. *J. Polym. Sci., Part A: Polym. Chem.* **1996**, *34*, 1359–1363.

68. Zhang, Y.; Wada, T.; Sasabe, H. *Polymer* **1997**, *38*, 2893–2897.
69. Lebib, A.; Natali, M.; Li, S. P.; Cambril, E.; Manin, L.; Chen, Y.; Janssen, H. M.; Sijbesma, R. P. *Microelectron Engng.* **2001**, *57/58*, 411–416.
70. Slark, A. T.; Sherrington, D. C.; Titterton, A.; Martin, I. K. J. *J. Mater. Chem.* **2003**, *13*, 2711 – 2720.
71. Sato, T.; Nakamura, T.; Seno, M.; Hirano, T. *Polymer* **2006**, *47*, 4630 – 4637.
72. Hawker, C. J.; Fréchet, J. M. J.; Grubbs, Dao, J. *J. Am. Chem. Soc.* **1995**, *117*, 10763–10764.
73. Yoon, J. A.; Young, T.; Matyjaszeski, K.; Kowaleski, T. *ACS Appl. Mater & Interfaces* **2010**, *2*, 2475–2480.
74. Weimer, W. M.; Fréchet, J. M. J.; Gitsov, I. *J. Polym. Sci., Part A: Polym. Chem.* **1998**, *36*, 955–970.
75. Muthukrishnan, S.; Mori, H.; Müller, A. H. E. *Macromolecules* **2005**, *38*, 3108–3119.
76. Matyjaszeski, K.; Pyun, J.; Gaynor, S. G. *Macromol. Rapid Commun.* **1998**, *19*, 665–670.
77. Matyjaszewski, K.; Gaynor, S. G. *Macromolecules* **1997**, *30*, 7042–7049.
78. Matyjaszewski, K.; Gaynor, S. G.; Müller, A. H. E. *Macromolecules* **1997**, *30*, 7034–7041.
79. Matyjaszewski, K.; Gaynor, S. G.; Kulfan, A.; Podwika, M. *Macromolecules* **1997**, *30*, 5192–5194.
80. Gaynor, S. G.; Edelman, S.; Matyjaszewski, K. *Macromolecules* **1996**, *29*, 1079–1081.
81. Wickline, S. A.; Wooley, K. L. *Biomacromolecules* **2008**, *9*, 2826–2833.
82. Cheng, C.; Wooley, K. L.; Khoshdel, E. *J. Polym. Sci., Part A: Polym. Chem.* **2005**, *43*, 4754−4770.
83. Tsarevsky, N. V.; Huang, J.; Matyjaszewski, K. *J. Polym. Sci., Part A: Polym. Chem.* **2009**, *47*, 6839−6851.
84. Wang, X.; Graff, R. W.; Shi, Y.; Gao, H. *Polym. Chem.* **2015**, *6*, 6739–6745.
85. Min, K.; Gao, H. *J. Am. Chem. Soc.* **2012**, *134*, 15680–15683.
86. Rikkou-Kalourkoti, M.; Matyjaszewski, K, M.; Patrickios, C. S. *Macromolecules* **2012**, *45*, 1313–1320.
87. Graff, R. W.; Wang, X.; Gao, H. *Macromolecules* **2015**, *48*, 2118–2126.
88. Sun, H.; Kabb, C. P.; Sumerlin, B. S. *Chem. Sci.* **2014**, *5*, 4646–4655.
89. Wang, Z.; He, J.; Tao, Y.; Yang, L.; Jiang, H.; Yang, H. Y. *Macromolecules* **2003**, *36*, 7446−7452.
90. Rimmer, S.; Carter, S. R.; Rutkaite, R.; Haycock, J. W.; Swanson, L. *Soft Matter* **2007**, *3*, 971−973.
91. Rikkou-Kalourkoti, M.; Elladiou, M.; Patrickios, C. S. *J. Polym. Sci., Part A: Polym. Chem.* **2015**, *53*, 1310−1319.
92. Carter, S. R.; England, R. M.; Hunt, B.; Rimmer, S. *Macromol. Biosci.* **2007**, *7*, 975−986.
93. Carter, S.; Hunt, B.; Rimmer, S. *Macromolecules* **2005**, *38*, 4595−4603.
94. Ishizu, K.; Kojima, T.; Ohta, Y.; Shibuya, T. *J. Colloidal and Interface Sci.* **2004**, *272*, 76−81.
95. Tao, Y.; He, J.; Wang, Z.; Pan, J.; Jjiang, H.; Chen, S.; Yang, Y. *Macromolecules* **2001**, *34*, 4742−4748.
96. Niu, A.; Li, C.; Zhao, Y.; He, J.; Yang, Y.; Wu. C. *Macromolecules* **2001**, *34*, 460−464.
97. Fréchet, J. M. J.; Henmi, M.; Gitsov, I.; Aoshima, S.; Leduc, M. R.; Grubbs, R. B. *Science* **1995**, *269*, 1080–1083.
98. Simon, P. F. W.; Müller, A. H. E.; Pakula, T. *Macromolecules* **2001**, *34*, 1677–1684.
99. Simon, P. F. W.; Müller, A. H. E. *Macromolecules* **2001**, *34*, 6206–6213.

100. Simon, P. F. W.; Radke, W.; Müller, A. H. E. *Macromol. Rapid Commun.* **1997**, *18*, 865–873.
101. Allcock, H. R.; Lampe, F. W. "Contemporary Polymer Chemistry" 2nd ed., Prentice Hall: Englewood Cliffs, 1990.
102. Queslel, J. P.; Mark, J. E. *J. Chem. Phys.* **1985**, *82*, 3449–3452.
103. Hild, G. *Prog. Polym. Sci.* **1998**, *23*, 1019–1149.
104. Triftaridou, A. I.; Kafouris, D.; Vamvakaki, M.; Georgiou, T. K.;Krasia, T. C.; Themistou, E.; Hadjiantoniou, N.; Ppatrickios, C. S. *Polym. Bull.* **2007**, *58*, 185–190.
105. Vega, D. A.; Villar, M. A.; Alessandrini, J. L.; Valles, E. M. *Macromolecules* **2001**, *34*, 4591–4596.
106. Rodriquez, E.; Katime, I. *Macromol. Mater. Eng.* **2003**, *288*, 607–612.
107. Weismüller, M.; Buchard, W. *Polymer International* **1997**, *44*, 380–390.
108. Mun, G. A.; Nurkeeva, Z. S.; Khutorvanskiy, V. V.; Sergaziyev, A. D. *Colloid. Polym. Sci.* **2002**, *9*, 280–282.
109. Dan, Y.; Chen, S.; Zhang, Y.; Xiang, F. *J. Polym. Sci., Part B: Polym. Phys.* **2000**, *38*, 1069–1077.
110. Kaczmarek, H.; Szalla, A.; Kaminska, A. *Polymer* **2001**, *42*, 6057–6069.
111. Beyer, P.; Nordmeier, E. *Eur. Polym. J.* **1999**, *35*, 1351–1365.
112. Nurkeeva, Z. S.; Mun, G. A.; Khutoryanskiy, V. V.; Zotov, A. A.; Mangazbaeva, R. A. *Polymer* **2000**, *41*, 7641–7651.
113. Zhumadilova, G. T.; Gazizov, A. D.; Bimendina, L. A.; Kudaibergenov, S. E. *Polymer* **2001**, *42*, 2985–2989.
114. Gazizov, A.D.; Zhumadilova, G. T.; Bimendina, L. A.; Kudaibergenov, S. E. *Polymer* **2000**, *41*, 5793–5797.
115. Porasso, R. D.; Benegas, J. C.; Van den Hoop, M. A. G. T. *J. Phys. Chem. B* **1999**, *103*, 2361–2365.
116. Miyajima, T.; Mori, M.; Ishiguro, S.-I. *J. Colloid. Interf. Sci.* **1997**, *187*, 259–266.
117. Morlay, C.; Cromer, M.; Mouginot, Y.; Vittori, O. *Talanta* **1999**, *48*, 1159–1166.
118. Heitz, C.; Francois, J. *Polymer* **1999**, *40*, 3331–3344.
119. Mori, H.; Müller, A. H. E.; Klee, J. E. *J. Am. Chem. Soc.* **2003**, *125*, 3712–3713.
120. Förster, S.; Antonietti, M. *Adv. Mater.* **1998**, *10*,195–217.
121. Förster, S.; Plantenberg, T. *Angew. Chem. Int. Ed.* **2002**, *41*, 688–714.
122. Liu, T.; Burger, C.; Chu, B. *Prog. Polym. Sci.* **2003**, *28*, 5–26.
123. Mayer, A. B. R. *Polym. Adv. Technol*. **2001**, *12*, 96–106.
124. Discher, D. E.; Eisenberg, A. *Science* **2002**, *297*, 967–973.
125. Rosler, A.; Vandermeulen, G. W. M.; Klok, H.-A. *Adv. Drug. Delivery Rev.* **2001**, *53*, 95–108.
126. Sauer, M.; Meier, W. *Aust. J. Chem.* **2001**, *54*, 149–151.
127. Nakahama, S.; Hirao, A. *Prog. Polym. Sci.* **1990**, *15*, 299–335.
128. Hirao, A.; Nakahama, S. *Acta. Polym.* **1998**, *49*, 133–144.
129. Mykytiuk, J.; Armes, S. P.; Billingham, N. C. *Polym. Bull.* **1992**, *29*, 139–145.
130. Patrickios, C. S.; Hertler, W. R.; Abbott, N. L.; Hatton, T. A. *Macromolecules* **1994**, *27*, 930–937.
131. Lowe, A. B.; Billingham, N. C.; Armes, S. P. *Chem. Commun.* **1997**, 1035–1036.
132. Lowe, A. B.; Billingham, N. C.; Armes, S. P. *Macromolecules* **1998**, *31*, 5991–5998.
133. Bütün, V.; Lowe, A. B.; Billingham, N. C.; Armes, S. P. *J. Am. Chem. Soc.* **1999**, *121*, 4288–4289.
134. Van Camp, W.; Du Prez, F. E.; Bon, S. A. F. *Macromolecules* **2004**, *37*, 6673–6675.

135. Hoogenboom, R.; Schubert, U. S.; Van Camp, W.; Du Prez, F. E. *Macromolecules* **2005**, *38*, 7653–7659.
136. Allen, R. D.; Long, T. E.; McGrath, J. E. *Polym. Bull.* **1986**, *15*, 127–134.
137. Kilian, L.; Wang, Z.-H.; Long, T. E. *J. Polym. Sci., Part A: Polym. Chem.* **2003**, *41*, 3083–3093.
138. Förster, S.; Zisenis, M.; Wenz, E.; Antonietti, M. *J. Chem. Phys.* **1996**, *104*, 9956–9970.
139. Krishnamoorthy, S.; Pugin, R.; Brugger, J.; Heinzelmann, H.; Hinderling, C. *Adv. Funct. Mater.* **2006**, *16*, 1469–1475.
140. Kang, M.; Moon, B. *Macromolecules* **2009**, *42*, 455−458.
141. Zhao, H.; Sterner, E. S.; Coughlin, E. B.; Theato, P. *Macromolecules* **2012**, *45*, 1723−1736.
142. Cline, G. W.; Hanna, S. B. *J. Am. Chem. Soc.* **1987**, *109*, 3087−3091.
143. Zhang, Q.; Schattling, P.; Theato, P.; Hoogenboom, R. *Polym. Chem.* **2012**, *3*, 1418−1426.
144. Eberhardt, M.; Mruk, R.; Zentel, R.; Théato, P. *Eur. Polym. J.* **2005**, *41*, 1569−1575.
145. Nilles, K.; Theato, P. *Eur. Polym. J.* **2007**, *43*, 2901−2912.
146. Eberhardt, M. ; Theato, P. *Macromol. Rapid. Commun.* **2005**, *26*, 1488−1493.
147. Qin, S.-H.; Qiu, K.-Y. *J. Polym. Sci. Part A: Polym. Chem.* **2001**, *39*, 1450–1455.
148. Esker, A. R.; Mengel, C.; Wegner, G. *Science* **1998**, *280*, 892–895.
149. Lai, J. *Macromolecules* **1984**, *17*, 1010–1012.
150. Scott, G. *Degradable Polymers Principles and Applications*; 2nd ed., Springer–Science+Business Media B. V.: Dordrecht, 2002.
151. Gates, B. D.; Xu, Q.; Stewart, M.; Ryan, D.; Willson, C. G.; Whitesides, G. M. *Chem. Rev.* **2005**, *105*, 1171–1196.
152. Reichmanis, E.; Thompson, L.F. *Chem. Rev.* **1989**, *89*, 1273–1289.
153. Guo, Y.; Feng, F.; Miyashita, T. *Macromolecules* **1999**, *32*, 1115–1118.
154. Long, B. K.; Keitz, B. K.; Willson, C. G. *J. Mater. Chem.* **2007**, *17*, 3575–3580.
155. Li. T.; Mitsuishi, M.; Miyashita, T. *Thin Solid Films* **2001**, *389*, 267–271.
156. Siracusa, V.; Rocculi, P.; Romani, S.; Dalla Rosa, M. Trends in Food Science & Technology **2008**, *19*, 634–643.
157. Arvanitoyannis, I. S. *J. Macrom. Sci., Part C: Polymer Reviews* **2007**, 205–271.
158. Davis, G.; Song, J. H. *Industrial Crops and Products* **2006**, *23*, 147–161.
159. Poirier, Y.; Nawrath, C.; Somerville, C. *Nat. Biotechnol.* **1995**, *13*, 142–150.
160. Domb, A. J. *Polymeric Site-Specific Pharmacotherapy*; John Wiley & Sons: Chicester, U.K., 1999.
161. Park, K. Controlled Drug Delivery Challenges and Strategies; American Chemical Society: Washington, DC, 1997.
162. Uhrich, K. E.; Cannizaro, S. M.; Langer, R. S.;Shakesheff, K. M. Chem. Rev. **1999**, *99*, 3181–3198.
163. Soppimath, K. S.; Aminabhavi, T. M.; Kulkarni, A. R.; Rudzinski, W. A. *J. Controlled Release* **2001**, *70*, 1–20.
164. Ulbricht, K.; Subr, V.; Seymour, L. W.; Duncar, R. *J. Controlled Release* **1993**, *24*, 181–190.
165. Brannon-Peppas, L. *Int. J. Pharmaceutics* **1995**, *116*, 1–9.
166. Vert, M. *J. Mater. Sci.: Mater. Med.* **2009**, *20*, 437–446.
167. Martina, M.; Hutmacher, D. W. *Polym. Int.* **2007**, *56*, 145–157.
168. Hoffman, A. S. *Advanced Drug Delivery Reviews* **2002**, *54*, 3–12.
169. Gunatillake, P. A.; Adhikari, R. *Eur. Cells Mater.* **2003**, *5*, 1–16.

170. Zhang, Z.; Kuijer, R.; Bulstra, S. K.; Grijpma, D. K.; Feijen, J. *Biomaterials* **2006**, *27*, 1741–1748.
171. Kim, J.;Lee, K. WW.q;Hefferan, T. E.; Currier, B. L.; Yaszemski, M. J.; Lu, L. *Biomacromolecules* **2008**, *9*, 149–157.
172. Fang, E.; Sherman, O. *J. Arthrosc. Relat. Surg.* **2004**, *20*, 273–286.
173. Martens, P. J.; Bryant, S. J.; Anseth, K. S. *Biomacromolecules* **2003**, *4*, 283–292.
174. Levy, G.; Nichols, M. A.; Miller, T. W. *ACS Symp. Ser.* **1993**, *520*, 202–212.
175. Brannon-Peppas, L. *ACS Symp. Ser.* **1993**, *520*, 42–52.
176. Chandra, R.; Rustgi, R. *Prog. Polym. Sci.* **1998**, *26*, 1273–1335.
177. Eglin, D.; Alini, M. *Eur. Cells Mater.* **2008**, *16*, 80–91.
178. Middleton, J. C.; Tipton, A. J. *Biomaterials* **2000**, *21*, 2335–2346.
179. Barrows, T. H. *Clin. Mater.* **1986**, *1*, 233–257.
180. Jain, J. P.; Modi, S.; Domb, A. J.; Kumar, N. *J. Controlled Release* **2005**, *103*, 541–563.
181. Ikada, Y.; Tsuji, H. *Macromol. Rapid Commun.* **2000**, *21*, 117–132.
182. Themistou, E.; Patrickios, C. S. *Macromolecules* **2006**, *39*, 73–80.
183. Themistou, E.; Patrickios, C. S. *Macromolecules* **2007**, *40*, 5231–5234.
184. Themistou, E.; Patrickios, C. S. *Macromol. Chem. Phys.* **2008**, *209*, 1021–1028.
185. Themistou, E.; Patrickios, C. S. *J. Polym. Sci., Part A: Polym. Chem.* **2009**, *75*, 5853–5870.
186. Murthy, N.; Thang, Y. X.; Schunk, S.; Xu, M. C.; Fréchet, J. M. *J. Am. Chem. Soc.* **2002**, *124*, 12398–12399.
187. Murthy, M.; Xu, M.; Schuck, S.; Kunisawa, J.; Shastri, N.; Fréchet, J. M. J. *Proc. Natl. Acad. Sci. USA* **2003**, *100*, 4995–5000.
188. Standley, S. M.; Kwon, Y. J.; Murthy, N.; Kunisawa, J.; Shastri, N.; Guillaudeu, S. J.; Lau, L.; Fréchet, J. M. J. *Bioconjugate Chem.* **2004**, *15*, 1281–1288.
189. Kwon, Y. J.; Standley, S. M.; Goh, S. L.; Fréchet, J. M. J. *J. Controlled Release* **2005**, *105*, 199–212.
190. Chan, Y.; Bulmus, V.; Zareie, M. H.; Byrne, F. L.; Barner, L.; Kavallaris, M. *J. Controlled Release* **2006**, *115*, 197–207.
191. Bulmus, V.; Chan, Y.; Nguyen, Q.; Tran, H. L. *Macromol. Biosci.* **2007**, *7*, 446–455.
192. Chan, Y.; Wong, T.; Byrne, F.; Kavallaris, M.; Bulmus, V. *Biomacromolecules* **2008**, *9*, 1826–1836.
193. Knorr, V.; Russ, V.; Allmendinger, L.; Ogris, M.; Wagner, E. *Bioconjugate Chem.* **2008**, *19*, 1625–1634.
194. Jain, R.; Standley, S. M.; Fréchet, J. M. J. *Macromolecules* **2007**, *40*, 452–457.
195. Kaihara, S.; Matsumura, S.; Fisher, J. P. *Macromolecules* **2007**, *40*, 7625–7632.
196. Shi, Y.; Fu, Z. F.; Sui, X. C. *Chin. Chem. Lett.* **2011**, *22*, 374–377.
197. Ruckenstein, E.; Zhang, H. *Macromolecules* **1999**, *32*, 3979–3983.
198. Heyden, K; Babooram, K.; Ahmed, M.; Narain, R. *Eur. Polym. J.* **2009**, *45*, 1689–1697.
199. Kwon, Y. J.; Standley, S. M.; Goodwin, A. P.; Gillies, E. R.; Fréchet, J. M. J. *Mol. Pharm.* **2004**, *2*, 83–91.
200. Shi, L.; Berkland, C. *Adv. Mater.* **2006**, *18*, 2315–2319.
201. Shi, L.; Berkland, C. *Macromolecules* **2007**, *40*, 4635–4643.
202. Shi, L.; Khondee, S.; Linz, T. H.; Berkland, C. *Macromolecules* **2008**, *41*, 6546–6554.
203. Heath, W. H.; Palmieri, F.; Adams, J. R.; Long, B. K.; Chute, J.; Holcombe, T. W., Zieren, S.; Truit, M. J.; White, J. L.; Willson, C. G. *Macromolecules* **2008**, *41*, 719–726.

204. Bhuchar, N.; Sunasee, R.; Ishihara, K.; Yhundat, T,; Narain, R. *Bioconjugate Chem.* **2012**, *23*, 75–83.
205. Hu, X.; Yang, T.; Gu, R.; Cui, Y.; Yuan, C.; Ge, H.; Wu, W.; Li, W.; Chen, Y. *J. Mater. Chem. C* **2014**, *2*, 1836–1843.
206. Themistou, E.; Patrickios, C. S. *Macromolecules* **2004**, *37*, 6734–6748.
207. Parrott, M. C.; Luft, J. C.; Byrne, J. D. Fain, J. H.; Napier, M. E.; DeSimone, J. M. *J. Am. Chem. Soc.* **2010**, *132*, 17928–17932.
208. Montague, M. F.; Hawker, C. J. *Chem.Mater.* **2007**, *19*, 526–534.
209. Mather, B. D. Williams, S. R.; Long, T. E. *Macromol. Chem. Phys.* **2007**, *208*, 1949–1955.
210. Kafouris, D.; Themistou, E.; Patrickios, C. S. *Chem. Mater.* **2005**, *18*, 85–93.
211. Ogino, K.; Chen, J.; Ober, C. K. *Chem, Mater.* **1998**, *10*, 3833–3838.
212. Kilian, L.; Yamauchi, K.; Sinani, V. A.; Hudelson, C. L.; Long, T. E. *J. Polym. Prep.* **2002**, *124*, 916–917.
213. Metz, N.; Theato, P. *Macromolecules* **2009**, *42*, 37–39.
214. Nicolaÿ, R,; Kamada, J.; Van Wassen, A.; Matyjaszewski, K. *Macromolecules* **2010**, *43*, 4355–4361.
215. Fenoli, C. R.; Wydra, J. W.; Bowman, C. N. *Macromolecules* **2014**, *47*, 907–915.
216. Van Dijk-Wolthuis, W. N. E.; Tsang, S. K. Y.; Kettenes Van den Bosch, J. J.; Hennink, W. E. *Polymer* **1997**, *38*, 6235–6242.
217. Bruining, M. J.; Blaauwgeers, H. G. T.; Kuijer, R.; Pels, E.; Nuijts, R. M. M. A.; Koole, L. H. *Biomaterials* **2000**, *21*, 595–604.
218. Gallagher, J. J.; Hillmyer, M. A.; Reineke, T. M. *Macromolecules* **2014**, *47*, 498–505.
219. Themistou, E.; Kanari, A.; Patrickios, C. S. *J. Polym. Sci., Part A: Polym. Chem.* **2007**, *45*, 5811–5823.
220. Burkoth, A. M.; Anseth, K. S. *Macromolecules* **1999**, *32*, 1438–1444.
221. Metters, A. T.; Anseth, K. S.; Bowman, C. N. *Polymer* **2000**, *41*, 3993–4004.
222. Eichenbaum, K. D.; Thomas, A. A.; Eichenbaum, G. M.; Gibney, B. R.; Needham, D.; Kiser, P. F. *Macromolecules* **2005**, *38*, 10757–10762.
223. Timmer, M. D.; Horch, R. A.; Ambrose, C. G.; Mikos, A. G. *J. Biomater. Sci. Polym. Ed* **2003**, *14*, 369–382.
224. Rikkou, M. D.; Patrickios, C. S. *Prog. Polym. Sci.* **2011**, *36*, 1079–1097.
225. Wang, J. S.; Matyjaszewski, K. *J. Am. Chem. Soc.* **1995**, *117*, 5614–5615.
226. Matyjaszewski, K.; Xia, J. *Chem. Rev.* **2001**,*101*, 2921–2990.
227. Kato, M.; Kamigaito, M.; Sawamoto, M.; Higashimura, T. *Macromolecules* **1995**, *28*,1721–1723.
228. Kamigaito, M.; Ando, T.; Sawamoto, M. *Chem. Rev.* **2001**, *101*,3689–3746.
229. Hawker, C.J.; Bosman, A.W.; Harth, E. *Chem. Rev.* **2001**, *101*, 3661–3688.
230. Chiefari, J.; Chong, Y. K.; Ercole, F.; Krstina, J.; Jeffery, J.; Le, T. P. T.; Mayadynne, R. T. A.; Meijs, G. F.; Moad, C. L.; Moad, G.; Rizzardo, E.; Thang, S. H. *Macromolecules* **1998**, *31*, 5559–5562.
231. Moad, G. *Aust. J. Chem.* **2006**, *59*, 661–662.
232. Moad, G.; Rizzardo, E.; Thang, S. H. *Aust. J. Chem.* **2006**, *59*, 669–692.
233. Moad, G.; Rizzardo, E.; Thang, S. H. *Polymer* **2008**, *49*, 1079–1131.
234. Webster, O. W.; Hertler, W. R.; Sogah, D. Y.; Farnham, W. B.; RajanBabu, T. V. *J. Am. Chem. Soc.* **1983**, *105*, 5706–5708.
235. Sogah, D. Y.; Hertler, W. R.; Webster, O. W.; Cohen, G. M. *Macromolecules* **1987**, *20*,1473–1488.
236. Webster, O. W. J. Polym. Sci. Part A: Polym. Chem. **2000**, *38*, 2855–2860.
237. Webster, O. W. Adv. Polym. Sci. **2004**, *167*, 1–34.

238. Raynaud, J.; Ciolino, J.; Baceiredo, A.; Destarac, M.; Bonnette, F.; Kato, T.; Gnanou, Y.; Taton, D. *Angew. Chem. Int. Ed.* **2008**, *47*, 5390–5393.
239. Raynaud, J.; Gnanou, Y.; Taton, D. *Macromolecules* **2009**, *42*, 5996–6005.
240. Dechy-Cabaret, O.; Martin-Vaca, B.; Bourissou, D. *Chem. Rev.* **2004**, *104*, 6147–6176.
241. Kamber, N. E.; Jeong, W.; Waymouth, R. M.; Pratt, R. C.; Lohmeijer, B. G. G.; Hedrick, J. L. *Chem. Rev.* **2007**, *107*, 5813–5840.
242. He, T.; Adams, D. J.; Butler, M. F.; Cooper, A. I.; Rannard, S. P. *J. Am. Chem. Soc.* **2009**, *131*, 1495 – 1501.
243. Li, C.; Madsen, J.; Armes, S. P.; Lewis, A. L. *Angew. Chem. Int. Ed.* **2006**, *45*, 3510 – 3513.
244. Madsen, J.; Armes, S. P.; Bertal, K.; Lomas, H.; MacNeil, S.; Lewis, A. L. *Biomacromolecules* **2008**, *9*, 2265 – 2275.
245. Tsarevsky, N. V.; Matyjaszewski, K. *Macromolecules* **2002**, *35*, 9009 – 9014.
246. Tsarevsky, N. V.; Matyjaszewski, K. *Macromolecules* **2005**, *38*, 3087 – 3092.
247. Yoshimoto, K.; Hhirase, T.; Madsen, J.; Armes, S. P.; Nagasaki, Y. *Macromol. Rapid Commun.* **2009**, *30*, 2136 – 2140.
248. Rikkou, M. D.; Loizou, E.; Porcar, L.; Matyjaszewski, K.; Patrickios, C. S. *Polym. Chem.* **2012**, *3*, 105 – 116.
249. Rikkou, M. D.; Patrickios, C. S. *Macromolecules* **2008**, *41*, 5957 – 5961.
250. Rikkou, M. D.; Loizou, E.; Porcar, L.; Butler, P.; Patrickios, C. S. *Macromolecules* **2009**, *42*, 9412 – 9421.
251. Gallucci, R. R.; Going, R. C. *J. Org. Chem.* **1982**, *47*, 3517 – 3521.
252. Rikkou, M. D.; Patrickios, C. S. *Macromolecules* **2012**, *45*, 7890 – 7899.
253. Johnson, J. A.; Lewis, D. R.; Díaz, D. D.; Finn, M. G.; Koberstein, J. T.; Turro, N. J. *J. Am. Che. Soc.* **2006**, *128*, 6564 – 6565.
254. Syrett, A. A.; Becer, C. R.; Haddleton, D. M. *Polym. Chem.* **2010**, *1*, 978 – 987.
255. Johnson, J. A.; Baskin, J. M.; Bertozzi, C. R.; Koberstein, J. T.; Turro, N. J. *Chem. Commun.* **2008**, 3064 – 3066.
256. Johnson, J. A.; Finn, M. G.;Koberstein, J. T.; Turro, N. J. *Macromolecules* **2007**, *40*, 3589 – 3598.
257. Ge, Z.; Chen, D.; Zhang, J.; Rao, J.; Yin, J.; Wang, D.; Wan, X.; Shi, W.; Liu, S. *J. Polym. Sci.: Part A Polym. Chem.* **2007**, *45*, 1432 – 1445.
258. Li, C.; He, J.; Li, J.; Cao, J.; Yang, Y. *Macromolecules* **1999**, *32*, 7012−7014.
259. Raynaud, J.; Liu, N.; Gnanou, Y.; Taton, D. *Macromolecules* **2010**, *43*, 8853−8861.
260. Mayadunne, R. T. A.; Rizzardo, E.; Chiefari, J.; Chong, K. Y.; Moad, G.; Thang, S. H. *Macromolecules* **1999**, *32*, 6977−6980.
261. Luo, Y.; Cui, X. *J. Polym. Sci., Part A: Polym. Chem.* **2006**, *44*, 2837−2847.
262. Patten, E. T.; Matyjaszewski, K. *Adv. Mater.* **1998**, *10*, 901–915.
263. Skoog, D. A.; Holler, J. F.; Crouch, S. R. "Principles of Instrumental Analysis" 6th Ed., Brooks/Cole, Cengage Learning, 2013.
264. McMurry, J. "Oorganic Chemistry" 6th Ed., Brooks/Cole, Cengage Learning, 2008.
265. Gill, P.; Moghadam, T. T.; Ranjbar, B. *J. Biomol. Tech.* **2010**, *21*, 167−193.
266. Höhne, G.; Hemminger, W. F.; Flammersheim, H.-J. Differential Scanning Calorimetry; 2nd ed., Springer-Verlag Bberlin Heidberg, 2003.
267. Gabbott, P. "Principles and Applications of Thermal Analysis" Wiley-Blackwell, Oxford, 2008.
268. http://www.tainstruments.com/
269. Schmitz, K. C. "An Introduction to Dynamic Light Scattering by Macromolecules" Academic Press, Boston, 1990.

270. Berne, B.; Pecora, R. "Dynamic Light Scattering with Applications to Chemistry, Biology and Physics" Wiley, New Work, 1976.
271. Uversky, V. N.; Longhi, S. "Dynamic and Static Light Scattering" Wiley, New Work, 2010.
272. Binning, G.; Quate, C.; Gerber. C. *Phys. Rev. Lett.* **1986**, *56*, 930.
273. Schönherr, H.; Vancso, G. J. "*Scanning Force Microscopy of Polymers*" Springer, Heidelberg, 2010.
274. Sitterberg, J.; Ozcetin, A.; Ehrhardt, C.; Bakowsky, U. *Eur. J. Pharm. Biopharm.* **2010**, *74*, 2−13.
275. Elladiou, M.; Patrickios, C. S. *Polym. Chem.* **2012**, *3*, 3228−3231.
276. Mori, H.; Müller, A. H. E. *Prog. Polym. Sci.* **2003**, *28*, 1403−1439.
277. Elladiou, M.; Patrickios, C. S. *Macromolecues* **2015**, *48*, 7503−7512.
278. Pafiti, K. S.; Elladiou, M.; Patrickios, C. S. *Macromolecules* **2014**, *47*, 1819−1827.
279. Elladiou, M.; Patrickios, C. S. *Chem. Commun.* **2016**, *52*, 3135−3138.
280. Elladiou, M.; Kalogirou A. S.; Patrickios, C. S. Submitted for publication in *Polym. Sci. Part A: Polym. Chem.* February 2017.
281. Elladiou, M.; Patrickios, C. S. A Degradable ATRP Inimer Cleavable Under Thermolysis or Alkaline Hydrolysis Conditions: Synthesis, Polymerization and Cleavage, Unpublished Results.
282. Dicker, B.; Cohen, G. M.; Farnham, W. B.; Hhertler, W. R.; Laganis, E. D.; Sogah, D. Y. *Macromolecules* **1990**, *23*, 4034−4041.
283. Nicolas, J.; San Miguel, V.; Mantovani, G.; Haddleton, D. M. *Chem. Commun.* **2006**, 4697−4699.
284. Lowen, G. T.; Almond, M. R.; Rideout, J. L. *J. Heterocyclic Chem.* **1992**, *29*, 1663−1665.
285. Barnden, R. L.; Evans, R. M.; Hamlet, J. C.; Hems, B. A.; Jansen, A. B. A.; Trevett, M. E.; Webb, G. B. *J. Chem. Soc.* **1953**, 3733−3739.
286. Vaganova, E.; Wachtel, E.; Leitus, G.; Danovich, D.; Lesnichin, S.; Shenderovich, I. G.; Limbach, H.-H.; Yitzhaik, S. *J. Phys. Chem.* **2010**, *114*, 10728–10733.
287. Tsutsuminai, S.; Kanno, K.; Tachikura, M. United States Pub. No.: US 2012/0010434 A1.
288. Friedrich, S.; Schubarta, M.; Gade, L. H.; Scowen, I. J.; Edwards, A. J.; McPartlinb, M. *Chem. Ber./Recueil* **1997**, *130*, 1751 – 1759.
289. Fraenkel, G.; Cooper, J. W. *J. Am. Chem. Soc.* **1971**, *93*, 7228 – 7238.
290. Pasquinet, E.; Rocca, P.; Marsais, F.; Godard, A.; Quéguiner, G. *Tetrahedron* **1998**, *54*, 8771 – 8782.
291. Kearns, J. E.; McLean, C. D.; Solomon, D. H. J. Macromol. Sci.: Part A Chem. 1974, 673 – 685.
292. Kelly, W. S. J.; Ford, G. H.; Nelson, S. M. *J. Chem. Soc. A* **1971**, 388–396.
293. Löffler, K.; Thiel, L. *Chem. Berichte* **1909**, *42*, 132–140.
294. Furukawa, N.; Iida, K.; Kkawai, T.; Ogawa, S.; Oae, S. Phosphorous and Sulfur **1984**, *19*, 239–253.
295. Rayer, A.; Sumon, K. Z.; Jaffari, L.; Henni, A. *J. Chem. Eng. Data* **2014**, *59*, 3805–3813.
296. Fraser, R. R.; Mansour, T. S.; Savard, S. *J. Org. Chem.* **1985**, *50*, 3232–3234.
297. Alunni, S.; Ottavi, L. *J. Org. Chem.* **2004**, *69*, 2272–2283.
298. Taylor, R. J. *Chem. Soc., Perkin Trans. II*, **1979**, 1730–1737
299. Norfolk, S. B.; Taylor, R. *J. Chem. Soc. Perkin II **1976***, 280–285.
300. Taylor, R.; Thorne, M. P. *J. Chem. Soc. Perkin II* **1976**, 799–802.
301. Amin, H. B.; Taylor, R.; Thorne, M. P. *J. Chem. Soc. Perkin II* **1978**, 1090–1095.
302. Taylor, R. J. Chem. Soc. **1962**, 4881–4888.

303. Güven, A. *Int. J. Mol. Sci.* **2005**, *6*, 257 – 275.
304. Li, W.; Li, J.; Lin, M.; Wacharasindhu, S.; Tabei, K.; Mansour, T. S. *J. Org. Chem.* **2008**, *72*, 6016–6021.
305. Katritzky, A.; Khan, G. R.; Schwarz, O. A. *Tetrahedron Letters* **1984**, *25*, 1223–1226.
306. Lund, B. W.; Knapp, A. E.; Piu, F.; Gauthier, N. K.; Begtrup, M.; Hacksell, U.; Olsson, R. *J. Med. Chem.* **2009**, *52*, 1540–1545.
307. Meth-Cohn, O.; Yu, C.-Y. *Tetrahedron Lett.* **1999**, *40*, 6665–6668.
308. Kessler, H.; Becker, G.; Kogler, H.; Friese, J.; Kerssebaum, R. *Int. J. Peptide Protein Res.* **1986**, *28*, 342–346.
309. Kessler, H.; Becker, G.; Kogler, H.; Wolff, M. *Tetrahedron Lett.* **1984**, *25*, 3971–3974.
310. Kunz, H.; Birnbach, S. *Tetrahedron Lett.* **1984**, *25*, 3567–3570.
311. Matsumoto, A.; Enomoto, T.; Aota, H. *Sci. Technol. Rep. Kansai University* No. 54, **2012**, 171–181.
312. Georgiou, T. K.; Patrickios, C. S. *Biomacromolecules* **2008**, *9*, 574-582.
313. Pafiti, K. S.; Philippou, Z.; Loizou, E.; Porcar, L.; Patrickios, C. S. *Macromolecules* **2011**, *44*, 5352-5362.
314. Pafiti, K. S.; Loizou, E.; Patrickios, C. S.; Porcar, L. *Macromolecules* **2010**, *43*, 5195-5204.
315. Achilleos, M.; Legge, T. M.; Perrier, S.; Patrickios, C. S. *J. Polym. Sci., Part A: Polym. Chem.* **2008**, *46*, 7556-7565.
316. Achilleos, M.; Krasia-Christoforou, T.; Patrickios, C. S. *Macromolecules* **2007**, *40*, 5575-5581.
317. Krasia, T. C.; Patrickios, C. S. *Macromolecules* **2006**, *39*, 2467-2473.
318. Kudaibergenov, S. E.; Nuraje, N.; Khutoryanskiy, V. V. *Soft Matter* **2012**, *8*, 9302–9321.
319. Demosthenous, E.; Hadjiyannakou, S. C.; Vamvakaki, M.; Patrickios, C. S. *Macromolecules* **2002**, *35*, 2252-2260.
320. Patrickios, C. S. *J. Colloid Interface Sci.* **1995**, *175*, 256-260.
321. Patrickios, C. S.; Yamasaki, E. N. *Anal. Biochem.* **1995**, *231*, 82-91.
322. Kashiwagi, T.; Inaba, A.; Brown, J. E.; Hatada, K.; Kitayama, T.; Masuda, E. *Macromolecules* **1986**, *19*, 2160-2168.

Publications

1. Elladiou, M.; Patrickios, C. S. "2-(Pyridin-2-yl)ethanol as a Protecting Group for Carboxylic Acids: Chemical and Thermal Cleavage, and Conversion of Poly[2-(pyridin-2-yl)ethyl Methacrylate] to Poly(methacrylic Acid)." *Polym. Chem.* **2012**, *3*, 3228−3231.

2. Pafiti, K. S.; Elladiou, M.; Patrickios, C. S. "Inverse Polyampholyte" Hydrogels from Double-cationic Hydrogels: Synthesis by RAFT Polymerization and Characterization." *Macromolecules* **2014**, *47*, 1819−1827.

3. Rikkou-Kalourkoti, M.; Elladiou, M.; Patrickios, C. S. "Synthesis and Characterization of Hyperbranched Amphiphilic Block Copolymers Prepared via Self-condensing RAFT Polymerization." *J. Polym. Sci., Part A: Polym. Chem.* **2015**, *53*, 1310−1319.

4. Elladiou, M.; Patrickios, C. S. "ABC Triblock Terpolymers with Orthogonally Deprotectable Blocks: Synthesis, Characterization, and Deprotection." *Macromolecules* **2015**, *48*, 7503−7512.

5. Constantinou, A. P.; Elladiou, M.; Patrickios, C. S. "Regular and Inverse Polyampholyte Hydrogels: A Detailed Comparison." *Macromolecules* **2016**, *49*, 3869−3880.

6. Elladiou, M.; Patrickios, C. S. "A Dimethacrylate Cross-linker Cleavable Under Thermolysis or Alkaline Hydrolysis Conditions: Synthesis, Polymerization, and Degradation." *Chem. Commun.* **2016**, *52*, 3135−3138.

7. Elladiou, M.; Kalogirou A. S.; Patrickios, C. S. "Symmetrical Polymer Systems Prepared Using a Degradable Bifunctional ATRP Initiator: Synthesis, Polymerization, and Degradation." Under revision in *The Journal of Polymer Science Part A: Polymer Chemistry.* February 2017.

8. Elladiou, M.; Patrickios, C. S. "A Degradable ATRP Inimer Cleavable Under Thermolysis or Alkaline Hydrolysis Conditions: Synthesis, Polymerization and Cleavage." In preparation for submission in *Macromolecular Rapid Communications*.

9. Elladiou, M.; Patrickios, C. S. "Poly(Pyridinylalkyl Methacrylates): A Class of Addition Polymers With Rich Chemical Properties." In preparation for submission in *Chemical Science.*

Appendix

Thermal Stability of the Poly(Pyridinylalkyl Methacrylate) Homologues. The DSC and TGA thermograms for the poly(pyridinylalkyl methacrylate) homologues are presented in Figures 1 and 2, respectively.

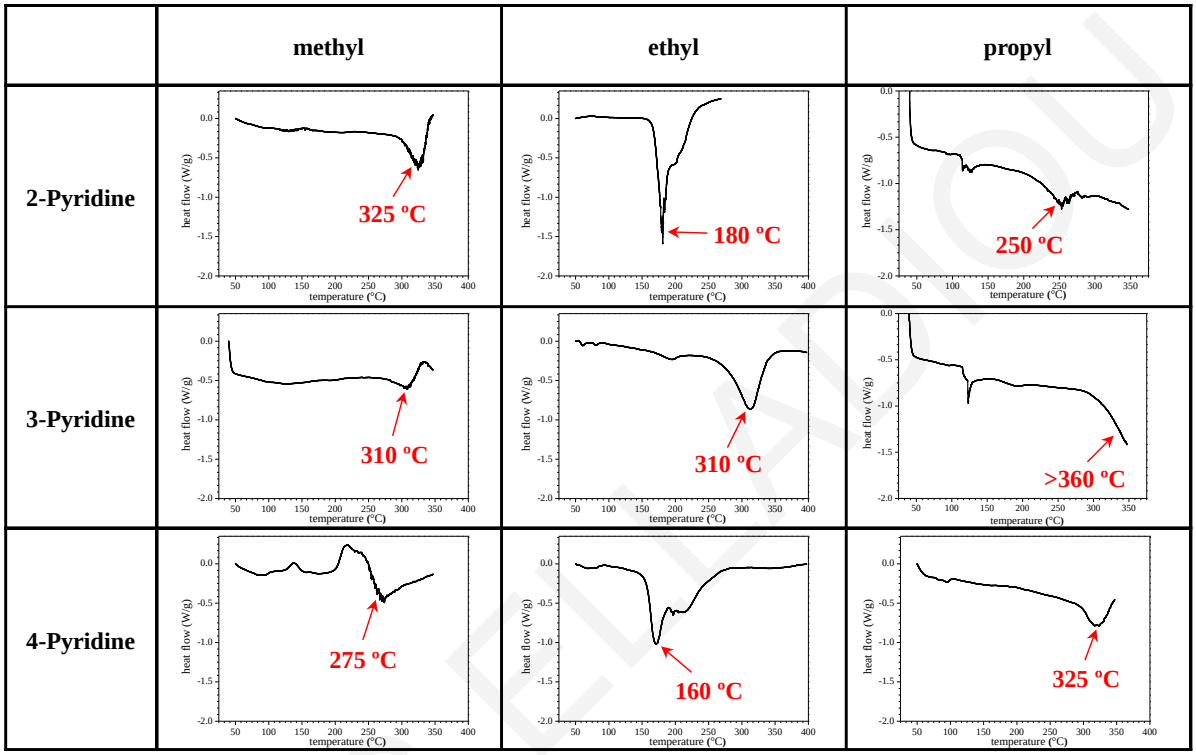

Figure 1. DSC thermograms for the poly(pyridinylalkyl methacrylate) homologues.

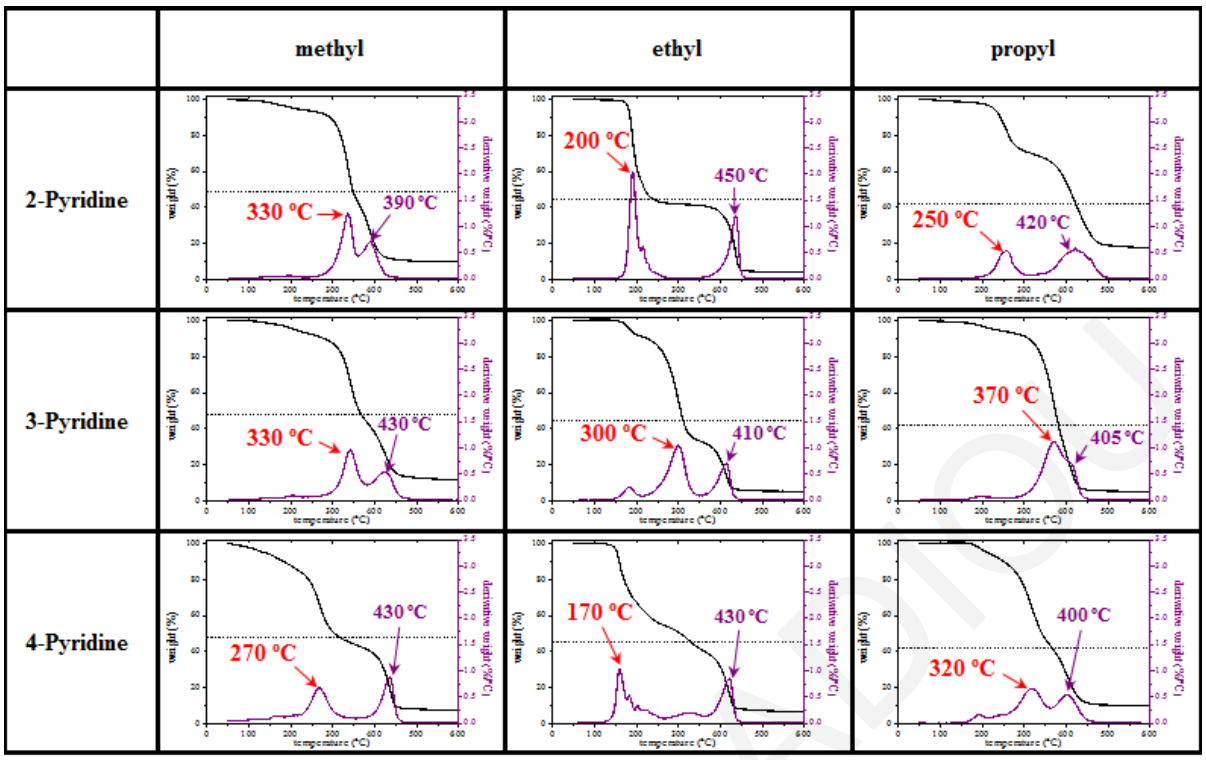

Figure 2. TGA thermograms for the poly(pyridinylalkyl methacrylate) homologues.

Thermal Stability of the Related Homopolymers. The DSC and TGA thermograms for the related homopolymers are presented in Figure 3-5.

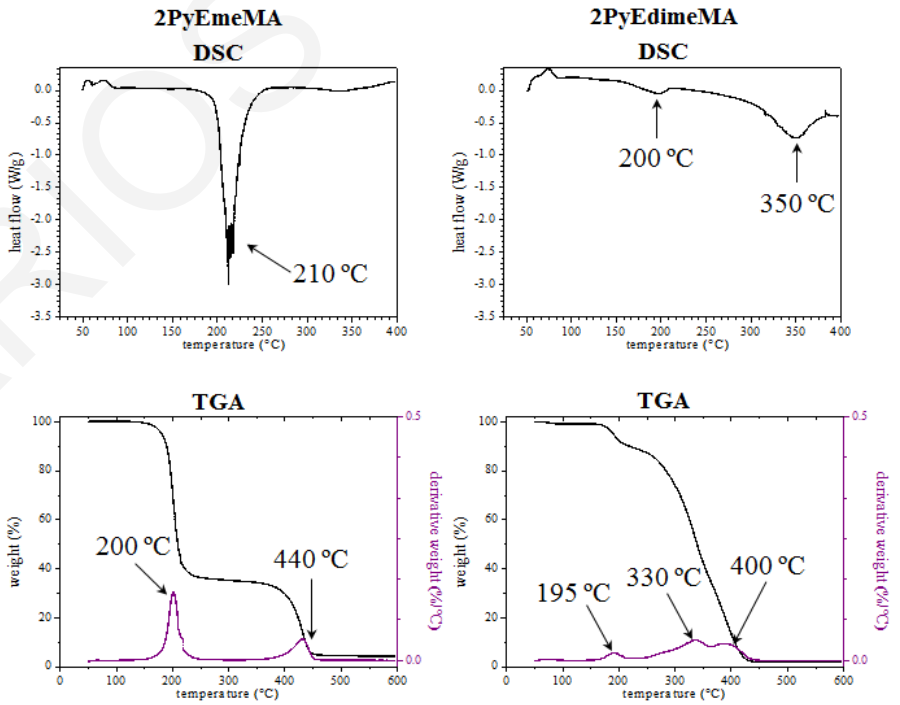

Figure 3. DSC and TGA thermograms for the 2PyEmeMA and 2PyEdimeMA.

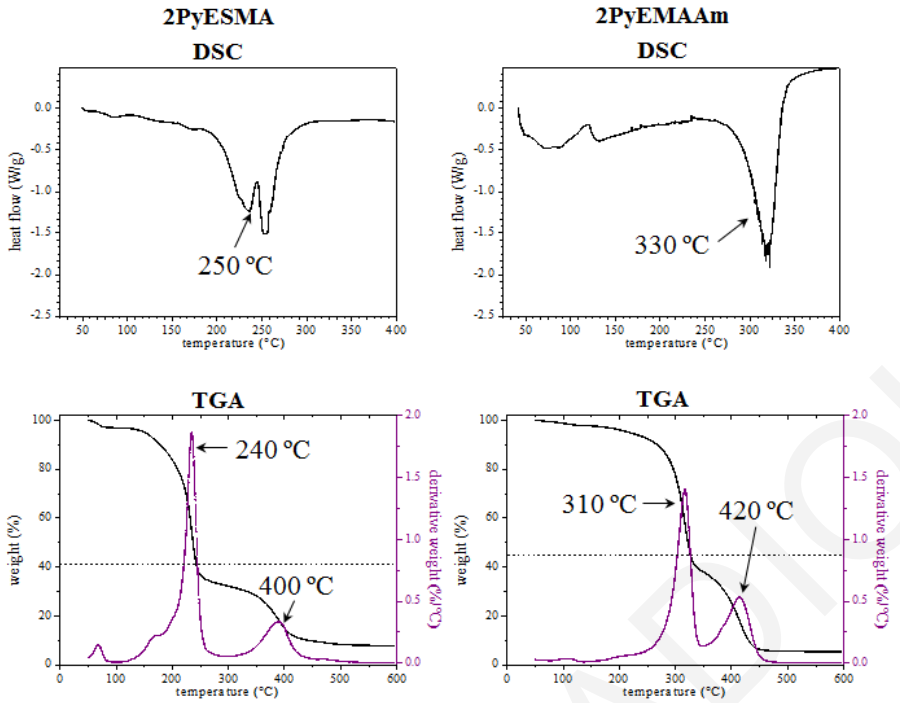

Figure 4. DSC and TGA thermograms for the 2PyESMA and 2PyEMAAm.

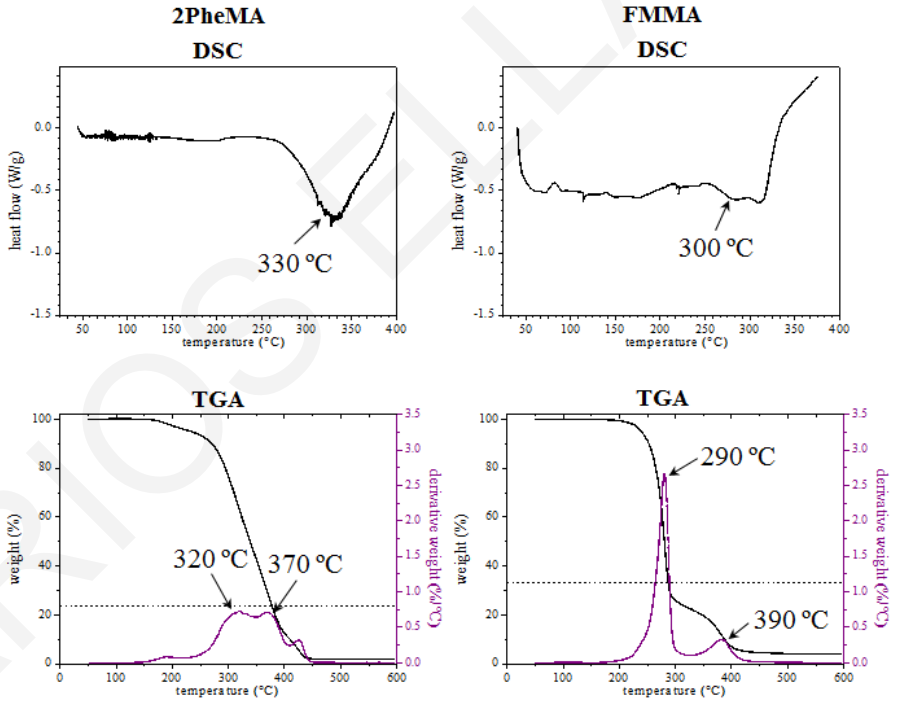

Figure 5. DSC and TGA thermograms for the 2PheMA and FMMA.

Alkaline Hydrolysis of Poly(Pyridinylalkyl Methacrylate) Homologues. The ^{1}H NMR spectra of the polymeric homologues obtained after subjecting them to alkaline hydrolysis conditions are presented in Figure 6.

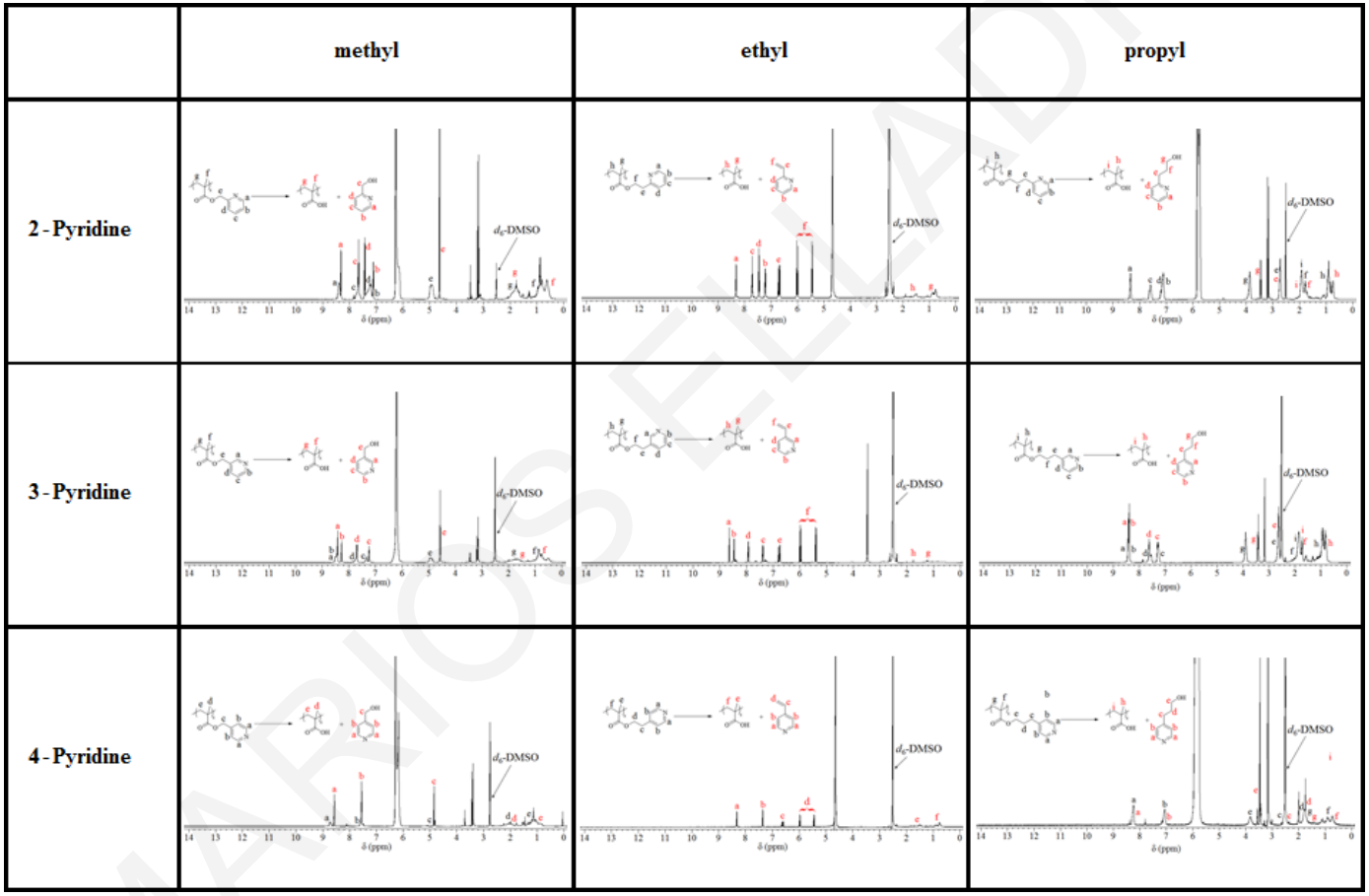

Figure 6. ^{1}H NMR spectra in d_6-DMSO of the nine pyridinylalkyl methacrylates after alkaline hydrolysis using NaOD in d_6-DMSO.

Acidic Hydrolysis of Poly(Pyridinylalkyl Methacrylate) Homologues. The ^{1}H NMR spectra of the polymeric homologues obtained after subjecting them to acidic hydrolysis conditions are presented in Figure 7.

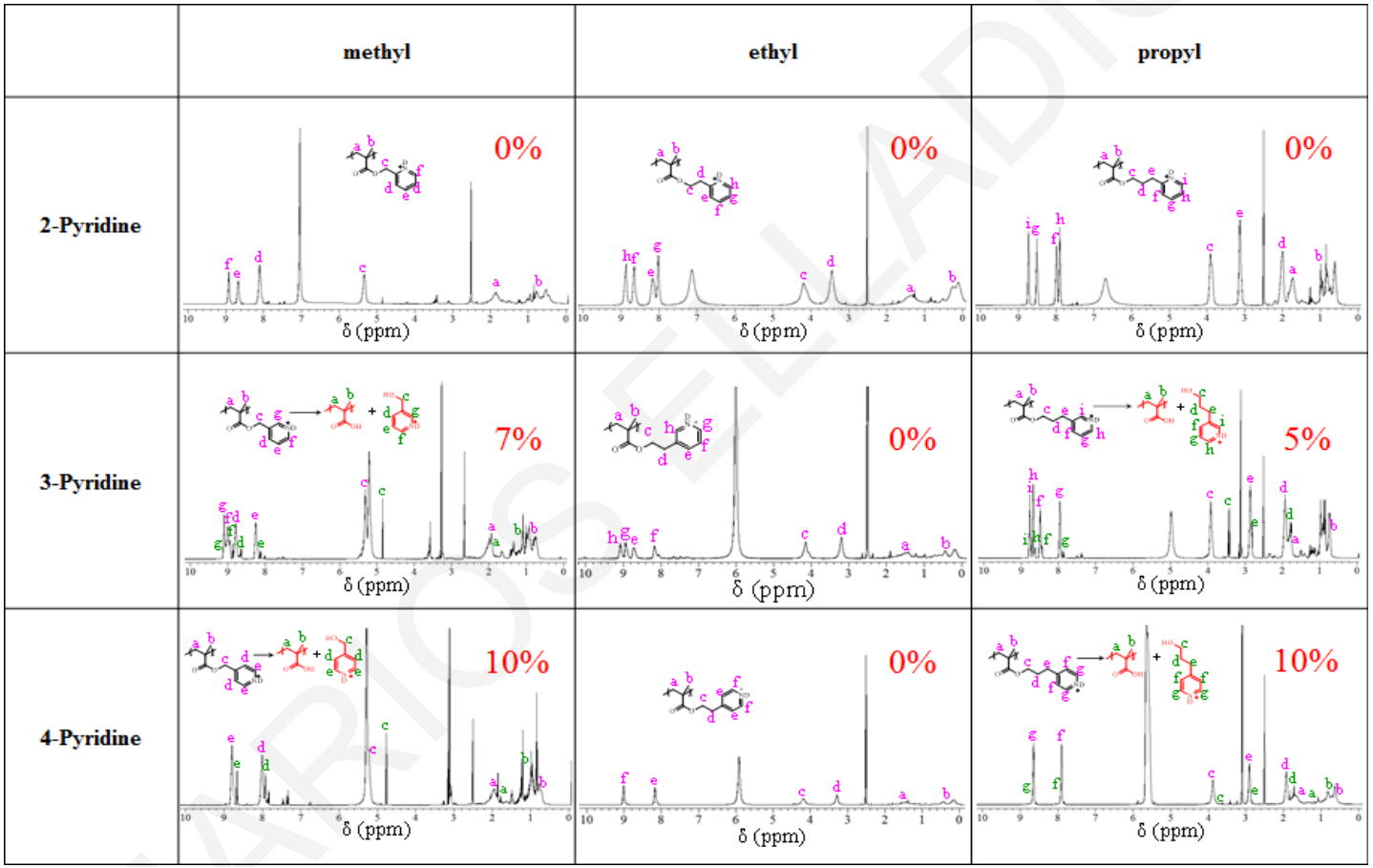

Figure 7. ^{1}H NMR spectra in d_6-DMSO of the nine pyridinylalkyl methacrylates after acidic hydrolysis using DCl in d_6-DMSO.

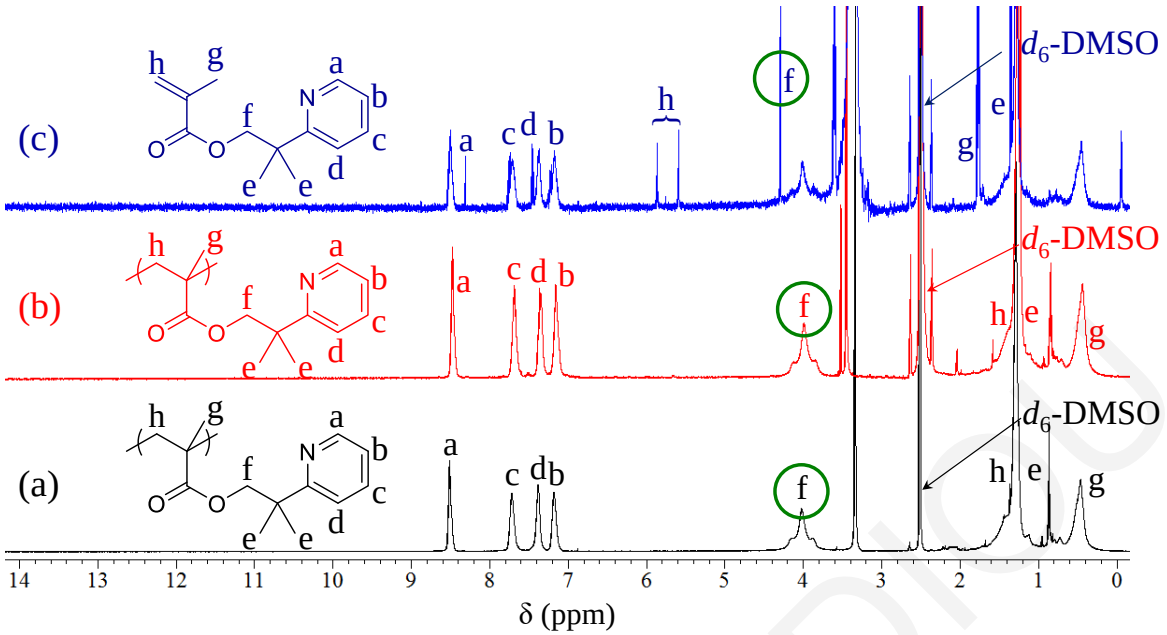

Figure 8. ^{1}H NMR spectra in d_6-DMSO of (a) the original 2PyEdimeMA$_{50}$ homopolymer (black), (b) the 2PyEmeMA$_{50}$ homopolymer after alkaline hydrolysis (red), and (c) the 2PyEmeMA$_{50}$ homopolymer after thermolysis in DSC up to 220 °C (blue).